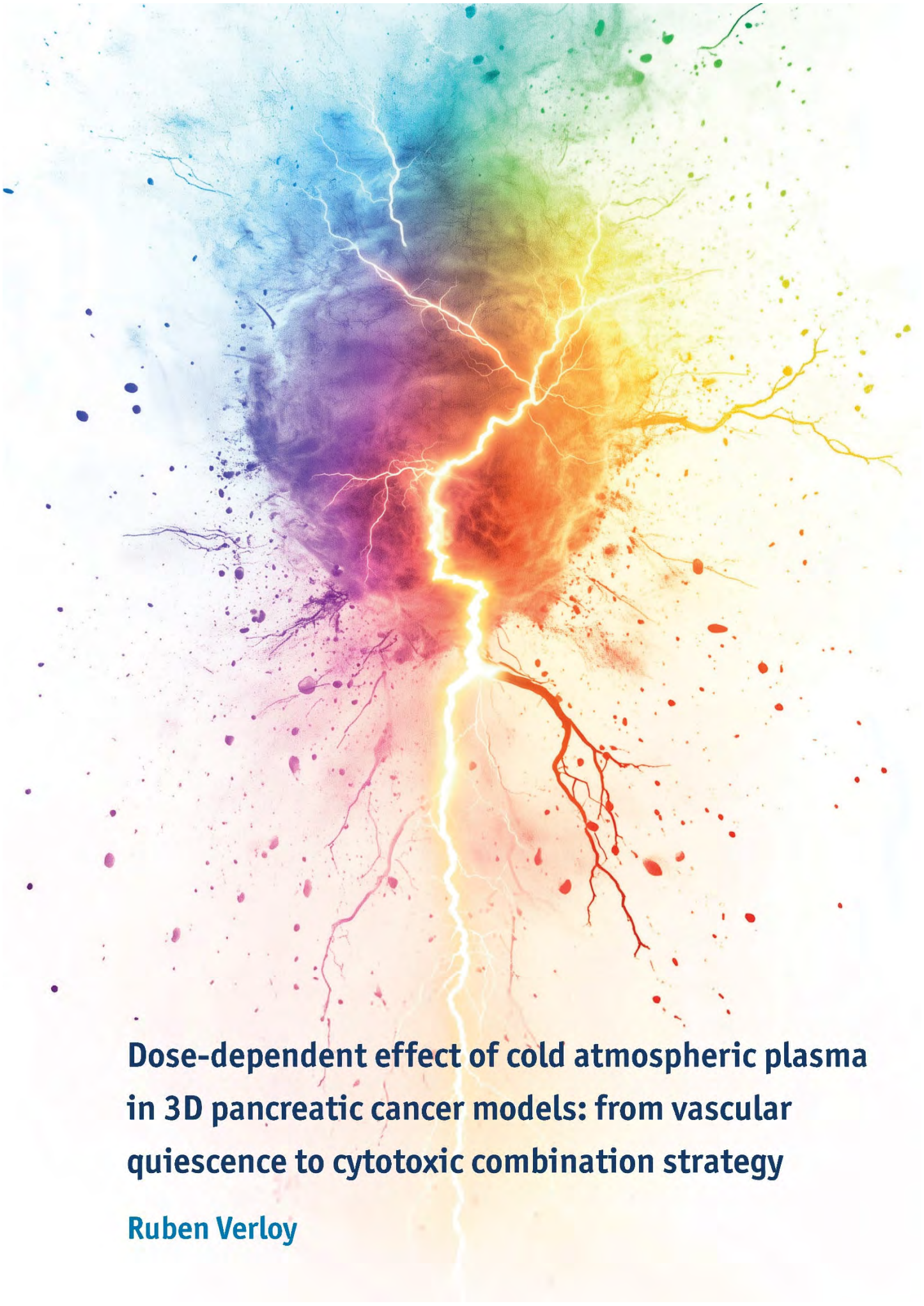

Dose-dependent effect of cold atmospheric plasma in 3D pancreatic cancer models: from vascular quiescence to cytotoxic combination strategy

Ruben Verloy

University of Antwerp

Faculty of Science
Department of Chemistry

Dose-dependent effect of cold atmospheric plasma in 3D pancreatic cancer models: from vascular quiescence to cytotoxic combination strategy

Dosisafhankelijk effect van koud atmosferische plasma in 3D pancreasmodellen: van vasculaire rust tot cytotoxische combinatiestrategie

Thesis submitted for the degree of Doctor of Science: Chemistry at the University of Antwerp to be defended by Ruben Verloy

Supervisors:
Prof. Dr. Annemie Bogaerts, Prof. Dr. Evelien Smits, Dr. Angela Privat-Maldonado

Antwerp, 2025

Disclaimer:

The research described in this dissertation was performed at the Plasma Lab for Applications in Sustainability and Medicine Antwerp (PLASMANT) and Center for Oncological Research (CORE) at the University of Antwerp. This work was supported financially by Research Foundation Flanders (FWO).

The PhD researcher and supervisor(s) declare that the PhD research was conducted according to the principles of scientific integrity, as mentioned in the general PhD regulations and charter for PhD researchers of UAntwerp and the integrity charter for PhD researchers and supervisors affiliated with the University of Antwerp.

De doctoraatsonderzoeker en promotor(en) verklaren dat het doctoraatsonderzoek werd uitgevoerd volgens de principes van de wetenschappelijke integriteit, zoals vermeld in het algemeen doctoraatsreglement en algemeen charter van de doctorandus van UAntwerpen en het integriteitscharter voor doctorandi en promotoren verbonden aan de Universiteit Antwerpen.

Members of the jury

Promotors

Prof. Dr. Annemie Bogaerts

Prof. Dr. Evelien Smits

Dr. Angela Privat-Maldonado

Internal Jury Members

Prof Dr. An Wouters (Chair)

Dr. Abraham Lin

External Jury Members

Prof. Dr. Cristina Canal

Dr. Augusto Stancampiano

Funding Acknowledgement

Fonds voor Wetenschappelijk Onderzoek (FWO) was the main funder of this PhD research.

Table of contents

List of abbreviations

2D	Two-dimensional
3D	Three-dimensional
α-SMA	α-smooth muscle actin
Ang-2	Angiopoietin-2
ATP	Adenosine triphosphate
BH	BxPC-3:hPSC21
BHH	BxPC-3:hPSC21:HMEC-1
CAF	Cancer-associated fibroblast
CAM	Chorioallantoic membrane
CAP	Cold atmospheric plasma
CTGF	Connective tissue growth factor
PDGF	Platelet-derived growth factor
DAMP	Danger-associated molecular pattern
DC	Dendritic cell
DBD	Dielectric barrier discharge
EC	Endothelial cell
ECM	Extracellular matrix
EMT	Epithelial-to-mesenchymal transition
FGF	Fibroblast growth factor
FAP	Fibroblast activation protein-α
FFX	FOLFIRINOX
GEM	Gemcitabine
GFAP	Glial fibrillary acidic protein
GNP	Gemcitabine/Nab-paclitaxel
HDI	Human development index
HIF-1α	Hypoxia inducible factor-1α
H_2O_2	Hydrogen peroxide
HMGB-1	High mobility group box 1
IL-1	Interleukin-1
IL-6	Interleukin-6
IL-8	Interleukin-8
ICD	Immunogenic cell death
LTE	Local thermodynamic equilibrium
MCP-1	Monocyte chemoattractant protein-1
MMP	Matrix metalloproteinase
MSDC	Myeloid-derived suppressor cell
MR	MiaPaCa-2:RLT-PSC
MRH	MiaPaCa-2:RLT-PSC:HMEC-1
N	Atomic nitrogen
·NO	Nitric oxide
NO_2^-	Nitrite

NO_3^-	Nitrate
NTP	Non-thermal plasma
O	Atomic oxygen
$O_2\cdot^-$	Superoxide
$^1O_2$	Singlet oxygen
O_3	Ozone
·OH	Hydroxyl radical
$ONOO^-$	Peroxynitrite
PanIN	Pancreatic intraepithelial neoplasia
PBS	Phosphate-buffered saline
PCC	Pancreatic cancer cell
PCX	Paclitaxel
PDAC	Pancreatic ductal adenocarcinoma
PSC	Pancreatic stellate cell
PTL	Plasma-treated liquid
RONS	Reactive oxygen and nitrogen species
Slm	Standard liter per minute
T-reg	Regulatory T cell
TCC	Triple co-culture
TGF-β	Transforming growth factor-β
TME	Tumor microenvironment
TNF-α	Tumor necrosis factor-α
VEGF	Vascular endothelial growth factor

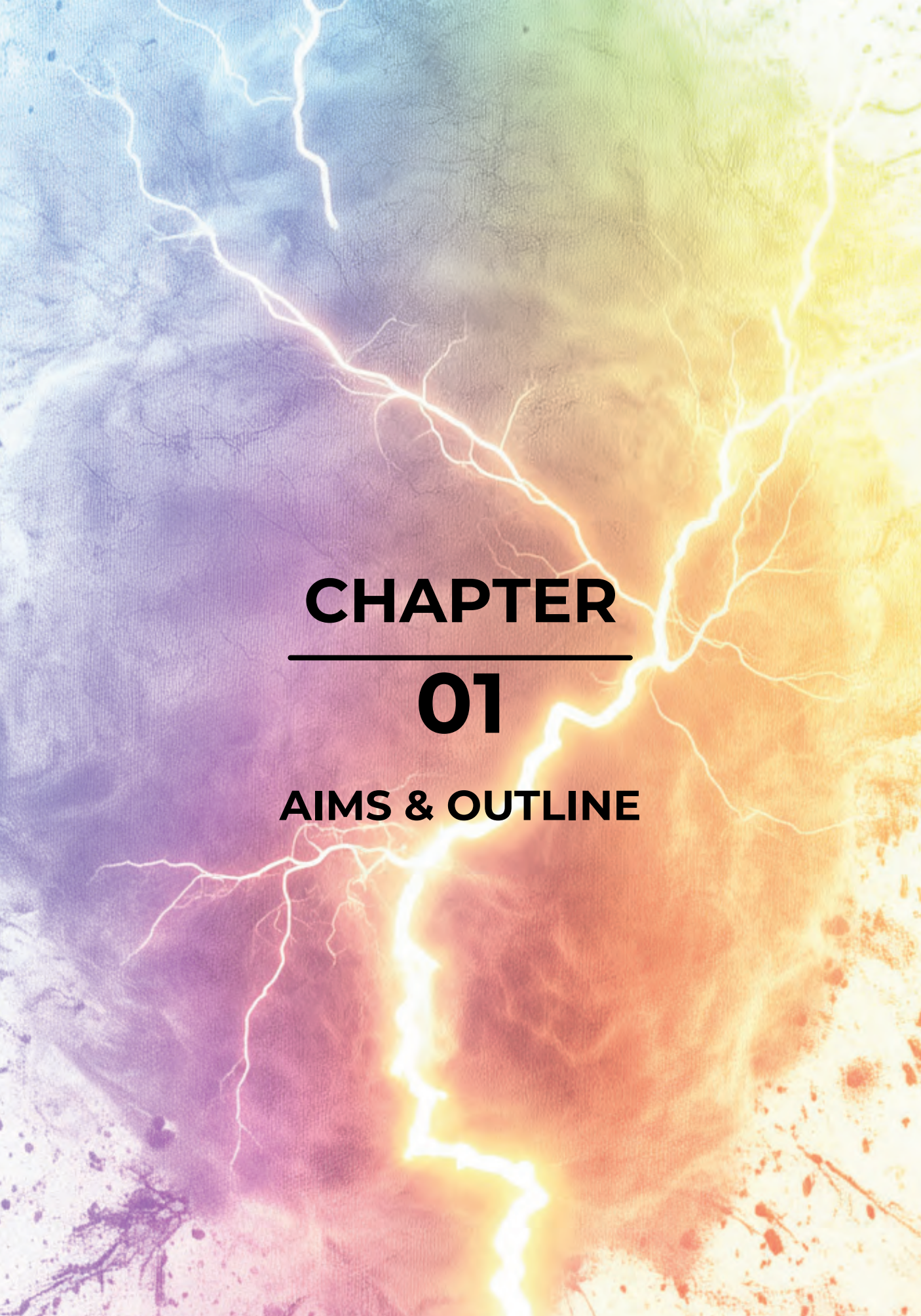

CHAPTER 01

AIMS & OUTLINE

1.1 Rationale and positioning with regard to state-of-the-art

1.1.1 Problem definition of PDAC

Pancreatic cancer has become the sixth leading cause of death by cancer globally [1]. In 2022, global pancreatic cancer incidence and mortality were 511,000 and 467,000, respectively [1]. Pancreatic ductal adenocarcinoma (PDAC), the most common type of pancreatic cancer with approximately 85% of all cases [2], is characterized by a desmoplastic reaction, which triggers the formation of a dense, fibrous tissue [3]. This dense tissue creates high intratumoral pressure, causing vascular compression and hypovascularity, which inhibits drug delivery and induces chemoresistance [4]. Activated pancreatic stellate cells (PSCs) can be seen as the guardians of PDAC and are major contributors to this desmoplastic reaction [5]. Due to their cross-talk with pancreatic cancer cells (PCCs), they cause the creation of a complex tumor microenvironment (TME), leading to the acquisition of properties like rapid growth, high invasive and metastatic potential, survival in hypoxic and low-nutrient condition, etc. [6]. Surgery in combination with conventional therapies is currently the only potential treatment for PDAC [7]. The five-year survival rate for this disease is only around 10 % and confirms once again that pancreatic cancer is the deadliest type of cancer and underscores why alternative treatment options are highly needed [1, 8, 9]. Failure to significantly increase survival rates of this disease is highly related to the tumor complexity, e.g. dense desmoplastic shield due to PSCs. Looking into the different parameters that create this complexity, such as the PSCs and the TME, and using models that can mimic this complexity, are highly important in research towards a novel therapy for PDAC.

1.1.2 Current treatment of PDAC patients

Currently, surgery with adjuvant chemotherapy (FOLFIRINOX or Gemcitabine/Nab-Paclitaxel) is the most successful treatment strategy for PDAC [7]. Out of 30% of all PDAC patients that are potentially eligible for surgery at time of diagnosis, only 15-20% of all patients are candidates for surgical resection, as others are limited by the local progression of the disease towards other organs [10]. For others, total removal cannot be achieved due

to safety reasons concerning arteries (including borderline resectable and/or locally advanced tumors) [11]. Thus, this strategy presents multiple limitations for the treatment of PDAC: i) metastases are not removed; and ii) remaining PCCs in the tumor site have the risk to form secondary tumors. Although chemotherapy provides an increase in overall survival for PDAC patients, this improvement is only with a few months, and overall survival is barely prolonged with one year [12, 13]. Compared to other types of cancer, PDAC has an increased resistance to chemotherapy, partially due to the vascular compression and hypovascularity caused by the desmoplastic shield [14]. Radiotherapy for PDAC is only used for improving surgical resection or in combination with chemotherapy, known as radiochemotherapy [15]. Immunotherapy was awarded to be the biggest scientific breakthrough in 2013 [16] and has found its way to the therapeutic armamentarium of several cancer types, however, its efficacy in clinical trials is still limited in PDAC [17, 18].

The current conventional therapies leave significant room to improve the survival of PDAC patients. Novel combination therapies for PDAC are necessary to improve the therapeutic outcome, which is a big need of PDAC patients. Therefore, this PhD thesis aims to explore the ability of cold atmospheric plasma (CAP) treatment in combination with chemotherapy to treat this lethal disease [19].

1.1.3 Implementation of CAP for PDAC treatment

CAP is a partially ionized gas that operates below 40°C, which includes a cocktail of electrons, various types of ions, radicals, and excited species. In N_2/O_2 mixtures (or air), the reactive species formed are referred to as reactive oxygen and nitrogen species (RONS). These RONS disrupt the oxidative balance within cells, which causes cellular oxidative stress and could lead to various effects, e.g., protein and DNA damage, destruction of lipid membranes, activation of the immune system, etc. [19, 20]. CAP treatment can have positive effects on tissues when delivering low levels of RONS, e.g., promote wound healing by blood coagulation, angiogenesis and tissue regeneration [21, 22]. When higher levels of RONS are exogenously applied with CAP, it can induce cell death, as the oxidative balance in cancer cells and tissues becomes disturbed [19]. The intracellular RONS level in cancer cells is higher than in healthy cells due to a higher metabolic activity, suggesting a selective

killing effect of CAP on cancer cells [23-25]. In all cases, the administered concentration of RONS depends on the treatment time, the distance from the nozzle of the device to the tissue, the type of feed gas used, the device itself, the treatment liquid and its supplements. This difference in cellular effects provides a large variety of applications for CAP treatment and lies at the basis of this PhD thesis.

High-dose CAP has shown great potential for its therapeutic capabilities against cancer and has demonstrated to effectively eliminate several cancer cell types both in vitro and in vivo [23, 26, 27]. Early studies have shown that CAP is also able to alter the extracellular matrix (ECM) by oxidation and denaturation of ECM proteins [28], which is very interesting for the desmoplastic tissue of PDAC and could relief intratumoral pressure, however more research is needed regarding this topic. Other benefits of CAP are the permeabilization of the cell membrane and tissues like skin [29], which can sensitizes cells to chemotherapeutics [30], and the induction of immunogenic cell death [31]. The advantage of CAP is its multimodal nature that can simultaneously attack multiple targets in cancer cells and their TME, overcoming some of the limitations of current therapies. Adding CAP treatment to conventional chemotherapy in PDAC, could potentially lead to a more effective combinational therapy to improve clinical outcome of this aggressive cancer. Currently, only three studies have investigated the effect of CAP treatment on PDAC including PSCs. However, they only focused on cell viability of mono-culture PSCs [31-33]. To fill the knowledge gap, my PhD thesis focused on co-culture and three-dimensional (3D) models to recapitulate the TME more accurately. A more detailed explanation of PDAC, the importance of the PSCs, the TME, current treatment methods and their limitations, and the potential of CAP for (pancreatic) cancer can be found in my published review article [6].

1.1.4 Low-dose CAP to induce angiogenesis in PDAC, in order to enhance chemotherapeutic delivery and efficacy

Significant attention in cancer research has been given to anti-angiogenic approaches to inhibit vascularity and tumor growth. However, these approaches highly struggle with retaining their promising pre-clinical effects when moving onto clinical models [34]. For

PDAC, tumor aggressiveness is often increased, while chemotherapeutic effects are decreased due to the inhibition of drug delivery and the induction of hypoxia [35]. Pro-angiogenic approaches for PDAC have been suggested to facilitate the delivery and effect of chemotherapeutics, showing a reduction in tumor growth, metastasis and desmoplasia, and an increased survival, blood vessel density and perfusion [35, 36]. The first study made use of a combination of the calcium channel blocker Verapamil and the anti-angiogenic drug Cilengitide. The second study aimed to create therapeutic vulnerabilities by inducing a senescence-associated secretory phenotype, which causes the release of pro-angiogenic factors and promotes tumor angiogenesis.

CAP treatment received increasing attention in anti-cancer research for its ability to selectively kill cancer cells. However, CAP treatment has also been used for wound healing due to the induction of angiogenesis and tissue regeneration [22, 37, 38]. As discussed in the previous section, this difference in application originates from the RONS concentration dependence of cellular effects [19]. Mild CAP treatment to provide a pro-angiogenic strategy to fight cancer is a novel and potential high-impact breakthrough in (plasma) oncology. It could contribute to breaking the current anti-angiogenic dogma, which has drastically shown its limitations. Furthermore, pro-angiogenic CAP treatment offers multiple advantages over angiogenic drugs, such as the multimodal nature of CAP to influence cancer cells or tissues in multiple ways, as described earlier. Importantly, CAP is a highly localized, temporal and non-invasive treatment which significantly reduces side effects compared to systemic drug administration [28].

1.2 Aims

1.2.1 Hypothesis

I can summarize previous information as follows: 1) PDAC tumors show hypovascularity and vascular compression providing chemoresistance; 2) low CAP treatment times can induce angiogenesis alongside other effects (e.g. selective elimination of cancer cells, alteration of the ECM, cell membrane & tissue permeation, which sensitizes cells to chemotherapy); 3) high CAP treatment times are cytotoxic to cancer cells due to oxidative

damage which could be selective to cancer cells over healthy cells; and 4) cross-talk between PCCs and PSCs majorly contributes to creating the ideal TME to benefit tumor growth, resilience and survival. This has led to the first hypothesis of my PhD thesis that low-dose CAP treatment can enhance the uptake and efficacy of chemotherapeutics in PDAC by inducing angiogenesis, causing a synergistic effect. The second hypothesis is that cytotoxic high-dose CAP treatment could increase the efficacy of eliminating PCCs in combination with chemotherapy by inducing cell death through oxidative stress, which is a different mechanism of action than that of gemcitabine and paclitaxel.

1.2.2 Aims and objectives

This PhD thesis explores two therapeutic approaches using CAP treatment to tackle the complex TME of PDAC, using novel and complex in vitro and in ovo 3D models. The first aim of my PhD thesis is to evaluate whether angiogenesis can be induced in cancer by low-dose CAP treatment, which could facilitate the delivery and effect of chemotherapeutics, while retaining an anti-cancer effect, and combined lead to a better prognosis [39]. The second aim is to evaluate the synergistic potential of high-dose CAP treatment combined with chemotherapeutics. I will use 3D co-culture in vitro and in ovo models of PSCs, PCCs and endothelial cells (ECs) to mimic a more accurate TME.

My specific objectives are:

1. Establish in vitro 3D tumor-stroma-endothelial spheroid models of PDAC
2. Evaluate the effect of low-dose CAP treatment on angiogenesis using 3D in vitro and in ovo co-culture models
3. Investigate the potential synergistic effect of high-dose CAP treatment with chemotherapy in 3D in vitro and in ovo co-culture models

1.3 Outline

An overview of this PhD thesis is visualized in Figure 1.1.

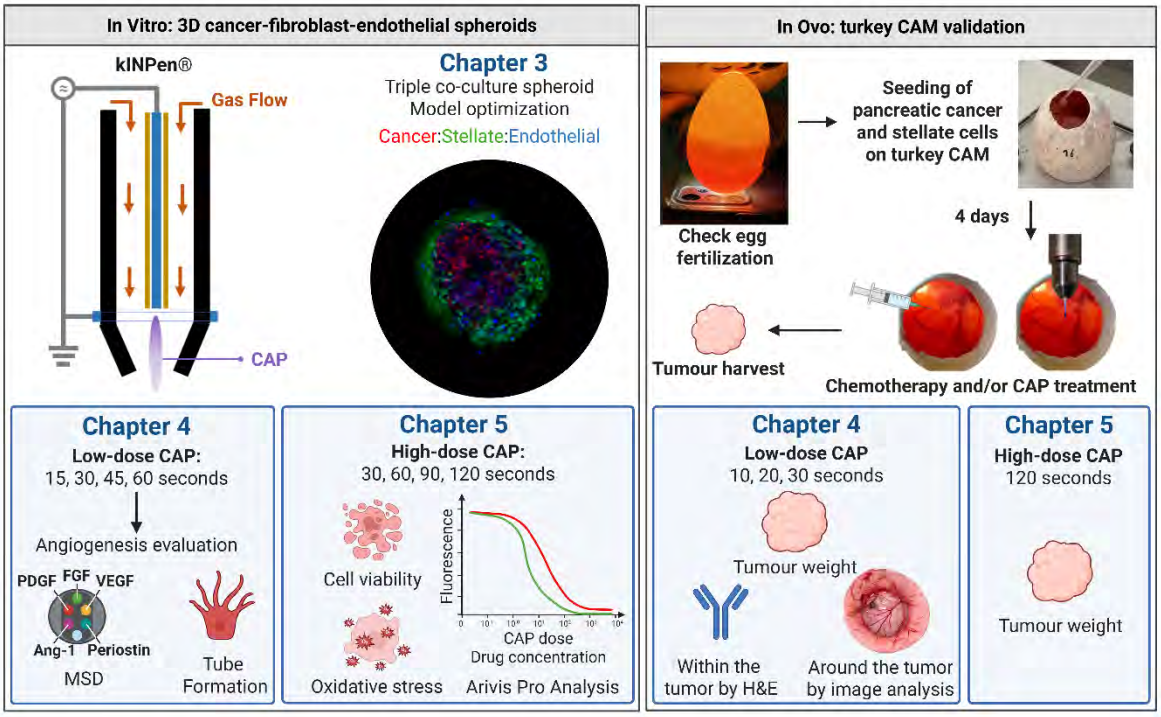

***Figure 1.1**. Outline of the doctoral PhD thesis. Overview of the two experimental models used to evaluate CAP effects: a 3D in vitro tumor-stroma-endothelial spheroid model and an in ovo turkey CAM model. Both models were treated with low- or high-dose CAP to assess angiogenesis, cell viability, oxidative stress, and tumor shrinkage.*

Chapter 2 provides a general and more detailed literature overview to lay the foundation for the experimental research presented in this PhD thesis. PDAC is introduced, emphasizing its hallmark features, such as dense desmoplasia, poor vascularization, and resistance to therapy. Special attention is given to the role of PSCs in promoting these treatment barriers, as well as to the emerging potential of CAP as an innovative, non-invasive therapeutic modality. CAP's dual behavior of stimulating wound healing and angiogenesis at low doses and inducing cytotoxicity at higher doses is discussed in the context of cancer treatment, highlighting gaps in the current research, especially the lack of relevant 3D and multicellular in vitro models.

Chapter 3 addresses this gap by describing the development of a set of clinically relevant triple co-culture (TCC) spheroid models that integrate PCCs, PSCs, and ECs. Four distinct

spheroid types are proposed to recreate the heterogeneity of the PDAC TME, making this model more suitable for studying both angiogenic and cytotoxic responses to treatment.

In **chapter 4**, these models are used to investigate whether low-dose CAP treatment can promote angiogenesis, with the aim of improving vascular perfusion and chemotherapeutic drug delivery in PDAC. The angiogenic response is assessed using both the TCC spheroids and a turkey chorioallantoic membrane (CAM) in ovo model for further validation. Results demonstrated that CAP did not induce angiogenesis in PDAC but rather preserved vascular quiescence.

Building on earlier findings, **chapter 5** explores whether high-dose CAP can enhance the efficacy of chemotherapeutic agents by directly increasing tumor cell death. Both the TCC spheroid model and the turkey in ovo CAM model are used. Notably, I applied an innovative technique using the in ovo model, where chemotherapy is injected directly into the tumor vasculature. This allows for targeted drug delivery in a vascularized setting, enabling a more accurate assessment of CAP–chemotherapy synergy in a physiologically relevant context. Intravenous administration of chemotherapy in the turkey in ovo model resulted in significant tumor shrinkage, proving this technique to be successful. Additionally, CAP treatment resulted in tumor shrinkage in the in vitro experiments with low-dose chemotherapy or without chemotherapy, but failed to further decrease cell viability (in vitro) or tumor shrinkage (in ovo) upon combination with high-dose chemotherapy

Chapter 6 discusses the key findings from all experimental chapters and places them in the broader context of current literature. This chapter critically evaluates the potential of CAP as both a vascular modulator and cytotoxic agent in PDAC. In addition, it discusses the impact of model complexity, CAP treatment parameters, and tumor heterogeneity on the observed outcomes. Particular attention is given to the challenges and opportunities of integrating CAP into combination therapies with chemotherapy. Finally, future perspectives are proposed to optimize CAP application, refine delivery methods, and better understand its mechanistic effects within the PDAC tumor microenvironment.

1.4 References

1. Bray, F., M. Laversanne, H. Sung, J. Ferlay, R.L. Siegel, I. Soerjomataram, et al., *Global cancer statistics 2022: GLOBOCAN estimates of incidence and mortality worldwide for 36 cancers in 185 countries.* CA Cancer J Clin, 2024. **74**(3): p. 229-263.
2. Hasan, S., R. Jacob, U. Manne, and R. Paluri, *Advances in pancreatic cancer biomarkers.* Oncol Rev, 2019. **13**(1): p. 410.
3. Pandol, S., M. Edderkaoui, I. Gukovsky, A. Lugea, and A. Gukovskaya, *Desmoplasia of pancreatic ductal adenocarcinoma.* Clin Gastroenterol Hepatol, 2009. **7**(11 Suppl): p. S44-7.
4. de Sousa Cavalcante, L. and G. Monteiro, *Gemcitabine: metabolism and molecular mechanisms of action, sensitivity and chemoresistance in pancreatic cancer.* Eur J Pharmacol, 2014. **741**: p. 8-16.
5. Wu, Y., C. Zhang, K. Jiang, J. Werner, A.V. Bazhin, and J.G. D'Haese, *The Role of Stellate Cells in Pancreatic Ductal Adenocarcinoma: Targeting Perspectives.* Front Oncol, 2020. **10**: p. 621937.
6. Verloy, R., A. Privat-Maldonado, E. Smits, and A. Bogaerts, *Cold Atmospheric Plasma Treatment for Pancreatic Cancer-The Importance of Pancreatic Stellate Cells.* Cancers (Basel), 2020. **12**(10): p. 2782.
7. McGuigan, A., P. Kelly, R.C. Turkington, C. Jones, H.G. Coleman, and R.S. McCain, *Pancreatic cancer: A review of clinical diagnosis, epidemiology, treatment and outcomes.* World J Gastroenterol, 2018. **24**(43): p. 4846-4861.
8. Siegel, R.L., A.N. Giaquinto, and A. Jemal, *Cancer statistics, 2024.* CA Cancer J Clin, 2024. **74**(1): p. 12-49.
9. Sung, H., J. Ferlay, R.L. Siegel, M. Laversanne, I. Soerjomataram, A. Jemal, et al., *Global Cancer Statistics 2020: GLOBOCAN Estimates of Incidence and Mortality Worldwide for 36 Cancers in 185 Countries.* CA Cancer J Clin, 2021. **71**(3): p. 209-249.
10. Hackert, T., *Surgery for Pancreatic Cancer after neoadjuvant treatment.* Ann Gastroenterol Surg, 2018. **2**(6): p. 413-418.
11. Fogel, E.L., S. Shahda, K. Sandrasegaran, J. DeWitt, J.J. Easler, D.M. Agarwal, et al., *A Multidisciplinary Approach to Pancreas Cancer in 2016: A Review.* Am J Gastroenterol, 2017. **112**(4): p. 537-554.
12. Williet, N., A. Saint, A.L. Pointet, D. Tougeron, S. Pernot, A. Pozet, et al., *Folfirinox versus gemcitabine/nab-paclitaxel as first-line therapy in patients with metastatic pancreatic cancer: a comparative propensity score study.* Therap Adv Gastroenterol, 2019. **12**: p. 1756284819878660.
13. Von Hoff, D.D., T. Ervin, F.P. Arena, E.G. Chiorean, J. Infante, M. Moore, et al., *Increased survival in pancreatic cancer with nab-paclitaxel plus gemcitabine.* N Engl J Med, 2013. **369**(18): p. 1691-703.
14. Van Audenaerde, J.R.M., J. De Waele, E. Marcq, J. Van Loenhout, E. Lion, J.M.J. Van den Bergh, et al., *Interleukin-15 stimulates natural killer cell-mediated killing of both human pancreatic cancer and stellate cells.* Oncotarget, 2017. **8**(34): p. 56968-56979.

15. Brunner, T.B. and M. Scott-Brown, *The role of radiotherapy in multimodal treatment of pancreatic carcinoma.* Radiat Oncol, 2010. **5**: p. 64.
16. Couzin-Frankel, J., *Breakthrough of the year 2013. Cancer immunotherapy.* Science, 2013. **342**(6165): p. 1432-3.
17. Schizas, D., N. Charalampakis, C. Kole, P. Economopoulou, E. Koustas, E. Gkotsis, et al., *Immunotherapy for pancreatic cancer: A 2020 update.* Cancer Treat Rev, 2020. **86**: p. 102016.
18. Farhangnia, P., H. Khorramdelazad, H. Nickho, and A.A. Delbandi, *Current and future immunotherapeutic approaches in pancreatic cancer treatment.* J Hematol Oncol, 2024. **17**(1): p. 40.
19. Privat-Maldonado, A., A. Schmidt, A. Lin, K.D. Weltmann, K. Wende, A. Bogaerts, et al., *ROS from Physical Plasmas: Redox Chemistry for Biomedical Therapy.* Oxid Med Cell Longev, 2019. **2019**: p. 29.
20. Miller, V., A. Lin, and A. Fridman, *Why Target Immune Cells for Plasma Treatment of Cancer.* Plasma Chemistry and Plasma Processing, 2016. **36**(1): p. 259-268.
21. von Woedtke, T., A. Schmidt, S. Bekeschus, K. Wende, and K.D. Weltmann, *Plasma Medicine: A Field of Applied Redox Biology.* In Vivo, 2019. **33**(4): p. 1011-1026.
22. Arndt, S., P. Unger, M. Berneburg, A.K. Bosserhoff, and S. Karrer, *Cold atmospheric plasma (CAP) activates angiogenesis-related molecules in skin keratinocytes, fibroblasts and endothelial cells and improves wound angiogenesis in an autocrine and paracrine mode.* J Dermatol Sci, 2018. **89**(2): p. 181-190.
23. Guerrero-Preston, R., T. Ogawa, M. Uemura, G. Shumulinsky, B.L. Valle, F. Pirini, et al., *Cold atmospheric plasma treatment selectively targets head and neck squamous cell carcinoma cells.* Int J Mol Med, 2014. **34**(4): p. 941-6.
24. Kim, S.J. and T.H. Chung, *Cold atmospheric plasma jet-generated RONS and their selective effects on normal and carcinoma cells.* Sci Rep, 2016. **6**: p. 20332.
25. Biscop, E., A. Lin, W.V. Boxem, J.V. Loenhout, J. Backer, C. Deben, et al., *Influence of Cell Type and Culture Medium on Determining Cancer Selectivity of Cold Atmospheric Plasma Treatment.* Cancers (Basel), 2019. **11**(9).
26. Lin, A., Y. Gorbanev, J. De Backer, J. Van Loenhout, W. Van Boxem, F. Lemiere, et al., *Non-Thermal Plasma as a Unique Delivery System of Short-Lived Reactive Oxygen and Nitrogen Species for Immunogenic Cell Death in Melanoma Cells.* Adv Sci (Weinh), 2019. **6**(6): p. 1802062.
27. Liedtke, K.R., S. Bekeschus, A. Kaeding, C. Hackbarth, J.P. Kuehn, C.D. Heidecke, et al., *Non-thermal plasma-treated solution demonstrates antitumor activity against pancreatic cancer cells in vitro and in vivo.* Sci Rep, 2017. **7**(1): p. 8319.
28. Gouarderes, S., A.-F. Mingotaud, P. Vicendo, and L. Gibot, *Vascular and extracellular matrix remodeling by physical approaches to improve drug delivery at the tumor site.* Expert Opinion on Drug Delivery, 2020: p. 1-24.
29. Vijayarangan, V., Z. Maaroufi, A. Rouillard, S. Gaetan-Zin, S. Dozias, P. Escot-Bocanegra, et al., *Plasma jet and plasma treated aerosol induced permeation of reconstructed human epidermis.* Bioelectrochemistry, 2026. **167**: p. 109060.

30. Privat-Maldonado, A., C. Bengtson, J. Razzokov, E. Smits, and A. Bogaerts, *Modifying the Tumour Microenvironment: Challenges and Future Perspectives for Anticancer Plasma Treatments.* Cancers (Basel), 2019. **11**(12).
31. Van Loenhout, J., T. Flieswasser, L. Freire Boullosa, J. De Waele, J. Van Audenaerde, E. Marcq, et al., *Cold Atmospheric Plasma-Treated PBS Eliminates Immunosuppressive Pancreatic Stellate Cells and Induces Immunogenic Cell Death of Pancreatic Cancer Cells.* Cancers (Basel), 2019. **11**(10).
32. Kumar, N., P. Attri, S. Dewilde, and A. Bogaerts, *Inactivation of human pancreatic ductal adenocarcinoma with atmospheric plasma treated media and water: a comparative study.* Journal of Physics D: Applied Physics, 2018. **51**(25): p. 255401.
33. Privat-Maldonado, A., R. Verloy, E. Cardenas Delahoz, A. Lin, S. Vanlanduit, E. Smits, et al., *Cold Atmospheric Plasma Does Not Affect Stellate Cells Phenotype in Pancreatic Cancer Tissue in Ovo.* Int J Mol Sci, 2022. **23**(4).
34. Comunanza, V. and F. Bussolino, *Therapy for Cancer: Strategy of Combining Anti-Angiogenic and Target Therapies.* Front Cell Dev Biol, 2017. **5**: p. 101.
35. Wong, P.P., F. Demircioglu, E. Ghazaly, W. Alrawashdeh, M.R. Stratford, C.L. Scudamore, et al., *Dual-action combination therapy enhances angiogenesis while reducing tumor growth and spread.* Cancer Cell, 2015. **27**(1): p. 123-37.
36. Ruscetti, M., J.P.t. Morris, R. Mezzadra, J. Russell, J. Leibold, P.B. Romesser, et al., *Senescence-Induced Vascular Remodeling Creates Therapeutic Vulnerabilities in Pancreas Cancer.* Cell, 2020. **181**(2): p. 424-441 e21.
37. Schmidt, A., F. Nießner, T.v. Woedtke, and S. Bekeschus, *Hyperspectral Imaging of Wounds Reveals Augmented Tissue Oxygenation Following Cold Physical Plasma Treatment in Vivo.* IEEE Transactions on Radiation and Plasma Medical Sciences, 2020: p. 1-1.
38. Bolgeo, T., A. Maconi, M. Gardalini, D. Gatti, R. Di Matteo, M. Lapidari, et al., *The Role of Cold Atmospheric Plasma in Wound Healing Processes in Critically Ill Patients.* J Pers Med, 2023. **13**(5).
39. Katsuta, E., Q. Qi, X. Peng, S.N. Hochwald, L. Yan, and K. Takabe, *Pancreatic adenocarcinomas with mature blood vessels have better overall survival.* Sci Rep, 2019. **9**(1): p. 1310.

CHAPTER 02

BACKGROUND ON PANCREATIC DUCTAL ADENOCARCINOMA AND COLD ATMOSPHERIC PLASMA

Adapted from:
Verloy, R., Privat-Maldonado, A., Smits, E., and Bogaerts, A. Cold Atmospheric Plasma Treatment for Pancreatic Cancer-The Importance of Pancreatic Stellate Cells. Cancers (Basel), 2020. 12(10), 2782. doi:10.3390/cancers12102782

2.1 PDAC: etiology, incidence and treatments

2.1.1 Cancer

Cancer is a group of diseases resulting from the transformation of normal cells into rapidly proliferating, invasive, and therapy-resistant cells [1]. It is currently responsible for one in six deaths overall, and for one in four deaths from noncommunicable diseases [2]. According to the 2022 Global Cancer Statistics, there were 20.0 million new cases and 9.7 million cancer deaths worldwide [2], with Europe accounting for 20.4% of global cancer mortality (Figure 2.1). In Belgium, 76,220 new cases were reported in 2022, and about one in three men and one in four women are diagnosed with cancer before the age of 75 [3]. About 47% of all new cancer cases worldwide in 2022 were associated with countries with a very high human development index (HDI, an index based on life expectancy, education and gross national income per capita), while only 4% is related to low-HDI countries [2]. Certain aggressive cancers exhibit high invasiveness, therapy resistance, and metastatic potential. Between 2000 and 2014, these “hard-to-kill” cancers showed low five-year survival rates, including pancreatic, liver, lung and stomach cancer [2].

Cancer is fundamentally a genetic disease, driven by mutations in key regulatory genes such as tumor suppressor genes, oncogenes, and stability genes [4]. These mutations contribute to the acquisition of biological capabilities known as the hallmarks of cancer [5-7]. Originally six were defined in 2000, later expanded to ten in 2011, and most recently to fourteen hallmarks in 2022, reflecting emerging insights into tumor biology [5-7]. These now include: sustaining proliferative signaling, evading growth suppressors, resisting cell death, enabling replicative immortality, inducing angiogenesis, activating invasion and metastasis, reprogramming metabolism, avoiding immune destruction, genome instability, tumor-promoting inflammation, phenotypic plasticity, non-mutational epigenetic reprogramming, influence of the microbiome, and senescent cell effects (Figure 2.2) [7].

Tumor development and progression also rely on dynamic interactions with TME, which supplies immune cells, growth factors, cytokines, and matrix metalloproteinases (MMPs) that remodel the ECM [8]. This reciprocal signaling between cancer cells and the TME

supports tumor growth, metastasis, and resistance [9, 10]. In cancers like PDAC, such TME-driven ECM remodeling contributes significantly to the aggressive characteristics [11].

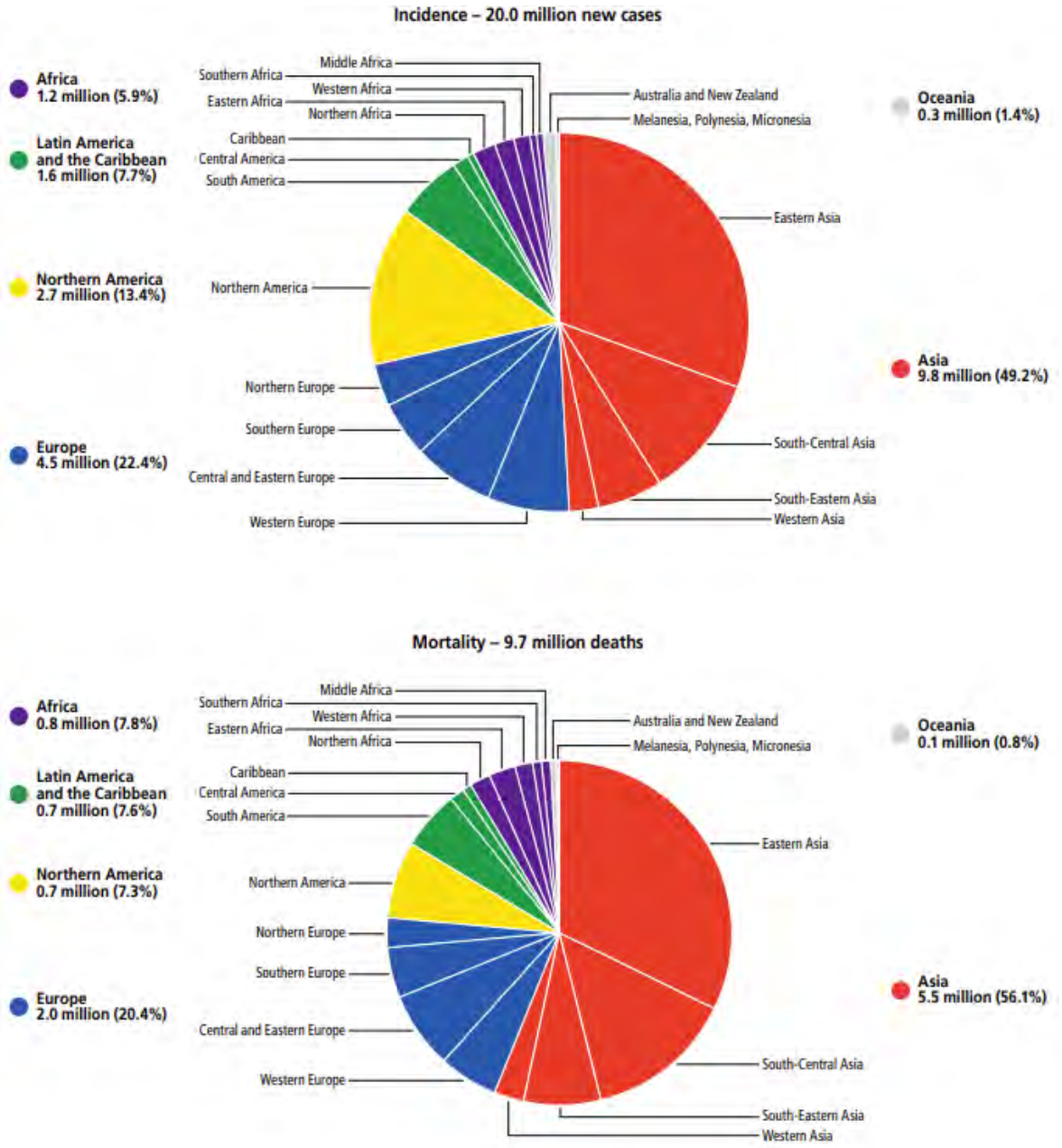

Figure 2.1. *Global cancer incidence and mortality by region. The top pie chart shows estimated new cancer cases in 2022, totaling 20.0 million worldwide. Asia accounts for nearly half of cases (49.2%), followed by Europe (22.4%), Northern America (13.4%), Latin America and the Caribbean (7.7%), Africa (5.9%), and Oceania (1.4%). The bottom pie chart depicts cancer-related deaths, totaling 9.7 million globally, with Asia contributing the largest share (56.1%), highlighting the regional disparities in cancer burden and outcomes. Image retrieved from [2].*

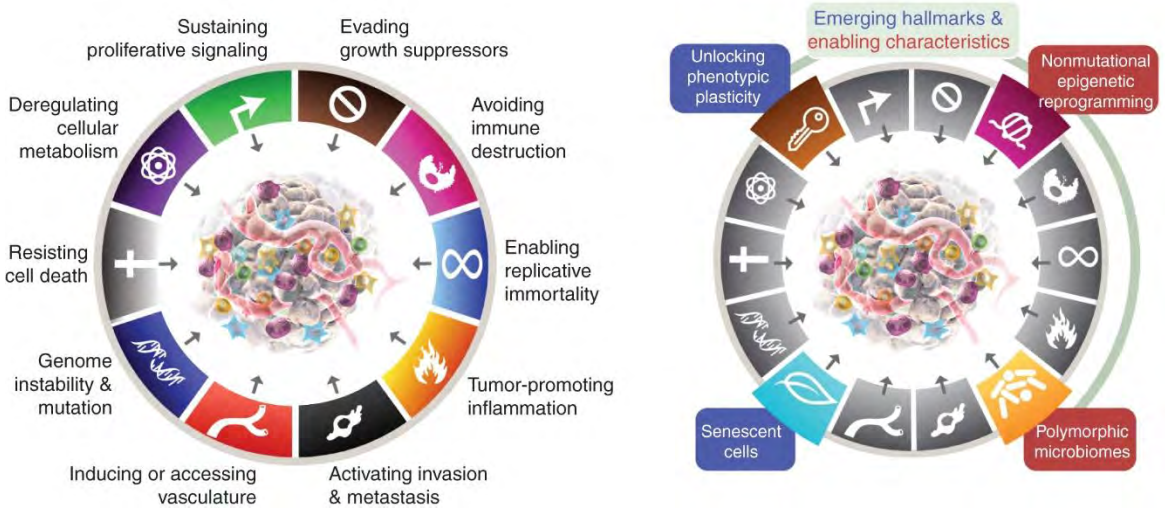

Figure 2.2. *The hallmarks of cancer and emerging enabling characteristics. The diagram on the left illustrates the classical hallmarks of cancer. The diagram on the right highlights emerging hallmarks and enabling characteristics. Together, these traits underpin cancer development and therapeutic resistance. Image retrieved from [7].*

2.1.2 PDAC

PDAC is one of the most lethal types of cancer and is refractory to most of the current treatment approaches, as the five-year survival rate of patients subjected to surgery, radio- and chemotherapy is barely 8% [12]. In 2022, the incidence and mortality of pancreatic cancer counted 510,566 and 467,005, respectively [2]. PDAC is related to a poor prognosis being ranked sixth in the leading causes of cancer mortality and is predicted to increase in the near future [2]. Together, these numbers highlight the need for therapeutic alternatives for this disease. High contributing factors to the development of PDAC include obesity, smoking and a family history of the disease [13]. The acinar and ductal cells of the pancreas are important in this development [12]. Upon environmental stimuli, e.g., stress, inflammatory conditions, etc., acinar cells transform into ductal-like cells (Figure 2.3) [14]. Through this transformation, the acinar cells become more sensitive towards mutations in, e.g., proto-oncogene KRAS, resulting in pancreatic intraepithelial neoplasia (PanIN-1, -2 and -3) [12, 14]. Followed by other oncogenic mutations, these can lead to the progression towards PDAC. KRAS mutations are present in approximately 90% of PDAC cases and are associated with poor prognosis, often occurring alongside alterations in CDKN2A [15, 16]. Besides KRAS, other important mutations in PDAC are CDKN2A, SMAD4, and TP53 [17].

Mutations in SMAD4 have been linked to enhanced metastatic potential and therapy resistance, while alterations in TP53 are known to reshape the immune environment and foster inflammation, thereby supporting tumor progression [18, 19].

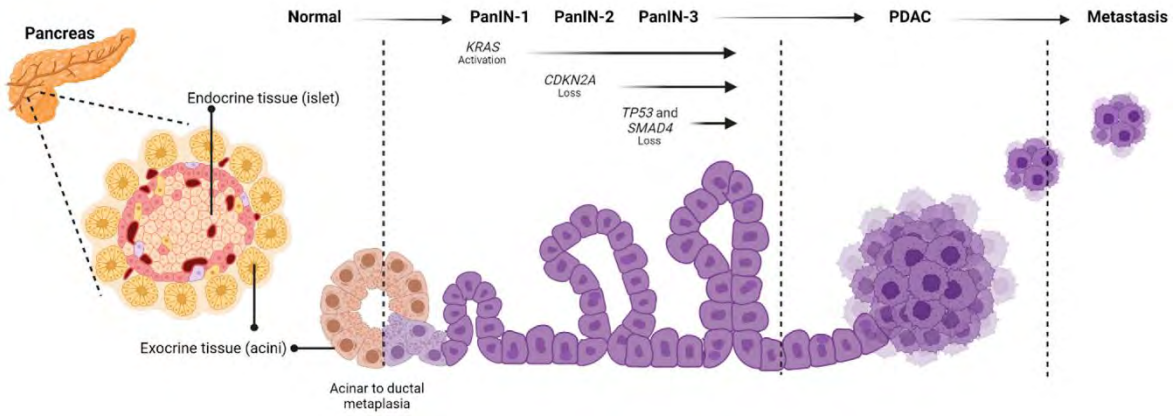

Figure 2.3. *Schematic representation of PDAC development and progression. PDAC originates predominantly from exocrine tissue (acinar cells) through a multistep process, starting with acinar-to-ductal metaplasia and progressing through various stages of pancreatic intraepithelial neoplasia (PanIN-1, -2, and -3). Key genetic mutations characterize these transitions, including activation of KRAS and subsequent loss of tumor suppressor genes CDKN2A, TP53, and SMAD4. Ultimately, advanced PDAC can metastasize, spreading cancerous cells to distant sites. Image retrieved from [20].*

PDAC is characterized by the development of early metastasis, a unique immunosuppressive TME and desmoplasia, which is the formation of a dense fibrous tissue (Figure 2.4) [21, 22]. This tissue accounts for 50-80% of the total tumor volume and is largely a consequence of the activity of stromal cells present in PDAC [23-25]. In PDAC, this unique TME is responsible for the aggressiveness and resistance to therapy due to rapid growth, invasiveness, survival in hypoxic and low-nutrient environments, a high interstitial pressure and immunosuppression in PDAC [26, 27]. This high interstitial pressure due to the extensive desmoplastic reaction leads to vascular compression and hypovascularity (Figure 2.4).

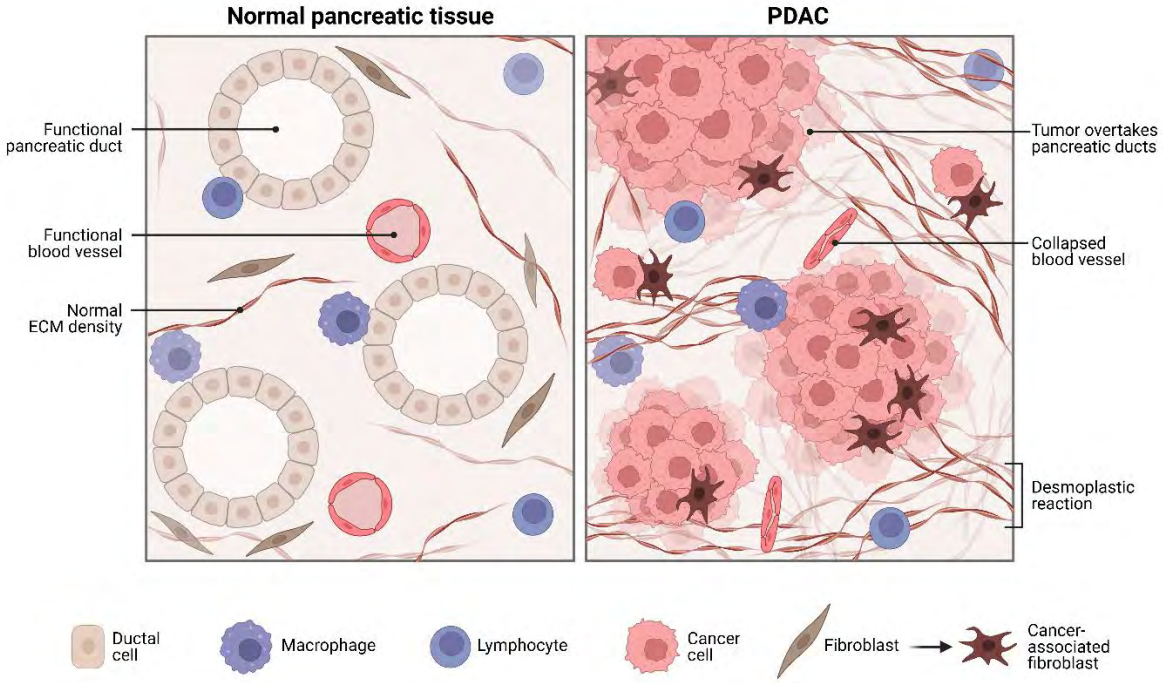

Figure 2.4. *Comparison of normal pancreatic tissue and PDAC TME. Normal tissue features organized ductal structures, functional blood vessels, and balanced ECM density, with resident immune cells and fibroblasts. In PDAC, cancer cells overtake pancreatic ducts, blood vessels become compressed or collapsed, and extensive desmoplastic stroma develops, characterized by dense ECM deposition and activation of cancer-associated fibroblasts (CAFs). This altered TME contributes to hypoxia, impaired drug delivery, and tumor progression. Image retrieved from BioRender.*

2.1.3 Current therapies for PDAC

The type of therapy that is given to PDAC patients is highly dependent on the tumor stage (Figure 2.5). Currently, surgery with adjuvant chemotherapy is the only potential treatment for PDAC [28, 29]. However, only 15-20% of patients have a chance of a successful surgical resection at the time of diagnosis, and it is only performed when a positive response to neoadjuvant therapy is observed [28, 30, 31]. Surgical resection is not an option when the tumor is too advanced or metastases have already been formed [12, 30]. Thus, this technique presents some limitations for the treatment of PDAC: i) it cannot remove metastases; and ii) remaining cancer cells in the tumor site have the risk to form secondary tumors. In addition, bleeding, short-term pain, and damage to adjacent tissues or organs have been reported as negative side effects [32, 33]. The combination of surgery with other therapies is still highly recommended for circulating cancer cells or metastatic niches, as well as to avoid recurrence of the main tumor.

The most used chemotherapeutic drugs for patients with metastatic, locally advanced, or unresectable PDAC are FOLFIRINOX (FFX) or gemcitabine combined with nab-paclitaxel (GNP) (Figure 2.5) [12, 34]. FFX was observed to be more effective than GNP, with overall survival of approximately 14 months compared to nine months, respectively [35]. In another study, the overall survival of patients treated with FFX was 11.1 months, while it was only 6.8 months with gemcitabine (GEM) alone [36]. The enhanced effect of combining GEM with nab-paclitaxel has been observed, by an overall survival of 8.5 months for GNP and only 6.7 months for GEM alone [37]. In a more recent study, a similar trend is observed in the clinical outcome of FFX, GNP or GEM alone [34]. These results highlight why FFX is the most used first-line therapy for PDAC patients [34]. Although an increase in overall survival is observed, this increase spans only a few months. The high toxicity of chemotherapeutics in normal cells is particularly important, as it prevents their use in the elderly and patients with poor health status [12].

Compared to other types of cancers, PDAC has an increased resistance to radiotherapy due to the desmoplastic shield [12]. Radiotherapy is used for improving surgical possibilities or together with chemotherapy, known as radiochemotherapy [28, 38]. This has proven to be effective in borderline PDAC according to the PREOPANC trial, but not for resectable PDAC as shown by the ESPAC-1 multicenter trial [28]. Radiosensitizing agents, such as capecitabine, GEM and fluorouracil (5-FU), combined with radiotherapy can reduce the radioresistance of PDAC [12]. Adjuvant radiotherapy treatment has great potential to attack both cancer cells remaining in the tumor bed after surgery and the circulating, invasive cells. Nevertheless, 71–76% of patients relapsed within two years [29, 38]. Radiochemotherapy as neoadjuvant treatment could offer the advantage of improving surgical possibilities for PDAC patients with borderline-resectable tumors, yet more research on this strategy is necessary [29, 38].

Immunotherapy was stated to be the biggest breakthrough in cancer research in 2013 and is also actively investigated for PDAC [39-41], but to date, its efficacy in PDAC is still limited [41, 42]. More efforts are needed in this direction to overcome the immunosuppressive

and therapy-resistant TME of PDAC and to identify specific target molecules on cancer cells, without targeting normal cells [41-45].

As discussed here, the current conventional therapies cannot significantly improve the survival of PDAC patients. Novel combination therapies for PDAC could be used to improve the therapeutic outcome.

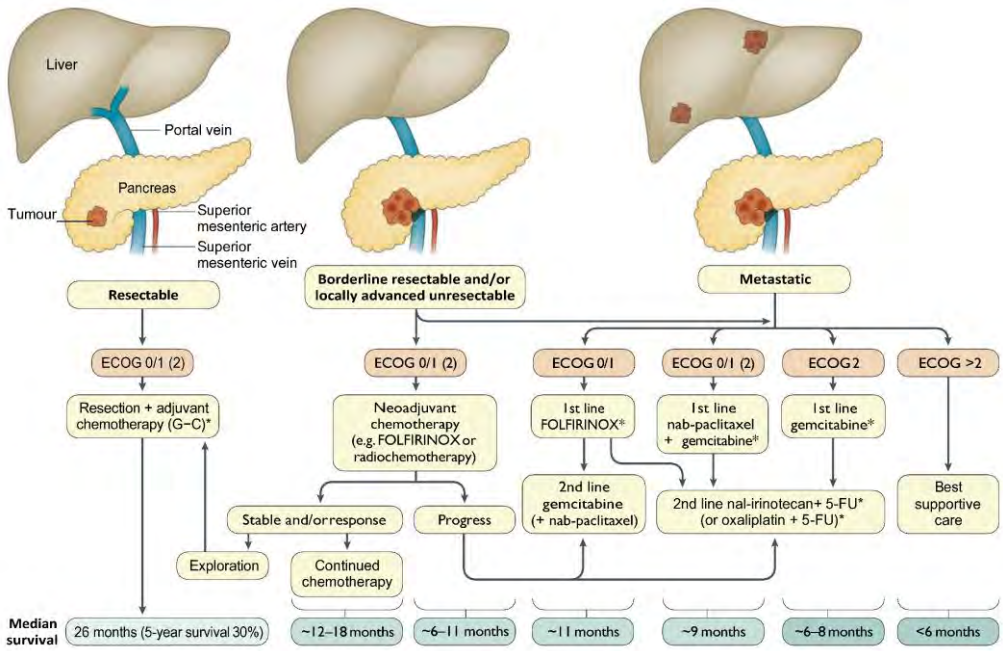

Figure 2.5. *Treatment strategies and median survival outcomes for PDAC based on disease stage and patient performance status (ECOG score). For resectable tumors, surgical resection followed by adjuvant chemotherapy yields a median survival of 26 months and a five-year survival of approximately 30%. Borderline resectable or locally advanced disease patients receive treatment based on ECOG score, disease progression and therapy response with varying outcomes. Metastatic PDAC is treated with systemic chemotherapy regimens tailored to performance status (ECOG score), including FFX, GEM with or without nab-paclitaxel, or best supportive care, with median survival ranging from 6 to 11 months depending on treatment and patient condition [46].*

2.1.4 The PDAC tumor microenvironment

2.1.4.1 The importance of pancreatic stellate cells in the creation of a complex tumor microenvironment

PSCs are a type of CAFs specific to the pancreas and are the major contributors in the creation of the ideal TME of PDAC (Figure 2.6). They are responsible for the secretion of MMPs, which degrade and remodel the ECM. This ECM remodeling has several effects: (1) it allows growth factors, e.g., platelet-derived growth factor (PDGF) to be released, causing

tumor growth; (2) it increases PCC motility to promote invasion and metastasis; (3) it increases intra-tumoral pressure and hypoxia, and (4) it creates a barrier and provides resistance towards chemotherapy [47, 48]. Besides creating an ideal TME for tumor growth and resistance towards treatments, PSCs are also responsible for inducing an inflammatory response and creating an immunosuppressive environment. PSCs recruit immunosuppressive cells, such as myeloid-derived suppressor cells (MDSCs) and regulatory T-cells (T-regs) by secreting C-X-C motif chemokine 12 [48], inflammatory cytokines, e.g., interleukin-6 (IL-6) [49], and immunosuppressive cytokines, e.g., transforming growth factor (TGF-β) [48]. In the low-nutrient and hypoxic environment of PDAC tumors, PSCs can contribute to the PDAC metabolism by secreting non-essential amino acids (e.g., alanine and aspartate), which can be used as an alternative energy source during a scarcity of glucose [50, 51]. The secretion of these amino acids results from an autophagic PSC death, induced by the PCCs [52]. In these conditions, PCCs with defects in their apoptotic mechanism can survive and overtake normal cells.

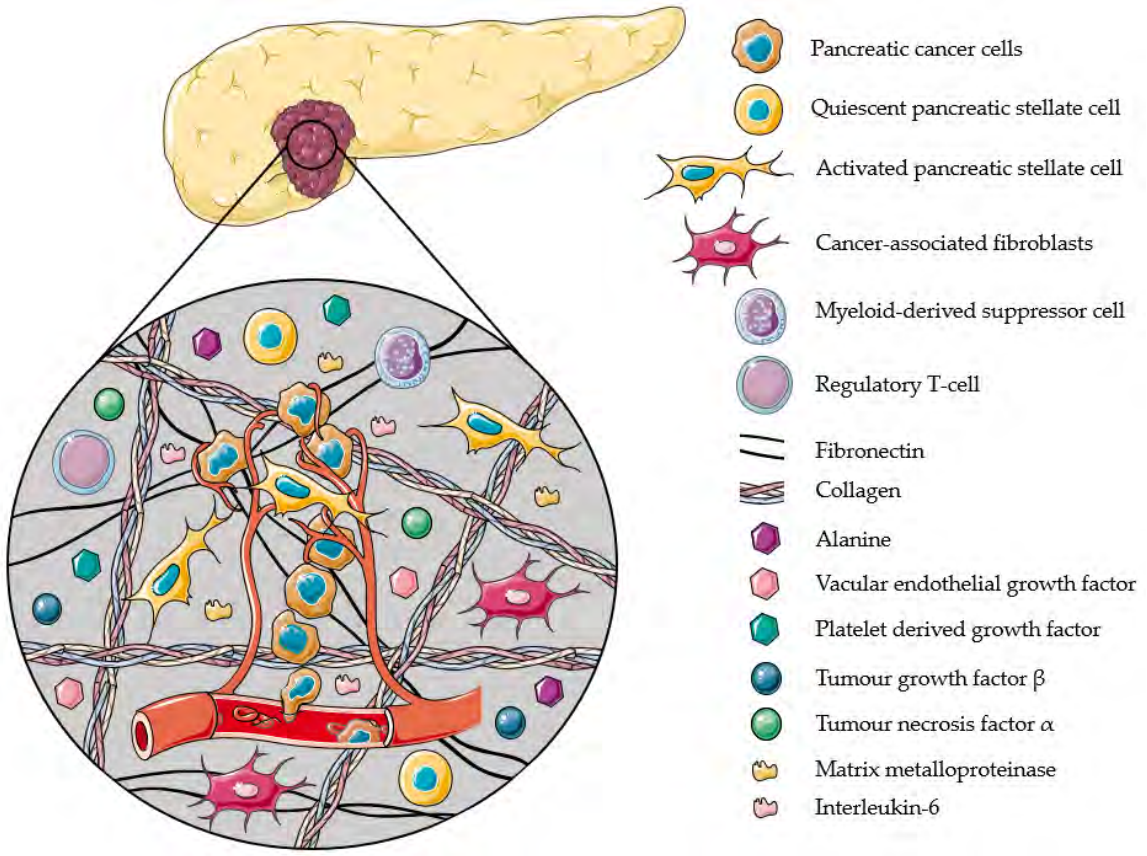

Figure 2.6. *Schematic representation of the TME of PDAC and its dense desmoplastic stroma. PSCs, as main type of CAFs in this case, account for nearly 50% of the total stroma and are typically activated in PDAC. PSCs recruit immunosuppressive cells (e.g., MDSC and T-reg) and secrete ECM molecules (e.g., collagen and fibronectin), immunosuppressive (e.g., TGF-β) and inflammatory (e.g., IL-6 and TNF-α) cytokines, pro-angiogenic factors (e.g., VEGF), MMPs (e.g., MMP-2 and MMP-9), growth factors (e.g., PDGF), and non-essential amino acids (e.g., alanine). The complexity of this TME due to PSCs causes PDAC to acquire crucial properties like rapid growth, high invasion and metastatic potential, survival in hypoxic and low-nutrient conditions, and resistance to therapy.*

2.1.4.2 Activated pancreatic stellate cells: key players for the progression of PDAC

Quiescent PSCs are responsible for maintaining the stromal composition in the healthy pancreas and are involved in the storage of vitamin-A rich lipid droplets [47, 48]. When activated, the quiescent PSC changes from a regular, circular phenotype to a star-shaped, myofibroblast-like phenotype. This activation is the result of different stimuli, such as TGF-β, tumor necrosis factor (TNF-α), oxidative stress, etc., and is typical for PDAC (Figure 2.7A) [47, 53].

One of the main reasons for the resistance of PDAC to treatment is the desmoplastic reaction induced by activated PSCs [47]. This reaction causes high intra-tumoral pressure

and creates a fibrotic shield that surrounds the tumor, limits the blood flow and the delivery of therapeutic agents, oxygen, and immune cells [50]. Activated PSCs are key players in PDAC and can induce tumor growth, PCC and PSC motility, invasion and metastasis, immune evasion, an inflammatory response, hypoxia, a metabolic alternative, etc. (Figure 2.7B), as discussed before. The secretion of cytokines and other molecules by PSCs will also cause a proliferative and migrational effect on PSCs, and sustain their activation (Figure 2.7C). In addition, PCCs stimulate PSC activation and growth, resulting in a reciprocal stimulation (Figure 2.7D). This loop of stimulation is a major reason for the aggressiveness of PDAC [47].

It is known that oxidative stress can induce the activation of PSCs [47, 48, 53]. CAP treatment provides an external source of RONS that, in principle, could favor the activation of PSCs or exacerbate their response to RONS (Figure 2.7E). However, research has shown that CAP treatment does not cause the activation of PSCs, as mRNA expression and immunofluorescence staining of activation markers (αSMA, vimentin and GFAP) remained unchanged (see red cross in Figure 2.7E) [54].

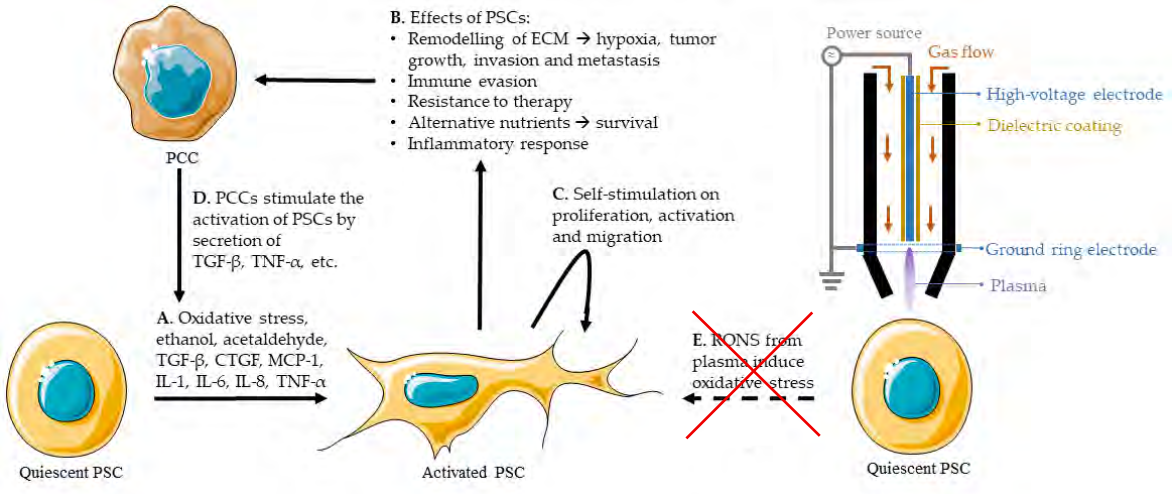

Figure 2.7. *Mechanism of reciprocal stimulation of PSCs and PCCs and the hypothetical influence of CAP (represented by treatment with a plasma jet).* ***(A)*** *Activation of PSCs due to different stimuli, e.g., oxidative stress, ethanol, acetaldehyde, TGF-β, connective tissue growth factor (CTGF), monocyte chemoattractant protein-1 (MCP-1), IL-1, IL-6, IL-8, TNF-α.* ***(B)*** *PSCs secrete immunosuppressive and inflammatory cytokines, MMPs, growth factors, pro-angiogenic factors, ECM molecules, and non-essential amino acids, by autophagic cell death and they recruit immune cells. These create an environment that allows PCCs to proliferate, evade cell death and the immune system, survive in hypoxia and low-nutrient environments, recruit immune cells and resist therapy. This has a major stimulation effect on PCCs and the survival and progression of the tumor.*

(C) *Self-stimulation of PSCs on their proliferation, activation and migration.* ***(D)*** *Stimulation of the activation of PSCs by PCCs.* ***(E)*** *CAP-derived RONS were demonstrated to not induce activation of quiescent PSCs.*

Activated PSCs can be distinguished from quiescent ones by evaluating the expression of specific markers. Commonly used markers for activated PSCs in literature are α-smooth muscle actin (α-SMA), glial fibrillary acidic protein (GFAP), desmin, vimentin, and fibroblast activation protein-α (FAP) (Table 2.1). Besides these markers, epithelial-to-mesenchymal transition (EMT) markers could also be useful, as the EMT-transition process is suspected to be related to the activation of PSCs [55]. Some of these markers and relevant to investigate PSCs are e-cadherin, n-cadherin, and slug.

Table 2.1*. List of markers for quiescent and activated PSCs. (x) = could be expressed, x = expressed, x(x) = expression could be increased, xx = increased expression.*

Marker	Quiescent PSC	Activated PSC	References
Desmin	x	x(x)	[53, 56-59]
Vimentin	x	x(x)	[53, 55, 57, 59-63]
GFAP	x	x(x)	[53, 56-59, 62]
α-SMA		xx	[47, 53, 57, 59, 60, 63, 64]
FAP	(x)	x	[64, 65]
E-cadherin	xx	x	[55, 60, 61]
N-cadherin	x	xx	[55, 61]
Slug	x	x(x)	[55, 61]

Except for α-SMA, there is still uncertainty on the expression profiles of the markers for quiescent and activated PSCs. Tian et al. have compared the expression of e-cadherin, n-cadherin, vimentin and slug between quiescent and activated PSCs, validating the expression profile given in Table 2.1 [55]. However, the authors stated that PSCs upregulate the expression of α-SMA, vimentin, desmin, and GFAP, while they do not make a distinction between markers for quiescent and activated PSCs. In previous publications, these markers are suggested to be related to PSC activation, but no comparison of the protein expression between quiescent and activated PSCs was made, nor did the cited literature experimentally validate these differences in expression [47, 58, 59, 66, 67]. Based on current research, it is difficult to determine the exact difference in expression profiles

between quiescent and activated PSCs for these markers (Table 2.1). Therefore, a pool of markers is still required to evaluate the activation of PSCs, as was partly done by Tian et al. [55].

2.1.4.3 Pancreatic stellate cells as major contributors to the hallmarks of PDAC

The aggressiveness of the disease can be summarized in a set of hallmarks for PDAC that explain and reveal the importance of PSCs in the PDAC TME [12, 47, 68], as PSCs can:

- Increase resistance to cell death by apoptosis in hypoxic regions
- Favor an immunosuppressive and inflammatory TME
- Induce a desmoplastic environment that shields the tumor and increases resistance to therapy
- Induce angiogenesis, favoring invasion and metastasis
- Provide an adaptive metabolic strategy when glucose is scarce
- Boost an excessive proliferative capacity and reciprocal stimulation due to the crosstalk between PCCs and PSCs

It is clear that the stromal PSCs significantly contribute to the hallmarks and act as the guardians of PDAC. They favor the rapid growth of PCCs, their survival in abnormal conditions, resistance to therapy, etc., by creating the ideal TME. This crosstalk between PSCs and PCCs is an important aspect to tackle and is key for the development of novel therapeutic approaches for PDAC.

2.1.5 Angiogenesis in PDAC: a unique feature

2.1.5.1 The tumor vasculature in PDAC: a hypovascular and abnormal network

One of the most distinctive features of PDAC is its paradoxical hypovascularity, despite the frequent expression of pro-angiogenic factors [69, 70]. Unlike many other solid tumors, PDAC lesions are poorly perfused, with a low microvessel density and irregular vascular architecture [71]. This abnormal vasculature is partially a consequence of the extensive desmoplastic stroma, which generates high interstitial pressure, physically compressing blood vessels and reducing perfusion [72]. These conditions promote hypoxia, which

paradoxically fails to induce efficient angiogenesis, in contrast to other cancers [73]. As a result, vessels that do form are sparse, poorly organized, leaky, and often non-functional. Ultrastructural and immunohistochemical studies have shown that PDAC vessels are irregular in shape, lack proper basement membranes, and exhibit incomplete endothelial coverage [74]. The resulting dysfunctional vasculature contributes to limited drug delivery, increased tumor hypoxia, and a more aggressive tumor phenotype. Furthermore, the surrounding stroma, rich in activated PSCs, fibroblasts, and ECM proteins, acts as both a physical and biochemical barrier to vessel formation and function [75]. This creates a unique TME in which pro- and anti-angiogenic cues are imbalanced or spatially dysregulated. In sum, PDAC vasculature is not simply insufficient in quantity but deeply altered in quality. Its structural and functional abnormalities play a central role in tumor progression, immune exclusion, and resistance to therapy.

2.1.5.2 Molecular drivers in PDAC angiogenesis

Angiogenesis in PDAC is shaped by an atypical set of molecular signals. Canonical pro-angiogenic factors like vascular endothelial growth factor A (VEGF-A), fibroblast growth factors (FGFs), and angiopoietins are expressed in PDAC but fail to trigger effective neovascularization due to the dense, hypoxic, and desmoplastic TME [76-79]. VEGF-A, upregulated via hypoxia-inducible factor 1-α (HIF-1α), is a central player, yet PDAC remains hypovascular [80]. This is partly due to stromal barriers, vessel compression, and disrupted VEGF receptor signaling [69, 77, 81]. Angiopoietin-2 (Ang-2) acts as a context-dependent modulator of angiogenesis, as in the presence of VEGF, it promotes vascular remodeling and sprouting, whereas in its absence, Ang-2 induces vessel regression and destabilization [82-84]. Other modulators like PDGF, TGF-β, and IL-6 drive both angiogenesis and fibrosis, often leading to aberrant or non-functional vessels [85-87]. IL-6/STAT3 signaling, for instance, promotes angiogenesis while fostering immune suppression and stroma activation [85]. Recent single-cell RNA-seq studies have revealed distinct endothelial subtypes and gene expression patterns in PDAC, suggesting a tumor-specific reprogramming of angiogenesis [88]. These findings underline that angiogenesis in PDAC is not merely suppressed but fundamentally altered.

2.1.5.3 The role of pancreatic stellate cells in angiogenesis

PSCs play a pivotal role in the desmoplastic TME of PDAC, and their influence on angiogenesis is both multifaceted and context-dependent. In their activated state, PSCs secrete a range of growth factors, including VEGF, FGF, PDGF, angiopoietin-1, hepatocyte growth factor, among others, all of which are capable of promoting EC proliferation, migration, and tube formation [58, 80, 89]. In vitro models such as aortic ring assays have demonstrated the capacity of activated PSCs to induce sprouting angiogenesis, suggesting that PSCs may actively support vascular development in certain regions of the TME [90, 91]. However, this pro-angiogenic capacity is counterbalanced by anti-angiogenic effects that PSCs exert through ECM production and paracrine signaling [24, 89]. The extensive deposition of fibrillar collagen and hyaluronan by PSCs contributes to elevated interstitial fluid pressure, compressing blood vessels and reducing perfusion [92]. Moreover, PSCs express inhibitors of angiogenesis such as vasohibin-1 and stimulate tumor cells to release endostatin, further impairing functional vessel formation [58]. This dichotomy gives rise to spatial heterogeneity within PDAC tumors, wherein peritumoral regions may exhibit relatively more vascularization while the tumor core remains hypovascular and poorly perfused. Such uneven vascular architecture impairs drug delivery, fosters treatment resistance, and perpetuates hypoxia-driven tumor progression. Importantly, the dynamic nature of PSCs suggests potential for therapeutic modulation. In summary, PSCs in PDAC serve as both architects and gatekeepers of angiogenesis, simultaneously enabling and restricting vascular development in a context-dependent manner.

2.1.5.4 Anti-angiogenic therapy in PDAC: why has it failed?

Despite the strong theoretical appeal of starving tumors by blocking their blood supply, anti-angiogenic therapies have consistently failed to deliver survival benefits in patients with PDAC (Figure 2.8) [93]. The rationale behind these therapies, primarily targeting VEGF, is based on the idea that inhibiting neovascularization will deprive tumors of oxygen and nutrients. While this approach has shown efficacy in several cancers, PDAC presents a unique and resistant biological landscape [76, 94]. Paradoxically, PDAC is a hypovascular tumor, despite often exhibiting elevated VEGF expression. This is largely due to its dense

desmoplastic stroma and the resulting elevated interstitial fluid and solid stress, which compress existing vessels and prevent the formation of functional new ones [81, 92]. In contrast to other tumor types where hypoxia stimulates angiogenesis, in PDAC the fibrotic and inflammatory TME imposes physical and molecular barriers that hinder both vessel sprouting and perfusion. Endothelial recruitment is impaired, basement membranes are disrupted, and pro-angiogenic signals are dysregulated or blocked by surrounding matrix and stromal cells, as explained before [94]. Consequently, inhibiting VEGF signaling in PDAC does not significantly reduce vascularization, as the vasculature is already sparse and dysfunctional, but may instead intensify hypoxia and promote tumor aggressiveness and therapy resistance [93]. These factors help explain why anti-angiogenic agents have failed to translate into clinical benefit in this cancer type. Clinical trials have reflected these challenges. For instance, the addition of bevacizumab, a monoclonal antibody against VEGF-A, to GEM did not yield significant improvements in overall survival for PDAC patients [95, 96]. Similarly, trials combining other anti-angiogenic agents with standard chemotherapy have not produced meaningful clinical benefits [97]. These outcomes suggest that anti-angiogenic therapies are insufficient in the context of PDAC's complex TME. Emerging strategies in cancer research propose combining anti-angiogenic agents with immunotherapies or other targeted treatments to overcome these limitations [98]. Such combinations aim to normalize or promote the tumor vasculature, enhance immune

cell infiltration, and improve drug delivery (Figure 2.8). However, these approaches are still new and under investigation, and their efficacy in PDAC has yet to be determined.

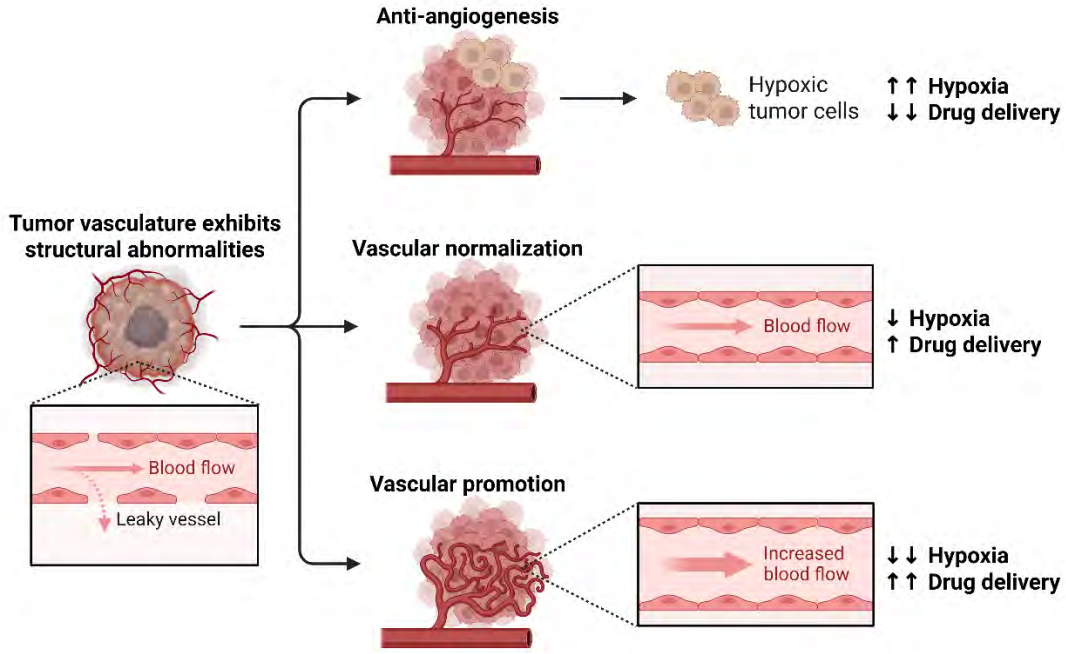

Figure 2.8. *Strategies targeting abnormal tumor vasculature and their effects on hypoxia and drug delivery. Tumor blood vessels are structurally abnormal in PDAC, leading to poor blood flow and leakiness. Anti-angiogenic therapies aim to reduce vessel formation but can worsen hypoxia and impair drug delivery. Vascular normalization aims to restore vessel structure, improving blood flow, reducing hypoxia, and enhancing drug delivery. Vascular promotion increases vessel density and blood flow, further decreasing hypoxia and possibly further enhancing drug delivery to the tumor. Image retrieved from BioRender.*

2.2 Plasma

2.2.1 What is CAP?

CAP is a partially ionized gas generated at atmospheric pressure and near room temperature, making it distinct from thermal plasmas that operate at high temperatures. CAP consists of electrons, ions, neutral molecules, UV photons, an electric field, radicals and excited species. When created in N_2/O_2 mixtures (or air), it produces a mixture of short- and long-lived RONS, such as hydrogen peroxide (H_2O_2), nitric oxide (·NO), superoxide ($O_2\cdot^-$) and peroxynitrite ($ONOO^-$) (Figure 2.9) [99]. These components interact synergistically with biological systems, enabling CAP to trigger a range of bio-responses without inducing thermal damage.

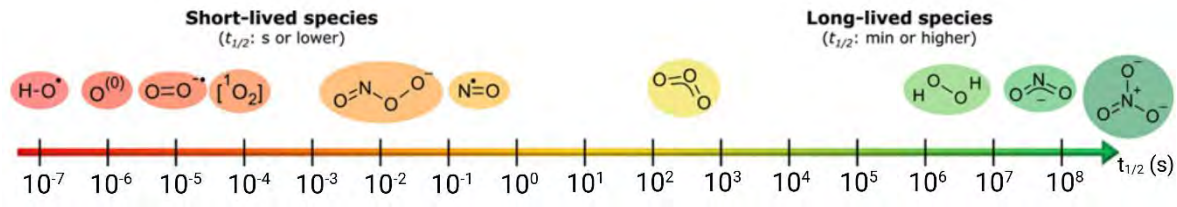

Figure 2.9. *Lifespans of RONS generated by CAP. Short-lived species, such as hydroxyl radicals (·OH), atomic oxygen (O), $O_2{\cdot}^-$, singlet oxygen ($^1O_2$), $ONOO^-$ and ·NO, have half-lives in seconds or less and act locally. Long-lived species, including H_2O_2, ozone (O_3), nitrite (NO_2^-), and nitrate (NO_3^-), persist for minutes or longer, enabling diffusion and extended biological effects. The half-life scale emphasizes the diverse reactivity and biological impact of different RONS in plasma medicine applications. Image retrieved from [100].*

In a controlled setting, plasma is created by applying a high electric field across two electrodes, accelerating electrons and initiating collisions that generate reactive species [101]. This process gives rise to a broad range of plasma types, which are typically classified into thermal and non-thermal plasmas [101, 102]. In thermal plasmas, all species are in equilibrium and the gas reaches temperatures exceeding (several) 1000 K. In contrast, non-thermal plasmas (NTP) transfer energy primarily to electrons which can reach average temperatures of ~10,000 K, while heavier species remain near room temperature (up to ca. 1000 K) [101]. This non-local thermodynamic equilibrium (non-LTE) allows NTP to treat heat-sensitive materials, including biological tissues [101, 102]. CAPs are non-LTE plasmas. These characteristics have driven increasing interest in biomedical uses of CAP, such as antimicrobial & antiviral applications, wound healing, and cancer therapy [99, 103-107].

2.2.2 Plasma devices

The biological effectiveness of CAP is determined not only by its reactive species, but also by device configuration and environmental conditions. In plasma medicine, two types of plasma devices are most commonly used: floating electrode dielectric barrier discharge (FE-DBD) and plasma jets, each with unique properties and applications [102, 108] (Figure 2.10).

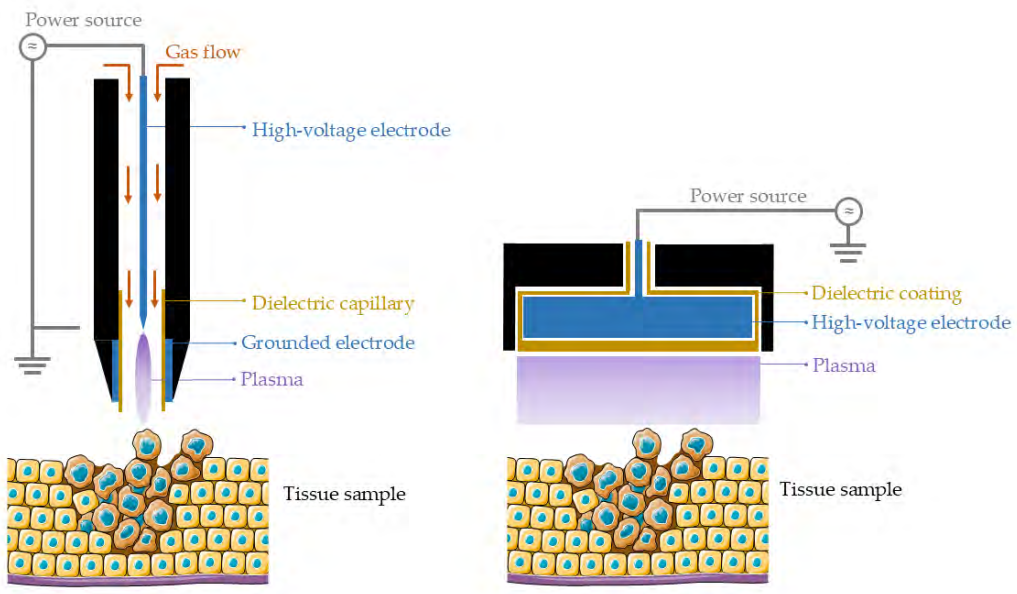

Figure 2.10. *Schematic representation of CAP device configurations for biomedical applications. (a) Plasma jet design, where gas flows through a system comprising a high-voltage electrode, dielectric coating, and grounded ring electrode, generating CAP directed toward the tissue surface. (b) FE-DBD setup, in which CAP is generated between a dielectric-coated high-voltage electrode and the tissue surface (acting as grounded electrode), allowing direct CAP exposure.*

2.2.2.1 Floating Electrode Dielectric barrier discharge

FE-DBD devices create CAP by applying high-voltage alternating current across two "electrodes" (one real electrode, built-in to the device, the other being the grounded tissue sample), separated by one or more dielectric barriers, typically made of quartz, glass, or ceramic (Figure 2.10b). The barrier prevents arc formation, producing a series of microdischarges within the gas-filled gap. These non-thermal discharges result in a (more or less) homogeneous CAP suitable for treating broad, flat surfaces [109]. FE-DBD systems are often used in dermatology, dentistry, wound care, and surface decontamination. Their planar configuration allows for even distribution of reactive species but also limits their use in applications requiring deep tissue access or treatment of irregular geometries [110]. A prominent example of a FE-DBD system used clinically is the PlasmaDerm® VU-2010 applied for chronic wound disinfection and skin regeneration studies [111].

2.2.2.2 Plasma jet

Plasma jets, also known as atmospheric pressure plasma jets (APPJs), generate a focused plume of partially ionized gas (created by the applied electrical field inside the device) by accelerating a carrier gas, typically helium or argon, through a narrow nozzle (Figure 2.10a) [112]. These jets produce a CAP that can be precisely directed at specific targets, including small or internal treatment areas, without causing thermal damage to surrounding tissues [113]. One of the most well-characterized and widely used plasma jet devices in biomedical research is the kINPen MED, a CE-certified device that is clinically approved for wound healing, typically operating with argon [107, 114]. It has been extensively used in cancer research as well, including pancreatic, skin, head-and-neck cancer models, among others [54, 115-125]. The kINPen generates a stable CAP plume rich in RONS, such as H_2O_2, NO_2^-, and $ONOO^-$, with secondary species, generated by contact with the treated sample, varying depending on the treatment medium [107, 114, 126]. Another notable plasma jet is the COST-Jet [127]. Plasma jets are particularly advantageous in biomedical contexts requiring localized treatment, such as treatment of irregular surfaces, endoscopic applications, targeted bacterial decontamination, and selective tumor eradication, due to their thin shape, precision and low temperature [99, 107, 128-134].

2.2.3 CAP for medicine: important reactive species and their effects on cells

2.2.3.1 Mechanism of action at the molecular level

CAP induces a variety of biological effects primarily through the generation of RONS, such as H_2O_2, ·NO, $O_2\cdot^-$, ·OH, and $ONOO^-$ [102, 135, 136]. These species interact with cellular membranes, DNA, proteins, and lipids, resulting in oxidative and nitrosative stress that can lead to apoptosis, autophagy, or immunogenic cell death depending on the cell type and exposure conditions [116, 135-140].

On the molecular level, one of the earliest events following CAP exposure is lipid peroxidation, particularly of the phospholipid bilayer, which compromises membrane integrity and increases permeability [102, 135, 136]. This facilitates the influx of RONS and calcium ions, promoting mitochondrial dysfunction and caspase activation [135-137]. CAP-

generated H_2O_2 and ·NO can also diffuse into the cytoplasm and nucleus, where they induce DNA strand breaks and activate p53 and other DNA damage response pathways, further reinforcing apoptotic signaling [102, 136].

Importantly, CAP has been shown to modulate key molecular signaling cascades, including downregulation of pro-survival pathways such as PI3K/AKT and upregulation of stress-responsive elements like MAPK and NF-κB, depending on the context [136, 141, 142]. The cellular response is highly dependent on the balance between intracellular antioxidants (e.g., glutathione, catalase) and the oxidative burden imposed by CAP treatment [136]. The observed molecular changes ultimately converge to activate regulated cell death pathways in cancer cells, with minimal effects on non-malignant cells when dosed appropriately, a feature that underpins the therapeutic potential of CAP [137, 143-145].

2.2.3.2 CAP interaction with the tumor microenvironment

The TME plays a critical role in cancer progression, immune evasion, and resistance to therapy. CAP has emerged as a promising modality capable of modulating multiple components of the TME, including stromal cells, ECM, vasculature, and immune cells [24, 102, 136]. One of the primary effects of CAP in the TME is the induction of oxidative stress, which could affect stromal cells such as CAFs and ECs [146]. In vitro studies have shown that CAP treatment reduces the viability and pro-tumorigenic activity of CAFs using the kINPen IND or a Helium DBD-jet, potentially weakening the stromal support system for tumors [54, 147]. Similarly, ECs exposed directly to CAP using the kINPen (15s) or MiniJet (30s) show impaired tube formation and decreased cell viability and proliferation, suggesting a suppressive effect on tumor vascularization [148]. However, in other studies CAP showed an enhancing effect on ECs, e.g., enhanced migration and tube formation in vitro, and increased angiogenesis in vivo using a 3D printed plasma jet from polylactic polymer (60s per mL), or increased mRNA expression of pro-angiogenic genes and tube formation using the Adtec SteriPlas (30s) [149-151]. These differential results highlight the duality of CAP treatment based on device, exposure time, etc. CAP also interacts with the ECM by oxidizing matrix proteins and degrading structural components, such as hyaluronan, collagen and fibronectin, which can reduce the physical barriers that prevent

immune infiltration and drug delivery [152-154]. Furthermore, CAP has been reported to modulate the immune TME by inducing immunogenic cell death (ICD) in tumor cells [116, 118, 138-140, 155, 156]. This process involves the release of danger-associated molecular patterns (DAMPs) such as calreticulin, adenosine triphosphate (ATP), and high mobility group box 1 HMGB1, which act as signals to recruit and activate dendritic cells and cytotoxic T lymphocytes [116, 118, 138-140, 155, 156]. In this way, CAP may help shift the TME from immunosuppressive to immunostimulatory, thereby enhancing the efficacy of immune-based therapies. Overall, CAP exerts multifaceted effects on the TME, disrupting tumor-supportive elements, while promoting immune surveillance and therapeutic accessibility.

2.2.4 Is there a selectivity of CAP towards cancer cells?

Research suggested that cancer cells are more sensitive towards CAP treatment than normal cells, providing a selective effect [157-162]. The probable underlying reason is the increased concentration of RONS present inside cancer cells compared to normal cells (Figure 2.11) [103, 136, 163]. Another factor could be their higher vulnerability to DNA damage due to an abnormal dividing capacity [164]. The high expression of aquaporins [165-167] and a lower level of cholesterol in the membrane in cancer cells [168, 169] could also increase the transport of RONS into the cytoplasm, damaging cancer cells more than their healthy counterpart. However, the above observations on selectivity must be evaluated critically. Recent research has provided evidence on the importance of the treatment conditions, such as the difference between the cell culture media used for different cell lines and the cell type of healthy and cancerous cells, and it is recommended that the same treatment conditions are applied to compare the effect on both cancer and normal cells [170]. During in vivo treatment, cancerous and normal cells are treated simultaneously and without difference in tissue environment (cf. culture medium). Given these considerations, resembling the TME as closely as possible during in vitro experiments may improve the ability to predict treatment responses in vivo and help reduce the risk of future CAP treatment failures in patients.

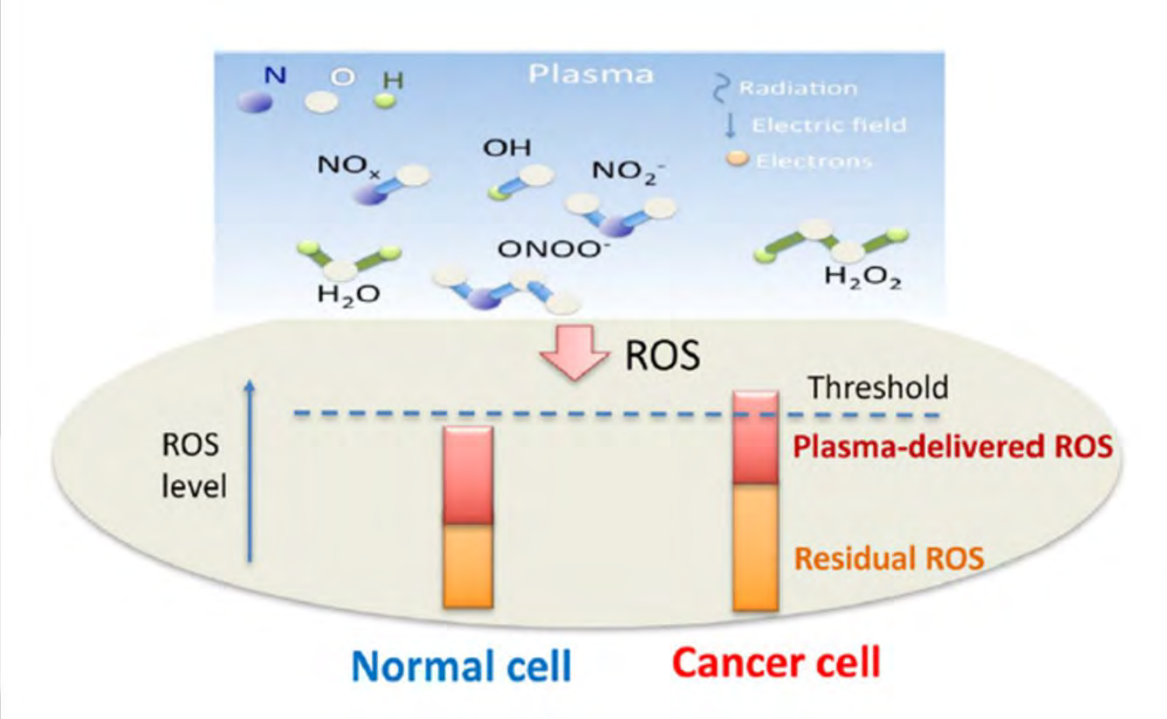

Figure 2.11. *Selective cytotoxicity mechanism of CAP via RONS. CAP generates various reactive species, including ·OH, ·NO, $ONOO^-$, NO_2^-, and H_2O_2, through radiation, electric fields, and electron interactions. Cancer cells typically have elevated baseline (residual) RONS levels, positioning them closer to a critical oxidative threshold. CAP-derived RONS further elevate intracellular RONS levels, pushing cancer cells above this threshold and inducing cell death. In contrast, normal cells remain below the cytotoxic ROS threshold, preserving viability and enabling CAP's selective anti-cancer effects [143].*

2.2.5 Delivery methods and clinical application of CAP

The clinical application of CAP depends not only on the type of CAP device but also on how the CAP is delivered to the target. CAP can be applied either directly or indirectly, with each approach offering distinct advantages depending on the biological context, tissue accessibility, and therapeutic goal (Figure 2.12). While direct treatment involves the application of the CAP plume to the tissue, indirect methods use CAP-treated phosphate-buffered saline (PBS), media, hydrogels or other liquids and materials that could retain the biological activity of CAP-generated species. This section outlines both approaches and highlights their relevance in current and emerging clinical practices.

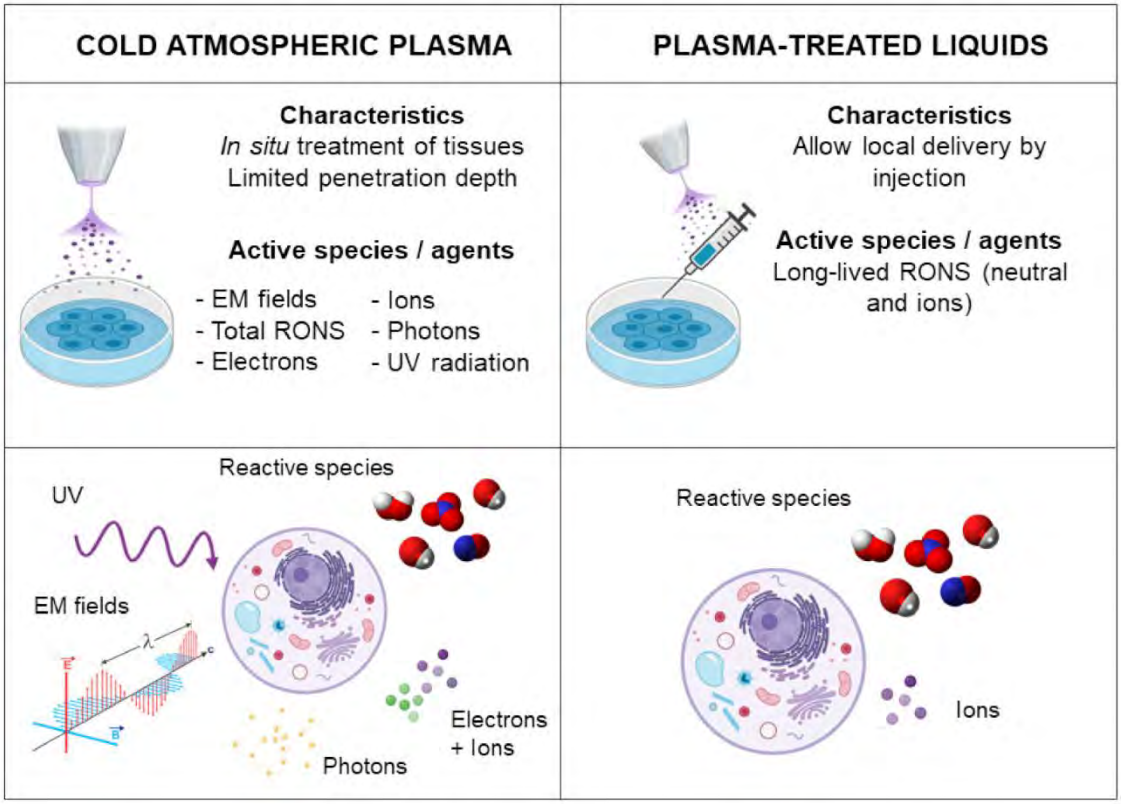

Figure 2.12. *Comparison of direct and indirect CAP treatments. Direct CAP treatment involves CAP exposure of tissues, characterized by limited penetration depth and delivery of electromagnetic fields, RONS, electrons, ions, photons, and ultraviolet radiation (depending on whether a DBD or plasma jet is used, not all of these effects would be included). Indirect CAP treatment employs plasma-treated liquids (or hydrogels), enabling localized delivery via injection or localized application, primarily carrying long-lived reactive species (neutral molecules and ions). Each method offers distinct advantages for biomedical applications depending on therapeutic goals, tissue accessibility, and biological context. Image retrieved from [171].*

2.2.5.1 Indirect CAP treatment

With indirect CAP treatment, tissues or cells are not exposed to the CAP itself but to its reactive components, typically through a plasma-treated liquid (PTL) such as phosphate-buffered saline (PBS), water, cell culture medium or hydrogels (Figure 2.12 right). During CAP exposure, these liquids absorb long-lived RONS (e.g., H_2O_2, NO_2^-, NO_3^-), forming a biologically active solution that can retain therapeutic effects even after CAP exposure has ended [172]. This method offers several advantages: It avoids thermal and electrical interaction with tissue, making it ideal for sensitive areas (e.g., ocular surface, mucosa). It enables storage and transport of long-lived RONS and their CAP effects, allowing treatment outside the CAP generation setting [173]. It offers a practical treatment option across

irregular surfaces or internal cavities [174]. PTLs have demonstrated promising results in oncology, where they induce apoptosis and inhibit proliferation in various cancer cell types, however not as effective as direct treatment [174-178]. Moreover, the chemical stability and reproducibility of PTLs can be influenced by factors such as liquid composition, treatment time, gas type, and storage conditions [174, 176-178]. Optimization of these parameters is currently an active area of research to standardize protocols for clinical translation, especially in the use of hydrogels [140, 177, 179, 180].

Indirect CAP treatment represents a highly adaptable and non-invasive strategy with broad potential for topical application, targeted delivery through injection, or irrigation of cancer-affected tissues in clinical settings. However, it is noteworthy that no short-lived species are included in indirect treatment resulting in a weaker effect compared to direct treatment [178]. In addition, PTL is not suitable for intravenous injection, as it is known that blood quenches RONS, limiting their effect before reaching the tumor site and [181]. Finally, liquids are hard to control and retain to a local site of treatment as it might leak and flow to other spaces and through cavities. In addition, it is known that a “mock” solution, in which the individual components of PTLs are mixed and the pH is adjusted, results in the same biological effects [100]. Hydrogels solve this issue partially as they are more controlled and retained to their position [177, 179, 180].

2.2.5.2 Direct CAP treatment

In direct CAP treatment, the reactive CAP is applied directly to the target tissue (Figure 2.12 left). This approach enables the immediate delivery of both short-lived and long-lived reactive species, along with electric fields, UV radiation, and charged particles (depending on a DBD or plasma jet), allowing for multifactorial interaction with cells and tissues in real time and therefore larger effects [178].

The key advantage of direct CAP treatment lies in the comprehensive and synergistic effects of these CAP components. Short-lived species such as ·OH, $^1O_2$, and atomic nitrogen (N), which are not retained in PTLs, play a crucial role in the oxidative burst and localized stress response of directly exposed cells. These species can modulate membrane potential,

induce oxidative damage, and activate apoptotic or necrotic cell death pathways, particularly in cancer cells which are more susceptible to oxidative imbalance [136, 178, 182, 183]. A limitation of direct CAP treatment is the limited penetration depth of tissues [171].

Direct CAP treatment has shown promising results in preclinical models of skin, head-and-neck, breast, and pancreatic cancer, where it induces cell death, inhibiting or stimulating angiogenesis, and alters the TME by affecting stromal and immune cell signaling [54, 116, 118, 139, 148, 149, 156, 178, 184]. Moreover, it can be precisely applied using plasma jets, making it suitable for small tumor nodules, superficial surgical cavities and lesions, including intraoperative settings in a controlled and localized manner.

2.2.5.3 Clinical applications

CAP has demonstrated substantial clinical relevance in different types of biomedical applications. One of these is wound healing, where CAP can effectively promote wound closure, reduce bacterial load, and stimulate tissue regeneration by modulating inflammation, enhancing angiogenesis, and accelerating cell proliferation and migration [107, 184-186]. This makes CAP a successful treatment for chronic wounds, diabetic ulcers, and burn injuries.

The use of CAP for sterilization and disinfection is another important field, particularly in hospital and clinical environments. CAP efficiently eliminates pathogens on medical instruments, surfaces, and even biological tissues, thus reducing infection risks [187, 188]. In dentistry, CAP has demonstrated efficacy in oral biofilm removal, tooth bleaching, treatment of periodontal diseases, and improvement of implant surface sterilization, thus significantly contributing to oral healthcare [106, 189-191].

The most recent addition to clinical applications of CAP lies in oncology. CAP has demonstrated significant potential through its RONS-mediated cytotoxicity towards cancer cells, with a less substantial effect on normal cells and the possibility to be combined with current first-line therapies [54, 119, 140, 144, 156, 157, 175, 178, 192-194]. Direct treatment could be used for easily accessible tumors, such as, head and neck cancer and

melanoma, or in combination with surgery which allows for superficial treatment of the surgical bed. Indirect treatment, and especially hydrogels that allow for a controlled release of RONS, could be interesting for tumors that are more difficult to reach, such as osteosarcoma [140, 177, 179, 180].

CAP offers many clinical advantages, such as the ability to treat locally, minimizing side effects on healthy tissue. In addition, it allows treating irregular surfaces like wounds, oral cavities, and surgical beds and to be integrated into an endoscopic/laparoscopic device for internal tumor sites [195, 196].

Recent years have seen growing interest in translating CAP into oncology, including for the treatment of PDAC. Although clinical research in PDAC remains limited, the first clinical data have emerged, offering a potential path toward clinical application.

The most significant step forward in CAP research for PDAC has been the first FDA-approved Phase I clinical trial using the Canady Helios Cold Plasma (CHCP) system as an intra-operative adjunct therapy for patients with advanced solid tumors, including pancreatic cancer [197]. In this multicenter trial (NCT04267575), twenty patients with stage IV or recurrent solid tumors underwent surgical resection followed by intra-operative CHCP treatment applied directly to surgical margins. Among these was one case of pancreatic cancer, where CAP was administered intra-operatively after a Whipple procedure. The trial primarily assessed safety and reported no intraoperative physiological disturbances or significant CAP-related adverse events, underscoring its tolerability. Histological analysis confirmed tumor cell death in ex vivo treated tissue, and molecular markers indicated apoptosis and reduced cancer stem cell signatures. Notably, local regional recurrence rates were lower in patients achieving an R0 or R0-MPM resection combined with CAP treatment, suggesting a potential role for CAP in improving local control in pancreatic cancer surgery. Although the patient cohort was small and heterogeneous, this trial provides the first clinical evidence supporting the safety and feasibility of intra-operative CAP in PDAC.

In addition to this first step in PDAC, clinical experience with CAP has been acquired in other solid tumors, particularly head and neck cancers. In one study, CAP applied via the kINPen MED plasma jet in patients with advanced squamous cell carcinoma of the head and neck induced visible tumor surface changes and increased apoptotic tumor cell death in resected tissues, with no evidence of enhanced tumor growth and no severe adverse effects [198]. Another clinical report described partial tumor remission lasting at least nine months in two of six patients with locally advanced oropharyngeal cancer treated with CAP, accompanied by reduced pain, odor, and improved social function, though responses were not universally sustained [115].

Collectively, these clinical experiences establish a foundation for exploring CAP as a novel adjuvant therapy in oncological surgery, including for PDAC. While further studies are needed to define its precise role and optimize delivery modalities, the initial clinical evidence suggests CAP can be safely integrated into surgical workflows and may contribute to reducing local recurrence by eradicating microscopic residual disease in pancreatic cancer.

2.3 CAP treatment for PDAC

In order to perform clinical trials, we require pre-clinical in vitro and in vivo data to support the added value of CAP treatment on first-line therapies. In this section, I discuss all the current research on CAP treatment of PDAC and cells of the TME to the best of our knowledge. Studies that only included PCCs will be described first, followed by the limited number of reports that also investigated PSCs. It is due to this limited number of publications including PSCs in their research that I want to emphasize the importance of these cells in the response to treatment for future CAP research. These studies are summarized in Table 2.2.

***Table 2.2**. Overview of the state-of-the-art on CAP treatment of PDAC.*

PDAC Cell Lines	PSC Cell Lines	Observed Effects	Plasma Device	Treatment	Model	Ref.
Murine 6606PDA		Increased cell death & slight surface temperature	kINPen09	Direct	In vitro	[199]
Murine 6606PDA		Decreased metabolic activity & cell proliferation Increased apoptosis	kINPen MED	Indirect Direct	In vitro In vivo	[200]
Murine 6606PDA		Decreased metabolic activity Increased cell death & apoptosis	kINPen MED	Direct	In vitro In ovo	[201]
MiaPaCa-2		Reduced tumor growth after GEM and CAP combination treatment	Plasma gun	Direct	In vitro In vivo	[202]
MiaPaCa-2 PANC-1		Decreased metabolic activity & cell viability Unchanged metastatic potential	kINPen	Direct	In vitro In ovo	[203]
BxPC-3 MiaPaCa-2 Capan-2 PANC-1		Increased apoptosis & cell death Selectivity toward cancer cells	Plasma jet	Indirect	In vitro In vivo	[204]
PANC-1		Decreased cell viability Increased apoptosis	PetriPlas	Indirect	In vitro	[139]
BxPC-3		Decreased metabolic activity	Plasma jet	Indirect	In vitro	[205]
Murine PDA6606		Decreased cell viability & migration & apoptosis Reduced tumor growth in ovo Altering cytokine expression	kINPen	Direct	In vitro In ovo	[206]
BxPC-3 MiaPaCa-2 Capan-2 PANC-1	hPSC128 hPSC21 RLT-PSC	Increased cell death Increased ICD markers Increased phagocytosis by dendritic cells (DCs) Maturation of DCs	kINPen IND	Indirect	In vitro	[116]
MiaPaCa-2 BxPC-3	hPSC128	Decreased cell viability Increased apoptosis Increased intracellular RONS levels Decreased expression of tumor biomarkers	kINPen IND	Indirect	In vitro	[207]
MiaPaCa-2 PANC-1	RLT-PSC	Increased apoptosis Unchanged EMT or metastasis	kINPen	Direct	In vitro In ovo	[208]
MiaPaCa-2	RLT-PSC	Increased cell death Decreased proliferation Unchanged PSC activation & ECM remodelling	kINPen IND	Direct	In ovo	[54]

2.3.1 CAP treatment of PDAC cells

Multiple efforts have been made to determine the mechanisms of action and efficacy of CAP on PDAC cells. One of the first studies on CAP treatment for PDAC investigated the effect of CAP using the kINPen09 on the surface temperature of cell culture dishes to evaluate the safety of CAP treatment and cell death of in vitro murine PDAC 6606PDA cells [199]. Results revealed an increase in surface temperature of only approximately 2–3 °C after 5–20 seconds and a significant increase in cell death after CAP treatment compared to untreated controls.

Liedtke et al. investigated the murine PDAC cell line 6606PDA with the kINPen MED [200, 201]. In vitro, cell metabolic activity and cell proliferation both decreased after CAP treatment, with a larger effect for 6606PDA cells compared to fibroblasts. No difference between indirect and direct treatment was seen. N-acetylcysteine is a known RONS-scavenging anti-oxidant that showed reversal of the CAP-mediated cytotoxicity. In vivo, cell apoptosis was significantly increased after indirect CAP treatment compared to controls. Apoptosis was also observed in deeper parts of the tumor, implicating penetration of the medium. No side effects were observed from these CAP treatments on mice.

Brullé et al. used a plasma jet to investigate the combinatorial effect of CAP treatment and GEM on tumor growth by tumor volume, weight and bioluminescence [202]. Both GEM and CAP treatment caused significant tumor growth reduction, but CAP treatment produced a larger anti-tumor effect. The combination of CAP and GEM enhanced the anti-tumor effect by 33% compared to only CAP treatment.

Bekeschus and Freund et al. have demonstrated that direct CAP treatment with a plasma jet significantly decreased the metabolic activity of MiaPaCa-2 and PANC-1 in two-dimensional (2D) cultures in vitro, which correlated with a reduced cell viability [203]. PANC-1 showed higher resilience against CAP treatment (−6% metabolic activity) compared to MiaPaCa-2 (−38% metabolic activity). In addition, the authors performed similar assays using the in ovo model. Both cell lines showed a reduction in the metabolic activity in tissues collected from this experimental model, but PANC-1 showed a higher sensitivity to

CAP treatment. Further experiments in 3D spheroids in vitro suggest that CAP does not have a stimulating effect on the metastatic potential of PDAC cells.

Another study investigated the effect of indirect CAP treatment with a plasma jet on apoptosis and cell viability of the human PDAC cell lines BxPC-3, MiaPaCa-2, Capan-2, and PANC-1 [204]. CAP treatment of 1 min on the culture medium resulted in differences in sensitivity between cell lines. Capan-2 showed higher cell death than other cell lines for all three different seeding densities and PANC-1 did only show significant cell death for the lowest seeding density, which is unlike other cell lines. The higher resilience of PANC-1 to CAP treatment compared to MiaPaCa-2 was also seen in this study, but only to a minor extent compared to the previously mentioned study of Bekeschus and Freund et al [203]. Changing treatment time to 3 or 5 min resulted in effective cell death for all cell lines with a slightly higher cytotoxic effect after 5 min of treatment [204]. Interestingly, 5 min of CAP treatment showed highest cell death for the highest seeding density in all cell lines, which was not observed for the other treatment times. Comparison of the cell viability between Capan-2 PCCs and human pancreatic epithelial non-cancer cells (HDPE6/C7) showed a higher selectivity to CAP treatment for the cancer cells. Besides these findings, apoptosis was suggested to be induced due to the observation of caspase-3/7 activation and typical morphological changes. The anti-tumor effect of CAP treatment was validated in mice by a reduction in tumor volume of 64% compared to the control group.

Azzariti et al. investigated the effect of DBD CAP-treated medium on PANC-1 cells, assessing cell viability and cell death [139]. CAP treatment significantly reduced cell viability and increased apoptosis in PANC-1 cells, however, autophagy was not observed. Based on the exposure of calreticulin and release of adenosine triphosphate, it was suggested that CAP induced ICD, a process that activates the immune system to promote cell death in cancer cells and evoke a long-lasting protective antitumor immunity [209].

Chen et al. investigated the effects of CAP-treated saline solution with a plasma jet on the survival of BxPC-3 and H6c7 cells [205]. A cell viability assay based on relative metabolic activity compared to untreated controls has shown a higher sensitivity of BxPC-3 cells to indirect CAP treatment.

Khabipov et al. investigated how CAP treatment affects PCCs and the subsequent inflammatory response of murine macrophages [206]. Using the kINPen plasma jet, they showed that CAP treatment reduced viability and migration of PDA6606 PDAC cells in vitro and significantly decreased tumor growth and induced apoptosis in tumors grown on the CAM of chicken embryos. Importantly, co-culture experiments revealed that plasma-treated cancer cells modulated macrophage polarization, reducing M2-type cluster formation and altering cytokine profiles with decreased levels of tumor-promoting factors like TGF-β and VEGF, while increasing certain pro-inflammatory signals. Overall, plasma-inactivated PCCs influenced macrophages toward a mixed M1/M2 phenotype, suggesting a potentially favorable shift in the TME for pancreatic cancer therapy.

2.3.2 CAP effect on pancreatic stellate cells

Although PSCs play a key role in the treatment outcome of PDAC, to date only four studies, of which three are from our group, have addressed the effect of CAP on these cells [54, 116, 207, 208].

We investigated the potential of CAP treatment to induce ICD with CAP-treated PBS using a plasma jet [116]. Four PCC lines (MiaPaCa-2, PANC-1, BxPC3 and Capan-2) and three PSC lines (hPSC128, hPSC21, and RLT-PSC) were included. MiaPaCa-2 showed the highest percentage of cell death, followed by Capan-2, whereas BxPC-3 and PANC-1 showed the highest resistance to CAP-treated PBS treatment. PSCs showed a lower sensitivity to CAP-treated PBS treatment than PCCs, highlighting a selectivity effect of CAP treatment toward the preservation of PSCs. Different ICD markers (CRT, ATP, HMGB1) were investigated and suggested that indeed ICD is induced in the PCCs, and not in PSCs.

In the second study, indirect CAP treatment with a plasma jet was used for MiaPaCa-2 and BxPC3 PCCs and the PSC cell line hPSC128-SV with CAP-treated medium and CAP-treated water [207]. Cell viability (determined by MTT assay) was hardly reduced after CAP treatment on all three cell lines. Observed cell death was mostly due to apoptosis and necrosis (determined by Annexin V/PI staining). Intracellular RONS levels were dramatically increased in all cell lines upon treatment with PTL. Downregulated expression of tumor

biomarkers indicated a restoration of the apoptotic pathway (MPK7 and BCL2) and induction of double-stranded DNA breaks and chromosomal fragmentation (CHEK1) and can be correlated to the increase in cell death.

To date, there are only two studies on the effect of CAP on co-cultures of PDAC and PSC cells [54, 208]. In the third study from our group [54], we investigated the effect of CAP treatment on the tumor reduction and the activation of PSCs and the ECM remodeling in mono- and co-cultures. Based on protein expression of selected markers shown by immunohistochemistry and mRNA expression, no activation of PSCs (αSMA, vimentin and GFAP) or ECM remodeling (MMP1 and TIMP2) due to the PSCs upon CAP treatment was observed. In addition, CAP was able to shrink MiaPaCa-2 and MiaPaCa-2:RLT-PSC tumors, with a less pronounced effect in the latter. This reveals the potential of CAP to effectively eliminate tumors without causing activation of PSCs and the importance of including co-cultures to study therapy responses.

Finally, Freund et al. investigated whether CAP treatment with the kINPen plasma jet might promote EMT or inflammation in metastatic PDAC cells [208]. They examined cell viability, apoptosis, metastasis and cytokine expression in two PDAC cell lines in tumor spheroids co-cultured with PSCs, and in mono-culture tumors grown on chicken embryos. CAP treatment induced apoptosis in tumors but did not significantly change adhesion molecules, EMT marker expression, or promote tumor cell detachment and outgrowth. Cytokine responses varied among cell lines, but no consistent pro-metastatic or pro-inflammatory shift was observed. Overall, CAP treatment did not induce EMT or metastasis-related changes, suggesting its safety as a cancer therapy for pancreatic cancer.

Clearly, the lack of knowledge on the effect of CAP treatment on clinically relevant co-culture 3D models could give unforeseen drawbacks when moving onto in vivo experiments or clinical trials. Therefore, it is important to include PSCs in the experimental approaches of future studies.

2.3.3 CAP treatment of endothelial cells

ECs are the most important cell type when investigating angiogenesis. CAP has demonstrated both pro- and anti-angiogenic effects on ECs, depending strongly on device type, treatment parameters, and experimental conditions.

At low intensities, CAP can promote angiogenesis, with RONS such as ·NO, H_2O_2, $O_2{\cdot}^-$ and ·OH playing central roles in activating angiogenic pathways. These species induce controlled oxidative stress, or oxidative eustress, which stimulates cell proliferation pathways [184, 210, 211]. ECs respond to CAP by expressing pro-angiogenic factors like FGF-2 and Ang-2, fostering EC proliferation and migration, e.g., by using the MicroPlaSter β plasma torch system (Microwave 2.45 GHz, 80 W, argon flow 4.0 l/min, treatment diameter ∼5 cm) [150, 184, 211]. Paracrine signaling between fibroblasts and ECs further enhances this activation [150]. Additionally, RONS can disrupt EC membranes, triggering the release of more FGF-2 and stimulating neighboring EC proliferation [184]. For example, one study using a DBD device (1.5 kHz, 20 kV peak-to-peak) showed that CAP enhanced EC proliferation, migration, and tube formation via ROS-induced FGF-2 release [184]. Similarly, supernatants from CAP-treated fibroblasts have been shown to promote angiogenesis [150].

However, CAP's effects on ECs can also be inhibitory. Direct CAP exposure (15 sec) using the kINPen®MED reduced cell growth, metabolism, tube formation, and 2D migration in human dermal microvascular ECs [148].

These contrasting findings underscore CAP's dual-edged nature: its impact on cells varies considerably based on device configuration, feed gas composition, treatment duration, and TME context. Importantly, the type and quantity of RONS produced by CAP are highly dependent on these parameters, leading to diverse biological outcomes [126]. Overall, while CAP holds promise for modulating EC behavior and angiogenesis, achieving a consistent pro-angiogenic response requires careful optimization of CAP parameters to balance oxidative eustress without tipping into detrimental oxidative distress.

2.3.4 Towards clinical relevance: integrating 3D co-culture models into CAP research for PDAC

A crucial limitation in cancer research, particularly for PDAC, is the reliance on traditional 2D cell culture systems, which fail to replicate the intricate architecture and cellular interactions of the TME. The TME in PDAC is uniquely complex, characterized by dense stromal components, abundant ECM, hypoxia, and a dynamic interplay between PCCs, PSCs, ECs, immune cells, and other stromal elements. These interactions govern critical processes, such as angiogenesis, immune evasion, drug resistance, and metastatic spread. 3D co-culture models, including spheroids, organoids, and tissue-engineered constructs offer a more physiologically relevant platform by mimicking cell–cell and cell–matrix interactions, nutrient and oxygen gradients, and the mechanical properties of the tissue [212-216]. In PDAC, 3D co-culture systems enable researchers to investigate tumor biology in a context that more accurately mirrors in vivo conditions, improving the predictive power of preclinical studies for therapeutic efficacy and safety. They are especially valuable for evaluating how stromal elements like PSCs and the extracellular matrix contribute to the notorious chemoresistance and aggressive behavior of PDAC.

Despite the promise of CAP as a novel anti-cancer modality, the research conducted thus far on CAP treatment in PDAC has been predominantly confined to 2D monoculture systems, without incorporating the complexity of the TME properly. The summarized studies show encouraging results, including cytotoxicity against cancer cells, modulation of immune responses, and potential anti-tumor effects on cells in the TME. However, the absence of comprehensive 3D co-culture models limits the understanding of how CAP influences the interactions between PCCs and crucial stromal components like PSCs and ECs, which can significantly modulate treatment outcomes. For instance, PSCs can shield cancer cells from therapeutic effects or, conversely, be targeted to disrupt tumor-supportive stroma. Likewise, ECs can respond variably to CAP, leading to either pro- or anti-angiogenic effects depending on treatment parameters. Without 3D co-culture models that integrate these elements, it remains uncertain whether the in vitro cytotoxic effects of CAP will translate into effective and safe treatments in patients. Therefore, incorporating 3D co-

culture systems into CAP research for PDAC is essential to accurately predict therapeutic efficacy, understand potential side effects, and guide the development of optimized CAP-based treatment strategies.

2.4 References

2. Bray, F., M. Laversanne, H. Sung, J. Ferlay, R.L. Siegel, I. Soerjomataram, et al., *Global cancer statistics 2022: GLOBOCAN estimates of incidence and mortality worldwide for 36 cancers in 185 countries.* CA Cancer J Clin, 2024. **74**(3): p. 229-263.
3. vzw, K.o.t.K. *Hoe vaak komt kanker voor?*
4. Vogelstein, B. and K.W. Kinzler, *Cancer genes and the pathways they control.* Nat Med, 2004. **10**(8): p. 789-99.
5. Hanahan, D. and R.A. Weinberg, *The hallmarks of cancer.* Cell, 2000. **100**(1): p. 57-70.
6. Hanahan, D. and R.A. Weinberg, *Hallmarks of cancer: the next generation.* Cell, 2011. **144**(5): p. 646-74.
7. Hanahan, D., *Hallmarks of Cancer: New Dimensions.* Cancer Discov, 2022. **12**(1): p. 31-46.
8. Leight, J.L., A.P. Drain, and V.M. Weaver, *Extracellular Matrix Remodeling and Stiffening Modulate Tumor Phenotype and Treatment Response.* Annual Review of Cancer Biology, 2017. **1**(1): p. 313-334.
9. Goenka, A., F. Khan, B. Verma, P. Sinha, C.C. Dmello, M.P. Jogalekar, et al., *Tumor microenvironment signaling and therapeutics in cancer progression.* Cancer Commun (Lond), 2023. **43**(5): p. 525-561.
10. de Visser, K.E. and J.A. Joyce, *The evolving tumor microenvironment: From cancer initiation to metastatic outgrowth.* Cancer Cell, 2023. **41**(3): p. 374-403.
11. Perez, V.M., J.F. Kearney, and J.J. Yeh, *The PDAC Extracellular Matrix: A Review of the ECM Protein Composition, Tumor Cell Interaction, and Therapeutic Strategies.* Front Oncol, 2021. **11**: p. 751311.
12. Orth, M., P. Metzger, S. Gerum, J. Mayerle, G. Schneider, C. Belka, et al., *Pancreatic ductal adenocarcinoma: biological hallmarks, current status, and future perspectives of combined modality treatment approaches.* Radiat Oncol, 2019. **14**(1): p. 141.
13. Mekapogu, A.R., S.P. Pothula, R.C. Pirola, J.S. Wilson, and M.V. Apte, *Multifunctional role of pancreatic stellate cells in pancreatic cancer.* Annals of Pancreatic Cancer, 2019. **2**.
14. Wang, L., D. Xie, and D. Wei, *Pancreatic Acinar-to-Ductal Metaplasia and Pancreatic Cancer.* Methods Mol Biol, 2019. **1882**: p. 299-308.
15. Nusrat, F., A. Khanna, A. Jain, W. Jiang, H. Lavu, C.J. Yeo, et al., *The Clinical Implications of KRAS Mutations and Variant Allele Frequencies in Pancreatic Ductal Adenocarcinoma.* J Clin Med, 2024. **13**(7).
16. Stefanoudakis, D., M. Frountzas, D. Schizas, N.V. Michalopoulos, A. Drakaki, and K.G. Toutouzas, *Significance of TP53, CDKN2A, SMAD4 and KRAS in Pancreatic Cancer.* Curr Issues Mol Biol, 2024. **46**(4): p. 2827-2844.

17. Hayashi, H., T. Higashi, T. Miyata, Y.I. Yamashita, and H. Baba, *Recent advances in precision medicine for pancreatic ductal adenocarcinoma.* Ann Gastroenterol Surg, 2021. **5**(4): p. 457-466.
18. Racu, M.L., D. Bernardi, A. Chaouche, E. Zindy, J. Navez, P. Loi, et al., *SMAD4 Positive Pancreatic Ductal Adenocarcinomas Are Associated with Better Outcomes in Patients Receiving FOLFIRINOX-Based Neoadjuvant Therapy.* Cancers (Basel), 2023. **15**(15).
19. McCubrey, J.A., L.V. Yang, S.L. Abrams, L.S. Steelman, M.Y. Follo, L. Cocco, et al., *Effects of TP53 Mutations and miRs on Immune Responses in the Tumor Microenvironment Important in Pancreatic Cancer Progression.* Cells, 2022. **11**(14).
20. Myo Min, K.K., C.B. Ffrench, C.F. Jessup, M. Shepherdson, S.G. Barreto, and C.S. Bonder, *Overcoming the Fibrotic Fortress in Pancreatic Ductal Adenocarcinoma: Challenges and Opportunities.* Cancers (Basel), 2023. **15**(8).
21. Kane, S., A. Engelhart, J. Guadagno, A. Jones, I. Usoro, and E. Brutcher, *Pancreatic Ductal Adenocarcinoma: Characteristics of Tumor Microenvironment and Barriers to Treatment.* J Adv Pract Oncol, 2020. **11**(7): p. 693-698.
22. Miquel, M., S. Zhang, and C. Pilarsky, *Pre-clinical Models of Metastasis in Pancreatic Cancer.* Front Cell Dev Biol, 2021. **9**: p. 748631.
23. Kim, W., S. Lee, D. Seo, D. Kim, K. Kim, E. Kim, et al., *Cellular Stress Responses in Radiotherapy.* Cells, 2019. **8**(9).
24. Verloy, R., A. Privat-Maldonado, E. Smits, and A. Bogaerts, *Cold Atmospheric Plasma Treatment for Pancreatic Cancer-The Importance of Pancreatic Stellate Cells.* Cancers (Basel), 2020. **12**(10): p. 2782.
25. Bulle, A. and K.H. Lim, *Beyond just a tight fortress: contribution of stroma to epithelial-mesenchymal transition in pancreatic cancer.* Signal Transduct Target Ther, 2020. **5**(1): p. 249.
26. Carvalho, T.M.A., D. Di Molfetta, M.R. Greco, T. Koltai, K.O. Alfarouk, S.J. Reshkin, et al., *Tumor Microenvironment Features and Chemoresistance in Pancreatic Ductal Adenocarcinoma: Insights into Targeting Physicochemical Barriers and Metabolism as Therapeutic Approaches.* Cancers (Basel), 2021. **13**(23).
27. Hartupee, C., B.M. Nagalo, C.Y. Chabu, M.Z. Tesfay, J. Coleman-Barnett, J.T. West, et al., *Pancreatic cancer tumor microenvironment is a major therapeutic barrier and target.* Front Immunol, 2024. **15**: p. 1287459.
28. Bugazia, D., E. Al-Najjar, A. Esmail, S. Abdelrahim, K. Abboud, A. Abdelrahim, et al., *Pancreatic ductal adenocarcinoma: the latest on diagnosis, molecular profiling, and systemic treatments.* Front Oncol, 2024. **14**: p. 1386699.
29. McGuigan, A., P. Kelly, R.C. Turkington, C. Jones, H.G. Coleman, and R.S. McCain, *Pancreatic cancer: A review of clinical diagnosis, epidemiology, treatment and outcomes.* World J Gastroenterol, 2018. **24**(43): p. 4846-4861.
30. Hackert, T., *Surgery for Pancreatic Cancer after neoadjuvant treatment.* Ann Gastroenterol Surg, 2018. **2**(6): p. 413-418.
31. Fogel, E.L., S. Shahda, K. Sandrasegaran, J. DeWitt, J.J. Easler, D.M. Agarwal, et al., *A Multidisciplinary Approach to Pancreas Cancer in 2016: A Review.* Am J Gastroenterol, 2017. **112**(4): p. 537-554.

32. Biondetti, P., E.M. Fumarola, A.M. Ierardi, and G. Carrafiello, *Bleeding complications after pancreatic surgery: interventional radiology management.* Gland Surgery, 2019. **8**(2): p. 150-163.
33. Ho, C.K., J. Kleeff, H. Friess, and M.W. Buchler, *Complications of pancreatic surgery.* HPB (Oxford), 2005. **7**(2): p. 99-108.
34. Aseafan, M., A.H. Alfakeeh, E. Tashkandi, M. Mahrous, M. Alghamdi, B. Alshamsan, et al., *Real-world clinical outcome of unresectable locally advanced & de-novo metastatic pancreatic ductal adenocarcinoma: a multicentre retrospective study.* BMC Cancer, 2025. **25**(1): p. 7.
35. Williet, N., A. Saint, A.L. Pointet, D. Tougeron, S. Pernot, A. Pozet, et al., *Folfirinox versus gemcitabine/nab-paclitaxel as first-line therapy in patients with metastatic pancreatic cancer: a comparative propensity score study.* Therap Adv Gastroenterol, 2019. **12**: p. 1756284819878660.
36. Conroy, T., F. Desseigne, M. Ychou, O. Bouche, R. Guimbaud, Y. Becouarn, et al., *FOLFIRINOX versus gemcitabine for metastatic pancreatic cancer.* N Engl J Med, 2011. **364**(19): p. 1817-25.
37. Von Hoff, D.D., T. Ervin, F.P. Arena, E.G. Chiorean, J. Infante, M. Moore, et al., *Increased survival in pancreatic cancer with nab-paclitaxel plus gemcitabine.* N Engl J Med, 2013. **369**(18): p. 1691-703.
38. Brunner, T.B. and M. Scott-Brown, *The role of radiotherapy in multimodal treatment of pancreatic carcinoma.* Radiat Oncol, 2010. **5**: p. 64.
39. Couzin-Frankel, J., *Breakthrough of the year 2013. Cancer immunotherapy.* Science, 2013. **342**(6165): p. 1432-3.
40. Schizas, D., N. Charalampakis, C. Kole, P. Economopoulou, E. Koustas, E. Gkotsis, et al., *Immunotherapy for pancreatic cancer: A 2020 update.* Cancer Treat Rev, 2020. **86**: p. 102016.
41. Farhangnia, P., H. Khorramdelazad, H. Nickho, and A.A. Delbandi, *Current and future immunotherapeutic approaches in pancreatic cancer treatment.* J Hematol Oncol, 2024. **17**(1): p. 40.
42. Zheng, R., X. Liu, Y. Zhang, Y. Liu, Y. Wang, S. Guo, et al., *Frontiers and future of immunotherapy for pancreatic cancer: from molecular mechanisms to clinical application.* Front Immunol, 2024. **15**: p. 1383978.
43. Torphy, R.J., Y. Zhu, and R.D. Schulick, *Immunotherapy for pancreatic cancer: Barriers and breakthroughs.* Ann Gastroenterol Surg, 2018. **2**(4): p. 274-281.
44. Xu, J.W., L. Wang, Y.G. Cheng, G.Y. Zhang, S.Y. Hu, B. Zhou, et al., *Immunotherapy for pancreatic cancer: A long and hopeful journey.* Cancer Lett, 2018. **425**: p. 143-151.
45. Rosenberg, S.A., *Decade in review-cancer immunotherapy: entering the mainstream of cancer treatment.* Nat Rev Clin Oncol, 2014. **11**(11): p. 630-2.
46. Neoptolemos, J.P., J. Kleeff, P. Michl, E. Costello, W. Greenhalf, and D.H. Palmer, *Therapeutic developments in pancreatic cancer: current and future perspectives.* Nat Rev Gastroenterol Hepatol, 2018. **15**(6): p. 333-348.

47. Erkan, M., G. Adler, M.V. Apte, M.G. Bachem, M. Buchholz, S. Detlefsen, et al., *StellaTUM: current consensus and discussion on pancreatic stellate cell research.* Gut, 2012. **61**(2): p. 172-8.
48. Schnittert, J., R. Bansal, and J. Prakash, *Targeting Pancreatic Stellate Cells in Cancer.* Trends Cancer, 2019. **5**(2): p. 128-142.
49. Mace, T.A., M. Bloomston, and G.B. Lesinski, *Pancreatic cancer-associated stellate cells: A viable target for reducing immunosuppression in the tumor microenvironment.* Oncoimmunology, 2013. **2**(7): p. e24891.
50. Ferdek, P.E. and M.A. Jakubowska, *Biology of pancreatic stellate cells-more than just pancreatic cancer.* Pflugers Arch, 2017. **469**(9): p. 1039-1050.
51. Graeber, T.G., C. Osmanian, T. Jacks, D.E. Housman, C.J. Koch, S.W. Lowe, et al., *Hypoxia-mediated selection of cells with diminished apoptotic potential in solid tumours.* Nature, 1996. **379**(6560): p. 88-91.
52. Sousa, C.M., D.E. Biancur, X. Wang, C.J. Halbrook, M.H. Sherman, L. Zhang, et al., *Pancreatic stellate cells support tumour metabolism through autophagic alanine secretion.* Nature, 2016. **536**(7617): p. 479-483.
53. Apte, M.V., R.C. Pirola, and J.S. Wilson, *Pancreatic stellate cells: a starring role in normal and diseased pancreas.* Front Physiol, 2012. **3**: p. 344.
54. Privat-Maldonado, A., R. Verloy, E. Cardenas Delahoz, A. Lin, S. Vanlanduit, E. Smits, et al., *Cold Atmospheric Plasma Does Not Affect Stellate Cells Phenotype in Pancreatic Cancer Tissue in Ovo.* Int J Mol Sci, 2022. **23**(4).
55. Tian, L., Z.P. Lu, B.B. Cai, L.T. Zhao, D. Qian, Q.C. Xu, et al., *Activation of pancreatic stellate cells involves an EMT-like process.* Int J Oncol, 2016. **48**(2): p. 783-92.
56. Apte, M.V., P.A. Phillips, R.G. Fahmy, S.J. Darby, S.C. Rodgers, G.W. McCaughan, et al., *Does alcohol directly stimulate pancreatic fibrogenesis? Studies with rat pancreatic stellate cells.* Gastroenterology, 2000. **118**(4): p. 780-794.
57. Bachem, M.G., Z. Zhou, S. Zhou, and M. Siech, *Role of stellate cells in pancreatic fibrogenesis associated with acute and chronic pancreatitis.* J Gastroenterol Hepatol, 2006. **21 Suppl 3**: p. S92-6.
58. Pothula, S.P., Z. Xu, D. Goldstein, R.C. Pirola, J.S. Wilson, and M.V. Apte, *Key role of pancreatic stellate cells in pancreatic cancer.* Cancer Lett, 2016. **381**(1): p. 194-200.
59. Jesnowski, R., D. Furst, J. Ringel, Y. Chen, A. Schrodel, J. Kleeff, et al., *Immortalization of pancreatic stellate cells as an in vitro model of pancreatic fibrosis: deactivation is induced by matrigel and N-acetylcysteine.* Lab Invest, 2005. **85**(10): p. 1276-91.
60. Kikuta, K., A. Masamune, T. Watanabe, H. Ariga, H. Itoh, S. Hamada, et al., *Pancreatic stellate cells promote epithelial-mesenchymal transition in pancreatic cancer cells.* Biochem Biophys Res Commun, 2010. **403**(3-4): p. 380-4.
61. Wu, Y.S., I. Chung, W.F. Wong, A. Masamune, M.S. Sim, and C.Y. Looi, *Paracrine IL-6 signaling mediates the effects of pancreatic stellate cells on epithelial-mesenchymal transition via Stat3/Nrf2 pathway in pancreatic cancer cells.* Biochim Biophys Acta Gen Subj, 2017. **1861**(2): p. 296-306.
62. Han, S., D. Delitto, D. Zhang, H.L. Sorenson, G.A. Sarosi, R.M. Thomas, et al., *Primary outgrowth cultures are a reliable source of human pancreatic stellate cells.* Lab Invest, 2015. **95**(11): p. 1331-40.

63. Omary, M.B., A. Lugea, A.W. Lowe, and S.J. Pandol, *The pancreatic stellate cell: a star on the rise in pancreatic diseases.* J Clin Invest, 2007. **117**(1): p. 50-9.
64. Lunardi, S., R.J. Muschel, and T.B. Brunner, *The stromal compartments in pancreatic cancer: are there any therapeutic targets?* Cancer Lett, 2014. **343**(2): p. 147-55.
65. Lee, H.O., S.R. Mullins, J. Franco-Barraza, M. Valianou, E. Cukierman, and J.D. Cheng, *FAP-overexpressing fibroblasts produce an extracellular matrix that enhances invasive velocity and directionality of pancreatic cancer cells.* BMC Cancer, 2011. **11**: p. 245.
66. Cabrera, M.C., E. Tilahun, R. Nakles, E.S. Diaz-Cruz, A. Charabaty, S. Suy, et al., *Human Pancreatic Cancer-Associated Stellate Cells Remain Activated after in vivo Chemoradiation.* Front Oncol, 2014. **4**: p. 102.
67. Birbrair, A., *Tumor Microenvironment*. First ed. Advances in Experimental Medicine and Biology. 2020: Springer International Publishing.
68. Sun, Q., B. Zhang, Q. Hu, Y. Qin, W. Xu, W. Liu, et al., *The impact of cancer-associated fibroblasts on major hallmarks of pancreatic cancer.* Theranostics, 2018. **8**(18): p. 5072-5087.
69. de Sousa Cavalcante, L. and G. Monteiro, *Gemcitabine: metabolism and molecular mechanisms of action, sensitivity and chemoresistance in pancreatic cancer.* Eur J Pharmacol, 2014. **741**: p. 8-16.
70. Katsuta, E., Q. Qi, X. Peng, S.N. Hochwald, L. Yan, and K. Takabe, *Pancreatic adenocarcinomas with mature blood vessels have better overall survival.* Sci Rep, 2019. **9**(1): p. 1310.
71. Olive, K.P., M.A. Jacobetz, C.J. Davidson, A. Gopinathan, D. McIntyre, D. Honess, et al., *Inhibition of Hedgehog Signaling Enhances Delivery of Chemotherapy in a Mouse Model of Pancreatic Cancer.* Science, 2009. **324**(5933): p. 1457-1461.
72. Neesse, A., P. Michl, K.K. Frese, C. Feig, N. Cook, M.A. Jacobetz, et al., *Stromal biology and therapy in pancreatic cancer.* Gut, 2011. **60**(6): p. 861-8.
73. Longo, V., O. Brunetti, A. Gnoni, S. Cascinu, G. Gasparini, V. Lorusso, et al., *Angiogenesis in pancreatic ductal adenocarcinoma: A controversial issue.* Oncotarget, 2016. **7**(36): p. 58649-58658.
74. Hexige, S., C.M. Ardito-Abraham, Y. Wu, Y. Wei, Y. Fang, X. Han, et al., *Identification of novel vascular projections with cellular trafficking abilities on the microvasculature of pancreatic ductal adenocarcinoma.* J Pathol, 2015. **236**(2): p. 142-154.
75. Natarajan, V., S. Ha, A. Delgado, R. Jacobson, L. Alhalhooly, Y. Choi, et al., *Acquired alphaSMA Expression in Pericytes Coincides with Aberrant Vascular Structure and Function in Pancreatic Ductal Adenocarcinoma.* Cancers (Basel), 2022. **14**(10).
76. Erkan, M., S. Hausmann, C.W. Michalski, A.A. Fingerle, M. Dobritz, J. Kleeff, et al., *The role of stroma in pancreatic cancer: diagnostic and therapeutic implications.* Nat Rev Gastroenterol Hepatol, 2012. **9**(8): p. 454-67.
77. Angelescu, R., F. Burada, C. Angelescu, D.I. Gheonea, S. Iordache, F. Mixich, et al., *Expression of Vascular Endothelial Growth Factor and Epidermal Growth Factor Receptor in Pancreatic Ductal Adenocarcinomas, Neuroendocrine Tumours and Chronic Pancreatitis.* Endoscopic Ultrasound, 2013. **2**(2).

78. Ohta, T., M. Yamamoto, M. Numata, S. Iseki, Y. Tsukioka, T. Miyashita, et al., *Expression of basic fibroblast growth factor and its receptor in human pancreatic carcinomas.* British Journal of Cancer, 1995. **72**(4): p. 824-831.
79. Schulz, P., C. Fischer, K.M. Detjen, S. Rieke, G. Hilfenhaus, Z. von Marschall, et al., *Angiopoietin-2 drives lymphatic metastasis of pancreatic cancer.* The FASEB Journal, 2011. **25**(10): p. 3325-3335.
80. Masamune, A., K. Kikuta, T. Watanabe, K. Satoh, M. Hirota, and T. Shimosegawa, *Hypoxia stimulates pancreatic stellate cells to induce fibrosis and angiogenesis in pancreatic cancer.* Am J Physiol Gastrointest Liver Physiol, 2008. **295**(4): p. G709-17.
81. Olive, K.P., M.A. Jacobetz, C.J. Davidson, A. Gopinathan, D. McIntyre, D. Honess, et al., *Inhibition of Hedgehog signaling enhances delivery of chemotherapy in a mouse model of pancreatic cancer.* Science, 2009. **324**(5933): p. 1457-61.
82. Lobov, I.B., P.C. Brooks, and R.A. Lang, *Angiopoietin-2 displays VEGF-dependent modulation of capillary structure and endothelial cell survival in vivo.* Proc Natl Acad Sci U S A, 2002. **99**(17): p. 11205-10.
83. Fagiani, E. and G. Christofori, *Angiopoietins in angiogenesis.* Cancer Lett, 2013. **328**(1): p. 18-26.
84. Roos-Mattila, M., T. Kaprio, H. Mustonen, J. Hagstrom, P. Saharinen, C. Haglund, et al., *The possible dual role of Ang-2 in the prognosis of pancreatic cancer.* Sci Rep, 2023. **13**(1): p. 18725.
85. van Duijneveldt, G., M.D.W. Griffin, and T.L. Putoczki, *Emerging roles for the IL-6 family of cytokines in pancreatic cancer.* Clin Sci (Lond), 2020. **134**(16): p. 2091-2115.
86. Sabbadini, F., M. Bertolini, S. De Matteis, D. Mangiameli, S. Contarelli, S. Pietrobono, et al., *The Multifaceted Role of TGF-beta in Gastrointestinal Tumors.* Cancers (Basel), 2021. **13**(16).
87. Pandey, P., F. Khan, T.K. Upadhyay, M. Seungjoon, M.N. Park, and B. Kim, *New insights about the PDGF/PDGFR signaling pathway as a promising target to develop cancer therapeutic strategies.* Biomed Pharmacother, 2023. **161**: p. 114491.
88. Oh, K., Y.J. Yoo, L.A. Torre-Healy, M. Rao, D. Fassler, P. Wang, et al., *Coordinated single-cell tumor microenvironment dynamics reinforce pancreatic cancer subtype.* Nat Commun, 2023. **14**(1): p. 5226.
89. Masamune, A., T. Watanabe, K. Kikuta, and T. Shimosegawa, *Roles of pancreatic stellate cells in pancreatic inflammation and fibrosis.* Clin Gastroenterol Hepatol, 2009. **7**(11 Suppl): p. S48-54.
90. Di Maggio, F., P. Arumugam, F.R. Delvecchio, S. Batista, T. Lechertier, K. Hodivala-Dilke, et al., *Pancreatic stellate cells regulate blood vessel density in the stroma of pancreatic ductal adenocarcinoma.* Pancreatology, 2016. **16**(6): p. 995-1004.
91. Apte, M.V., J.S. Wilson, A. Lugea, and S.J. Pandol, *A starring role for stellate cells in the pancreatic cancer microenvironment.* Gastroenterology, 2013. **144**(6): p. 1210-9.

92. Chauhan, V.P., Y. Boucher, C.R. Ferrone, S. Roberge, J.D. Martin, T. Stylianopoulos, et al., *Compression of pancreatic tumor blood vessels by hyaluronan is caused by solid stress and not interstitial fluid pressure.* Cancer Cell, 2014. **26**(1): p. 14-5.
93. Comunanza, V. and F. Bussolino, *Therapy for Cancer: Strategy of Combining Anti-Angiogenic and Target Therapies.* Front Cell Dev Biol, 2017. **5**: p. 101.
94. Feig, C., A. Gopinathan, A. Neesse, D.S. Chan, N. Cook, and D.A. Tuveson, *The pancreas cancer microenvironment.* Clin Cancer Res, 2012. **18**(16): p. 4266-76.
95. Kindler, H.L., D. Niedzwiecki, D. Hollis, S. Sutherland, D. Schrag, H. Hurwitz, et al., *Gemcitabine plus bevacizumab compared with gemcitabine plus placebo in patients with advanced pancreatic cancer: phase III trial of the Cancer and Leukemia Group B (CALGB 80303).* J Clin Oncol, 2010. **28**(22): p. 3617-22.
96. Van Cutsem, E., W.L. Vervenne, J. Bennouna, Y. Humblet, S. Gill, J.L. Van Laethem, et al., *Phase III trial of bevacizumab in combination with gemcitabine and erlotinib in patients with metastatic pancreatic cancer.* J Clin Oncol, 2009. **27**(13): p. 2231-7.
97. Rougier, P., H. Riess, R. Manges, P. Karasek, Y. Humblet, C. Barone, et al., *Randomised, placebo-controlled, double-blind, parallel-group phase III study evaluating aflibercept in patients receiving first-line treatment with gemcitabine for metastatic pancreatic cancer.* Eur J Cancer, 2013. **49**(12): p. 2633-42.
98. Hodi, F.S., D. Lawrence, C. Lezcano, X. Wu, J. Zhou, T. Sasada, et al., *Bevacizumab plus ipilimumab in patients with metastatic melanoma.* Cancer Immunol Res, 2014. **2**(7): p. 632-42.
99. von Woedtke, T., S. Reuter, K. Masur, and K.D. Weltmann, *Plasmas for medicine.* Physics Reports, 2013. **530**(4): p. 291-320.
100. Tampieri, F., Y. Gorbanev, and E. Sardella, *Plasma-treated liquids in medicine: Let's get chemical.* Plasma Processes and Polymers, 2023. **20**(9): p. e2300077.
101. Snoeckx, R. and A. Bogaerts, *Plasma technology - a novel solution for CO2 conversion?* Chem Soc Rev, 2017. **46**(19): p. 5805-5863.
102. Yan, D., J.H. Sherman, and M. Keidar, *Cold atmospheric plasma, a novel promising anti-cancer treatment modality.* Oncotarget; Vol 8, No 9, 2016.
103. Keidar, M., *A prospectus on innovations in the plasma treatment of cancer.* Physics of Plasmas, 2018. **25**(8): p. 083504.
104. von Woedtke, T., A. Schmidt, S. Bekeschus, K. Wende, and K.D. Weltmann, *Plasma Medicine: A Field of Applied Redox Biology.* In Vivo, 2019. **33**(4): p. 1011-1026.
105. Weltmann, K.D. and T. von Woedtke, *Plasma medicine—current state of research and medical application.* Plasma Physics and Controlled Fusion, 2016. **59**(1): p. 014031.
106. Hoffmann, C., C. Berganza, and J. Zhang, *Cold Atmospheric Plasma: methods of production and application in dentistry and oncology.* Med Gas Res, 2013. **3**(1): p. 21.
107. Bekeschus, S., A. Schmidt, K.-D. Weltmann, and T. von Woedtke, *The plasma jet kINPen – A powerful tool for wound healing.* Clinical Plasma Medicine, 2016. **4**(1): p. 19-28.
108. Fridman, A.A., *Plasma chemistry*. First paperback edition. ed. 2012, Cambridge: Cambridge University Press. xlii, 978 pages.

109. Kong, M.G., G. Kroesen, G. Morfill, T. Nosenko, T. Shimizu, J. van Dijk, et al., *Plasma medicine: an introductory review.* New Journal of Physics, 2009. **11**(11): p. 115012.
110. Scholtz, V., J. Pazlarova, H. Souskova, J. Khun, and J. Julak, *Nonthermal plasma--A tool for decontamination and disinfection.* Biotechnol Adv, 2015. **33**(6 Pt 2): p. 1108-19.
111. Brehmer, F., H.A. Haenssle, G. Daeschlein, R. Ahmed, S. Pfeiffer, A. Gorlitz, et al., *Alleviation of chronic venous leg ulcers with a hand-held dielectric barrier discharge plasma generator (PlasmaDerm((R)) VU-2010): results of a monocentric, two-armed, open, prospective, randomized and controlled trial (NCT01415622).* J Eur Acad Dermatol Venereol, 2015. **29**(1): p. 148-55.
112. Fridman, G., G. Friedman, A. Gutsol, A.B. Shekhter, V.N. Vasilets, and A. Fridman, *Applied Plasma Medicine.* Plasma Processes and Polymers, 2008. **5**(6): p. 503-533.
113. Weltmann, K.D., E. Kindel, R. Brandenburg, C. Meyer, R. Bussiahn, C. Wilke, et al., *Atmospheric Pressure Plasma Jet for Medical Therapy: Plasma Parameters and Risk Estimation.* Contributions to Plasma Physics, 2009. **49**(9): p. 631-640.
114. Reuter, S., T. von Woedtke, and K.-D. Weltmann, *The kINPen—a review on physics and chemistry of the atmospheric pressure plasma jet and its applications.* Journal of Physics D: Applied Physics, 2018. **51**(23): p. 233001.
115. Metelmann, H.-R., C. Seebauer, V. Miller, A. Fridman, G. Bauer, D.B. Graves, et al., *Clinical experience with cold plasma in the treatment of locally advanced head and neck cancer.* Clinical Plasma Medicine, 2018. **9**: p. 6-13.
116. Van Loenhout, J., T. Flieswasser, L. Freire Boullosa, J. De Waele, J. Van Audenaerde, E. Marcq, et al., *Cold Atmospheric Plasma-Treated PBS Eliminates Immunosuppressive Pancreatic Stellate Cells and Induces Immunogenic Cell Death of Pancreatic Cancer Cells.* Cancers (Basel), 2019. **11**(10).
117. Biscop, E., E.C. De La Hoz, H. Verswyvel, J. De Backer, H.W. Lau, A. Privat-Maldonado, et al., *Dose-dependent induction of epithelial-mesenchymal transition in 3D melanoma models by non-thermal plasma treatment.* Mol Oncol, 2025.
118. Lin, A., J. De Backer, D. Quatannens, B. Cuypers, H. Verswyvel, E.C. De La Hoz, et al., *The effect of local non-thermal plasma therapy on the cancer-immunity cycle in a melanoma mouse model.* Bioeng Transl Med, 2022. **7**(3): p. e10314.
119. Alimohammadi, M., M. Golpur, F. Sohbatzadeh, S. Hadavi, S. Bekeschus, H.A. Niaki, et al., *Cold Atmospheric Plasma Is a Potent Tool to Improve Chemotherapy in Melanoma In Vitro and In Vivo.* Biomolecules, 2020. **10**(7).
120. Vermeylen, S., J. De Waele, S. Vanuytsel, J. De Backer, J. Van der Paal, M. Ramakers, et al., *Cold atmospheric plasma treatment of melanoma and glioblastoma cancer cells.* Plasma Processes and Polymers, 2016. **13**(12): p. 1195-1205.
121. Mateu-Sanz, M., M.P. Ginebra, J. Tornin, and C. Canal, *Cold atmospheric plasma enhances doxorubicin selectivity in metastasic bone cancer.* Free Radic Biol Med, 2022. **189**: p. 32-41.
122. Jung, J.M., H.K. Yoon, S.Y. Kim, M.R. Yun, G.H. Kim, W.J. Lee, et al., *Anticancer Effect of Cold Atmospheric Plasma in Syngeneic Mouse Models of Melanoma and Colon Cancer.* Molecules, 2023. **28**(10).

123. Zimmermann, T., S. Staebler, R.V. Taudte, S. Unuvar, S. Grosch, S. Arndt, et al., *Cold Atmospheric Plasma Triggers Apoptosis via the Unfolded Protein Response in Melanoma Cells.* Cancers (Basel), 2023. **15**(4).
124. Weiss, M., D. Gumbel, E.M. Hanschmann, R. Mandelkow, N. Gelbrich, U. Zimmermann, et al., *Cold Atmospheric Plasma Treatment Induces Anti-Proliferative Effects in Prostate Cancer Cells by Redox and Apoptotic Signaling Pathways.* PLoS One, 2015. **10**(7): p. e0130350.
125. Rostami, Z., R. Alizadeh-Navaei, M. Golpoor, Z. Yazdani, and A. Rafiei, *Synergistic effects of cold atmospheric plasma and doxorubicin on melanoma: A systematic review and meta-analysis.* Sci Rep, 2025. **15**(1): p. 7870.
126. Khlyustova, A., C. Labay, Z. Machala, M.-P. Ginebra, and C. Canal, *Important parameters in plasma jets for the production of RONS in liquids for plasma medicine: A brief review.* Frontiers of Chemical Science and Engineering, 2019. **13**(2): p. 238-252.
127. Golda, J., J. Held, B. Redeker, M. Konkowski, P. Beijer, A. Sobota, et al., *Concepts and characteristics of the 'COST Reference Microplasma Jet'.* Journal of Physics D: Applied Physics, 2016. **49**(8): p. 084003.
128. Holanda, A.G.A., B.C. Cesario, V.M. Silva, L.E.C. Francelino, B.H.M. Nascimento, K.F.A. Damasceno, et al., *Use of Cold Atmospheric Plasma in the Treatment of Squamous Cell Carcinoma: in vitro Effects and Clinical Application in Feline Tumors: A Pilot Study.* Top Companion Anim Med, 2023. **53-54**: p. 100773.
129. Isbary, G., G. Morfill, H.U. Schmidt, M. Georgi, K. Ramrath, J. Heinlin, et al., *A first prospective randomized controlled trial to decrease bacterial load using cold atmospheric argon plasma on chronic wounds in patients.* Br J Dermatol, 2010. **163**(1): p. 78-82.
130. Laroussi, M., *Sterilization of contaminated matter with an atmospheric pressure plasma.* IEEE Transactions on Plasma Science, 1996. **24**(3): p. 1188-1191.
131. Sebastian, S., R. McLoughlin, A. Qasim, C.A. O'Morain, and M.J. Buckley, *Endoscopic argon plasma coagulation for the treatment of gastric antral vascular ectasia (watermelon stomach): long-term results.* Dig Liver Dis, 2004. **36**(3): p. 212-7.
132. Robert, E., M. Vandamme, L. Brullé, S. Lerondel, A. Le Pape, V. Sarron, et al., *Perspectives of endoscopic plasma applications.* Clinical Plasma Medicine, 2013. **1**(2): p. 8-16.
133. Schubert, D., R. Kuhn, H. Lippert, and M. Pross, *Endoscopic treatment of benign gastrointestinal anastomotic strictures using argon plasma coagulation in combination with diathermy.* Surg Endosc, 2003. **17**(10): p. 1579-82.
134. Schlegel, J., J. Köritzer, and V. Boxhammer, *Plasma in cancer treatment.* Clinical Plasma Medicine, 2013. **1**(2): p. 2-7.
135. Yan, D., H. Cui, W. Zhu, A. Talbot, L.G. Zhang, J.H. Sherman, et al., *The Strong Cell-based Hydrogen Peroxide Generation Triggered by Cold Atmospheric Plasma.* Sci Rep, 2017. **7**(1): p. 10831.
136. Privat-Maldonado, A., A. Schmidt, A. Lin, K.D. Weltmann, K. Wende, A. Bogaerts, et al., *ROS from Physical Plasmas: Redox Chemistry for Biomedical Therapy.* Oxid Med Cell Longev, 2019. **2019**: p. 29.

137. Keidar, M., R. Walk, A. Shashurin, P. Srinivasan, A. Sandler, S. Dasgupta, et al., *Cold plasma selectivity and the possibility of a paradigm shift in cancer therapy.* Br J Cancer, 2011. **105**(9): p. 1295-301.
138. Lin, A., Y. Gorbanev, J. De Backer, J. Van Loenhout, W. Van Boxem, F. Lemiere, et al., *Non-Thermal Plasma as a Unique Delivery System of Short-Lived Reactive Oxygen and Nitrogen Species for Immunogenic Cell Death in Melanoma Cells.* Adv Sci (Weinh), 2019. **6**(6): p. 1802062.
139. Azzariti, A., R.M. Iacobazzi, R. Di Fonte, L. Porcelli, R. Gristina, P. Favia, et al., *Plasma-activated medium triggers cell death and the presentation of immune activating danger signals in melanoma and pancreatic cancer cells.* Sci Rep, 2019. **9**(1): p. 4099.
140. Zivanic, M., A. Espona-Noguera, A. Lin, and C. Canal, *Current State of Cold Atmospheric Plasma and Cancer-Immunity Cycle: Therapeutic Relevance and Overcoming Clinical Limitations Using Hydrogels.* Adv Sci (Weinh), 2023. **10**(8): p. e2205803.
141. Wu, P.S., T.H. Wong, C.W. Hou, T.P. Chu, J.W. Lee, B.S. Lou, et al., *Cold Atmospheric Plasma Jet Promotes Wound Healing Through CK2-Coordinated PI3K/AKT and MAPK Signaling Pathways.* Mol Cell Proteomics, 2025. **24**(5): p. 100962.
142. Liu, F., Y. Zhou, W. Song, and H. Wang, *Cold Atmospheric Plasma Inhibits the Proliferation of CAL-62 Cells through the ROS-Mediated PI3K/Akt/mTOR Signaling Pathway.* Science and Technology of Nuclear Installations, 2022. **2022**(1): p. 3884695.
143. Keidar, M., D. Yan, and J.H. Sherman, *Cold Plasma Cancer Therapy*. 2019, Morgan & Claypool Publishers.
144. Biscop, E., J. Baroen, J. De Backer, W. Vanden Berghe, E. Smits, A. Bogaerts, et al., *Characterization of regulated cancer cell death pathways induced by the different modalities of non-thermal plasma treatment.* Cell Death Discov, 2024. **10**(1): p. 416.
145. Yan, D., A. Horkowitz, Q. Wang, and M. Keidar, *On the selective killing of cold atmospheric plasma cancer treatment: Status and beyond.* Plasma Processes and Polymers, 2021. **18**(10): p. 2100020.
146. Hanahan, D. and L.M. Coussens, *Accessories to the crime: functions of cells recruited to the tumor microenvironment.* Cancer Cell, 2012. **21**(3): p. 309-22.
147. Bourdens, M., Y. Jeanson, M. Taurand, N. Juin, A. Carriere, F. Clement, et al., *Short exposure to cold atmospheric plasma induces senescence in human skin fibroblasts and adipose mesenchymal stromal cells.* Sci Rep, 2019. **9**(1): p. 8671.
148. Haralambiev, L., O. Neuffer, A. Nitsch, N.C. Kross, S. Bekeschus, P. Hinz, et al., *Inhibition of Angiogenesis by Treatment with Cold Atmospheric Plasma as a Promising Therapeutic Approach in Oncology.* Int J Mol Sci, 2020. **21**(19).
149. Duchesne, C., S. Banzet, J.J. Lataillade, A. Rousseau, and N. Frescaline, *Cold atmospheric plasma modulates endothelial nitric oxide synthase signalling and enhances burn wound neovascularisation.* J Pathol, 2019. **249**(3): p. 368-380.
150. Arndt, S., P. Unger, M. Berneburg, A.K. Bosserhoff, and S. Karrer, *Cold atmospheric plasma (CAP) activates angiogenesis-related molecules in skin keratinocytes, fibroblasts and endothelial cells and improves wound angiogenesis in an autocrine and paracrine mode.* J Dermatol Sci, 2018. **89**(2): p. 181-190.

151. Kang, S.U., H.J. Kim, S. Ma, D.Y. Oh, J.Y. Jang, C. Seo, et al., *Liquid plasma promotes angiogenesis through upregulation of endothelial nitric oxide synthase-induced extracellular matrix metabolism: potential applications of liquid plasma for vascular injuries.* Cell Commun Signal, 2024. **22**(1): p. 138.
152. Yusupov, M., A. Privat-Maldonado, R.M. Cordeiro, H. Verswyvel, P. Shaw, J. Razzokov, et al., *Oxidative damage to hyaluronan-CD44 interactions as an underlying mechanism of action of oxidative stress-inducing cancer therapy.* Redox Biol, 2021. **43**: p. 101968.
153. Wang, X.F., Q.Q. Fang, B. Jia, Y.Y. Hu, Z.C. Wang, K.P. Yan, et al., *Potential effect of non-thermal plasma for the inhibition of scar formation: a preliminary report.* Sci Rep, 2020. **10**(1): p. 1064.
154. Kang, S.U., Y.S. Kim, Y.E. Kim, J.K. Park, Y.S. Lee, H.Y. Kang, et al., *Opposite effects of non-thermal plasma on cell migration and collagen production in keloid and normal fibroblasts.* PLoS One, 2017. **12**(11): p. e0187978.
155. Khalili, M., A.E. Snook, W.B. Bowne, A. Fridman, and V. Miller, *Non-Thermal Plasma Induced Immunogenic Cell Death In Pancreatic Cancer.* Clinical Plasma Medicine, 2018. **9**: p. 17.
156. Verswyvel, H., *Boosting cancer immunotherapy : the immunogenic and therapeutic potential of non-thermal plasma in head and neck cancer*. 2025, University of Antwerp: UAntwerp Repository. p. 253.
157. Guerrero-Preston, R., T. Ogawa, M. Uemura, G. Shumulinsky, B.L. Valle, F. Pirini, et al., *Cold atmospheric plasma treatment selectively targets head and neck squamous cell carcinoma cells.* Int J Mol Med, 2014. **34**(4): p. 941-6.
158. Wang, M., B. Holmes, X. Cheng, W. Zhu, M. Keidar, and L.G. Zhang, *Cold atmospheric plasma for selectively ablating metastatic breast cancer cells.* PLoS One, 2013. **8**(9): p. e73741.
159. Zucker, S.N., J. Zirnheld, A. Bagati, T.M. DiSanto, B. Des Soye, J.A. Wawrzyniak, et al., *Preferential induction of apoptotic cell death in melanoma cells as compared with normal keratinocytes using a non-thermal plasma torch.* Cancer Biol Ther, 2012. **13**(13): p. 1299-306.
160. Kaushik, N., N. Kumar, C.H. Kim, N.K. Kaushik, and E.H. Choi, *Dielectric Barrier Discharge Plasma Efficiently Delivers an Apoptotic Response in Human Monocytic Lymphoma.* Plasma Processes and Polymers, 2014. **11**(12): p. 1175-1187.
161. Utsumi, F., H. Kajiyama, K. Nakamura, H. Tanaka, M. Hori, and F. Kikkawa, *Selective cytotoxicity of indirect nonequilibrium atmospheric pressure plasma against ovarian clear-cell carcinoma.* Springerplus, 2014. **3**: p. 398.
162. Kim, S.J. and T.H. Chung, *Cold atmospheric plasma jet-generated RONS and their selective effects on normal and carcinoma cells.* Sci Rep, 2016. **6**: p. 20332.
163. Dubuc, A., P. Monsarrat, F. Virard, N. Merbahi, J.P. Sarrette, S. Laurencin-Dalicieux, et al., *Use of cold-atmospheric plasma in oncology: a concise systematic review.* Ther Adv Med Oncol, 2018. **10**: p. 1758835918786475.
164. Hubenak, J.R., Q. Zhang, C.D. Branch, and S.J. Kronowitz, *Mechanisms of injury to normal tissue after radiotherapy: a review.* Plast Reconstr Surg, 2014. **133**(1): p. 49e-56e.

165. Yan, D., A. Talbot, N. Nourmohammadi, J.H. Sherman, X. Cheng, and M. Keidar, *Toward understanding the selective anticancer capacity of cold atmospheric plasma--a model based on aquaporins (Review).* Biointerphases, 2015. **10**(4): p. 040801.
166. Yusupov, M., J. Razzokov, R.M. Cordeiro, and A. Bogaerts, *Transport of Reactive Oxygen and Nitrogen Species across Aquaporin: A Molecular Level Picture.* Oxid Med Cell Longev, 2019. **2019**: p. 2930504.
167. Yusupov, M., D. Yan, R.M. Cordeiro, and A. Bogaerts, *Atomic scale simulation of H2O2permeation through aquaporin: toward the understanding of plasma cancer treatment.* Journal of Physics D: Applied Physics, 2018. **51**(12): p. 125401.
168. Van der Paal, J., C. Verheyen, E.C. Neyts, and A. Bogaerts, *Hampering Effect of Cholesterol on the Permeation of Reactive Oxygen Species through Phospholipids Bilayer: Possible Explanation for Plasma Cancer Selectivity.* Sci Rep, 2017. **7**: p. 39526.
169. Van der Paal, J., E.C. Neyts, C.C.W. Verlackt, and A. Bogaerts, *Effect of lipid peroxidation on membrane permeability of cancer and normal cells subjected to oxidative stress.* Chem Sci, 2016. **7**(1): p. 489-498.
170. Biscop, E., A. Lin, W.V. Boxem, J.V. Loenhout, J. Backer, C. Deben, et al., *Influence of Cell Type and Culture Medium on Determining Cancer Selectivity of Cold Atmospheric Plasma Treatment.* Cancers (Basel), 2019. **11**(9).
171. Mateu-Sanz, M., J. Tornin, M.P. Ginebra, and C. Canal, *Cold Atmospheric Plasma: A New Strategy Based Primarily on Oxidative Stress for Osteosarcoma Therapy.* J Clin Med, 2021. **10**(4).
172. Gorbanev, Y., A. Privat-Maldonado, and A. Bogaerts, *Analysis of Short-Lived Reactive Species in Plasma-Air-Water Systems: The Dos and the Do Nots.* Anal Chem, 2018. **90**(22): p. 13151-13158.
173. Zhou, R., R. Zhou, P. Wang, Y. Xian, A. Mai-Prochnow, X. Lu, et al., *Plasma-activated water: generation, origin of reactive species and biological applications.* Journal of Physics D: Applied Physics, 2020. **53**(30): p. 303001.
174. Fan, R., X. Zhao, M. Qi, H. Zhang, X. Zhang, J. Zhang, et al., *Properties and anticancer effects of plasma-activated medium stored at different temperatures.* AIP Advances, 2022. **12**(9): p. 095022.
175. Saadati, F., H. Mahdikia, H.-A. Abbaszadeh, M.-A. Abdollahifar, M.S. Khoramgah, and B. Shokri, *Comparison of Direct and Indirect cold atmospheric-pressure plasma methods in the B16F10 melanoma cancer cells treatment.* Scientific Reports, 2018. **8**(1): p. 7689.
176. Jezeh, M.A., T. Tayebi, M.R. Khani, H. Niknejad, and B. Shokri, *Direct cold atmospheric plasma and plasma-activated medium effects on breast and cervix cancer cells.* Plasma Processes and Polymers, 2020. **17**(11): p. 1900241.
177. Solé-Martí, X., C. Labay, Y. Raymond, J. Franch, R. Benitez, M.-P. Ginebra, et al., *Ceramic-hydrogel composite as carrier for cold-plasma reactive-species: Safety and osteogenic capacity in vivo.* Plasma Processes and Polymers, 2023. **20**(1): p. 2200155.
178. *Plasma Cancer Therapy*. 1 ed. 2020: Springer Charm. 310.

179. Sole-Marti, X., T. Vilella, C. Labay, F. Tampieri, M.P. Ginebra, and C. Canal, *Thermosensitive hydrogels to deliver reactive species generated by cold atmospheric plasma: a case study with methylcellulose.* Biomater Sci, 2022. **10**(14): p. 3845-3855.
180. Espona-Noguera, A., F. Tampieri, and C. Canal, *Engineering alginate-based injectable hydrogels combined with bioactive polymers for targeted plasma-derived oxidative stress delivery in osteosarcoma therapy.* Int J Biol Macromol, 2024. **257**(Pt 2): p. 128841.
181. Lin, A., E. Biscop, C. Breen, S.J. Butler, E. Smits, and A. Bogaerts, *Critical Evaluation of the Interaction of Reactive Oxygen and Nitrogen Species with Blood to Inform the Clinical Translation of Nonthermal Plasma Therapy.* Oxid Med Cell Longev, 2020. **2020**: p. 9750206.
182. Wang, Y., X. Mang, X. Li, Z. Cai, and F. Tan, *Cold atmospheric plasma induces apoptosis in human colon and lung cancer cells through modulating mitochondrial pathway.* Front Cell Dev Biol, 2022. **10**: p. 915785.
183. Tiwari, R., Y. Mondal, K. Bharadwaj, M. Mahajan, S. Mondal, and A. Sarkar, *Reactive Oxygen Species (ROS) and Their Profound Influence on Regulating Diverse Aspects of Cancer: A Concise Review.* Drug Dev Res, 2025. **86**(4): p. e70107.
184. Arjunan, K.P., G. Friedman, A. Fridman, and A.M. Clyne, *Non-thermal dielectric barrier discharge plasma induces angiogenesis through reactive oxygen species.* J R Soc Interface, 2012. **9**(66): p. 147-57.
185. Stratmann, B., T.C. Costea, C. Nolte, J. Hiller, J. Schmidt, J. Reindel, et al., *Effect of Cold Atmospheric Plasma Therapy vs Standard Therapy Placebo on Wound Healing in Patients With Diabetic Foot Ulcers: A Randomized Clinical Trial.* JAMA Netw Open, 2020. **3**(7): p. e2010411.
186. Bolgeo, T., A. Maconi, M. Gardalini, D. Gatti, R. Di Matteo, M. Lapidari, et al., *The Role of Cold Atmospheric Plasma in Wound Healing Processes in Critically Ill Patients.* J Pers Med, 2023. **13**(5).
187. Ullah, N., M.I. Khan, A. Qamar, N.U. Rehman, E. Tag elDin, M. Alkhedher, et al., *Metrology of Ar-N(2)/O(2) Mixture Atmospheric Pressure Pulsed DC Jet Plasma and its Application in Bio-Decontamination.* ACS Omega, 2023. **8**(13): p. 12028-12038.
188. Brany, D., D. Dvorska, E. Halasova, and H. Skovierova, *Cold Atmospheric Plasma: A Powerful Tool for Modern Medicine.* Int J Mol Sci, 2020. **21**(8).
189. Alqutaibi, A.Y., A. Aljohani, A. Alduri, A. Masoudi, A.M. Alsaedi, H.M. Al-Sharani, et al., *The Effectiveness of Cold Atmospheric Plasma (CAP) on Bacterial Reduction in Dental Implants: A Systematic Review.* Biomolecules, 2023. **13**(10).
190. Garcia, L., L. Rojas, G. Gonzales, D. Alvitez-Temoche, R. Mendoza, and F. Mayta-Tovalino, *The Role of Cold Atmospheric Plasma (CAP) in the Control of Biofilms on Titanium Surfaces: A Literature Review.* Journal of International Oral Health, 2021. **13**(4).
191. Hui, W.L., V. Perrotti, F. Iaculli, A. Piattelli, and A. Quaranta, *The Emerging Role of Cold Atmospheric Plasma in Implantology: A Review of the Literature.* Nanomaterials (Basel), 2020. **10**(8).
192. Aggelopoulos, C.A., A.M. Christodoulou, M. Tachliabouri, S. Meropoulis, M.E. Christopoulou, T.T. Karalis, et al., *Cold Atmospheric Plasma Attenuates Breast*

Cancer Cell Growth Through Regulation of Cell Microenvironment Effectors. Front Oncol, 2021. **11**: p. 826865.
193. Ahn, H.J., K.I. Kim, N.N. Hoan, C.H. Kim, E. Moon, K.S. Choi, et al., *Targeting cancer cells with reactive oxygen and nitrogen species generated by atmospheric-pressure air plasma.* PLoS One, 2014. **9**(1): p. e86173.
194. Tanaka, H., M. Mizuno, K. Ishikawa, K. Nakamura, H. Kajiyama, H. Kano, et al., *Plasma-Activated Medium Selectively Kills Glioblastoma Brain Tumor Cells by Down-Regulating a Survival Signaling Molecule, AKT Kinase.* 2011. **1**(3-4): p. 265-277.
195. Decauchy, H., A. Pavy, M. Camus, L. Fouassier, and T. Dufour, *Cold plasma endoscopy applied to biliary ducts: feasibility risk assessment on human-like and porcine models for the treatment of cholangiocarcinoma.* Journal of Physics D: Applied Physics, 2022. **55**(45): p. 455401.
196. Bastin, O., M. Thulliez, J. Servais, A. Nonclercq, A. Delchambre, A. Hadefi, et al., *Optical and Electrical Characteristics of an Endoscopic DBD Plasma Jet.* Plasma Medicine, 2020. **10**(2): p. 71-90.
197. Canady, J., S.R.K. Murthy, T. Zhuang, S. Gitelis, A. Nissan, L. Ly, et al., *The First Cold Atmospheric Plasma Phase I Clinical Trial for the Treatment of Advanced Solid Tumors: A Novel Treatment Arm for Cancer.* Cancers (Basel), 2023. **15**(14).
198. Schuster, M., C. Seebauer, R. Rutkowski, A. Hauschild, F. Podmelle, C. Metelmann, et al., *Visible tumor surface response to physical plasma and apoptotic cell kill in head and neck cancer.* J Craniomaxillofac Surg, 2016. **44**(9): p. 1445-52.
199. Partecke, L.I., K. Evert, J. Haugk, F. Doering, L. Normann, S. Diedrich, et al., *Tissue tolerable plasma (TTP) induces apoptosis in pancreatic cancer cells in vitro and in vivo.* BMC Cancer, 2012. **12**: p. 473.
200. Liedtke, K.R., S. Bekeschus, A. Kaeding, C. Hackbarth, J.P. Kuehn, C.D. Heidecke, et al., *Non-thermal plasma-treated solution demonstrates antitumor activity against pancreatic cancer cells in vitro and in vivo.* Sci Rep, 2017. **7**(1): p. 8319.
201. Liedtke, K.R., S. Diedrich, O. Pati, E. Freund, R. Flieger, C.D. Heidecke, et al., *Cold Physical Plasma Selectively Elicits Apoptosis in Murine Pancreatic Cancer Cells In Vitro and In Ovo.* Anticancer Res, 2018. **38**(10): p. 5655-5663.
202. Brulle, L., M. Vandamme, D. Ries, E. Martel, E. Robert, S. Lerondel, et al., *Effects of a non thermal plasma treatment alone or in combination with gemcitabine in a MIA PaCa2-luc orthotopic pancreatic carcinoma model.* PLoS One, 2012. **7**(12): p. e52653.
203. Bekeschus, S., E. Freund, C. Spadola, A. Privat-Maldonado, C. Hackbarth, A. Bogaerts, et al., *Risk Assessment of kINPen Plasma Treatment of Four Human Pancreatic Cancer Cell Lines with Respect to Metastasis.* Cancers (Basel), 2019. **11**(9).
204. Hattori, N., S. Yamada, K. Torii, S. Takeda, K. Nakamura, H. Tanaka, et al., *Effectiveness of plasma treatment on pancreatic cancer cells.* Int J Oncol, 2015. **47**(5): p. 1655-62.
205. Chen, Z., L. Lin, E. Gjika, X. Cheng, J. Canady, and M. Keidar, *Selective Treatment of Pancreatic Cancer Cells by Plasma-Activated Saline Solutions.* IEEE Transactions on Radiation and Plasma Medical Sciences, 2018. **2**(2): p. 116-120.

206. Khabipov, A., E. Freund, K.R. Liedtke, A. Kading, J. Riese, J. van der Linde, et al., *Murine Macrophages Modulate Their Inflammatory Profile in Response to Gas Plasma-Inactivated Pancreatic Cancer Cells.* Cancers (Basel), 2021. **13**(11).
207. Kumar, N., P. Attri, S. Dewilde, and A. Bogaerts, *Inactivation of human pancreatic ductal adenocarcinoma with atmospheric plasma treated media and water: a comparative study.* Journal of Physics D: Applied Physics, 2018. **51**(25): p. 255401.
208. Freund, E., C. Spadola, A. Schmidt, A. Privat-Maldonado, A. Bogaerts, T. von Woedtke, et al., *Risk Evaluation of EMT and Inflammation in Metastatic Pancreatic Cancer Cells Following Plasma Treatment.* Frontiers in Physics, 2020. **Volume 8 - 2020**.
209. Zhou, J., G. Wang, Y. Chen, H. Wang, Y. Hua, and Z. Cai, *Immunogenic cell death in cancer therapy: Present and emerging inducers.* J Cell Mol Med, 2019. **23**(8): p. 4854-4865.
210. Haertel, B., K. Eiden, A. Deuter, K. Wende, T.v. Woedtke, and U. Lindequist. *Differential effect of non-thermal atmospheric-pressure plasma on angiogenesis*. 2014. Letters in Applied NanoBioScience.
211. Boeckmann, L., M. Schäfer, T. Bernhardt, M.L. Semmler, O. Jung, G. Ojak, et al., *Cold Atmospheric Pressure Plasma in Wound Healing and Cancer Treatment.* Applied Sciences, 2020. **10**(19).
212. Zanoni, M., F. Piccinini, C. Arienti, A. Zamagni, S. Santi, R. Polico, et al., *3D tumor spheroid models for in vitro therapeutic screening: a systematic approach to enhance the biological relevance of data obtained.* Scientific Reports, 2016. **6**(1): p. 19103.
213. Mehta, G., A.Y. Hsiao, M. Ingram, G.D. Luker, and S. Takayama, *Opportunities and challenges for use of tumor spheroids as models to test drug delivery and efficacy.* J Control Release, 2012. **164**(2): p. 192-204.
214. Rodrigues, T., B. Kundu, J. Silva-Correia, S.C. Kundu, J.M. Oliveira, R.L. Reis, et al., *Emerging tumor spheroids technologies for 3D in vitro cancer modeling.* Pharmacol Ther, 2018. **184**: p. 201-211.
215. Pape, J., M. Emberton, and U. Cheema, *3D Cancer Models: The Need for a Complex Stroma, Compartmentalization and Stiffness.* Front Bioeng Biotechnol, 2021. **9**: p. 660502.
216. Zhu, Y., E. Kang, M. Wilson, T. Basso, E. Chen, Y. Yu, et al. *3D Tumor Spheroid and Organoid to Model Tumor Microenvironment for Cancer Immunotherapy*. Organoids, 2022. **1**, 149-167 DOI: 10.3390/organoids1020012.

CHAPTER 03

CAPTURING THE HETEROGENEITY OF THE PDAC TUMOR MICROENVIRONMENT: NOVEL TRIPLE CO-CULTURE SPHEROIDS FOR DRUG SCREENING AND ANGIOGENIC EVALUATION

Adapted from:
Verloy, R., Privat-Maldonado, A., Van Audenaerde, J., Rovers, S., Zaryouh, H., De Waele, J., Quatannens, D., Peeters, D., Roeyen, G., Deben, D., Smits, E. and Bogaerts, A. Capturing the Heterogeneity of the PDAC Tumor Microenvironment: Novel Triple Co-Culture Spheroids for Drug Screening and Angiogenic Evaluation. Cells, 2025. 14(6). doi:10.3390/cells14060450

3.1 Abstract

As discussed in previous chapter, PDAC presents significant treatment challenges due to its desmoplastic reaction, which impedes therapeutic effectiveness, highlighting the need for advanced in vitro models to better mimic the complex tumor environment. Currently 3D co-culture models of fibroblasts and endothelial cells are lacking, which presents a challenge for performing more comprehensive in vitro research. In this chapter I develop TCC spheroid models using MiaPaCa-2 and BxPC-3 cancer cell lines, with RLT-PSC and hPSC21 PSC lines and the EC line HMEC-1. These models are assessed through growth assays, multicolor flow cytometry to optimize cell ratios, cell viability assays to evaluate drug responses, and a tube formation assay with a spheroid-conditioned medium to examine angiogenesis. Our TCC spheroids effectively replicate the PDAC microenvironment, showing significant variations in drug responses influenced by cellular composition, density, and spatial arrangement. The tube formation assay showcases the potential of our models to quantitatively assess a treatment-induced angiogenic response. These cost-effective TCC in vitro spheroid models provide vital insights into the PDAC microenvironment, significantly improving the quality of the in vitro evaluation of treatment responses.

3.2 Introduction

As explained in previous chapter, PDAC is predicted to become the second leading cause of death by cancer before 2030, clearly emphasizing why improvement in treatment strategy is highly needed [1]. PDAC, which comprises approximately 85% of all pancreatic cancer cases [2], is characterized by a desmoplastic reaction, which triggers the formation of a dense, fibrous tumor stroma causing high intratumoral pressure. This serves as a physical barrier to therapy and causes vascular compression and hypovascularity, which inhibits drug delivery and induces chemoresistance [3]. In addition to their vital role in angiogenesis, ECs contribute to the complexity of the disease as CAFs through an endothelial-to-mesenchymal transition [4, 5]. Furthermore, activated PSCs, a specific type of fibroblast, act as the guardians of PDAC and are major contributors to the desmoplasia and the creation of a complex TME. This leads to the acquisition of properties like rapid growth, a highly invasive and metastatic potential; survival in hypoxic and low-nutrient conditions; and immunosuppression, among others [6]. Important point mutations in PDAC are *KRAS, SMAD4, CDKN2A*, and *TP53* [7]. *KRAS* is detected in 90% of the cases and is related to a worse prognosis alongside *CDKN2A* [8, 9]. *SMAD4* is correlated to an increased rate of metastasis and resistance to therapy, and *TP53* changes the immune milieu and promotes inflammation, which benefits the tumor [10, 11]. Single-cell RNA sequencing revealed that roughly 35% of all cells in PDAC tumors are cancerous, 26% are fibroblasts and PSCs, and 12% are ECs [12]. While other studies show similar results [13-16], it is important to note the cellular distribution spread among patients [12, 14]. The extreme cellular heterogeneity among patients (intertumoral) and within the tumors (intratumoral) increases the failure rate of therapies in clinical trials and highlights the importance of utilizing more complex models to capture this heterogeneity during the in vitro stage of research [17]. While pharmaceutical research and drug development has been ever-growing, the approval rate of new drugs is not experiencing the same uptrend [18]. This is partially caused by Phase III failures originating from inadequate preclinical screening [19].

To develop novel therapeutic approaches, we need better and more accessible in vitro models that can mimic the TME of PDAC. Simple models such as 2D cultures have been a

useful and economic approach for investigating fundamental questions for decades. However, these models are not sufficient to translate cellular responses to innovative treatment strategies that can tackle these complex diseases [20]. One simple and low-cost alternative is the use of 3D spheroids, which offer many advantages, including an oxygen gradient, scaffold-free tissue-like cellular organization, cellular crosstalk, high-throughput capabilities, and reproducibility [20-22]. Monoculture spheroids of cancer cells lack the stromal component of a tumor-like ECM deposition and a complex TME [21]. It has been stated that co-culture spheroids of a 1:1 and 2:1 ratio (cancer–stellate) are not representative of the PDAC stroma content [22-24]. In addition, attempts have been made to develop a TCC spheroid model for pancreatic cancer with fibroblasts and ECs. However, to our knowledge, they did not include enough PSCs, which are a highly specific cell population to PDAC that play a pivotal role in the desmoplastic response [25, 26]. In these studies, the authors used either lung fibroblasts or extremely low numbers of fibroblasts, which do not truly mimic PDAC tumors, and hence do not provide a full picture of the cell-to-cell interactions governing the PDAC TME. In addition, the intra- and intertumoral heterogeneity of the PDAC TME was not considered.

Another alternative is the use of patient-derived organoids (PDOs), which are gaining attention due to their clinical relevance and their value for understanding patient-specific drug responses for personalized cancer treatment [27]. However, they are reported to have low physical properties and a soft matrix [22, 28, 29]. Even though PDOs are highly valuable, in many laboratories there is still a lack of expertise and standardized protocols for the processing, culturing, and cryopreservation of these tissues with a high success rate [30]. In addition, most PDOs do not yet include the complex TME related to ECs and angiogenesis, and they require Matrigel or Cultrex (ECMs isolated from mouse sarcoma) which introduce unknown growth factors [31].

The translatability of in vitro research toward clinical observations will remain low without proper 3D models that consider the complex TME and its heterogeneity with clinically relevant numbers of different cell types to better study the treatment response. In this chapter, we therefore present a relevant panel of four high-throughput TCC spheroid

models of PDAC including both PSCs and ECs. To tackle the heterogeneity of the PDAC TME, we used cell lines with different characteristics for both PDAC cells and PSCs. Altogether, our four novel TCC spheroid models provide an affordable and relevant tool to advance the development of suitable therapies for PDAC that can be widely used for drug screening, angiogenic studies, and more.

3.3 Material and methods

3.3.1 Cell culture

The human PCC lines MiaPaCa-2 (ATCC®, Manassas, VA, USA) and BxPC-3 (ATCC®) were used in this chapter. The human immortalized PSC line RLT-PSC was kindly provided by Prof. Ralf Jesenofsky of the Faculty of Medicine, University of Mannheim [32], while the hPSC21 line was established at Tohoku University, Graduate School of Medicine, and was kindly provided by Prof. Atsushi Masamune [33]. In addition, the immortalized EC line HMEC-1 (ATCC®) was used. All cell lines were used for a maximum of 20 passages after thawing and tested for mycoplasma every 3 months, and short tandem repeats (STR) profiling has validated that the cell lines remained identical to the original cell line (see Supplementary Figures S3.1–S3.5 at the end of this chapter). PCCs and PSCs were cultured in Dulbecco's Modified Eagle Medium (DMEM, 10938025, Gibco, Grand Island, NY, USA) supplemented with 10% foetal bovine serum (FBS, 10270106, Life Technologies, Carlsbad, CA, USA), 100 U/mL penicillin, 100 µg/mL streptomycin (15140122, Life Technologies), and 2 mM L-glutamine (25030024, Life Technologies). PCCs and PSCs were transduced with NucLight Rapid Red (4741, Essen Biosciences, Ann Arbor, MI, USA) to express mKate2, and with NucLight Green (4475, Essen Biosciences) to express GFP, respectively. HMEC-1 cells were cultured in MCDB131 (10372019, ThermoFisher Scientific, Waltham, MA, USA) and supplemented with 10 ng/mL Epidermal Growth Factor (PHG0314, ThermoFisher Scientific), 1 µg/mL Hydrocortisone (H0396, Sigma Aldrich, St. Louis, MO, USA), 10 mM L-glutamine (25030024, Life Technologies), 10% FBS (10270106, Life Technologies), 100 U/mL penicillin, and 100 µg/mL streptomycin (15140122, Life Technologies). Cells were

maintained in a humidified incubator at 37 °C and 5% CO_2. HMEC-1 cells for the supplementary proliferation rate were transduced with CMV-GFP.

3.3.2 Proliferation rate

MiaPaCa-2, BxPC-3, RLT-PSC, hPSC21, and HMEC-1 cells were seeded in a flat 96-well plate (655180, Greiner Bio-One, Kremsmünster, Austria) in 200 µL (1000, 2000, 1000, 1000, and 1500 cells/well, respectively). Cells were either seeded in MCDB131 or DMEM (with or without supplements) to evaluate proliferation over time. Confluence was measured every 24 h using live-cell imaging with the Spark® Cyto (Tecan, Männedorf, Switzerland).

3.3.3 Triple co-culture spheroid seeding ratio optimization

To optimize the seeding densities for TCC spheroids of PCCs, PSCs, and ECs, initial pilot experiments tested cancer–stellate ratios (1:1 to 1:4) to ensure single, compact spheroid formation and qualitatively assess proportions via imaging (Figure S3.6a and b). The seeding density was tested in a range from 3000–7500 cells per spheroid to obtain a spheroid of 300–500 µm in diameter. Based on these results, ECs were added to form TCC, varying cancer–endothelial ratios (1:0.25 to 1:4). Spheroids were analyzed after 3 days using Orbits software to quantify relative proportions of each cell type (area-based) and were compared to clinical PDAC cellular percentages (Figure S3.6c and d). Due to the limitations of 2D image analysis, we continued final optimization using flow cytometry to accurately quantify cell-type proportions and refined seeding densities for clinically relevant spheroids.

3.3.4 Spheroid formation

3D co-culture spheroids were generated using the previously mentioned cell lines. Spheroids were seeded at 5000 (BxPC-3:RLT-PSC:HMEC-1 in a ratio of 7:2:4), 7000 (BxPC-3:hPSC21:HMEC-1 in a ratio of 6:5:3), 3500 (MiaPaCa-2:RLT-PSC:HMEC-1 in a ratio of 6:3:3), 4500 (MiaPaCA-2:hPSC21:HMEC-1 in a ratio of 5:6:4), 6000 (BxPC-3), and 4000 (MiaPaCa-2) cells per well, including 0.24% methylcellulose (M0512, Merck, Rahway, NJ, USA in ultra-low adherent (ULA) plates (7007, Corning®, Corning, NY, USA). Empty outer wells were filled with 200 µL of water to minimize evaporation and plates were sealed with a breathable

membrane (Z380059, Merck, Rahway, NJ, USA). The ULA plates were centrifuged at 453 × *g* for 10 min. Cells were incubated at 37 °C and 5% CO_2 for three days to promote spheroid formation, after which spheroids of 300–500 µm diameter were formed.

3.3.5 Flow cytometry

The characterization of the different cell types in the TCC spheroids was performed with multicolor flow cytometry. Forty-eight spheroids per condition were collected after three days of formation and dissociated with 1 mL of TrypLE (12604-021, Life Technologies) for 30 min while shaking and incubating at 37 °C and 5% CO_2. Mechanical stress was applied by pipetting up and down with 0.1% BSA-coated tips every 10 min. A total of 3 mL of medium was added, cells were pipetted up and down and vortexed, and a single cell suspension was obtained using a 70 µm strainer. All cells were resuspended in 200 µL FACS buffer and seeded in a 96-well round-bottom plate. Subsequently, all cell suspensions were pre-treated with human serum blocking solution (S1-100ML, Merck) for 15 min at room temperature (RT) to avoid non-specific binding and washed twice with FACS buffer. Cells were incubated with PE-Cy7 anti-human CD31 (303118, BioLegend, San Diego, CA, USA) antibody for 15 min at RT, then washed twice with FACS buffer. PCCs and PSCs were measured with mKate2 and GFP fluorophores that are expressed by the cell nuclei due to transduction, as explained earlier. Samples were measured on the NovoCyte Quanteon (Agilent Technologies, Santa Clara, CA, USA), and analysis of all flow cytometry experiments was performed using the FlowJo v10 software (Becton, Dickinson & Company, Franklin Lakes, NJ, USA).

3.3.6 Cell viability assay

Spheroids were formed over three days, as described earlier. The spheroid medium was refreshed by removing 100 µL of medium and adding 100 µL of fresh MCDB131 medium (50% medium renewal). GEM (S1714, 10 mM in DMSO, Selleck Chemicals, Houston, TX, USA) and PCX (S1150, 10 mM in DMSO, Selleck Chemicals) were applied as monotherapy or as combinational therapy using the D300e Digital Dispenser (Tecan). GEM and PCX were titrated in a range as monotherapy or in combination (Table 3.1). Cell viability curves were

set up by quantifying ATP from metabolically active cells with CellTiter-Glo® (G7571, Promega, Madison, WI, USA) after five days of drug treatment. DMSO normalization was performed based on the highest drug concentration to a maximum of 0.6% DMSO. Staurosporine (5 µM, S1421, Selleck Chemicals) was used as a 100% cell death control to normalize data. The area under the curve (AUC) value represents the area under the curve and is a measure for drug resistance. The higher the viability, the larger the AUC value will be, therefore indicating higher drug resistance.

Table 3.1. *Titration concentration range of gemcitabine and paclitaxel either as mono- or combinational therapy.*

Gemcitabine	Paclitaxel
2.5 nM	0.5 nM
5 nM	1 nM
25 nM	5 nM
50 nM	10 Nm
0.4 µM	80 nM
2.5 µM	0.4 µM
10 µM	2 µM

3.3.7 Enzyme-linked immunosorbent assay

Supernatant levels of VEGF in TCC spheroid-conditioned media were quantified using the LEGEND MAX™ Human VEGF ELISA Kit (446507, BioLegend) according to the manufacturer's instructions. Absorbance was measured at 450 nm and 570 nm (reference) using the Spark® Cyto (Tecan).

3.3.8 Tube formation assay

Assessment of angiogenesis was performed with a tube formation assay in a 384-well plate (3764, Corning®). The supernatant (spheroid-conditioned medium) of 3-day-old TCC spheroids cultured in 200 µL was refreshed by either renewing 100 µL with fresh medium to a total of 200 µL or removing 150 µL of medium and adding 50 µL of fresh medium for a total of 100 µL, both leading to a 50% medium refresh (indicated as 100 µL or 200 µL). Plates were then coated with 8 µL of Cultrex (3533, Bio-Techne, Minneapolis, MN, USA), centrifuged at 180 × *g* for three min and incubated for at least 60 min at 37 °C and 5% CO_2.

HMEC-1 cells were resuspended at 58,000 cells/mL (either in MCDB131 or spheroid-conditioned medium), and 40 µL of cell suspension was seeded on top of the Cultrex coating. Fresh MCDB131 medium was used as positive control, as this highly supports tube formation and loops. After 6 hours, images of the tubular network were taken using the Spark® Cyto (Tecan) with a 4× objective. This protocol was adapted to our application based on the literature [34, 35]. Python v3.12 was used to crop these images to a center-focused circular image to remove the out-of-focus outside regions of the well, caused by the meniscus shape of the Cultrex coating. Finally, the IKOSA® tube formation analysis (Kolaido, Altenrheim, Switzerland) was performed to gain four metrics: number of loops, covered area, total tube length, and number of branch points.

3.3.9 Patient samples

FFPE (Formalin-fixed paraffin-embedded) tissue blocks from 10 patients with PDAC were acquired from the Antwerp Biobank (Antwerp, Belgium; ID: BE71030031000). The usage of these samples was approved by the Ethics Committee at Antwerp University Hospital–University of Antwerp (UZA–UAntwerp) under the reference number EC14/47/48. Two patient samples were selected as representative tumors to represent multiple typical PDAC characteristics.

3.3.10 Immunohistochemistry

α-SMA staining was part of a previous study [36]. ETS-related gene (ERG) expression in the TME of clinical PDAC tumors was evaluated by staining for hematoxylin and eosin (H&E) and ERG of five µm-thick sections from formalin-fixed paraffin-embedded tissue blocks. Sections were baked at 60 °C for 2 h and heat-induced epitope retrieval was performed by incubation with Envision FLEX high pH antigen retrieval solution (GV80411-2, Dako, Glostrup, Denmark) for 20 min at 97 °C (PT-Link instrument, Dako). Next, peroxidase activity was quenched by incubating the slides in peroxidase blocking buffer (GE001, Dako) for 5 min. Incubation with an anti-ERG monoclonal antibody (GA65961-2, monoclonal anti-rabbit, clone EP111, Agilent Technologies) was performed for 20 min at room temperature. Visualization was achieved by using a rabbit-linker (K800921-2, Agilent) for 10 min and the

Envision FLEX detection kit (K802321-2, Agilent) for 20 min according to the manufacturer's instructions. All sections were counterstained with hematoxylin (105175, Merck) for 2 min, dehydrated, and mounted with mounting medium (SEA-1604-00A, Cellpath, Wales). Images were captured from digitized histological slides by using a Philips Ultra-Fast scanner and displayed at 200× final magnification.

3.3.11 Spheroid image analysis

Images of the TCC spheroids were captured using the non-confocal Spark® Cyto (Tecan) microscope with a 10× objective. Image acquisition was performed for brightfield, green (stellate), red (cancer), and blue (endothelial) fluorescent channels (Table 3.2).

Table 3.2. *Technical information on the image acquisition of TCC spheroids using the Spark® Cyto (Tecan).*

Dye	Excitation	Emission	LED Intensity (%)	Exposure Time (ms)
BxPC-3	543–566	580–611	25	300
MiaPaCa-2	543–566	580–611	20	60
RLT-PSC	461–487	500–530	10	50
hPSC21	461–487	500–530	20	80
HMEC-1	381–400	414–450	15	45

3.3.12 Statistical analysis

All experiments were performed at least three times with three replicates unless specified otherwise. The significances in the proliferation assay were evaluated using two-way ANOVA with Sidak's multiple comparison test using Prism v10.1.0 (GraphPad Software, San Diego, CA, USA). Dose-response curves were evaluated for significances using the AUC values ($p \leq 0.05$) and a linear mixed model with either the treatment or the spheroid combination as fixed effect using JMP Pro v17.0.0 software. Outlier tests were performed using Prism v10.1.0 (GraphPad Software). For multiple comparisons of all experimental groups, Tukey's honestly significant difference (HSD) was used. Statistical significances between the concentrations of VEGF in spheroid-conditioned media was also evaluated with linear mixed models using JMP Pro v17.0.0 software (JMP, Cary, NC, USA) and Tukey's HSD multiple comparisons test.

3.4 Results

3.4.1 MCDB131 medium is most optimal for triple co-culture spheroid formation

To include the heterogeneity of the PDAC TME, we used two PCC lines with different genetic backgrounds and associated characteristics (MiaPaCa-2 with CDKN2A gene deletion and KRAS and TP53 mutations, BxPC-3 with CDKN2A and SMAD4 gene deletion and BRAF, and TP53 mutations). PANC-1 and Capan-2 were also assessed in a preliminary monoculture spheroid formation assay. Unlike MiaPaCa-2, PANC-1, and Capan-2, BxPC-3 formed compact spheroids and was selected to introduce structural heterogeneity in our spheroid models. Capan-2 did not even form loose singular spheroids like MiaPaCa-2 and PANC-1. We decided to continue with MiaPaCA-2, which is frequently used in our lab and widely reported in the literature. Additionally, to increase heterogeneity, we also used two PSC lines with different origins (RLT-PSC originating from chronic pancreatitis, as this is one of the main causes of pancreatic cancer development, and hPSC21 originating from pancreatic cancer) and one EC line (HMEC-1) [32, 33]. As PCCs, PSCs, and ECs were cultured in different media, we evaluated the cell growth of each cell line in both DMEM (PCC and PSC culture medium) and MCDB131 (EC culture medium) to determine the optimal medium for TCC spheroid formation. Clearly, MCDB131 was able to sustain growth for all cell lines, similar to DMEM (MiaPaCa-2 and RLT-PSC) or better than DMEM (BxPC-3, hPSC21, and HMEC-1) (Figure S3.7). The DMEM medium supplemented with VEGF and FGF was not able to provide the required environment for ECs to grow to the same extent as they did in the MCDB131 medium (Figure S3.8). Therefore, the MCDB131 medium was chosen for spheroid culture.

3.4.2 Triple co-culture spheroids demonstrate the heterogeneity of the PDAC tumor microenvironment

To generate TCC spheroids with different characteristics of PDAC tumors, we first determined the optimal seeding densities for each cell type in a TCC environment. For this, we quantified the cell populations in 3-day-old spheroids by flow cytometry (Figures 3.1a

and S9). The seeding densities for each TCC spheroid type was adjusted to achieve similar population percentages in 3-day-old spheroids to those observed in patients' tumors, as reported in the literature (Table 3.3) [12-16]. These adjustments were made based on the quantitative data from the flow cytometry experiments (Figure S3.10). The final seeding ratios of the four distinct combinations of TCC spheroids that presented characteristics of clinical tumors and the different facets of the heterogeneous spectrum of PDAC (Figure 3.1b) were as follows: 7:2:4 BxPC-3:RLT-PSC:HMEC-1 (dense and round), 6:5:3 BxPC-3:RLT-PSC:HMEC-1 (well-defined fibrotic shield), 6:3:3 MiaPaCa-2:RLT-PSC:HMEC-1 (invasive PCCs protruding from spheroids), and 5:6:4 MiaPaCa-2:hPSC21:HMEC-1 (less-dense fibrotic shield). All four TCC combinations were able to form compact spheroids with diameters of 300–500 µm at 3 days post-seeding (Figure 3.1c). Notably, the seeding ratios of the different cell types did not correlate fully with the flow cytometry ratios after 3 days of formation (Figure 3.1b). This shows that the growth of these cells in a 3D co-culture environment is different from their 2D monoculture growth (Supplementary Figure S3.7).

We observed that the PSC line hPSC21 (which originates from pancreatic cancer) tended to organize itself around the tumor (Figure 3.1c), shielding it from the environment, a characteristic often seen in clinical PDAC tumors (Figure S3.11) and which has been linked to drug resistance. When this shield was not present (as observed in the spheroids generated with RLT-PSC that originates from chronic pancreatitis), the highly invasive nature of MiaPaCa-2 lead to the migration of PCCs out of the TCC spheroids, something not observed in TCC spheroids generated with BxPC-3. The TCC spheroid models showed typical characteristics of PDAC, including the presence of abundant fibroblasts with a fibrotic shield in some cases, invasive tumor edges (as observed in MiaPaCa-2 spheroids, Figure 3.1c), and a low number of ECs (characteristic of the limited vasculature present in PDAC tumors), as observed in human PDAC samples (Figure S3.11).

Altogether, these results show that the four different TCC spheroids developed here resemble PDAC tumor characteristics and have significant potential to improve in vitro research.

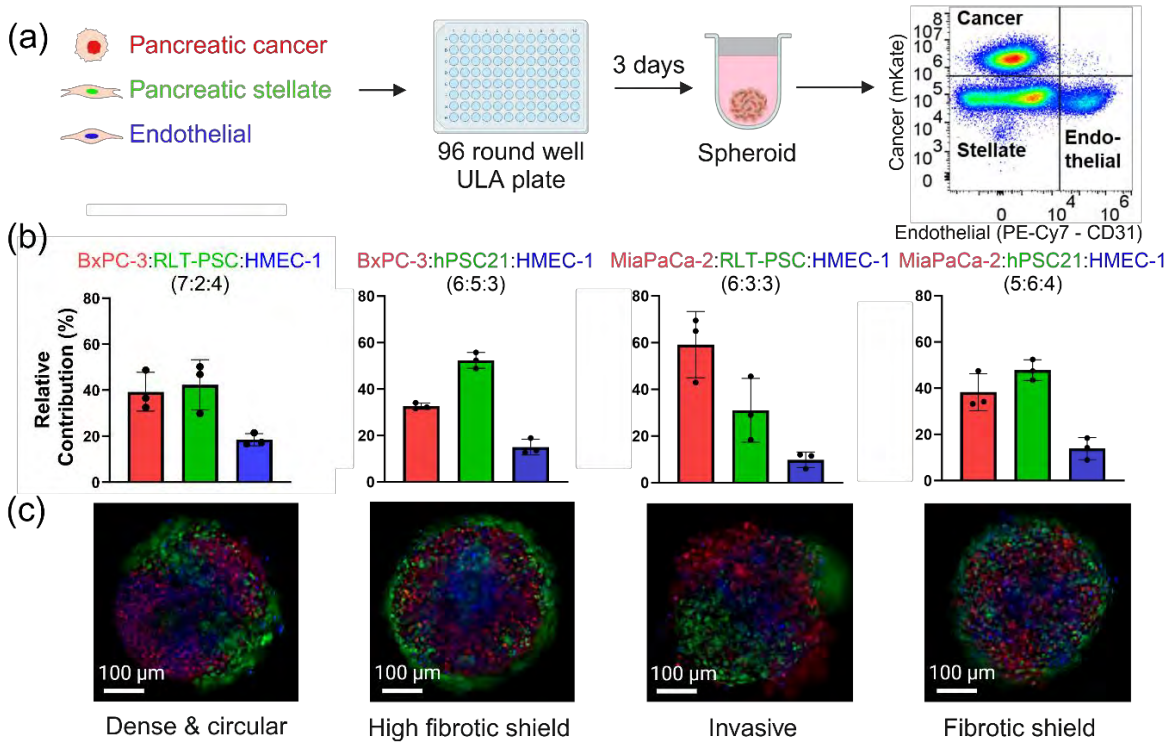

Figure 3.1. *Capturing the heterogeneity of PDAC in the scope of the TME with TCC spheroids.* ***(a)*** *Methodology for spheroid formation of pancreatic cancer (red fluorescently labelled nuclei), stellate (green fluorescently labelled nuclei), and ECs (CD31 positive).* ***(b)*** *Quantitative flow cytometric data showing the relative contribution of each cell population in our four spheroid combinations.* ***(c)*** *Representative live images of the TCC spheroids of pancreatic cancer (red), stellate (green), and endothelial (blue) cells. Data are represented as mean ± SD (n=3 of three independent experiments). Each dot represents one flow-cytometry measurement of a pool of 48 spheroids. ULA: ultra-low attachment.*

Table 3.3. *Cell population percentages in TCC spheroids after 3 days of formation, determined by flow cytometry and compared to literature [12].*

PDAC Tumor/Model	Cancer cells (%)	Stellate cells (%)	Endothelial cells (%)
BxPC-3:RLT-PSC:HMEC-1	39.25	42.29	18.46
BxPC-3:hPSC21:HMEC-1	32.63	52.35	15.02
MiaPaCa-2:RLT-PSC:HMEC-1	59.14	31.03	9.83
MiaPaCa-2:hPSC21:HMEC-1	38.30	47.80	13.90
Clinical PDAC tumors (recalculated excluding other cell types from literature) [12]	47.95	35.62	16.44

3.4.3 Improved spheroid compactness in the triple co-culture microenvironment better mimics the solid nature of PDAC

Given the solid nature of PDAC tumors, we quantitatively evaluated the spheroid diameter and qualitatively evaluated the compactness and general spheroid structure using live cell imaging (Figure 3.2), which we compared for TCC versus monoculture spheroids. We observed that both the monoculture and TCC spheroids of BxPC-3 cancer cells formed compact spheroids (Figure 3.2). In contrast, MiaPaCa-2 monoculture formed loose cell aggregates of roughly 1000 µm in diameter, which is different from the more solid and tightly packed structure observed when MiaPaCa-2 was seeded in combination with PSCs and ECs (approx. 400 µm diameter; Figure 3.2). This ability of MiaPaCa-2 to form compact spheroids upon co-culturing with PSCs and ECs highlights the influence and importance of the TME on the structure of PDAC tumors. This improved compactness in TCC spheroids is relevant, as PDAC is known to form highly solid and dense tumors in patients.

TCC spheroids generated with RLT-PSC in combination with BxPC3 or MiaPaCa-2 showed differences in their sensitivities to GEM, PCX, or both (Figure 3.3d). However, these differences were not present in TCC spheroids generated with hPSC21. Interestingly, BxPC-3:RLT-PSC:HMEC-1 spheroids exhibited higher resistance than any of the other three TCC spheroid models, as seen from the AUC values (Figure 3.3d). This suggests a distinct resistance profile in the context of the complex TME represented by this specific TCC spheroid.

Altogether, our results demonstrate that the different TMEs in our four spheroid combinations affect the drug response differently and highlight the importance of considering the TME heterogeneity in drug response studies.

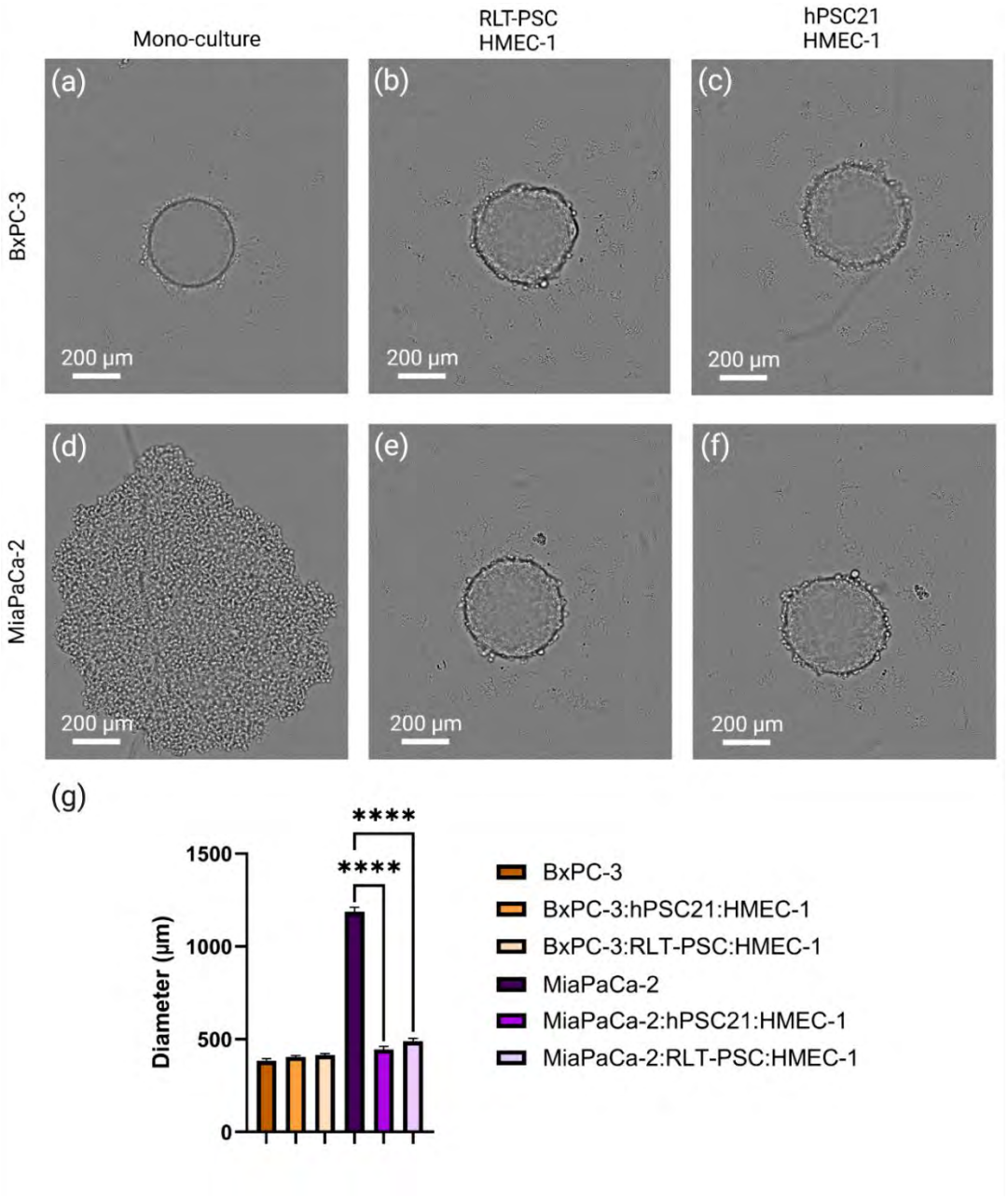

Figure 3.2. *A TCC environment ensures a dense spheroid structure. Representative brightfield images of (**a**) BxPC-3, (**b**) BxPC-3:RLT-PSC:HMEC-1 (7:2:4), (**c**) BxPC-3:hPSC21:HMEC-1 (6:5:3), (**d**) MiaPaCa-2, (**e**) MiaPaCa-2:RLT-PSC:HMEC-1 (6:3:3), and (**f**) MiaPaCa-2:hPSC21:HMEC-1 (5:6:4) spheroids. (**g**) Quantitative evaluation of the spheroid diameter as a mean of the width and length. Data are represented as mean ± SD (n = 9 from three independent experiments for TCC spheroids and n = 3 from one experiment for monoculture spheroids). **** = p ≤ 0.0001.*

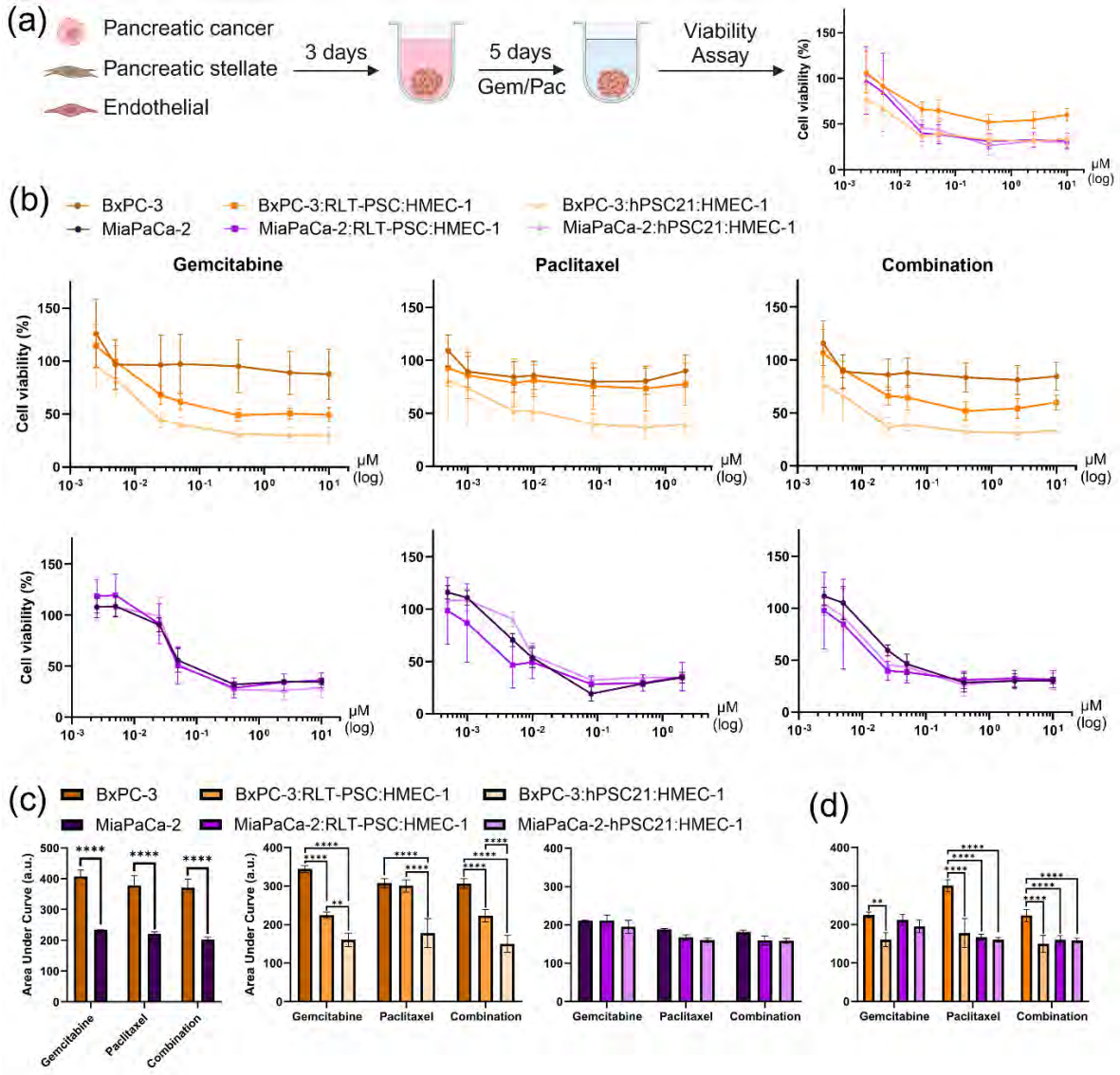

Figure 3.3. *GEM and PCX treatments of monoculture and TCC spheroids reveal different drug resistance profiles depending on the tumor microenvironment. (**a**) Methodology scheme to measure the cell viability of spheroids with CellTiter-Glo® after 5 days of drug treatment. (**b**) Cell viability curves of GEM- and PCX-treated monoculture and TCC spheroids. The x-axis in the combination plots corresponds to the GEM concentrations used; however PCX was co-administered in a 1:5 ratio (PCX–GEM). (**c**) Area under the curve as a measure of drug resistance of monoculture alone, and a comparison of monoculture and TCC spheroids per cancer cell line. (**d**) Area under the curve results of TCC spheroids. Data are represented as mean ± SD (n ≥ 7 from three independent experiments). All data were normalized to an untreated and 100% cell death control. A.u.: arbitrary units. ** = p ≤ 0.01; **** = p ≤ 0.0001.*

3.4.4 Triple co-culture spheroids and angiogenesis: exploring treatment response

Lastly, we investigated the value of our TCC spheroid models in angiogenesis studies using the tube formation assay in vitro (Figure 3.4a). We evaluated the presence of VEGF in the spheroid-conditioned medium when spheroids were cultured in 100 or 200 µL and after 24 or 72 h post-seeding. We concluded that a medium renewal of up to 100 µL 72 h post-seeding provided the highest VEGF concentrations (Figure 3.4b). In addition, we observed that MiaPaCa-2 TCC spheroid-conditioned media presented higher levels of VEGF than spheroid-conditioned media from BxPC3 TCC spheroids, showing a two-fold increase in TCC spheroids with hPSC21 (BxPC-3:hPSC21:HMEC-1, 214 pg/mL; MiaPaCa-2:hPSC21:HMEC-1; 383 pg/mL; $p \leq 0.0001$) and a three-fold increase in TCC spheroids with RLT-PSC (BxPC-3:RLT-PSC:HMEC-1, 185 pg/mL; MiaPaCa-2:RLT-PSC:HMEC-1; 487 pg/mL; $p \leq 0.0001$).

Tube formation in the EC monolayers was evaluated using the IKOSA® tube formation analysis, which provides four key parameters: number of loops, total tube length of the vessel network, total covered area of the vessels, and number of branch points (Figure 3.4c and d). In combination with the number of loops, the total tube length and covered area offered a better understanding of angiogenesis than the number of tubes alone, as the negative control often gave a high number of tubes due to the presence of single cells and disconnected short tubes. However, the presence of loops (Figure 3.4c and d positive control) represents a mature network of tubes [37], which was not present in the negative control or the spheroid-conditioned media. This correlates to the vascular compression and hypovascularity of PDAC. Compared to our negative and positive controls, BxPC-3:RLT-PSC:HMEC-1 and MiaPaCa-2:hPSC21:HMEC-1 spheroid-conditioned media showed high numbers of branching points, covered areas, and total tube lengths. In contrast, BxPC-3:hPSC21:HMEC-1 and MiaPaCa-2:RLT-PSC:HMEC-1 spheroid-conditioned media induced a lower number of branch points, total tube lengths, and covered areas (Figure 3.4d). Additionally, the number of loops is an interesting metric for studying a proangiogenic response, as none of the untreated spheroid-conditioned media resulted in a high number of loops, similar to the negative control (Figure 3.4d).

Our results demonstrate that the four TCC spheroids are valuable models for evaluating pro- or anti-angiogenic treatments, as shown by the differential production of VEGF in the spheroid-conditioned medium and the angiogenic response evoked in the ECs. Overall, we successfully developed four spheroid models that mimic the TME heterogeneity and its unique characteristics observed in patients with valuable potential for high-throughput screening of drug treatment and angiogenic evaluation (Table 3.4).

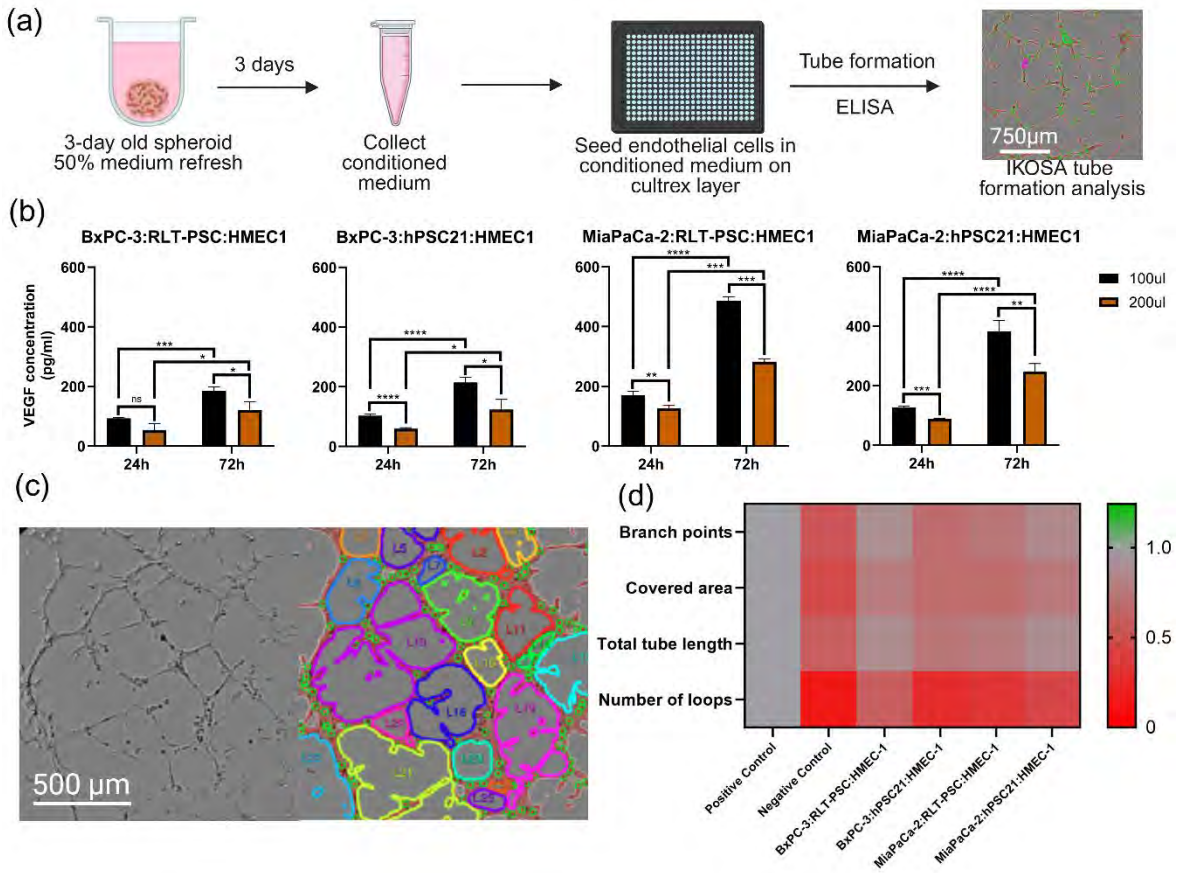

Figure 3.4. *Heterogenous PDAC TCC spheroids display distinct angiogenic profiles. (**a**) Methodology scheme of using spheroid-conditioned medium for a tube formation assay to evaluate angiogenesis. Three-day old spheroids could be treated with an angiogenic treatment schedule right after medium refreshment. (**b**) VEGF concentrations of spheroid-conditioned medium after 24 h or 72 h by ELISA (n = 3 from one independent experiment). (**c**) Raw (left) and IKOSA® analysis images (right) of a positive control showing tubes (red lines), branch points (small green circles, white arrow), and a high number of loops (colored perimeter lines). (**d**) Heat map of the IKOSA® tube formation analysis results for the positive and negative controls and the four combinations of untreated TCC spheroid-conditioned media. Data are represented as mean ± SD (n ≥ 8 from three independent experiments). * = p ≤ 0.05; ** = p ≤ 0.01; *** = p ≤ 0.001; **** = p ≤ 0.0001; ns = not significant. Color code of the heatmap was chosen to remain consistent with other heatmaps in this PhD thesis.*

Table 3.4. *Overview of the different proposed spheroid models, their seeding ratios, most visible characteristics, drug responses, and angiogenic responses.*

Spheroid Model	Seeding Ratio	Seeding Density (Cells)	Feature	Drug Response	Angiogenic Activity
BxPC-3:RLT-PSC:HMEC-1	7:2:4	5000	Dense	Low	High
BxPC-3:hPSC21:HMEC-1	6:5:3	7000	High fibrotic shield	High	Low
MiaPaCa-2:RLT-PSC:HMEC-1	6:3:3	3500	Invasive	High	Low
MiaPaCa-2:hPSC21:HMEC-1	5:6:4	4500	Fibrotic shield	High	High

3.5 Discussion

The complex and heterogeneous TME of PDAC, which is characterized by a dense stroma, limits drug delivery and can cause chemoresistance [3]. Recognizing the crosstalk between different cell types is essential for tackling PDAC and developing better screening tools for drug discovery [4-6]. In this chapter, we developed an innovative panel of four TCC spheroid models that represent the complex TME observed in different types of PDAC tumors, with high-throughput secondary screening potential for anti-cancer drugs and angiogenic compounds. Traditional 2D and monoculture models struggle with translatability towards in vivo and clinical studies, while the adoption of 3D co-culture in vitro models, particularly our clinically relevant and heterogeneous TCC spheroids, signify an important shift in PDAC research [20-22].

To generate the four TCC spheroid models presented in this study, we considered the literature-derived cell percentages observed in clinical tumors, determined by single-cell RNA sequencing (approximately 35% PCCs, 26% fibroblasts and PSCs, and 12% ECs, among other cell types with a notable spread between patients) [12, 14], which is also described in other studies [13-16]. This cellular distribution spread between patients also correlates to therapy response [13]. To account for the heterogeneity of the TME, a hallmark of PDAC, we used two different PCC and PSC lines, mirroring the inter- and intratumoral complexity and diversity, as well as cellular distribution, as observed in patient tumors [22]. Two TCC spheroid models containing hPSC21 cells presented different levels of fibrotic shields that correlate with the presence of desmoplastic tissue in PDAC samples. In contrast, TCC spheroids containing RLT-PSC cells formed dense and round spheroids (TCCs with BxPC3), as observed in the tightly packed invasive front in PDAC tumors, or a more disperse

distribution, characteristic of more aggressive and migratory PDAC (TCCs with MiaPaCa-2). It is known that BxPC-3 cells form dense spheroids that mimic the compactness of PDAC, and this could result in poor drug penetration and high drug resistance, as observed in our cell viability data as well [38]. In contrast, the structural support provided by PSCs and ECs to the TCC spheroids prevented the formation of loose spheroids with the aggressive MiaPaCa-2 cell line. This improved their compactness, which is true of clinical PDAC tumors, and resistance to common laboratory manipulation, e.g., pipetting of the spheroids without breaking their structure. This is an advantage of our TCC spheroids, because they allow the MiaPaCa-2 cell line to be investigated in a relevant 3D in vitro model, which is not possible otherwise with the overly loose and fragile monoculture cell aggregates.

It is important to consider the fact that MiaPaCa-2 presents more aggressive features than BxPC-3, such as a high expression of the mesenchymal marker vimentin, important for migration and invasion, and low expression of the epithelial marker e-cadherin, a tumor-suppressor protein involved both in EMT and tumor progression [39]. Indeed, it has been demonstrated that BxPC-3 spheroids express higher levels of cadherins than MiaPaCa-2, which are essential for spheroid formation [40]. Interestingly, we also observed the formation of a cluster of ECs in the core of 3-day old BxPC-3:hPSC21:HMEC-1 spheroids. This is in agreement with the distribution of ECs observed in 4-day-old PANC-1:MRC-5:HUVEC spheroids, where the cluster of HUVECs present in the core was progressively lost after 7 days [25]. The structural differences observed between monoculture and TCC spheroids highlight the importance of considering spatial arrangement, cell density, and the TME for mimicking clinical scenarios. The lack of crosstalk among different cell types in monoculture spheroids impacts various aspects, including responses to immunotherapy, growth rates, survival, invasion, metastasis, angiogenesis, and other critical factors [22, 41].

To validate the use of our models in drug screening, we assessed the drug response to first-line chemotherapeutics GEM and PAC in both monoculture and TCC spheroids. In this chapter, BxPC-3 monoculture spheroids exhibited higher resistance to treatment than BxPC-3 TCC spheroids. This agrees with a previous study demonstrating that BxPC-3 3D spheroids were more resistant to GEM than 2D cultures, although they only used

monoculture 3D spheroids [42]. In addition, in this chapter, the BxPC-3 spheroids demonstrated higher resistance to chemotherapy than the MiaPaCa-2 spheroids, and this was partially reversed in BxPC-3 TCC spheroids. Conversely, the TME of the TCC spheroids containing the MiaPaCa-2 cells did not significantly affect the overall survival of the cells exposed to chemotherapy. However, there are contradictory reports regarding the sensitivity to chemotherapeutic drugs of these PDAC cell lines. While BxPC-3 has been reported to be more sensitive to GEM than MiaPaCa-2 in 2D cultures [43, 44], another study reported the opposite [45]. This discrepancy could reflect the different responses achieved in the presence of a more complex TME and validates the use of diverse cell lines and TMEs exhibiting varying sensitivity to chemotherapy. This allows for a more comprehensive understanding of the dynamics of drug resistance. The differential drug response observed in TCC spheroids suggests specific interactions between cancer and stromal cells. Indeed, the genotypic and phenotypic characteristics of each cell line contribute to the creation of unique TMEs that influence growth, angiogenesis, and drug resistance, among others, where the specific communication between PCCs and PSCs is a key component [46]. The observed difference in drug responses in our TCC spheroid models matched the patient-specific drug resistance profiles recently shown in PDOs [47]. In this regard, we propose to use at least two TCC spheroid combinations to represent a highly resistant tumor (BxPC-3:RLT-PSC:HMEC-1) and a drug-sensitive tumor (MiaPaCa-2:hPSC21:HMEC-1). Both TCC spheroids consist of different PCC and PSC lines, which ensures heterogeneity. Our drug regimen serves as a proof-of-concept for TCC spheroid models and can be expanded to a broader spectrum of therapeutic agents for future investigations and high-throughput drug screening, assessing cell death of each cell type within the TCC spheroids to determine the effects of chemotherapy in a TCC environment.

We also tested the ability of our TCC spheroid models to induce angiogenesis, a hallmark of cancer, as the vasculature plays an important role in drug response, invasion, metastasis, and tumor growth [48]. It is known that cancer cells can release VEGF and other proangiogenic factors that modulate the development of ECs [49]. Using a tube formation assay and a spheroid-conditioned medium, we observed that TCC spheroids containing the

same type of cancer cells produced similar levels of VEGF and a notable difference in VEGF expression was observed in BxPC-3 TCC spheroids in comparison to MiaPaCa-2 TCC spheroids. However, the angiogenic potentials of the spheroid-conditioned media of each of them were different and highlights the importance of other growth factors (e.g., FGF, PDGF and PlGF secreted by or stimulated by PCCS, PSCs and ECs) in the tube formation of endothelial cells. These results suggest the presence of other angiogenic factors, such as TNF-α, IL-1, or IL-6, produced by the different cells of the TCCs [50]. A limitation of our model in this regard is the use of the commercial cell line HMEC-1, which is a dermal microvascular EC line that is not from pancreatic origin. Further research is needed to determine the types of factors and the cells in the TCCs secreting them that are responsible for the induction or inhibition of angiogenesis.

In comparison to the state-of-the-art 3D co-culture models [25, 26], we were able to include CAFs, more specifically PSCs, in a clinically relevant ratio to tumor cells, which created cell-to-cell interactions that reflected the complex TME of PDAC, as demonstrated by the comparison with the patient samples. Unlike other TCC spheroid models [25, 26], we developed four spheroid models that recreated the spread of cellular distribution observed among the patients and the TME heterogeneity, each of them with unique characteristics (Table 3.4). Our TCC spheroid models overcome some of the challenges still faced by PDOs, as the TCC spheroid models presented here incorporate the complex TME of PDAC while remaining a simple, low-cost, and easily accessible model suitable for high-throughput screening. Moreover, our TCC model can be combined and extended with PDOs, following full characterization and biobanking. We believe our models can also incorporate immune cells to provide an even more comprehensive understanding of the role of TME in treatment response, particularly in the context of immunotherapy [51]. Additionally, our TCC models can easily be extended toward PDOs instead of PCC lines, which would improve the clinical translatability of our models even further. Combined, our data show the importance and influence of the TME of PDAC in anti-cancer drug screening and angiogenic studies, for which we offer high-throughput in vitro 3D models that consider intra- and intertumoral heterogeneity.

3.6 Conclusions

We have established a panel of TCC spheroid models that capture the complexity and heterogeneity of the PDAC TME. Unlike other alternatives, we were able to achieve this with a simple, inexpensive, and easily reproducible method while ensuring that each cell population was present in a clinically relevant number. We showed the value of our TCC spheroids for high-throughput drug screening and angiogenesis evaluation; however, our model is not limited to these applications. We have provided a valuable tool for understanding this devastating disease and for exploring new treatment strategies with higher clinical translatability.

3.7 Supplementary figures

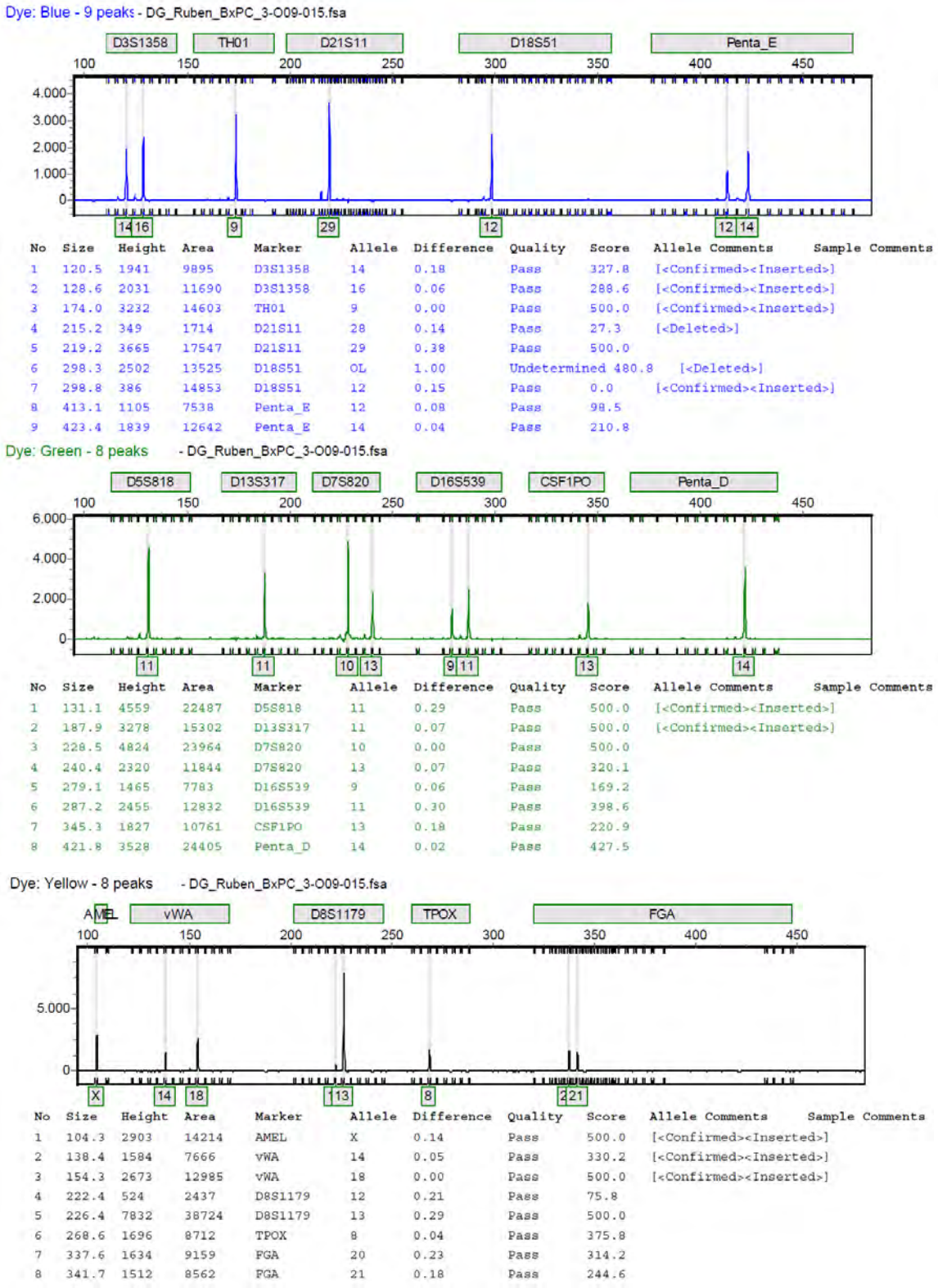

No	Size	Height	Area	Marker	Allele	Difference	Quality	Score	Allele Comments	Sample Comments
1	120.5	1941	9895	D3S1358	14	0.18	Pass	327.8	[<Confirmed><Inserted>]	
2	128.6	2031	11690	D3S1358	16	0.06	Pass	288.6	[<Confirmed><Inserted>]	
3	174.0	3232	14603	TH01	9	0.00	Pass	500.0	[<Confirmed><Inserted>]	
4	215.2	349	1714	D21S11	28	0.14	Pass	27.3	[<Deleted>]	
5	219.2	3665	17547	D21S11	29	0.38	Pass	500.0		
6	298.3	2502	13525	D18S51	OL	1.00	Undetermined	480.8	[<Deleted>]	
7	298.8	386	14853	D18S51	12	0.15	Pass	0.0	[<Confirmed><Inserted>]	
8	413.1	1105	7538	Penta_E	12	0.08	Pass	98.5		
9	423.4	1839	12642	Penta_E	14	0.04	Pass	210.8		

No	Size	Height	Area	Marker	Allele	Difference	Quality	Score	Allele Comments	Sample Comments
1	131.1	4559	22487	D5S818	11	0.29	Pass	500.0	[<Confirmed><Inserted>]	
2	187.9	3278	15302	D13S317	11	0.07	Pass	500.0	[<Confirmed><Inserted>]	
3	228.5	4824	23964	D7S820	10	0.00	Pass	500.0		
4	240.4	2320	11844	D7S820	13	0.07	Pass	320.1		
5	279.1	1465	7783	D16S539	9	0.06	Pass	169.2		
6	287.2	2455	12832	D16S539	11	0.30	Pass	398.6		
7	345.3	1827	10761	CSF1PO	13	0.18	Pass	220.9		
8	421.8	3528	24405	Penta_D	14	0.02	Pass	427.5		

No	Size	Height	Area	Marker	Allele	Difference	Quality	Score	Allele Comments	Sample Comments
1	104.3	2903	14214	AMEL	X	0.14	Pass	500.0	[<Confirmed><Inserted>]	
2	138.4	1584	7666	vWA	14	0.05	Pass	330.2	[<Confirmed><Inserted>]	
3	154.3	2673	12985	vWA	18	0.00	Pass	500.0	[<Confirmed><Inserted>]	
4	222.4	524	2437	D8S1179	12	0.21	Pass	75.8		
5	226.4	7832	38724	D8S1179	13	0.29	Pass	500.0		
6	268.6	1696	8712	TPOX	8	0.04	Pass	375.8		
7	337.6	1634	9159	FGA	20	0.23	Pass	314.2		
8	341.7	1512	8562	FGA	21	0.18	Pass	244.6		

Supplementary Figure 3.1. *STR profile of BxPC-3.*

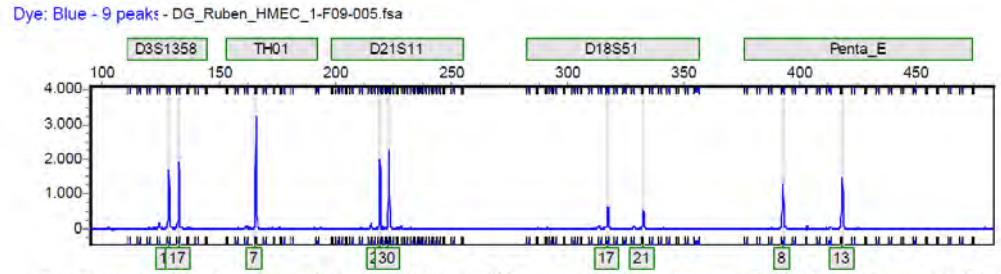

No	Size	Height	Area	Marker	Allele	Difference	Quality	Score	Allele Comments	Sample Comments
1	128.5	1682	8665	D3S1358	16	0.04	Pass	327.6	[<Confirmed><Inserted>]	
2	133.0	1591	9834	D3S1358	17	0.25	Pass	225.9	[<Confirmed><Inserted>]	
3	166.0	3212	14702	TH01	7	0.00	Pass	500.0	[<Confirmed><Inserted>]	
4	219.3	2010	9312	D21S11	29	0.28	Pass	481.0		
5	223.3	2249	10707	D21S11	30	0.23	Pass	500.0		
6	317.4	622	3381	D18S51	17	0.09	Pass	68.6		
7	332.6	543	2931	D18S51	21	0.19	Pass	55.6		
8	392.7	1269	7619	Penta_E	8	0.09	Pass	171.1		
9	418.4	1464	9353	Penta_E	13	0.15	Pass	190.7		

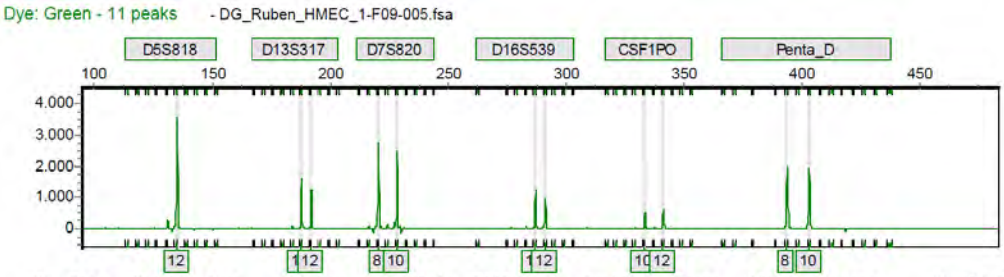

No	Size	Height	Area	Marker	Allele	Difference	Quality	Score	Allele Comments	Sample Comments
1	135.1	3515	17396	D5S818	12	0.20	Pass	500.0	[<Confirmed><Inserted>]	
2	188.0	1300	7765	D13S317	11	0.17	Pass	104.4	[<Confirmed><Inserted>]	
3	192.0	1265	5991	D13S317	12	0.33	Pass	158.8	[<Confirmed><Inserted>]	
4	220.4	2759	13563	D7S820	8	0.01	Pass	466.3		
5	228.4	2506	12473	D7S820	10	0.10	Pass	399.8		
6	287.1	1248	6382	D16S539	11	0.20	Pass	140.8		
7	291.1	993	5081	D16S539	12	0.16	Pass	98.4		
8	333.3	490	2539	CSF1PO	10	0.36	Pass	35.3		
9	341.4	610	3482	CSF1PO	12	0.18	Pass	42.9		
10	393.7	1995	12340	Penta_D	8	0.13	Pass	231.5		
11	403.2	1915	11838	Penta_D	10	0.05	Pass	217.0		

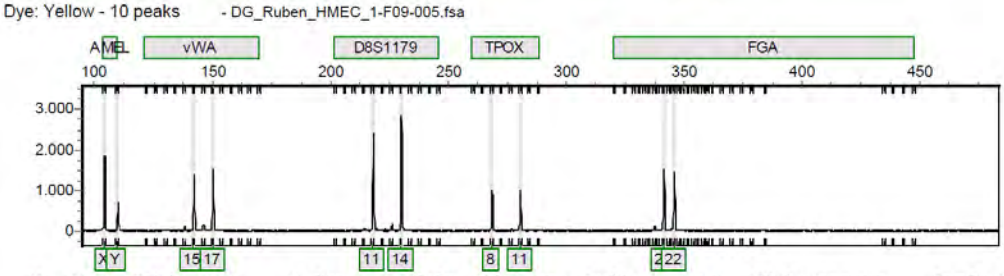

No	Size	Height	Area	Marker	Allele	Difference	Quality	Score	Allele Comments	Sample Comments
1	104.3	1850	9274	AMEL	X	0.14	Pass	499.3	[<Confirmed><Inserted>]	
2	110.0	706	3394	AMEL	Y	0.07	Pass	133.2	[<Confirmed><Inserted>]	
3	142.3	1360	6555	vWA	15	0.02	Pass	343.9	[<Confirmed><Inserted>]	
4	150.3	1524	7245	vWA	17	0.02	Pass	408.5	[<Confirmed><Inserted>]	
5	218.3	2412	11120	D8S1179	11	0.06	Pass	500.0		
6	230.3	2821	13308	D8S1179	14	0.16	Pass	500.0		
7	268.7	975	4918	TPOX	8	0.06	Pass	198.8		
8	280.7	1000	4992	TPOX	11	0.03	Pass	209.3		
9	341.7	1528	8414	FGA	21	0.18	Pass	334.8		
10	345.8	1440	7960	FGA	22	0.14	Pass	306.0		

Supplementary Figure 3.2. *STR profile of HMEC-1.*

Dye: Blue - 9 peaks - DG_Ruben_hPSC21-D09-003.fsa

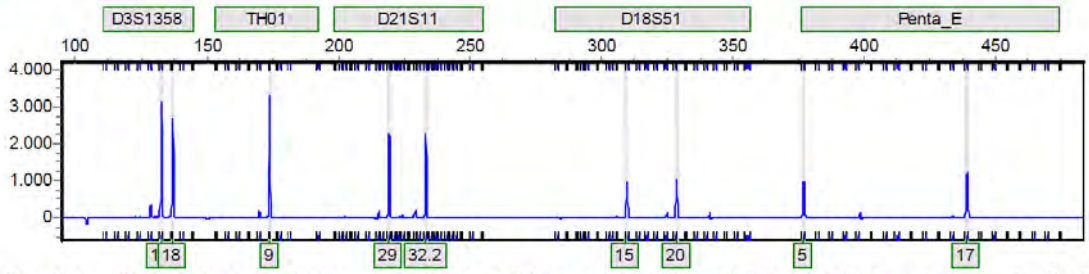

No	Size	Height	Area	Marker	Allele	Difference	Quality	Score	Allele Comments	Sample Comments
1	132.9	2977	15864	D3S1358	17	0.15	Pass	500.0	[<Confirmed><Inserted>]	
2	137.0	2641	12882	D3S1358	18	0.14	Pass	500.0	[<Confirmed><Inserted>]	
3	174.1	2782	15092	TH01	9	0.10	Pass	500.0	[<Confirmed><Inserted>]	
4	219.3	2250	10632	D21S11	29	0.28	Pass	493.7		
5	233.3	2276	10928	D21S11	32.2	0.18	Pass	492.1		
6	309.8	989	5244	D18S51	15	0.49	Pass	145.8		
7	328.8	1075	5734	D18S51	20	0.20	Pass	162.8		
8	377.1	984	5847	Penta_E	5	0.10	Pass	118.8		
9	439.3	1210	8172	Penta_E	17	0.07	Pass	148.2		

Dye: Green - 10 peaks - DG_Ruben_hPSC21-D09-003.fsa

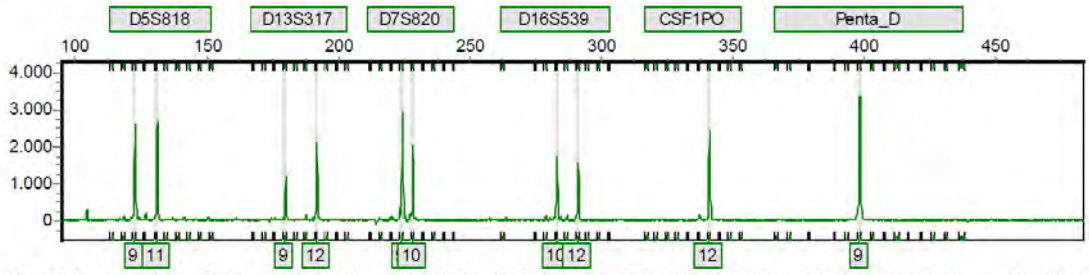

No	Size	Height	Area	Marker	Allele	Difference	Quality	Score	Allele Comments	Sample Comments
1	122.8	2362	12865	D5S818	9	0.34	Pass	326.2	[<Confirmed><Inserted>]	
2	131.2	2411	13235	D5S818	11	0.39	Pass	327.7	[<Confirmed><Inserted>]	
3	180.0	1213	5522	D13S317	9	0.24	Pass	124.0	[<Confirmed><Inserted>]	
4	191.8	2132	9674	D13S317	12	0.13	Pass	305.3	[<Confirmed><Inserted>]	
5	224.5	2933	14300	D7S820	9	0.09	Pass	438.2		
6	228.4	2009	10085	D7S820	10	0.10	Pass	248.1		
7	283.1	1731	8919	D16S539	10	0.08	Pass	207.5		
8	291.2	1566	8205	D16S539	12	0.06	Pass	174.9		
9	341.4	2403	13234	CSF1PO	12	0.18	Pass	328.4		
10	398.5	3351	20917	Penta_D	9	0.01	Pass	500.0		

Dye: Yellow - 7 peaks - DG_Ruben_hPSC21-D09-003.fsa

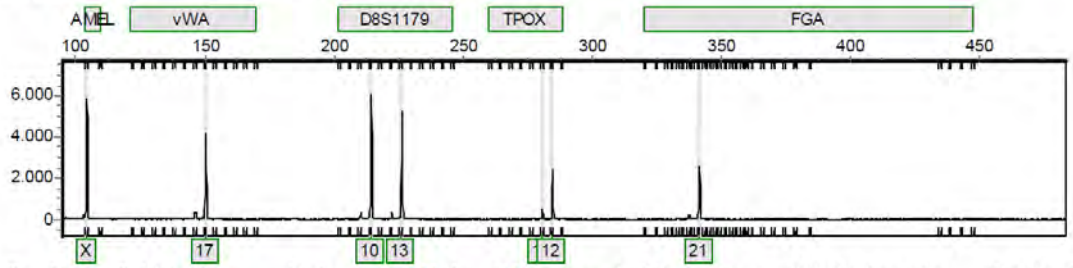

No	Size	Height	Area	Marker	Allele	Difference	Quality	Score	Allele Comments	Sample Comments
1	104.2	5837	28216	AMEL	X	0.04	Pass	500.0	[<Confirmed><Inserted>]	
2	150.3	4132	19573	vWA	17	0.02	Pass	500.0	[<Confirmed><Inserted>]	
3	214.4	6008	27895	D8S1179	10	0.12	Pass	500.0		
4	226.3	5238	24110	D8S1179	13	0.19	Pass	500.0		
5	280.7	488	2510	TPOX	11	0.03	Pass	67.2		
6	284.7	2361	11743	TPOX	12	0.02	Pass	500.0		
7	341.7	2553	13710	FGA	21	0.18	Pass	500.0		

Supplementary Figure 3.3. *STR profile of hPSC21.*

Dye: Blue - 9 peaks - DG_Ruben_MiaPACa_2-M09-013.fsa

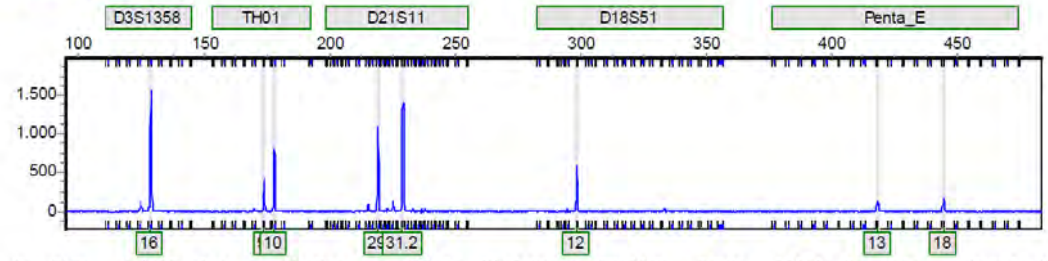

No	Size	Height	Area	Marker	Allele	Difference	Quality	Score	Allele Comments	Sample Comments
1	128.8	1551	7591	D3S1358	16	0.26	Pass	312.7	[<Confirmed><Inserted>]	
2	173.9	415	1983	TH01	9	0.10	Pass	49.6	[<Confirmed><Inserted>]	
3	177.9	807	3721	TH01	10	0.10	Pass	129.3	[<Confirmed><Inserted>]	
4	219.2	1090	5276	D21S11	29	0.38	Pass	217.2		
5	229.2	1402	6894	D21S11	31.2	0.27	Pass	304.0		
6	298.4	586	3085	D18S51	OL	1.00	Undetermined	75.6	[<Deleted>]	
7	298.7	208	3293	D18S51	12	0.25	Pass	0.0	[<Confirmed><Inserted>]	
8	418.3	142	1048	Penta_E	13	0.05	Pass	3.1	[<Confirmed>]	
9	444.6	172	1298	Penta_E	18	0.24	Pass	4.5	[<Confirmed>]	

Dye: Green - 12 peaks - DG_Ruben_MiaPACa_2-M09-013.fsa

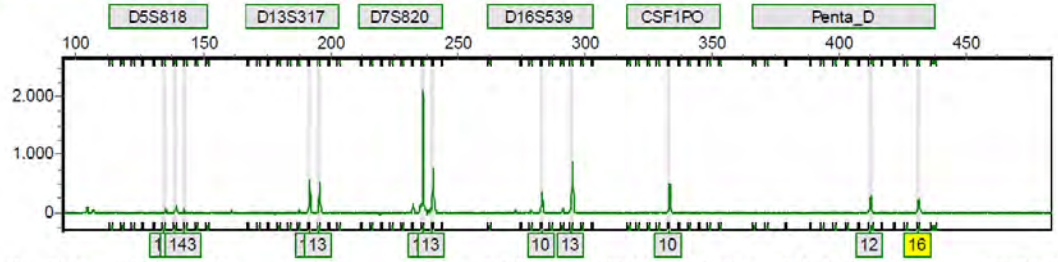

No	Size	Height	Area	Marker	Allele	Difference	Quality	Score	Allele Comments	Sample Comments
1	135.0	67	413	D5S818	12	0.10	Pass	0.9	[<Confirmed><Inserted>]	
2	139.3	140	715	D5S818	13	0.13	Pass	4.8	[<Confirmed><Inserted>]	
3	142.5	57	276	D5S818	143	0.76	Pass	1.1	[<Confirmed><Inserted>]	
4	191.8	552	2709	D13S317	12	0.13	Pass	51.9	[<Confirmed><Inserted>]	
5	195.9	525	2560	D13S317	13	0.23	Pass	48.3	[<Confirmed><Inserted>]	
6	236.4	2096	10556	D7S820	12	0.18	Pass	369.2		
7	240.4	761	3872	D7S820	13	0.07	Pass	82.9		
8	283.1	372	2030	D16S539	10	0.08	Pass	26.1		
9	295.2	866	4750	D16S539	13	0.11	Pass	100.1		
10	333.3	496	2805	CSF1PO	10	0.36	Pass	37.0		
11	412.5	275	1854	Penta_D	12	0.32	Pass	10.3		
12	431.4	244	1778	Penta_D	16	0.04	Check	6.5		

Dye: Yellow - 6 peaks - DG_Ruben_MiaPACa_2-M09-013.fsa

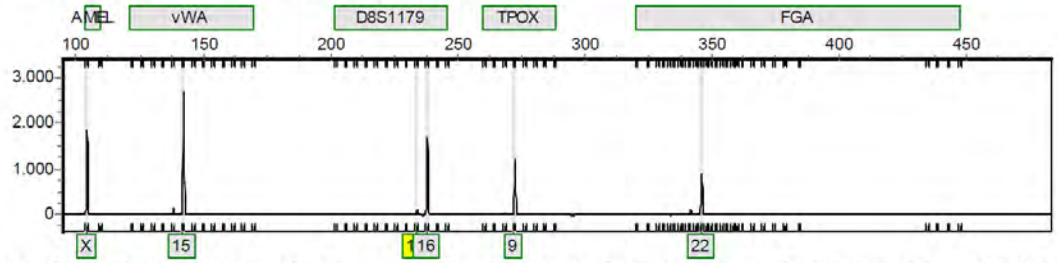

No	Size	Height	Area	Marker	Allele	Difference	Quality	Score	Allele Comments	Sample Comments
1	104.2	1852	9006	AMEL	X	0.04	Pass	404.9	[<Confirmed><Inserted>]	
2	142.3	2681	12966	vWA	15	0.02	Pass	500.0	[<Confirmed><Inserted>]	
3	234.2	123	541	D8S1179	15	0.04	Check	8.0		
4	238.2	1677	8176	D8S1179	16	0.06	Pass	397.4		
5	272.6	1195	6135	TPOX	9	0.01	Pass	228.8		
6	345.9	910	5071	FGA	22	0.24	Pass	134.8		

Supplementary Figure 3.4. *STR profile of MiaPaCa-2.*

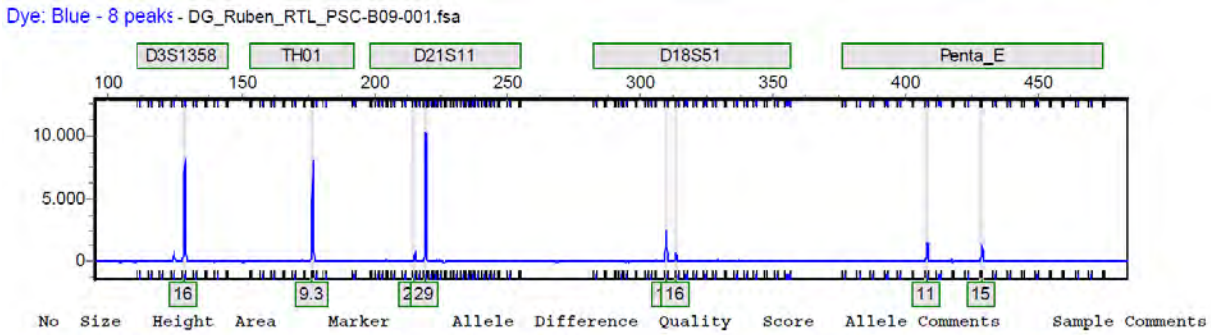

No	Size	Height	Area	Marker	Allele	Difference	Quality	Score	Allele Comments	Sample Comments
1	128.7	8207	40189	D3S1358	16	0.16	Pass	500.0	[<Confirmed><Inserted>]	
2	177.0	7001	36939	TH01	9.3	0.00	Pass	500.0	[<Confirmed><Inserted>]	
3	215.4	861	3967	D21S11	28	0.34	Pass	126.0		
4	219.3	10159	49690	D21S11	29	0.28	Pass	500.0	[<SAT (Repaired)><Confirmed>]	
5	309.9	2507	12898	D18S51	15	0.39	Pass	464.2		
6	313.8	498	3536	D18S51	16	0.47	Pass	20.2	[<Confirmed><Inserted>]	
7	408.1	1519	9089	Penta_E	11	0.02	Pass	202.0		
8	428.8	1393	9103	Penta_E	15	0.16	Pass	152.7		

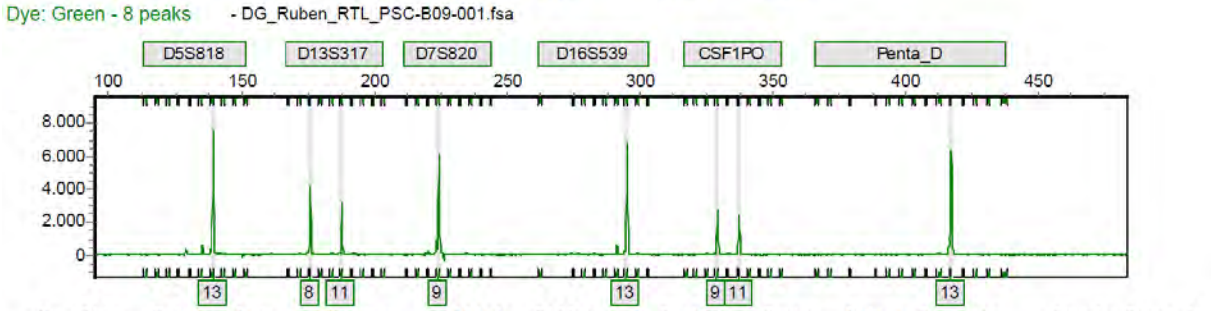

No	Size	Height	Area	Marker	Allele	Difference	Quality	Score	Allele Comments	Sample Comments
1	139.4	7479	37796	D5S818	13	0.23	Pass	500.0	[<Confirmed><Inserted>]	
2	176.0	4204	19100	D13S317	8	0.08	Pass	500.0	[<Confirmed><Inserted>]	
3	188.0	2927	14261	D13S317	11	0.17	Pass	379.2	[<Confirmed><Inserted>]	
4	224.4	6008	28658	D7S820	9	0.01	Pass	500.0		
5	295.2	6822	33962	D16S539	13	0.11	Pass	500.0		
6	329.3	2704	14098	CSF1PO	9	0.24	Pass	354.6		
7	337.3	2455	13203	CSF1PO	11	0.12	Pass	294.2		
8	417.2	6371	40378	Penta_D	13	0.07	Pass	500.0		

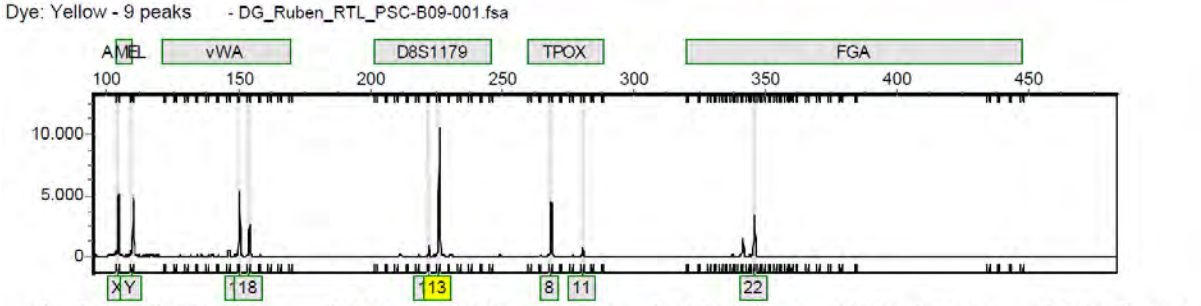

No	Size	Height	Area	Marker	Allele	Difference	Quality	Score	Allele Comments	Sample Comments
1	104.2	5029	25555	AMEL	X	0.04	Pass	500.0	[<Confirmed><Inserted>]	
2	110.0	4659	22431	AMEL	Y	0.07	Pass	500.0	[<Confirmed><Inserted>]	
3	150.3	5403	25638	vWA	17	0.02	Pass	500.0	[<Confirmed><Inserted>]	
4	154.3	2650	12277	vWA	18	0.00	Pass	500.0	[<Confirmed><Inserted>]	
5	222.3	934	4122	D8S1179	12	0.11	Pass	151.9		
6	226.3	10466	55948	D8S1179	13	0.19	Check	500.0	[<SAT (Repaired)>]	
7	268.7	4467	22335	TPOX	8	0.06	Pass	500.0		
8	280.8	746	3786	TPOX	11	0.07	Pass	101.8		
9	345.8	3376	17902	FGA	22	0.14	Pass	500.0		

Supplementary Figure 3.5. *STR profile of RLT-PSC.*

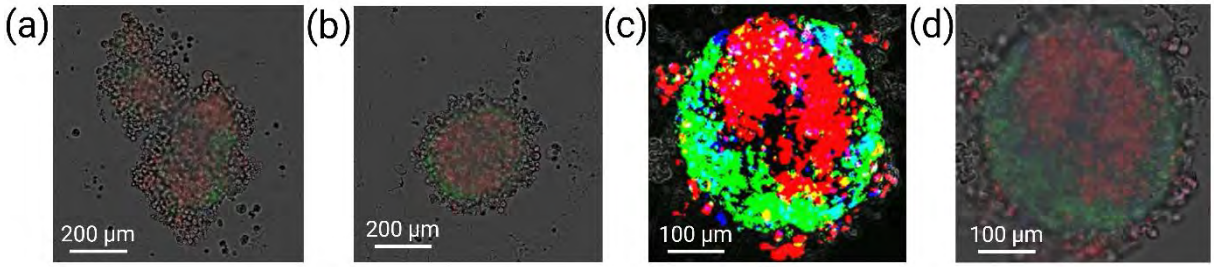

Supplementary Figure 3.6. *Initial optimization process of TCC spheroids. Representative images of (a) MiaPaCa-2:hPSC21 (1:1) spheroids which are not forming a single spheroid, and (b) MiaPaCa-2:hPSC21 (1:2) as a single spheroid. (c) Example of the masking of cancer (red), stellate (green) and endothelial (blue) cells using the Orbits image analysis software to quantify each cell type proportion on MiaPaCa-2:hPSC21:HMEC-1 (5:12:8) and (d) the original processed image of the Spark® Cyto (Tecan).*

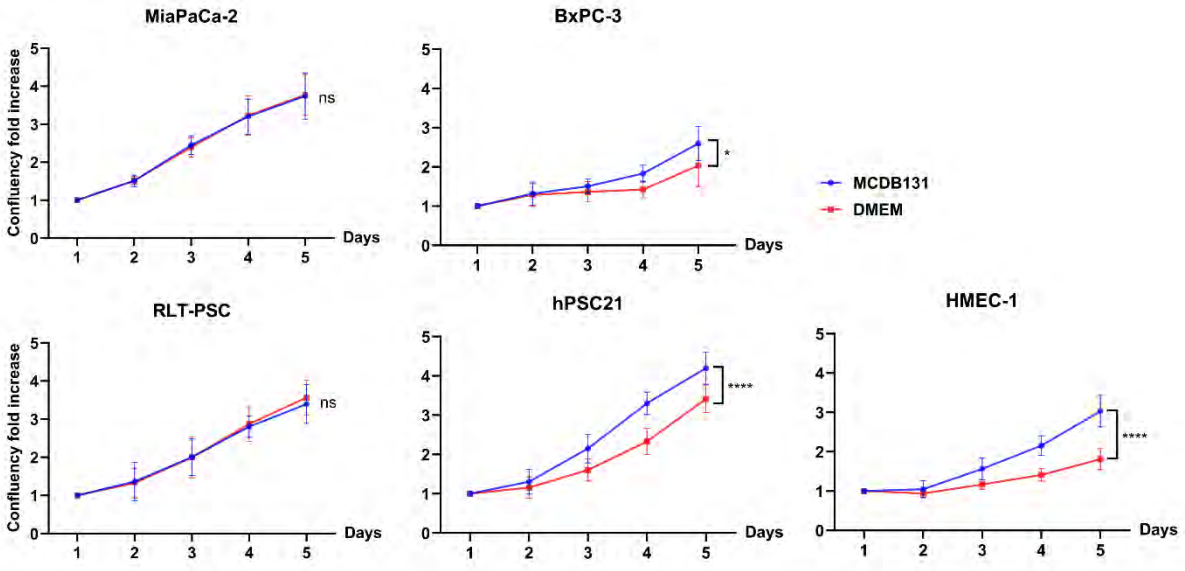

Supplementary Figure 3.7. *MCDB131 is the most suitable medium for spheroid culture. Proliferation rate comparison of MiaPaCa-2, BxPC-3, RLT-PSC, hPSC21, and HMEC-1 in DMEM and MCDB131 is showed based on the confluence fold ratio normalized to day 1. Data are represented as mean ± SD (n ≥ 10 from three independent experiments). Statistics were performed using two-way ANOVA with Sidak's multiple comparison test using Prism v10.1.0 (GraphPad Software, San Diego, CA, USA). * = p ≤ 0.05; **** = p ≤ 0.0001; ns = not significant.*

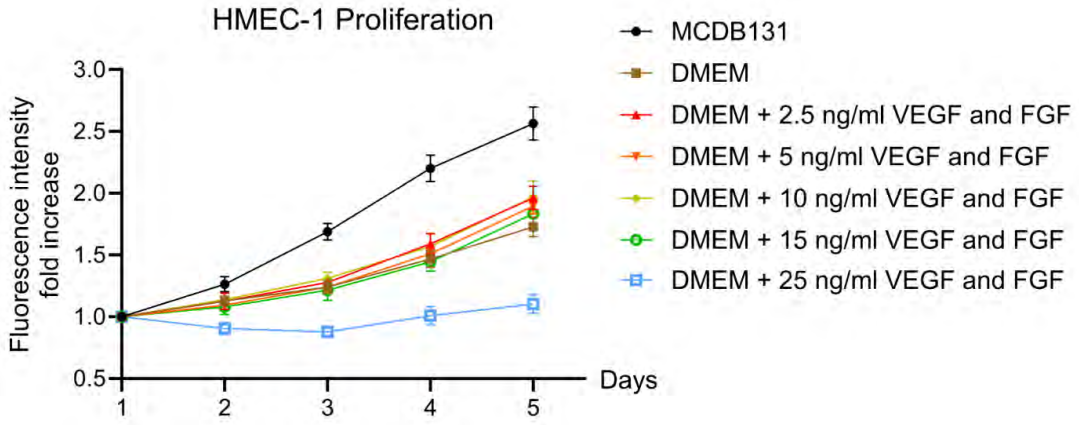

Supplementary Figure 3.8. *DMEM with VEGF/FGF supplements is not able to provide sufficient growth factors for HMEC-1 growth. Proliferation rate comparison of HMEC-1 growth in MCDB131 vs DMEM vs DMEM with supplements, based on green fluorescence intensity fold ratio as a measure of confluency normalized to day 1. Data are represented as mean ± SD (n ≥ 9 from three independent experiments).*

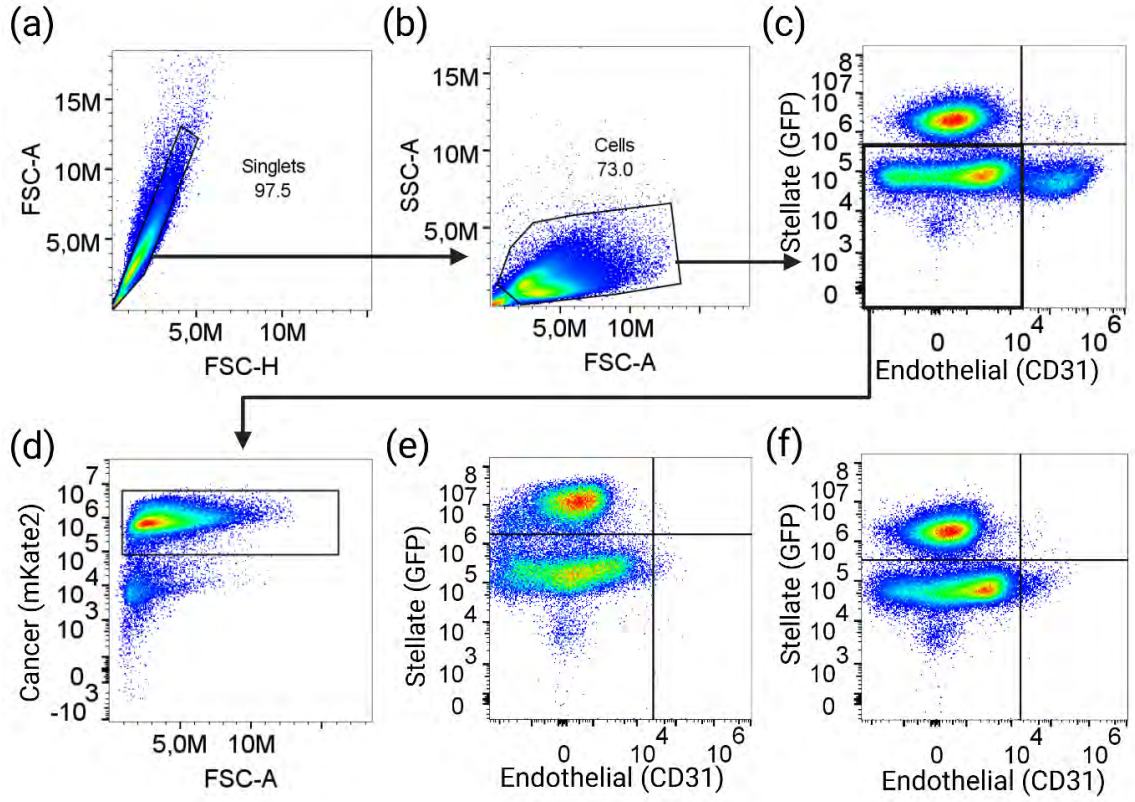

Supplementary Figure 3.9*. Flow cytometry gating strategy. (a) Singlets, (b) cells, (c) double negative population for GFP and CD31, (d) positive population of the mKate2 (Cancer). (e) FMO control for CD31 on BxPC-3:RLT-PSC:HMEC-1 spheroids. (f) FMO control for CD31 on MiaPaCa-2:hPSC21:HMEC-1.*

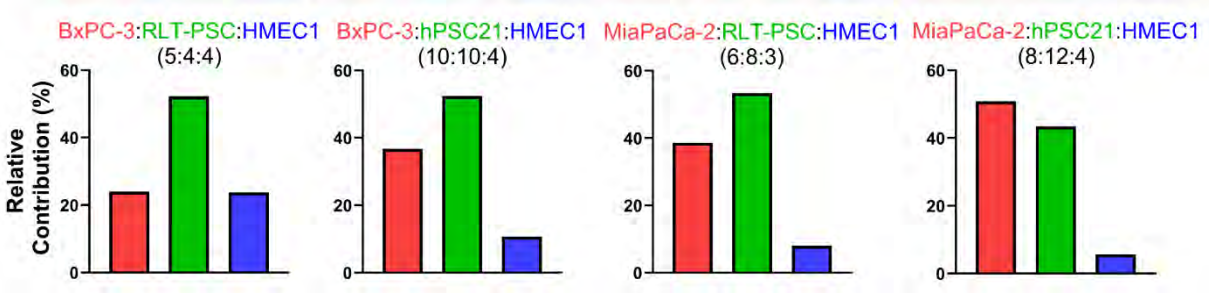

Supplementary Figure 3.10. Quantitative *flow cytometric data of TCC spheroid ratios that were not selected as optimal. Data shows the relative contribution of each cell population (each bar represents one flow cytometry measurement of a pool of 48 spheroids). Examples of TCC spheroids that were not selected due to an inaccurate representation of PDAC tumors.*

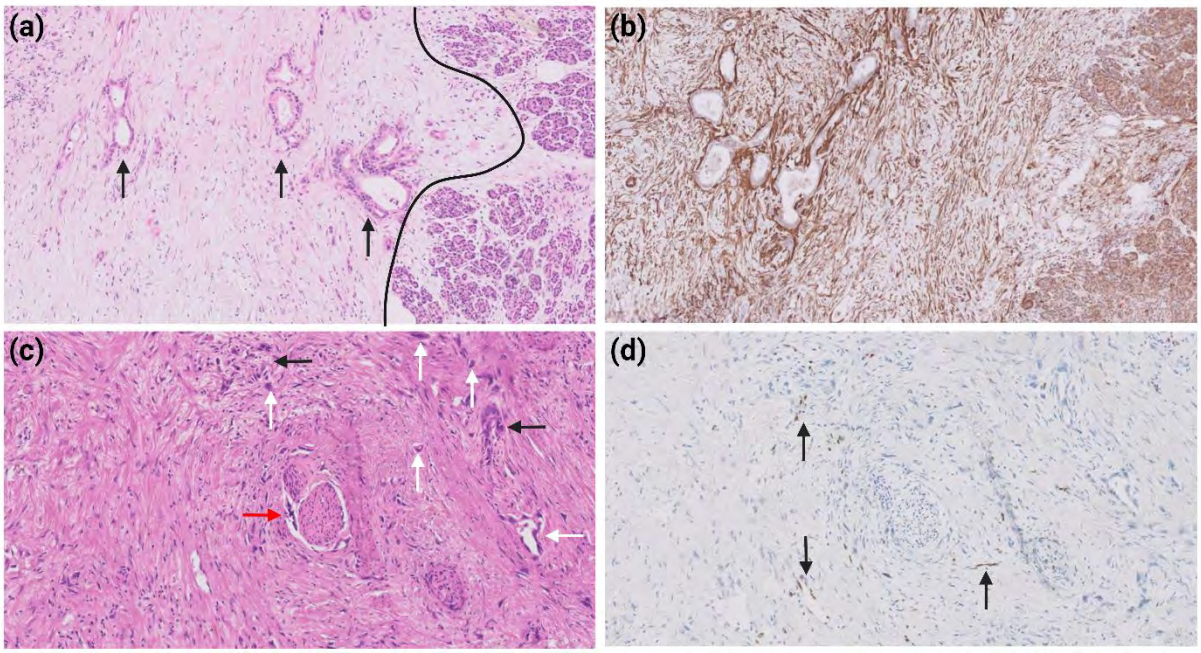

Supplementary Figure 3.11. *H&E and immunohistochemical staining of representative PDAC samples illustrating typical characteristics of the PDAC. (a) H&E staining of a PDAC sample at the invasive front of the tumor (black line). Note the abundant amount of desmoplastic stroma surrounding neoplastic ductular structures around the invasive carcinoma (left, black arrows). (b) Immunohistochemical staining for α-SMA of the same tumor as shown in (a), illustrating myofibroblastic differentiation of the tumor stroma. (c) Different tumor composed of perineural invasion (orange horizontal arrow), isolated tumor cells (white vertical arrows) and poorly formed ducts (black horizontal arrows) embedded in abundant desmoplastic stroma consisting of activated fibroblasts and myofibroblasts. (d) Immunohistochemical staining for ERG, a nuclear marker of ECs (brown), of the same tumor as shown in (c), illustrating sparse vasculature consisting of thin-walled capillary-size vessels with scanty luminal diameter (black arrows).*

3.8 References

1. Rahib, L., B.D. Smith, R. Aizenberg, A.B. Rosenzweig, J.M. Fleshman, and L.M. Matrisian, *Projecting cancer incidence and deaths to 2030: the unexpected burden of thyroid, liver, and pancreas cancers in the United States.* Cancer Res, 2014. **74**(11): p. 2913-21.
2. Hasan, S., R. Jacob, U. Manne, and R. Paluri, *Advances in pancreatic cancer biomarkers.* Oncol Rev, 2019. **13**(1): p. 410.
3. de Sousa Cavalcante, L. and G. Monteiro, *Gemcitabine: metabolism and molecular mechanisms of action, sensitivity and chemoresistance in pancreatic cancer.* Eur J Pharmacol, 2014. **741**: p. 8-16.
4. Zeisberg, E.M., S. Potenta, L. Xie, M. Zeisberg, and R. Kalluri, *Discovery of endothelial to mesenchymal transition as a source for carcinoma-associated fibroblasts.* Cancer Res, 2007. **67**(21): p. 10123-8.
5. Platel, V., S. Faure, I. Corre, and N. Clere, *Endothelial-to-Mesenchymal Transition (EndoMT): Roles in Tumorigenesis, Metastatic Extravasation and Therapy Resistance.* Journal of Oncology, 2019. **2019**: p. 8361945.
6. Verloy, R., A. Privat-Maldonado, E. Smits, and A. Bogaerts, *Cold Atmospheric Plasma Treatment for Pancreatic Cancer-The Importance of Pancreatic Stellate Cells.* Cancers (Basel), 2020. **12**(10): p. 2782.
7. Hayashi, H., T. Higashi, T. Miyata, Y.I. Yamashita, and H. Baba, *Recent advances in precision medicine for pancreatic ductal adenocarcinoma.* Ann Gastroenterol Surg, 2021. **5**(4): p. 457-466.
8. Nusrat, F., A. Khanna, A. Jain, W. Jiang, H. Lavu, C.J. Yeo, et al., *The Clinical Implications of KRAS Mutations and Variant Allele Frequencies in Pancreatic Ductal Adenocarcinoma.* J Clin Med, 2024. **13**(7).
9. Stefanoudakis, D., M. Frountzas, D. Schizas, N.V. Michalopoulos, A. Drakaki, and K.G. Toutouzas, *Significance of TP53, CDKN2A, SMAD4 and KRAS in Pancreatic Cancer.* Curr Issues Mol Biol, 2024. **46**(4): p. 2827-2844.
10. Racu, M.L., D. Bernardi, A. Chaouche, E. Zindy, J. Navez, P. Loi, et al., *SMAD4 Positive Pancreatic Ductal Adenocarcinomas Are Associated with Better Outcomes in Patients Receiving FOLFIRINOX-Based Neoadjuvant Therapy.* Cancers (Basel), 2023. **15**(15).
11. McCubrey, J.A., L.V. Yang, S.L. Abrams, L.S. Steelman, M.Y. Follo, L. Cocco, et al., *Effects of TP53 Mutations and miRs on Immune Responses in the Tumor Microenvironment Important in Pancreatic Cancer Progression.* Cells, 2022. **11**(14).
12. Peng, J., B.-F. Sun, C.-Y. Chen, J.-Y. Zhou, Y.-S. Chen, H. Chen, et al., *Single-cell RNA-seq highlights intra-tumoral heterogeneity and malignant progression in pancreatic ductal adenocarcinoma.* Cell Research, 2019. **29**(9): p. 725-738.
13. Wang, Y., Y. Liang, H. Xu, X. Zhang, T. Mao, J. Cui, et al., *Single-cell analysis of pancreatic ductal adenocarcinoma identifies a novel fibroblast subtype associated with poor prognosis but better immunotherapy response.* Cell Discov, 2021. **7**(1): p. 36.

14. Werba, G., D. Weissinger, E.A. Kawaler, E. Zhao, D. Kalfakakou, S. Dhara, et al., *Single-cell RNA sequencing reveals the effects of chemotherapy on human pancreatic adenocarcinoma and its tumor microenvironment.* Nat Commun, 2023. **14**(1): p. 797.
15. Ye, B., Q. Wang, X. Zhu, L. Zeng, H. Luo, Y. Xiong, et al., *Single-cell RNA sequencing identifies a novel proliferation cell type affecting clinical outcome of pancreatic ductal adenocarcinoma.* Front Oncol, 2023. **13**: p. 1236435.
16. Yu, Y., G. Yang, H. Huang, Z. Fu, Z. Cao, L. Zheng, et al., *Preclinical models of pancreatic ductal adenocarcinoma: challenges and opportunities in the era of precision medicine.* J Exp Clin Cancer Res, 2021. **40**(1): p. 8.
17. Cros, J., J. Raffenne, A. Couvelard, and N. Pote, *Tumor Heterogeneity in Pancreatic Adenocarcinoma.* Pathobiology, 2018. **85**(1-2): p. 64-71.
18. Wang, Y. and H. Jeon, *3D cell cultures toward quantitative high-throughput drug screening.* Trends Pharmacol Sci, 2022. **43**(7): p. 569-581.
19. Parasrampuria, D.A., L.Z. Benet, and A. Sharma, *Why Drugs Fail in Late Stages of Development: Case Study Analyses from the Last Decade and Recommendations.* AAPS J, 2018. **20**(3): p. 46.
20. Brüningk, S.C., I. Rivens, C. Box, U. Oelfke, and G. ter Haar, *3D tumour spheroids for the prediction of the effects of radiation and hyperthermia treatments.* Scientific Reports, 2020. **10**(1): p. 1653.
21. Pape, J., M. Emberton, and U. Cheema, *3D Cancer Models: The Need for a Complex Stroma, Compartmentalization and Stiffness.* Front Bioeng Biotechnol, 2021. **9**: p. 660502.
22. Tomas-Bort, E., M. Kieler, S. Sharma, J.B. Candido, and D. Loessner, *3D approaches to model the tumor microenvironment of pancreatic cancer.* Theranostics, 2020. **10**(11): p. 5074-5089.
23. Ware, M.J., V. Keshishian, J.J. Law, J.C. Ho, C.A. Favela, P. Rees, et al., *Generation of an in vitro 3D PDAC stroma rich spheroid model.* Biomaterials, 2016. **108**: p. 129-42.
24. Drifka, C.R., A.G. Loeffler, C.R. Esquibel, S.M. Weber, K.W. Eliceiri, and W.J. Kao, *Human pancreatic stellate cells modulate 3D collagen alignment to promote the migration of pancreatic ductal adenocarcinoma cells.* Biomed Microdevices, 2016. **18**(6): p. 105.
25. Lazzari, G., V. Nicolas, M. Matsusaki, M. Akashi, P. Couvreur, and S. Mura, *Multicellular spheroid based on a triple co-culture: A novel 3D model to mimic pancreatic tumor complexity.* Acta Biomater, 2018. **78**: p. 296-307.
26. Steinberg, E., N. Orehov, K. Tischenko, O. Schwob, G. Zamir, A. Hubert, et al., *Rapid Clearing for High Resolution 3D Imaging of Ex Vivo Pancreatic Cancer Spheroids.* International Journal of Molecular Sciences, 2020. **21**(20).
27. Yang, H., L. Sun, M. Liu, and Y. Mao, *Patient-derived organoids: a promising model for personalized cancer treatment.* Gastroenterol Rep (Oxf), 2018. **6**(4): p. 243-245.
28. Ohlund, D., A. Handly-Santana, G. Biffi, E. Elyada, A.S. Almeida, M. Ponz-Sarvise, et al., *Distinct populations of inflammatory fibroblasts and myofibroblasts in pancreatic cancer.* J Exp Med, 2017. **214**(3): p. 579-596.

29. Tsai, S., L. McOlash, K. Palen, B. Johnson, C. Duris, Q. Yang, et al., *Development of primary human pancreatic cancer organoids, matched stromal and immune cells and 3D tumor microenvironment models.* BMC Cancer, 2018. **18**(1): p. 335.
30. Rae, C., F. Amato, and C. Braconi, *Patient-Derived Organoids as a Model for Cancer Drug Discovery.* Int J Mol Sci, 2021. **22**(7).
31. Foo, M.A., M. You, S.L. Chan, G. Sethi, G.K. Bonney, W.P. Yong, et al., *Clinical translation of patient-derived tumour organoids- bottlenecks and strategies.* Biomark Res, 2022. **10**(1): p. 10.
32. Jesnowski, R., D. Furst, J. Ringel, Y. Chen, A. Schrodel, J. Kleeff, et al., *Immortalization of pancreatic stellate cells as an in vitro model of pancreatic fibrosis: deactivation is induced by matrigel and N-acetylcysteine.* Lab Invest, 2005. **85**(10): p. 1276-91.
33. Hamada, S., A. Masamune, T. Takikawa, N. Suzuki, K. Kikuta, M. Hirota, et al., *Pancreatic stellate cells enhance stem cell-like phenotypes in pancreatic cancer cells.* Biochemical and Biophysical Research Communications, 2012. **421**(2): p. 349-354.
34. Arndt, S., P. Unger, M. Berneburg, A.K. Bosserhoff, and S. Karrer, *Cold atmospheric plasma (CAP) activates angiogenesis-related molecules in skin keratinocytes, fibroblasts and endothelial cells and improves wound angiogenesis in an autocrine and paracrine mode.* J Dermatol Sci, 2018. **89**(2): p. 181-190.
35. Xu, Z., A. Vonlaufen, P.A. Phillips, E. Fiala-Beer, X. Zhang, L. Yang, et al., *Role of pancreatic stellate cells in pancreatic cancer metastasis.* Am J Pathol, 2010. **177**(5): p. 2585-96.
36. Van den Eynde, A., L. Gehrcken, T. Verhezen, H.W. Lau, C. Hermans, H. Lambrechts, et al., *IL-15-secreting CAR natural killer cells directed toward the pan-cancer target CD70 eliminate both cancer cells and cancer-associated fibroblasts.* J Hematol Oncol, 2024. **17**(1): p. 8.
37. Lee, H. and K.T. Kang, *Advanced tube formation assay using human endothelial colony forming cells for in vitro evaluation of angiogenesis.* Korean J Physiol Pharmacol, 2018. **22**(6): p. 705-712.
38. Han, S.J., S. Kwon, and K.S. Kim, *Challenges of applying multicellular tumor spheroids in preclinical phase.* Cancer Cell Int, 2021. **21**(1): p. 152.
39. Belvedere, R., V. Bizzarro, A. Popolo, F. Dal Piaz, M. Vasaturo, P. Picardi, et al., *Role of intracellular and extracellular annexin A1 in migration and invasion of human pancreatic carcinoma cells.* BMC Cancer, 2014. **14**: p. 961.
40. Svirshchevskaya, E., E. Doronina, M. Grechikhina, E. Matushevskaya, O. Kotsareva, G. Fattakhova, et al., *Characteristics of multicellular tumor spheroids formed by pancreatic cells expressing different adhesion molecules.* Life Sci, 2019. **219**: p. 343-352.
41. Kapalczynska, M., T. Kolenda, W. Przybyla, M. Zajaczkowska, A. Teresiak, V. Filas, et al., *2D and 3D cell cultures - a comparison of different types of cancer cell cultures.* Arch Med Sci, 2018. **14**(4): p. 910-919.
42. Longati, P., X. Jia, J. Eimer, A. Wagman, M.R. Witt, S. Rehnmark, et al., *3D pancreatic carcinoma spheroids induce a matrix-rich, chemoresistant phenotype offering a better model for drug testing.* BMC Cancer, 2013. **13**: p. 95.

43. Pan, X., T. Arumugam, T. Yamamoto, P.A. Levin, V. Ramachandran, B. Ji, et al., *Nuclear factor-kappaB p65/relA silencing induces apoptosis and increases gemcitabine effectiveness in a subset of pancreatic cancer cells.* Clin Cancer Res, 2008. **14**(24): p. 8143-51.
44. Maietta, I., A. Martinez-Perez, R. Alvarez, A.R. De Lera, A. Gonzalez-Fernandez, and R. Simon-Vazquez, *Synergistic Antitumoral Effect of Epigenetic Inhibitors and Gemcitabine in Pancreatic Cancer Cells.* Pharmaceuticals (Basel), 2022. **15**(7).
45. Patki, M., A. Saraswat, S. Bhutkar, V. Dukhande, and K. Patel, *In vitro assessment of a synergistic combination of gemcitabine and zebularine in pancreatic cancer cells.* Exp Cell Res, 2021. **405**(2): p. 112660.
46. Nilendu, P., S.C. Sarode, D. Jahagirdar, I. Tandon, S. Patil, G.S. Sarode, et al., *Mutual concessions and compromises between stromal cells and cancer cells: driving tumor development and drug resistance.* Cell Oncol (Dordr), 2018. **41**(4): p. 353-367.
47. Le Compte, M., E.C. De La Hoz, S. Peeters, F.R. Fortes, C. Hermans, A. Domen, et al., *Single-organoid analysis reveals clinically relevant treatment-resistant and invasive subclones in pancreatic cancer.* NPJ Precis Oncol, 2023. **7**(1): p. 128.
48. Nishida, N., H. Yano, T. Nishida, T. Kamura, and M. Kojiro, *Angiogenesis in cancer.* Vasc Health Risk Manag, 2006. **2**(3): p. 213-9.
49. Mercanti, L., M. Sindaco, M. Mazzone, M.C. Di Marcantonio, M. Piscione, R. Muraro, et al., *PDAC, the Influencer Cancer: Cross-Talk with Tumor Microenvironment and Connected Potential Therapy Strategies.* Cancers (Basel), 2023. **15**(11).
50. Barrera, L.N., A. Evans, B. Lane, S. Brumskill, F.E. Oldfield, F. Campbell, et al., *Fibroblasts from Distinct Pancreatic Pathologies Exhibit Disease-Specific Properties.* Cancer Res, 2020. **80**(13): p. 2861-2873.
51. Zhu, Y., E. Kang, M. Wilson, T. Basso, E. Chen, Y. Yu, et al. *3D Tumor Spheroid and Organoid to Model Tumor Microenvironment for Cancer Immunotherapy*. Organoids, 2022. **1**, 149-167 DOI: 10.3390/organoids1020012.

CHAPTER 04

LOW-DOSE CAP TREATMENT PRESERVES VASCULAR QUIESCENCE IN 3D TUMOR-STROMA-ENDOTHELIAL MODELS OF PDAC IN VITRO AND IN OVO

Adapted from:
Verloy, R.; Peeters, E.; Privat-Maldonado, A.; Rovers, S.; Lau, H.W.; Brants, L.; Hermans, C.; De Waele, J.; Deben, C.; Smits, E. and Bogaerts, A. Low-dose cold atmospheric plasma treatment preserves vascular quiescence in 3D tumor-stroma-endothelial models of pancreatic cancer in vitro and in ovo. Submitted manuscript

4.1 Abstract

As discussed in chapter 2, PDAC is characterized by a dense desmoplastic stroma that limits drug delivery and promotes chemoresistance. While anti-angiogenic strategies have shown limited clinical success, pro-angiogenic approaches may improve perfusion and treatment efficacy but remain underexplored. CAP, known for generating RONS, has demonstrated anti-cancer effects at high doses and pro-healing, angiogenic effects at low doses. In this chapter, we investigate the impact of low-dose CAP on angiogenesis in PDAC using the previously developed TCC spheroid models and a turkey in ovo model that mimic the TME. CAP is applied using the kINPen®MED for varying durations (15–60 seconds in vitro; 10–30 seconds in ovo). In vitro, CAP showed a dose-dependent inhibition of endothelial tube formation and a downward trend in VEGF-A secretion. Other angiogenic factors remain unchanged. In ovo, vascularization around and within tumors is not significantly altered. However, a slight increase in tumor weight is observed following 10-second CAP treatment in one cell line. These findings suggest that under standard conditions, low-dose CAP does not enhance angiogenesis in PDAC and may exert subtle tumor-modulating effects, highlighting the importance of treatment parameters and model complexity in CAP-based therapeutic strategies.

4.2 Introduction

As discussed in chapter 2, PDAC is projected to become the second leading cause of cancer-related death by 2030, highlighting the urgent need for advancements in treatment strategies [1]. Representing approximately 85% of all pancreatic cancer cases, PDAC is marked by a dense, fibrous tumor stroma caused by a desmoplastic reaction [2]. This reaction causes high intratumoral pressure, forming a physical barrier that compresses blood vessels, and reduces vascularity, thereby limiting drug delivery and fostering chemoresistance [3]. ECs, beyond their crucial role in angiogenesis, add to the complexity of PDAC by transitioning into CAFs through an endothelial-to-mesenchymal transition, exacerbating the disease [4, 5]. Additionally, activated PSCs , a specific fibroblast subtype, significantly contribute to desmoplasia and modulating the TME [6]. This complex milieu promotes PDAC traits such as rapid growth, high invasiveness and metastatic potential, survival under hypoxic and nutrient-poor conditions, and immunosuppression [6].

Significant attention in cancer research has been given to anti-angiogenic approaches to inhibit vascularity and tumor growth by starving the tumor, as also discussed in chapter 2. However, these approaches have struggled to maintain their promising pre-clinical effects when transitioning to clinical models [7]. In the context of PDAC, such strategies often exacerbate tumor aggressiveness and reduce the efficacy of chemotherapeutics by hindering drug delivery and inducing hypoxia [8]. Conversely, pro-angiogenic approaches for PDAC have been proposed to enhance the delivery and effectiveness of chemotherapeutics, demonstrating reductions in tumor growth, metastasis, and desmoplasia, alongside increases in survival rates, blood vessel density, and perfusion [9, 10].

Futhermore, as outlined in chapter 2, CAP treatment received increasing attention in anti-cancer research for its ability to selectively kill cancer cells [11, 12]. On the other hand, CAP also shows promising results in wound healing, which suggests it can promote angiogenesis, proliferation and tissue oxygenation at lower treatment intensities, consistent with the hermetic response included by CAP [13-19]. Low-intensity CAP

treatment can induce angiogenesis, with ·NO and other RONS like H_2O_2, $O_2{\cdot}^-$, and ·OH playing key roles in the angiogenesis pathway [19-21]. This controlled oxidative stress, or oxidative eustress, activates cell proliferation pathways [20]. ECs, crucial for new blood vessel formation, respond to CAP by expressing pro-angiogenic factors such as FGF-2 and angiopoietin-2, encouraging EC proliferation and migration [15, 20, 21]. Paracrine signaling between fibroblasts and ECs further enhances this activation [15]. Additionally, RONS disrupt EC membranes, releasing more FGF-2 and stimulating neighboring EC proliferation [21]. Based on information from the manufacturer of the kINPen MED, 30 to 60 s/cm^2 promotes tissue regeneration and is therefore seen as low-dose CAP treatment [22-24]. In addition, 60 s CAP treatment of 2D PDAC cell lines, 3D spheroids and in ovo PDAC tumors already showed significant tumor cell death [25, 26]. Thus, controlled RONS delivery via CAP could regulate blood vessel formation in tumors, offering a promising approach to modulate angiogenesis in cancer.

In the present chapter, we investigate whether low dose CAP's pro-angiogenic effects observed in wound healing can be achieved in cancer models to enhance chemotherapy delivery and efficacy against PDAC. For this, we have used our in-house developed TCC spheroid models, which incorporate cancer cells, PSCs, and ECs, presented in previous chapter [27]. Our in vitro TCC spheroid models overcome the limitations of 2D cultures and classic monoculture 3D spheroids by including different cell types to better mimic the tissue architecture and more accurately resemble cell-cell and cell-matrix interactions [28-30], better capturing the complexity of the TME [28]. In addition, we used the turkey in ovo model, a variant of the popular chick CAM model, which is ideal for angiogenesis studies due to its visible angiogenic network and longer embryonic development period [31, 32].

4.3 Material and methods

4.3.1 Cell culture

The human PCC lines MiaPaCa-2 (ATCC®, Manassas, VA, USA) and BxPC-3 (ATCC®, Manassas, VA, USA) were used in this study. The human immortalized PSC line RLT-PSC was kindly provided by Prof. Ralf Jesenofsky, of the Faculty of Medicine, University of Mannheim [33],

while the hPSC21 line was established at Tohoku University, Graduate School of Medicine, kindly provided by Prof. Atsushi Masamune [34]. In addition, the immortalized EC line HMEC-1 (ATCC®, Manassas, VA, USA) was used. All cell lines were used for a maximum of 20 passages after thawing, tested for mycoplasma every 3 months, and STR profiling has validated that the cell lines remained identical to the original cell line. PCCs and PSCs were cultured in Dulbecco's Modified Eagle Medium (DMEM, 10938025, Gibco, Waltham, MA, USA) supplemented with 10% fetal bovine serum (FBS, 10270106, Life Technologies, Carlsbad, CA, USA), 100 U/mL penicillin, 100 µg/mL streptomycin (15140122, Life Technologies, Carlsbad, CA, USA), and 2 mM L-glutamine (25030024, Life Technologies, Carlsbad, CA, USA). PCCs and PSCs were transduced with NucLight Rapid Red (4741, Essen Biosciences, Ann Arbor, MI, USA) to express mKate2, and with NucLight Green (4475, Essen Biosciences, Ann Arbor, MI, USA) to express GFP, respectively. HMEC-1 cells were cultured in MCDB131 (10372019, Thermo Fisher Scientific, Waltham MA, USA) supplemented with 10 ng/mL Epidermal Growth Factor (PHG0314, Thermo Fisher Scientific, Waltham, MA, USA), 1 µg/mL Hydrocortisone (H0396, Sigma Aldrich, Saint Louis, MO, USA), 10 mM L-glutamine (25030024, Life Technologies, Carlsbad, CA, USA), 10% FBS (10270106, Life Technologies, Carlsbad, CA, USA), and 100 U/mL penicillin, 100 µg/mL streptomycin (15140122, Life Technologies, Carlsbad, CA, USA). Cells were maintained in a humidified incubator at 37 °C and 5% CO_2.

4.3.2 Spheroid formation

Four different TCC spheroids were formed as previously described [27]. Briefly, spheroids were seeded at 7000 (BxPC-3:hPSC21:HMEC-1 in a ratio of 6:5:3) or 3500 (MiaPaCa-2:RLT-PSC:HMEC-1 in a ratio of 6:3:3) cells per well, including 0.24% methylcellulose (M0512, Merck, Rahway, NJ, USA) in ultra-low adherent (ULA) plates (7007, Corning®, Corning, NY, USA). Empty outer wells were filled with water to minimize evaporation and plates were sealed with a breathable membrane (Z380059, Merck, Rahway, NJ, USA). The ULA plates were centrifuged at 453 × *g* for 10 min.

4.3.3 Turkey chorioallantoic membrane model

The turkey eggs (Broeierij Claeys, Kruisem, Belgium) were introduced into the laboratory at day six of their embryonic development and kept in the dark at 19-21 °C overnight. The next day, after checking fertility with a flashlight, fertilized eggs were placed in an incubator at 37.7 °C with 65% humidity, cooled for two hours daily, and turned (lateral rotation from left to right) hourly to prevent adhesion and embryonic death. On day seven, eggs were disinfected with 70% isopropanol quick pads (QS0029, MLS, Menen, Belgium), punctured with a 20G needle (613-3937, VWR, Radnor, PA, USA) on the small side of the egg to relocate the air pocket, and sealed with Leukosilk tape (46834-00 AP, Essity, Stockholm, Sweden) before being incubated upright without cooling and turning. On day nine, PCCs and PSCs were seeded onto the CAM. After shell opening, a filter paper soaked in diethyl ether was applied to a large vessel to erode it, and a silicon ring was placed on top of the vessel. A two million cell pellet (2:1 ratio of PCC:PSC) was resuspended in 20 µL Matrigel (734-0269, VWR, Radnor, PA, USA) and was allowed to solidify as a droplet hanging from the tip for approximately 1 min before seeding within the ring. Eggs were sealed with Tegaderm (16002, 3M, Saint Paul, MN, USA) and placed back in the incubator for four days. On day thirteen, the tumors received CAP treatment. By day sixteen, tumors were harvested. The eggs were removed from the incubator, Tegaderm was taken off, and 750 µL paraformaldehyde was applied to fix the vascularized membrane. The egg was incised along the midline to flip the CAM and tumor into a weighing boat for photographing. The embryos were sacrificed by decapitation, and the tumors were dissected, weighed, and embedded in paraffin for hematoxylin and eosin (H&E) staining.

4.3.4 Cold atmospheric plasma treatment

The kINPen®MED (adjusted to operate below 4 slm) was used to treat the spheroids and in ovo tissues. As explained in chapter 2, the kINPen®MED is a plasma jet device that generates a CAP beam below 40 °C. Prior to CAP treatment of spheroids, 150 µL of medium was removed and 50 µL of fresh MCDB131 medium was added. Argon was used as ionizing gas at 2 standard liter per min (slm) to treat both spheroids and in ovo tissues in the turkey egg. The treatment was performed for 15, 30, 45 or 60 seconds, with a 12 mm gap in

MCDB131 medium (spheroids) or 10, 20, 30 seconds, based on the in vitro results, and a 10 mm gap (in ovo tissues) between the kINPen®MED nozzle and the liquid surface. The plasma setup was controlled by an automated stage using the program WinPC-NC. Spheroid-conditioned medium was collected 72h post-treatment for the tube formation assay and MSD analysis.

4.3.5 Tube formation assay

Assessment of angiogenesis was done with a tube formation assay in a 384-well plate (3764, Corning®, NY, USA) as described in previous chapter [27]. Finally, the IKOSA® tube formation analysis was performed on the images to gain four metrics: number of loops, covered area, total tube length, and number of branch points.

4.3.6 MSD

The Mesoscale Discovery (MSD) assay for angiogenesis was performed using the MSD V-PLEX Angiogenesis Panel 1 Kit (Catalogue No. K15190G-1, Rahway, NJ, USA) and an MSD MULTI-SPOT 96-well plate. The assay was performed following manufacturer's instructions.

4.3.7 Hematoxylin and eosin staining

The 5-µm thick sections were cut from paraffin embedded blocks containing the PDAC tumor tissue. These sections were baked on microscope slides for 2 h at 60 °C, ensuring secure attachment of the tissue to the slide surface. Next, the slides were dewaxed by washing in 100% xylene for 10 min, 100% isopropanol for 6 min, 95% isopropanol for 6 min, and 75% isopropanol for 6 min. Thereafter, H&E staining was performed with the following steps: 12 min incubation in hematoxylin, rinsing with water, 2 min incubation in sodium carbonate, rinsing with water, 5 min incubation in eosin, and rinsing with water. To finalize the staining process, slides were dehydrated with 75% isopropanol for 2 min, 95% isopropanol 2 min, 100% isopropanol for 2 min, and 100% xylene for 2 min. A coverslip with permanent mounting medium was carefully applied to the slide to preserve the stained tissue sections for microscopic examination.

4.3.8 Statistical analysis

All experiments were performed at least three times with three technical replicates, unless specified otherwise. Outlier tests were performed using GraphPad Software v10.1.0. Statistics for the tube formation assay were performed using linear mixed model with the treatment as fixed effect using JMP Pro v17.0.0 software. For multiple comparisons of the experimental groups to the untreated control, Dunnett's test was used. To calculate the statistical significances between the concentrations of angiogenic growth factors in spheroid-conditioned media using the MesoScale Discovery assay and the in ovo experiments, all experimental groups were compared to their control group using the one-way Anova, Brown-Forsythe and Welch ANOVA test, after the removal of the significant outliers using GraphPad Software v10.1.0.

4.4 Results

4.4.1 CAP treatment does not induce tube formation in vitro

First, we evaluated the angiogenic potential of CAP treatment on ECs. For this, we performed the tube formation assay using spheroid-conditioned medium collected 3 days after CAP treatment (indirect effect due to a change in secreted cytokines after CAP treatment) (Figure 4.1a). We observe that CAP treatment has a dose-dependent inhibitory effect, as it consistently reduced the number of branching points, number of tubes, covered area, and total tube length (Figure 4.1b). TCC spheroids with the Mia PaCa-2 cell line treated for 45 and 60s presented the most significant differences ($p<0.05$). The heatmaps reveal varying responses to CAP treatment across the different spheroid types, each representing a unique TME (Figure 4.1c). The shift from green to red indicates a general reduction in the measured angiogenic parameters with increasing treatment time, suggesting CAP treatment inhibits angiogenesis in these spheroid models. However, the extent of these changes varies among the spheroid types, e.g., with BxPC-3:RLT-PSC:HMEC-1 spheroids showing no change in tube formation upon CAP treatment, highlighting PDAC heterogeneity. This suggests that different tumor cell populations or TMEs respond

differently to the treatment, emphasizing the need to consider intra-tumor variability in therapeutic strategies.

Overall, these results indicate a dose-dependent inhibitory effect of CAP treatment on the angiogenic potential of ECs to form tubes.

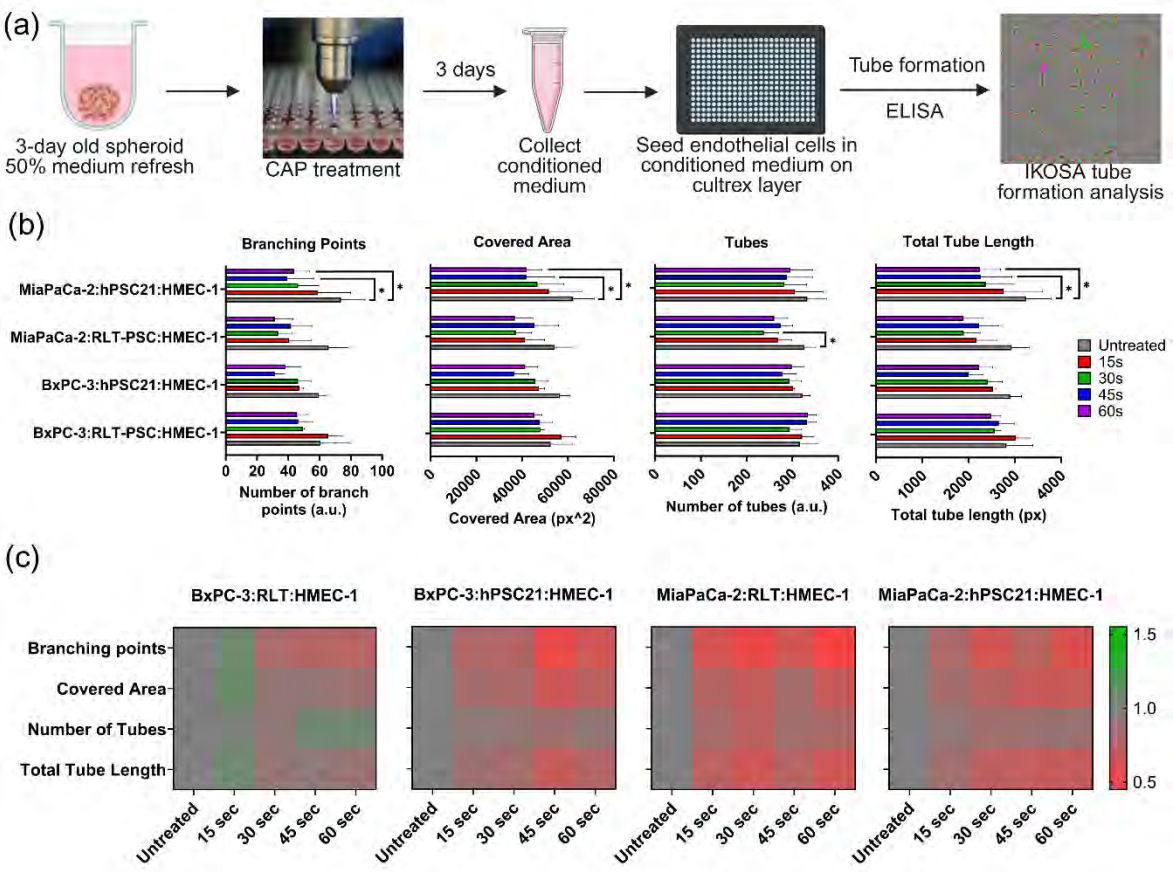

Figure 4.1. *CAP treatment inhibits tube formation in TCC spheroids.* ***(a)*** *Methodology scheme of using CAP-treated spheroid-conditioned medium for a tube formation assay to evaluate angiogenesis.* ***(b)*** *Bar plots of the IKOSA® tube formation analysis results for each quantitative parameter, showing the effects of CAP treatment per spheroid type.* ***(c)*** *Heat map of the IKOSA® tube formation analysis results of four different spheroid types, showing the effects of CAP treatment per quantitative parameter. Data is represented as mean ± SD (n ≥ 9 from three independent experiments) with each dot representing the mean of each independent experiment. * = p ≤ 0.05.*

4.4.2 Angiogenic cytokines do not change after CAP treatment

To investigate whether this subtle inhibition of angiogenesis was related to the secretion of angiogenic growth factors by the treated cancer, fibroblast and ECs, a MesoScale Discovery assay was performed (Figure 4.2a). While no statistically significant differences are observed in the secretion of VEGF-D, b-FGF, PlGF, and VEGF-A across different CAP treatment times and TCC spheroid types, several trends are noted (Figure 4.2b-e). VEGF-A concentrations decrease with increasing treatment times, suggesting reduced secretion of this angiogenic growth factor under prolonged treatment (Figure 4.2b). In addition, the BxPC-3:hPSC21:HMEC-1 spheroids have a notably higher secretion of VEGF-A compared to other spheroid types. VEGF-D data does not show a clear trend (Figure 4.2c). In contrast, b-FGF and PlGF secretions remain relatively stable across the different treatment times, with MiaPaCa-2 TCC spheroids secreting more b-FGF than BxPC-3 spheroids and MiaPaCa-2:hPSC21:HMEC-1 spheroids secreting lower amounts of PlGF (Figure 4.2d-e). Tie-2, Flt-1 and VEGF-C were not detected in the samples. Although these trends are not statistically robust, they suggest that the inhibitory effects of CAP treatment on tube formation could be due to a reduction in VEGF-A in the CAP-treated spheroid-conditioned media.

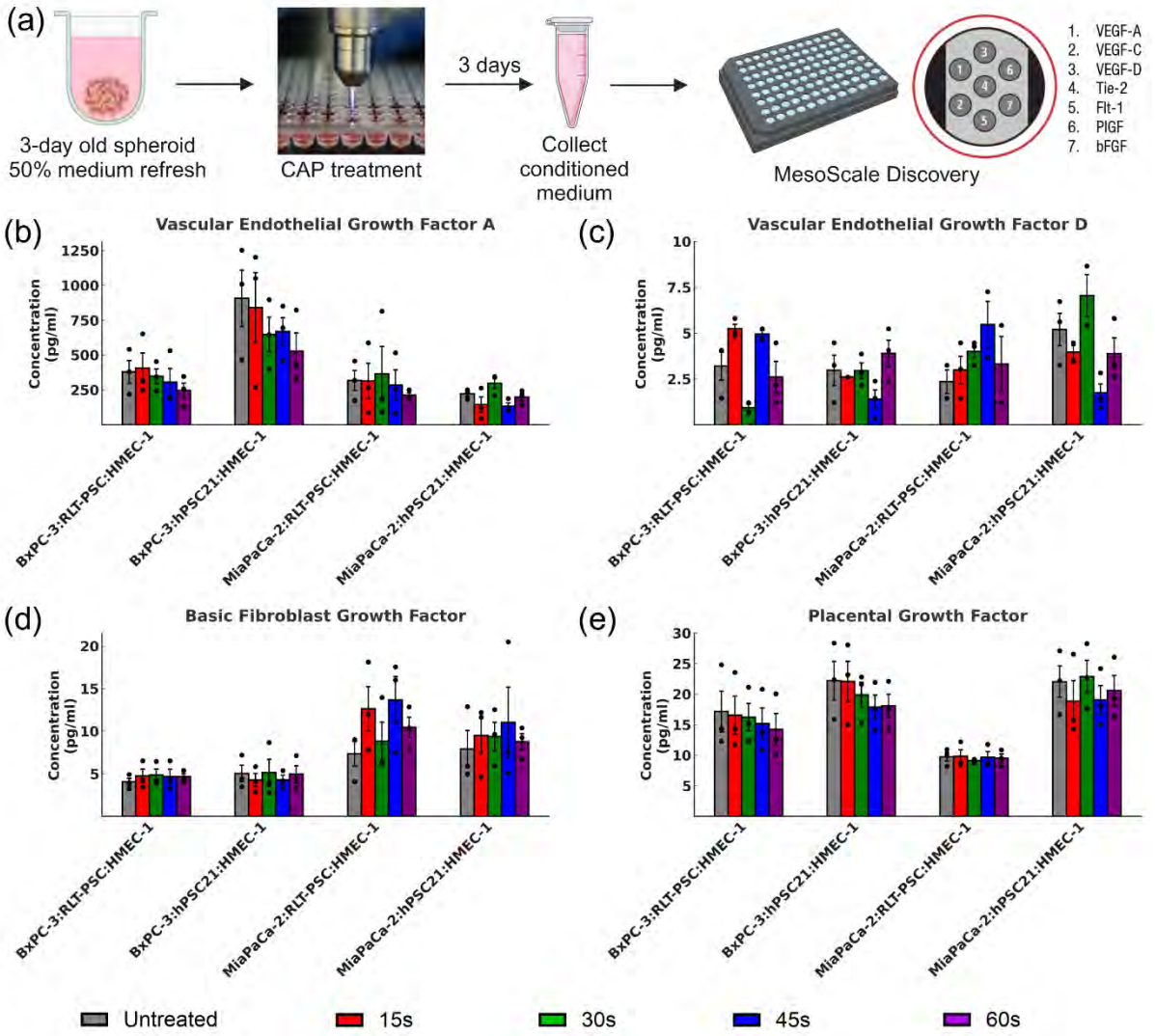

Figure 4.2. *Revealing the secretion profile of angiogenic growth factors in the TCC spheroids upon CAP treatment.* ***(a)*** *Methodology scheme of using CAP-treated spheroid-conditioned medium for a MesoScale Discovery assay of seven growth factors: VEGF-A, VEGF-C, VEGF-D, Tie-2, Flt-1, PlGF and bFGF. Bar plots of the secretion levels of* ***(b)*** *VEGF-A,* ***(c)*** *PlGF,* ***(d)*** *bFGF,* ***(e)*** *VEGF-D in TCC spheroid-conditioned medium. Data is represented as mean ± SEM (n = 2-3 from three independent experiments after removal of outliers) with each dot representing one independent experiment of 4-6 pooled TCC spheroids of the same condition. UT = untreated; VEGF-A/C/D = Vascular endothelial growth factor A/C/D; Tie-2 = Angiopoietin-1 reception; Flt-1 = Vascular endothelial growth factor receptor 1; PlGF = Placental growth factor; bFGF = Basic fibroblast growth factor.*

4.4.3 CAP treatment does not induce angiogenesis around the tumor in ovo

To investigate the effect of CAP treatment on tumor angiogenesis in a more complex model, we used the turkey in ovo model, as it has an extensive and visible vascular network. We evaluated three low-dose treatment times (10 s, 20 s and 30 s of CAP), as 45 s and 60 s

treatments showed signs of angiogenesis inhibition in vitro. To account for the heterogeneity of PDAC, we seeded two different co-cultures: MiaPaCa-2 with RLT-PSC (MR tumors) and BxPC-3 with hPSC21 (BH tumors). Macroscopic angiogenesis was evaluated by looking at the vascular network surrounding the tumor using the IKOSA® tool (Figure 4.3a), which provides quantitative measures of the vasculature around the tumor, including the total vessel length, the total vessel area, the mean vessel thickness and the number of branching points (Figure 4.3b and c).

For all four parameters, no statistically significant differences are observed between the three different treatment groups (10 s, 20 s and 30 s of CAP) and the untreated groups for both tumor types (Figure 4.3b and c). Within the MR tumors, 10 s CAP treatment shows a trend to increase the total vessel length, total vessel area and the number of branching points, however, no statistically significant differences are found. These results indicate that our proposed low-dose CAP treatment does not induce angiogenesis around the tumor in ovo. Moreover, the varying responses among tumor types highlight the importance of accounting for tumor heterogeneity in CAP research (Figure 4.3c).

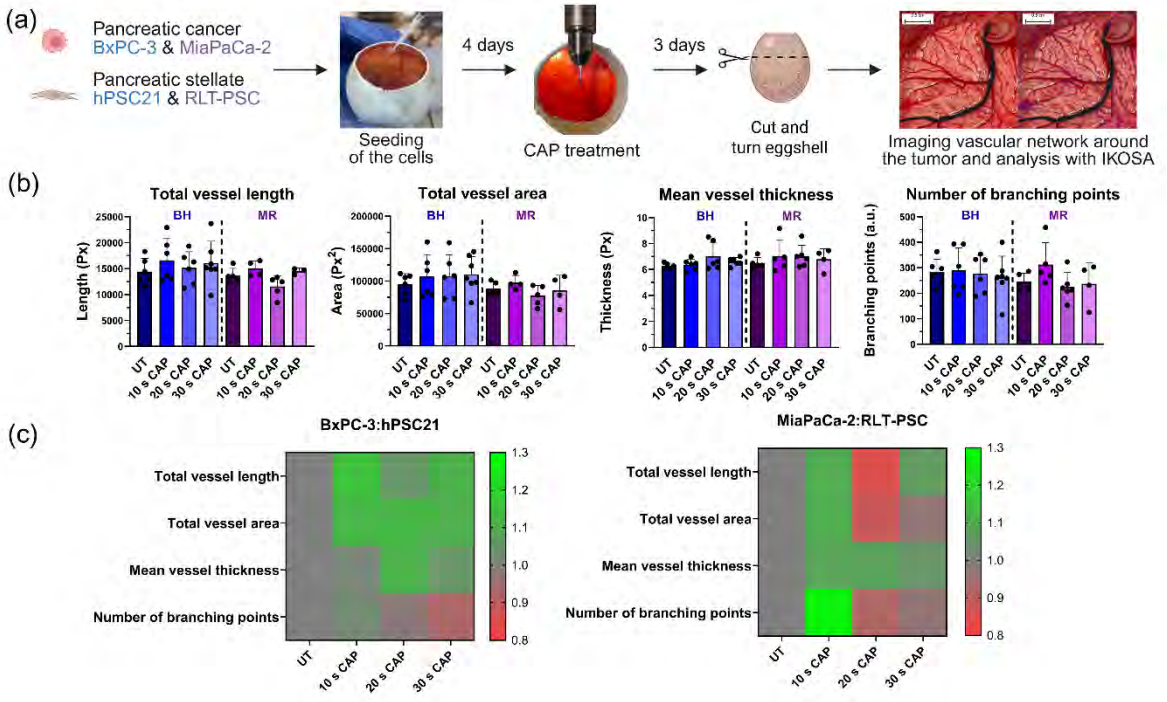

Figure 4.3. *Capturing the effect of CAP treatment on the macroscopic angiogenesis in the turkey in ovo model using the IKOSA® analysis.* ***(a)*** *Methodology scheme of tumor formation, CAP treatment and IKOSA® analysis using two different PCC and PSC lines. A representative raw image (left) and the*

IKOSA® analysis masking (right) are shown. ***(b)*** *Bar plots of the IKOSA® analysis results showing the total vessel length, total vessel area, mean vessel thickness and the number of branching points. Data is represented as mean ± SD (n ≥ 3 from three independent experiments). Each dot represents one egg.* ***(c)*** *Heat map of the IKOSA® analysis results of two different tumor types, showing the effects of CAP treatment per quantitative parameter. BH = BxPC-3 + hPSC21 tumor; MR = MiaPaCa-2 + RLT-PSC tumor; UT = untreated; Px = pixel; a.u. = arbitrary units.*

4.4.4 CAP treatment does not induce angiogenesis within the tumor in ovo

Next, angiogenesis was evaluated within the PDAC tumors of the turkey in ovo model by collecting them three days after CAP treatment, paraffin-embedding and staining them with H&E to differentiate the turkey red blood cells from the other human and turkey cells (Figure 4.4a). Pictures were taken of the stained tissue and analyzed with QuPath to quantify the percentage of turkey red blood cells within the tumor tissue, which indicate the presence of blood vessels (Figure 4.4b). For both tumor types, all three treatment groups show a trend to decrease the percentage of red blood cells compared to the untreated group. In general, small to no differences are observed in the percentage of red blood cells present in both tumor types treated with CAP for different times (Figure 4.4c). These observations suggest that CAP treatment might not effectively induce angiogenesis within the tumor.

Besides looking at the induced angiogenesis around and within the in ovo tumors, we measured the weight of the tumors on the day of harvesting (Figure 4.4d). For both BH and MR tumors, all CAP-treated groups show a higher mean tumor weight compared to the untreated groups, except the 30 s CAP treatment MR group. Furthermore, 10s and 30s CAP treatments seem to increase tumor weight of BH tumors, compared to the untreated group (Figure 4.4d, $p<0.05$). For both tumor types, 10 s CAP gives the highest mean tumor weight. Altogether, this in ovo data suggests that a low dose of CAP treatment does not induce angiogenesis, while slightly promotes tumor growth (Figure 4.3 and 4.4).

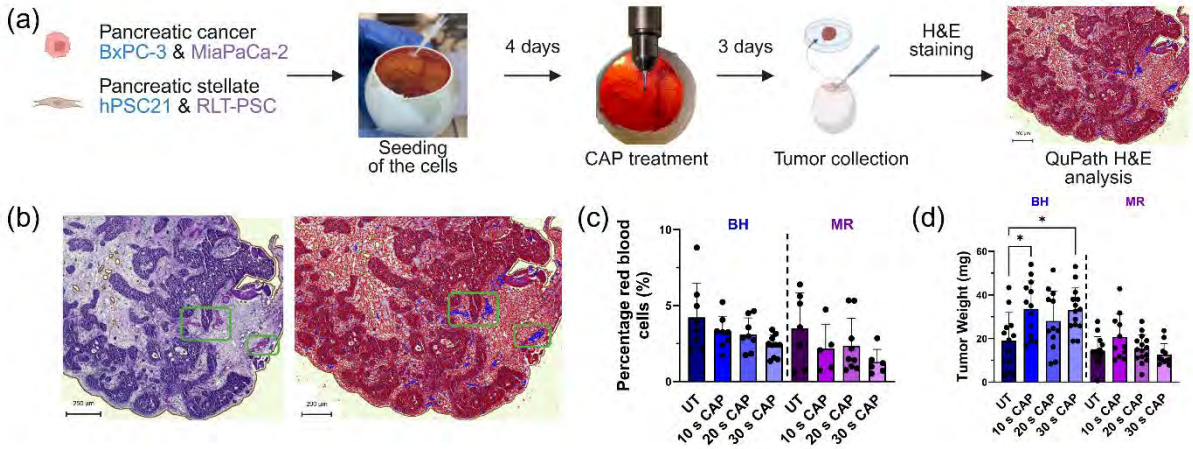

Figure 4.4. *Capturing the effect of CAP on microscopic angiogenesis and tumor weights in ovo.* ***(a)*** *Methodology scheme of tumor formation, CAP treatment and measuring the number of turkey red blood cells 3 days after treatment. Two different PCC and PSC lines were used.* ***(b)*** *QuPath analysis of the H&E stained tissue sample. The human tumor cells stained intensely blue/purple with hematoxylin and the turkey red blood cells stained intensely pink (left). The turkey red blood cells are indicated in blue after QuPath analysis (green boxes).* ***(c)*** *Bar plots of the QuPath H&E analysis results, showing the percentage of red blood cells compared to the total number of cells in the tumor. Data is represented as mean ± SD (n ≥ 5 from three independent experiments).* ***(d)*** *Bar plots representing the tumor weights per treatment group. Data is represented as mean ± SD (n ≥ 10 from four independent experiments). BH = BxPC-3 + hPSC21 tumor; MR = MiaPaCa-2 + RLT-PSC tumor; UT = untreated. Each dot represents one egg. * = p ≤ 0.05.*

4.5 Discussion

PDAC remains one of the most aggressive cancer types due to its dense stroma, poor vascularity, and resistance to therapies. Limited, but effective, pro-angiogenic strategies aim to enhance vascular perfusion, potentially improving drug delivery and treatment outcomes [9, 10]. However, systemic drugs have negative side effects as they induce an effect on the entire human body, which can be prevented using a local treatment, like CAP. CAP is known for its ability to generate RONS and has shown a pro-angiogenic potential, as shown in vitro, in ovo and in vivo with various devices [15, 18, 19, 21, 35-38]. We investigated whether CAP could promote angiogenesis in PDAC using in vitro TCC spheroid models and an in ovo turkey model. This could open opportunities to enhance the effects of chemotherapy in this hard-to-treat cancer.

However, CAP treatment slightly inhibited endothelial tube formation in vitro in a dose-dependent manner, and VEGF-A secretion in TCC spheroids trended downward with longer

CAP exposure. Other cytokines, such as b-FGF and PlGF, remained stable, indicating that CAP-induced oxidative stress may disrupt pro-angiogenic signaling without triggering compensatory increases in growth factors. Indeed, 60 seconds of CAP-treated nanoparticles have been associated with reduced VEGF mRNA expression in breast adenocarcinoma cells as well [39]. Similarly, direct CAP exposure (15 sec) using the kINPen®MED reduced cell growth, metabolism, tube formation, and 2D migration in human dermal microvascular ECs, comparable in origin to our HMEC-1 line [40]. In contrast, low-dose CAP using a DBD device has been shown to enhance EC proliferation and increase FGF-2 release [38]. The MicroPlaSter ß plasma torch (30 sec, 4 slm) also upregulated FGF-2, angiopoietin, and VEGF receptor expression in ECs, and FGF-2 in fibroblasts (2 min, 4 slm) [15]. Tube formation improved after 30 sec of direct CAP treatment, and supernatants from CAP-treated fibroblasts (1–2 min) also promoted angiogenesis [15], in contrast to our findings, where supernatants tended to suppress endothelial activity. Other studies using in-house plasma jets with helium (low-dose direct) or nitrogen (30–360 sec indirect) showed enhanced tube formation, migration, and VEGF receptor activation, with mechanisms involving eNOS and possibly MAPK signaling [36, 37]. Together, this suggests that inducing oxidative eustress at low CAP doses may be difficult to achieve with the kINPen®MED under standard conditions and highlight CAP's dual-edged nature: its angiogenic effects vary widely depending on factors such as device type, gas composition, type of liquid, cancer and EC type, TME, treatment mode and duration. Many of these factors critically influence not only the type but also the quantity of RONS generated, ultimately resulting in highly variable biological effects [41]. However, due to the complexity of this large number of variables, fully predicting the outcomes remains challenging.

Next, we investigated CAP's effect on angiogenesis using the in ovo model, as this model has an extensive vascular network, ideal to investigate angiogenesis. We used the turkey CAM model instead of chicken, as the extended development time of the turkey embryo is beneficial for combining CAP with chemotherapy in future studies as it provides a longer experimental time window. Analysis of vascularization around and within tumors revealed

no significant pro-angiogenic changes across treatment groups. However, a slight increase in tumor weight was observed with shorter CAP exposures, particularly at 10 seconds, suggesting CAP influences tumor growth, as expected with low-dose CAP due to hormesis, through mechanisms unrelated to angiogenesis [42]. In contrast, higher CAP doses of 60 seconds have previously been associated with tumor shrinkage in pancreatic cancer using the kINPen device, indicating that the therapeutic outcome is indeed dose dependent [25]. This tumor-promoting effect underscores the need to better understand CAP's broader biological impact, particularly its interaction with stromal components and cellular survival pathways.

In contrast, other studies have reported pro-angiogenic effects under different conditions and in non-cancer contexts. One study using a DBD device showed that plasma enhanced EC proliferation, migration, and tube formation via ROS-induced FGF-2 release [21]. Similarly, daily CAP treatment of mouse skin wounds over 10 days increased CD31 and FGF-2 mRNA expression [15]. In a separate in ovo study using the kINPen®MED, all treatment durations between 30 and 300 seconds increased vessel area, especially after several days [18]. However, this study evaluated angiogenesis in a healthy CAM model, without tumor tissue. Additionally, it used plasma-treated PBS (indirect treatment), lacking short-lived RONS like NO, supporting the idea that longer-lived RONS such as H_2O_2 may play a more prominent role in promoting angiogenesis, while short-lived RONS may be more detrimental. Both studies also relied on repeated treatments, which may be necessary to drive angiogenic responses. In our case, a single treatment was chosen to align with the clinical context of PDAC, where repeated CAP applications are currently not feasible. This distinction may explain the absence of pro-angiogenic effects in our model and highlights the challenge of overcoming the inherent oxidative stress and stromal complexity of PDAC. These findings emphasize the importance of using complex, disease-relevant models and staying mindful of clinical translation when assessing CAP's therapeutic potential.

Future pro-angiogenic CAP research should optimize CAP parameters, such as, a different plasma device, e.g. the MicroPlaSter ß plasma torch, as mentioned before, or changing the feed gas for the kINPen®MED to helium, or argon with admixtures of O_2 and N_2 as this might

lead to higher concentrations of relevant RONS for angiogenesis, such as ·NO, ·OH, H_2O_2 [36, 43-47]. Another future perspective is to further explore CAP's mechanistic effects on the tumor-stroma-vasculature interplay and investigate its potential synergistic use with chemotherapy. While CAP's ability to selectively target cancer cells remains promising, its limited pro-angiogenic effects and potential tumor-promoting effects at low doses in PDAC emphasize the need for careful dose optimization before integration into multimodal therapeutic strategies.

Overall, our findings show that low-dose CAP treatment using the kINPen MED with argon feed gas does not enhance angiogenesis, rather preserve vascular quiescence, in PDAC models and may even slightly promote tumor growth. However, these effects are highly context-dependent, and a pro-angiogenic response to improve the transport and efficacy of chemotherapeutics may still be achievable with alternative plasma devices, modified feed gases, or admixtures better suited to overcome the oxidative and stromal challenges of the PDAC TME.

4.6 Conclusions

CAP demonstrated no significant pro-angiogenic effects, with dose-dependent inhibition of endothelial tube formation and reduced VEGF-A secretion. In the in ovo model, CAP did not enhance vascularization, although a slight increase in tumor weight was observed with shorter CAP treatments, suggesting potential tumor-promoting effects unrelated to angiogenesis. While the kINPen®MED at short treatment times and argon as feed gas was not able to induce angiogenesis in PDAC, other experimental setups (e.g. a different feed gas, such as helium or argon with admixtures of O_2 and/or N_2, or a different device, such as the MicroPlaSter ß plasma torch or a DBD device) could be explored to achieve a pro-angiogenic response in PDAC with low-dose CAP treatment. These findings emphasize the complexity of modulating PDAC's TME and the need for more research using CAP treatment as a novel therapy. Future research should explore its mechanistic effects and potential synergy with chemotherapy to maximize therapeutic outcomes.

4.7 References

1. Rahib, L., B.D. Smith, R. Aizenberg, A.B. Rosenzweig, J.M. Fleshman, and L.M. Matrisian, *Projecting cancer incidence and deaths to 2030: the unexpected burden of thyroid, liver, and pancreas cancers in the United States.* Cancer Res, 2014. **74**(11): p. 2913-21.
2. Hasan, S., R. Jacob, U. Manne, and R. Paluri, *Advances in pancreatic cancer biomarkers.* Oncol Rev, 2019. **13**(1): p. 410.
3. de Sousa Cavalcante, L. and G. Monteiro, *Gemcitabine: metabolism and molecular mechanisms of action, sensitivity and chemoresistance in pancreatic cancer.* Eur J Pharmacol, 2014. **741**: p. 8-16.
4. Zeisberg, E.M., S. Potenta, L. Xie, M. Zeisberg, and R. Kalluri, *Discovery of endothelial to mesenchymal transition as a source for carcinoma-associated fibroblasts.* Cancer Res, 2007. **67**(21): p. 10123-8.
5. Platel, V., S. Faure, I. Corre, and N. Clere, *Endothelial-to-Mesenchymal Transition (EndoMT): Roles in Tumorigenesis, Metastatic Extravasation and Therapy Resistance.* Journal of Oncology, 2019. **2019**: p. 8361945.
6. Verloy, R., A. Privat-Maldonado, E. Smits, and A. Bogaerts, *Cold Atmospheric Plasma Treatment for Pancreatic Cancer-The Importance of Pancreatic Stellate Cells.* Cancers (Basel), 2020. **12**(10): p. 2782.
7. Annese, T., R. Tamma, S. Ruggieri, and D. Ribatti, *Angiogenesis in Pancreatic Cancer: Pre-Clinical and Clinical Studies.* Cancers (Basel), 2019. **11**(3).
8. Comunanza, V. and F. Bussolino, *Therapy for Cancer: Strategy of Combining Anti-Angiogenic and Target Therapies.* Front Cell Dev Biol, 2017. **5**: p. 101.
9. Wong, P.P., F. Demircioglu, E. Ghazaly, W. Alrawashdeh, M.R. Stratford, C.L. Scudamore, et al., *Dual-action combination therapy enhances angiogenesis while reducing tumor growth and spread.* Cancer Cell, 2015. **27**(1): p. 123-37.
10. Ruscetti, M., J.P.t. Morris, R. Mezzadra, J. Russell, J. Leibold, P.B. Romesser, et al., *Senescence-Induced Vascular Remodeling Creates Therapeutic Vulnerabilities in Pancreas Cancer.* Cell, 2020. **181**(2): p. 424-441 e21.
11. Ahn, H.J., K.I. Kim, N.N. Hoan, C.H. Kim, E. Moon, K.S. Choi, et al., *Targeting cancer cells with reactive oxygen and nitrogen species generated by atmospheric-pressure air plasma.* PLoS One, 2014. **9**(1): p. e86173.
12. Yan, D., A. Horkowitz, Q. Wang, and M. Keidar, *On the selective killing of cold atmospheric plasma cancer treatment: Status and beyond.* Plasma Processes and Polymers, 2021. **18**(10): p. 2100020.
13. Fridman, G., G. Friedman, A. Gutsol, A.B. Shekhter, V.N. Vasilets, and A. Fridman, *Applied Plasma Medicine.* Plasma Processes and Polymers, 2008. **5**(6): p. 503-533.
14. Schmidt, A., F. Nießner, T.v. Woedtke, and S. Bekeschus, *Hyperspectral Imaging of Wounds Reveals Augmented Tissue Oxygenation Following Cold Physical Plasma Treatment in Vivo.* IEEE Transactions on Radiation and Plasma Medical Sciences, 2020: p. 1-1.
15. Arndt, S., P. Unger, M. Berneburg, A.K. Bosserhoff, and S. Karrer, *Cold atmospheric plasma (CAP) activates angiogenesis-related molecules in skin keratinocytes,*

fibroblasts and endothelial cells and improves wound angiogenesis in an autocrine and paracrine mode. J Dermatol Sci, 2018. **89**(2): p. 181-190.
16. Bolgeo, T., A. Maconi, M. Gardalini, D. Gatti, R. Di Matteo, M. Lapidari, et al., *The Role of Cold Atmospheric Plasma in Wound Healing Processes in Critically Ill Patients.* J Pers Med, 2023. **13**(5).
17. Heinlin, J., J.L. Zimmermann, F. Zeman, W. Bunk, G. Isbary, M. Landthaler, et al., *Randomized placebo-controlled human pilot study of cold atmospheric argon plasma on skin graft donor sites.* Wound Repair Regen, 2013. **21**(6): p. 800-7.
18. Haertel, B., K. Eiden, A. Deuter, K. Wende, T.v. Woedtke, and U. Lindequist. *Differential effect of non-thermal atmospheric-pressure plasma on angiogenesis*. 2014. Letters in Applied NanoBioScience.
19. Haertel, B., T. von Woedtke, K.D. Weltmann, and U. Lindequist, *Non-thermal atmospheric-pressure plasma possible application in wound healing.* Biomol Ther (Seoul), 2014. **22**(6): p. 477-90.
20. Boeckmann, L., M. Schäfer, T. Bernhardt, M.L. Semmler, O. Jung, G. Ojak, et al., *Cold Atmospheric Pressure Plasma in Wound Healing and Cancer Treatment.* Applied Sciences, 2020. **10**(19).
21. Arjunan, K.P., G. Friedman, A. Fridman, and A.M. Clyne, *Non-thermal dielectric barrier discharge plasma induces angiogenesis through reactive oxygen species.* J R Soc Interface, 2012. **9**(66): p. 147-57.
22. Stratmann, B., T.C. Costea, C. Nolte, J. Hiller, J. Schmidt, J. Reindel, et al., *Effect of Cold Atmospheric Plasma Therapy vs Standard Therapy Placebo on Wound Healing in Patients With Diabetic Foot Ulcers: A Randomized Clinical Trial.* JAMA Netw Open, 2020. **3**(7): p. e2010411.
23. Strohal, R., S. Dietrich, M. Mittlbock, and G. Hammerle, *Chronic wounds treated with cold atmospheric plasmajet versus best practice wound dressings: a multicenter, randomized, non-inferiority trial.* Sci Rep, 2022. **12**(1): p. 3645.
24. GmbH, n.m. [cited 2025 15th of April]; Available from: https://neoplas-med.eu/en/studies/.
25. Privat-Maldonado, A., R. Verloy, E. Cardenas Delahoz, A. Lin, S. Vanlanduit, E. Smits, et al., *Cold Atmospheric Plasma Does Not Affect Stellate Cells Phenotype in Pancreatic Cancer Tissue in Ovo.* Int J Mol Sci, 2022. **23**(4).
26. Bekeschus, S., E. Freund, C. Spadola, A. Privat-Maldonado, C. Hackbarth, A. Bogaerts, et al., *Risk Assessment of kINPen Plasma Treatment of Four Human Pancreatic Cancer Cell Lines with Respect to Metastasis.* Cancers (Basel), 2019. **11**(9).
27. Verloy, R., A. Privat-Maldonado, J. Van Audenaerde, S. Rovers, H. Zaryouh, J. De Waele, et al., *Capturing the Heterogeneity of the PDAC Tumor Microenvironment: Novel Triple Co-Culture Spheroids for Drug Screening and Angiogenic Evaluation.* Cells, 2025. **14**(6).
28. Pape, J., M. Emberton, and U. Cheema, *3D Cancer Models: The Need for a Complex Stroma, Compartmentalization and Stiffness.* Front Bioeng Biotechnol, 2021. **9**: p. 660502.

29. Tomas-Bort, E., M. Kieler, S. Sharma, J.B. Candido, and D. Loessner, *3D approaches to model the tumor microenvironment of pancreatic cancer.* Theranostics, 2020. **10**(11): p. 5074-5089.
30. Kapalczynska, M., T. Kolenda, W. Przybyla, M. Zajaczkowska, A. Teresiak, V. Filas, et al., *2D and 3D cell cultures - a comparison of different types of cancer cell cultures.* Arch Med Sci, 2018. **14**(4): p. 910-919.
31. Kundekova, B., M. Macajova, M. Meta, I. Cavarga, and B. Bilcik, *Chorioallantoic Membrane Models of Various Avian Species: Differences and Applications.* Biology (Basel), 2021. **10**(4).
32. Guerra, A., J. Belinha, N. Mangir, S. MacNeil, and R. Natal Jorge, *Simulation of the process of angiogenesis: Quantification and assessment of vascular patterning in the chicken chorioallantoic membrane.* Comput Biol Med, 2021. **136**: p. 104647.
33. Jesnowski, R., D. Furst, J. Ringel, Y. Chen, A. Schrodel, J. Kleeff, et al., *Immortalization of pancreatic stellate cells as an in vitro model of pancreatic fibrosis: deactivation is induced by matrigel and N-acetylcysteine.* Lab Invest, 2005. **85**(10): p. 1276-91.
34. Hamada, S., A. Masamune, T. Takikawa, N. Suzuki, K. Kikuta, M. Hirota, et al., *Pancreatic stellate cells enhance stem cell-like phenotypes in pancreatic cancer cells.* Biochemical and Biophysical Research Communications, 2012. **421**(2): p. 349-354.
35. Priya Arjunan, K. and A. Morss Clyne, *Hydroxyl Radical and Hydrogen Peroxide are Primarily Responsible for Dielectric Barrier Discharge Plasma-Induced Angiogenesis.* Plasma Processes and Polymers, 2011. **8**(12): p. 1154-1164.
36. Duchesne, C., S. Banzet, J.J. Lataillade, A. Rousseau, and N. Frescaline, *Cold atmospheric plasma modulates endothelial nitric oxide synthase signalling and enhances burn wound neovascularisation.* J Pathol, 2019. **249**(3): p. 368-380.
37. Kang, S.U., H.J. Kim, S. Ma, D.Y. Oh, J.Y. Jang, C. Seo, et al., *Liquid plasma promotes angiogenesis through upregulation of endothelial nitric oxide synthase-induced extracellular matrix metabolism: potential applications of liquid plasma for vascular injuries.* Cell Commun Signal, 2024. **22**(1): p. 138.
38. Kalghatgi, S., G. Friedman, A. Fridman, and A.M. Clyne, *Endothelial cell proliferation is enhanced by low dose non-thermal plasma through fibroblast growth factor-2 release.* Ann Biomed Eng, 2010. **38**(3): p. 748-57.
39. Zhu, W., S.J. Lee, N.J. Castro, D. Yan, M. Keidar, and L.G. Zhang, *Synergistic Effect of Cold Atmospheric Plasma and Drug Loaded Core-shell Nanoparticles on Inhibiting Breast Cancer Cell Growth.* Sci Rep, 2016. **6**: p. 21974.
40. Haralambiev, L., O. Neuffer, A. Nitsch, N.C. Kross, S. Bekeschus, P. Hinz, et al., *Inhibition of Angiogenesis by Treatment with Cold Atmospheric Plasma as a Promising Therapeutic Approach in Oncology.* Int J Mol Sci, 2020. **21**(19).
41. Khlyustova, A., C. Labay, Z. Machala, M.-P. Ginebra, and C. Canal, *Important parameters in plasma jets for the production of RONS in liquids for plasma medicine: A brief review.* Frontiers of Chemical Science and Engineering, 2019. **13**(2): p. 238-252.
42. Privat-Maldonado, A., A. Schmidt, A. Lin, K.D. Weltmann, K. Wende, A. Bogaerts, et al., *ROS from Physical Plasmas: Redox Chemistry for Biomedical Therapy.* Oxid Med Cell Longev, 2019. **2019**: p. 29.

43. Bakhtiyari-Ramezani, M., M. Nasiri, and M. Baniasadi, *Helium and argon cold plasma effects on the 4T1 cancer cells and a triple negative mouse model of breast cancer.* Sci Rep, 2025. **15**(1): p. 10569.
44. Asghar, A.H. and A.R. Galaly, *The Effect of Oxygen Admixture with Argon Discharges on the Impact Parameters of Atmospheric Pressure Plasma Jet Characteristics.* Applied Sciences, 2021. **11**(15): p. 6870.
45. Barkhordari, A., S. Karimian, S. Shahsavari, D. Krawczyk, and A. Rodero, *Influence of the argon admixture on the reactive oxide species formation inside an atmospheric pressure oxygen plasma jet.* Sci Rep, 2024. **14**(1): p. 3425.
46. Ullah, N., M.I. Khan, A. Qamar, N.U. Rehman, E. Tag elDin, M. Alkhedher, et al., *Metrology of Ar-N(2)/O(2) Mixture Atmospheric Pressure Pulsed DC Jet Plasma and its Application in Bio-Decontamination.* ACS Omega, 2023. **8**(13): p. 12028-12038.
47. Babaeva, N.Y., G.V. Naidis, D.V. Tereshonok, E.E. Son, M.M. Vasiliev, O.F. Petrov, et al., *Production of active species in an argon microwave plasma torch.* Journal of Physics D: Applied Physics, 2018. **51**(46): p. 464004.

CHAPTER 05

BALANCING CYTOTOXICITY AND RESISTANCE: DOSE-DEPENDENT AND TUMOR-TYPE SPECIFIC RESPONSE TO CAP-CHEMOTHERAPY COMBINATIONS IN ADVANCED 3D PDAC MODELS

Adapted from:
Verloy, R.; Privat-Maldonado, A.; Palmiotto, G.; Rovers, S.; Peeters, E.; Brants, L.; Lau, H.W.; De Waele, J.; Nikiforov, A.; Gromov, M.; Deben, C.; Smits, E. and Bogaerts, A. Balancing cytotoxicity and resistance: dose-dependent and tumor-type specific response to cold atmospheric plasma-chemotherapy combinations in advanced 3D PDAC models. Manuscript in preparation.

5.1 Abstract

As written in chapter 2, PDAC is one of the most lethal cancers, with a five-year survival rate around 10%, primarily due to late diagnosis and high resistance to conventional therapies. This resistance is partially driven by the complex desmoplastic TME, which is created largely by the PSCs. CAP has shown promise in selectively targeting both cancer and stromal cells, including PSCs, key contributors to TME-mediated resistance. In this chapter, I evaluate the combination of CAP with GEM/PCX in two advanced PDAC models: a previously optimized TCC spheroid model mimicking the TME, and a turkey CAM model with intravascular drug delivery. CAP is applied using the kINPen MED device, and treatment effects are assessed by tumor size, viability, oxidative stress, and image-based analysis. Mono-CAP treatment and mono-chemotherapy show strong cytotoxic effects in vitro, and for chemotherapy in ovo as well. In addition, CAP enhances cancer cell killing at low chemotherapy doses in vitro but add no benefit at high doses and even enhances viability slightly in one type of spheroids. Image analysis reveals tumor-type-dependent selectivity: CAP spares PSCs in this type of spheroids but is broadly cytotoxic in the second type of spheroids. These differential outcomes in our two spheroid types stress the effects due to tumor heterogeneity, which are mimicked in both our in vitro and in ovo models. Overall, our results emphase the importance of tumor and dose context in optimizing CAP-chemotherapy strategies. In conclusion, combining CAP with low-dose chemotherapy shows therapeutic potential in PDAC and holds promise to lower chemotherapy doses for patients while retaining the anti-cancer effect, mitigating systemic toxicity and economic costs for patients, but this effectiveness is reduced with high-dose chemotherapy.

5.2 Introduction

As explained in chapter 2, PDAC remains one of the most lethal malignancies, characterized by rapid progression, late diagnosis, and poor prognosis, with an estimated five-year survival rate of only around 10% globally [1, 2]. Despite recent advances in chemotherapy, PDAC continues to show high resistance to standard treatment regimens, primarily due to the extensive desmoplastic reaction within the TME [3, 4]. Current first-line chemotherapy treatments for advanced or metastatic PDAC include FFX and GNP [5]. Although these regimens have improved overall survival compared to single-agent therapies, they are associated with significant toxicity and limited long-term efficacy, underscoring the urgent need for more effective therapeutic strategies [6-8]. With PDAC predicted to become the third leading cause of cancer-related deaths in Western countries by 2030, innovative approaches targeting both cancer cells and the complex tumor stroma are crucial for improving patient outcomes [2, 9].

A key feature of PDAC resistance to conventional treatments lies in its unique TME, characterized by extensive fibrosis and abundant stromal components, including PSCs and ECs [3, 7, 9]. These cells interact dynamically with cancer cells to promote tumor growth, therapy resistance, angiogenesis, and metastasis [7, 9]. Accurate modeling of these complex interactions is essential to better evaluate novel therapeutic combinations effectively.

As explained in previous chapters as well, an emerging and promising approach for overcoming therapy resistance in cancer treatment is the use of CAP, a partially ionized gas that generates RONS, which can induce apoptosis, oxidative stress, and cell death selectively in cancer cells [10]. In addition to its direct cytotoxic effects, CAP has demonstrated anti- and pro-angiogenic, immunomodulatory, and TME-modifying activities, highlighting its potential as a complementary therapeutic modality alongside conventional chemotherapy [11-16]. Although CAP's efficacy has been explored in multiple cancer models, most prior research has employed traditional 2D cultures or simple monoculture spheroids, limiting the translational relevance of findings.

Therefore, to better represent the complex interactions within the PDAC TME, advanced 3D co-culture models that closely mimic clinical tumor conditions are required. Such models integrate multiple cell types, including cancer cells, stromal cells, and ECs, enabling more accurate evaluation of therapeutic responses, as demonstrated in detail in chapter 3 [17]. Furthermore, innovative preclinical models such as the in ovo turkey CAM assay are valuable due to their accessibility, cost-effectiveness, and suitability for vascularized tumor development, allowing for direct assessment of intravascular delivery of therapeutics and the metastatic potential of cancer cells [18-21].

In this chapter, we aim to evaluate the therapeutic potential of combining CAP with chemotherapeutic agents GEM/PCX in overcoming PDAC resistance using two sophisticated preclinical models: the TCC spheroid model incorporating PDAC cells, PSCs, and ECs, developed in chapter 3, and a turkey CAM model enabling direct intravascular administration of chemotherapy. By employing these advanced approaches, we intend to investigate the effects of combining CAP treatment with chemotherapy on tumor growth, cell viability, oxidative stress, and cell population dynamics, providing novel insights into CAP as an adjuvant treatment modality for PDAC.

5.3 Materials and methods

5.3.1 Cell culture

The human PCC lines MiaPaCa-2 (ATCC®, Manassas, VA, USA) and BxPC-3 (ATCC®, Manassas, VA, USA) were used in this study. The human immortalized PSC line RLT-PSC was kindly provided by Prof. Ralf Jesenofsky, of the Faculty of Medicine, University of Mannheim [22], while the hPSC21 line was established at Tohoku University, Graduate School of Medicine, kindly provided by Prof. Atsushi Masamune [23]. In addition, the immortalized EC line HMEC-1 (ATCC®) was used. All cell lines were used for a maximum of 20 passages after thawing, tested for mycoplasma every 3 months, and STR profiling has validated that the cell lines remained identical to the original cell line. PCCs and PSCs cells were cultured in Dulbecco's Modified Eagle Medium (DMEM, 10938025, Gibco) supplemented with 10% fetal bovine serum (FBS, 10270106, Life Technologies), 100 U/mL penicillin, 100 µg/mL

streptomycin (15140122, Life Technologies), and 2 mM L-glutamine (25030024, Life Technologies). PCCs and PSCs were transduced with NucLight Rapid Red (4741, Essen Biosciences) to express mKate2, and with NucLight Green (4475, Essen Biosciences) to express GFP, respectively. HMEC-1 cells were cultured in MCDB131 (10372019, ThermoFisher Scientific) supplemented with 10 ng/mL Epidermal Growth Factor (PHG0314, ThermoFisher), 1 µg/mL Hydrocortisone (H0396, Sigma Aldrich), 10 mM L-glutamine (25030024, Life Technologies), 10% FBS (10270106, Life Technologies), and 100 U/mL penicillin, 100 µg/mL streptomycin (15140122, Life Technologies). Cells were maintained in a humidified incubator at 37 °C and 5% CO_2. HMEC-1 cells for the supplementary proliferation rate were transduced with CMV-GFP.

5.3.2 Spheroid formation

TCC spheroids of MiaPaCa-2:RLT-PSC:HMEC-1 (MRH) and BxPC-3:hPSC21:HMEC-1 (BHH) combinations were generated as described in chapter 3 [17]. Briefly, cells were seeded in defined ratios (MRH at 6:3:3 and BHH at 6:5:3) at densities of 3500 and 7000 cells per well, respectively, in ultra-low adherent (ULA) plates (7007, Corning®, Corning, NY, USA) containing 0.24% methylcellulose M0512, Merck, Rahway, NJ, USA). Plates were centrifuged at 453 × *g* for 10 min, incubated at 37 °C and 5% CO_2 for three days, resulting in the formation of spheroids with a diameter of approximately 300–500 µm.

5.3.3 Turkey chorioallantoic membrane model and intravenous drug injection

The turkey CAM model was used as previously described in chapter 4, section 4.3.3. Briefly, fertilized turkey eggs (Broeierij Claeys, Belgium) were incubated under controlled conditions. Eggs were pierced on embryonic day 7 with a 20G (613-3937, VWR, Radnor, PA, USA). On embryonic day 9, either 2 million cells of MiaPaCa-2 and RLT-PSC (MR) or BxPC-3 and hPSC21 (BH) (2:1 cancer:stellate cell ratio) were suspended in 20 µL Matrigel (CLS254320, Merck) and seeded onto the turkey CAM within a silicone ring. Tumors received intravenous chemotherapy (or PBS control) with CAP treatment (or gas flow control) on day 13 and were harvested and weighed on day 16 for RNA sequencing.

GEM/PCX were administered as a combination in 50 µL of PBS (Table 5.1). Using a 30G Micro-Fine insulin syringe (324826, BD), the injection was performed in one of the larger blood vessels that was most accessible. Care was taken to not pierce the blood vessel as this leads to excessive bleeding and increases the risk of embryonic death. Visually, the injection was confirmed by observing the flow of the transparent solution through the blood vessels. Before removing the needle, we waited for approximately 10 seconds to ensure all the liquid was absorbed in the bloodstream.

Table 5.1. *Titration concentration range of gemcitabine and paclitaxel in the turkey in ovo CAM model.*

Gemcitabine (ng/kg bodyweight)	Paclitaxel (ng/kg bodyweight)
5.3	1.1
16	3.2
48	9.6
144	28.8
432	86.4

5.3.4 CAP treatment

The kINPen®MED (adjusted to operate below 4 standard liter per minute (slm)) was used to treat the spheroids and in ovo tumors. Prior to CAP treatment of spheroids, 150 µL of medium was removed and 50 µL of fresh MCDB131 medium was added to a total of 100 µL. Argon was used as ionizing gas at 2 slm to treat both spheroids and in ovo tissues in the turkey egg. The treatment was performed for 60, 90 or 120 seconds with a 12 mm gap in MCDB131 medium (in vitro spheroids) and 120 seconds, based on the in vitro results, with a 10 mm gap (in ovo tissues) between the kINPen®MED nozzle and the liquid surface or in ovo tumor. For the in vitro experiments, the CAP setup was controlled by an automated stage using the program WinPC-NC. For the in ovo experiments, manual treatment was performed while carefully maintaining a 10 mm gap and moving the device from left to right, up and down, etc. to ensure treating the entire tumor.

5.3.5 Cell viability assay

The total cell viability of spheroids was measured with the CellTiter-Glo® assay (G7571, Promega) as described in chapter 3 [17]. Briefly, spheroids were treated for five days with

CAP or GEM in combination with PCX (Table 5.2) using a digital dispenser. Cell viability was assessed by ATP quantification (CellTiter-Glo®, G7571), normalized to vehicle control (≤0.6% DMSO).

Table 5.2. *Titration concentration range of gemcitabine and paclitaxel either as mono- or combinational therapy.*

Condition	Gemcitabine	Paclitaxel
T1	2.5 nM	0.5 nM
T2	5 nM	1 nM
T3	25 nM	5 nM
T4	50 nM	10 Nm
T5	0.4 µM	80 nM
T6	2.5 µM	0.4 µM
T7	10 µM	2 µM

5.3.6 Live imaging

PCCs and PSCs were transduced with NucLight Rapid Red (4741, Essen Biosciences) to express mKate2, and with NucLight Green (4475, Essen Biosciences) to allow for live-imaging. CellROX™ Orange (C10443, ThermoFischer Scientific) and Incucyte® Cytotox Green (4633, Sartorius) were used according to manufacturers' instructions at 24h and 72h after the mono- or combinational treatment of CAP and chemotherapy. Images of the TCC spheroids were captured using the non-confocal Spark® Cyto (Tecan) microscope with a 10× objective. Image acquisition was performed for brightfield, green (Cytotox) and red (CellROX) fluorescent channels (Table 5.3).

Table 5.3. *Technical information on the image acquisition of TCC spheroids using the Spark® Cyto (Tecan).*

Dye	Excitation	Emission	LED Intensity (%)	Exposure Time (ms)
BxPC-3	543–566	580–611	25	300
MiaPaCa-2	543–566	580–611	20	60
RLT-PSC	461–487	500–530	10	50
hPSC21	461–487	500–530	20	80
CellRox™ Orange	543–566	580–611	100	400
Incucyte® Cytotox Green	461-487	500-530	15	50

5.3.7 Image Analysis

In our analysis pipeline, raw multi-channel TIFF files were imported into Arivis Pro v4.3.1 using the Arivis SIS Converter. Spheroid segmentation was achieved using a Random Forest classifier implemented in ilastik (integrated within Arivis), which was trained on a subset of representative images to distinguish spheroid boundaries from background. Next, we individually segmented the green and red fluorescence channels, corresponding in the CAP-chemotherapy assay to PSCs and PCCs, and in the oxidative stress assay to oxidative stress (red) using the blobfinder algorithm in Arivis. To remove spurious objects, we filtered spheroid segments to exclude any regions smaller than 5,000 μm^2. We then isolated the largest contiguous spheroid in each field of view and applied a morphological closing operation to fill internal voids, yielding a single, solid spheroid mask. Finally, we applied the compartimentalization module of Arivis to map the blobfinder-identified dye signals onto the refined spheroid volume, enabling extraction of quantitative metrics for subsequent statistical analysis.

5.3.8 Statistical analysis

All experiments were performed at least three times with three technical replicates, unless specified otherwise. Outlier tests were performed using GraphPad Software v10.4.2. Statistics for the in vitro cell viability assay and in ovo chemotherapy titration were performed using linear mixed models with the treatment as fixed effect and experimental repeat as random effect and Dunnett's multiple comparison test using JMP Pro v17.0.0 software. To calculate the statistical significances for the in ovo experiments on the combination of CAP and chemotherapy, all experimental groups were compared using the Brown-Forsythe and Welch one-way ANOVA test and Dunnett's T3 multiple comparison test using GraphPad Software v10.4.2. The data that was acquired using Arivis Pro v4.3.1 was tested for significances (where indicated) with one-sample t-test compared to the control group.

5.4 Results

5.4.1 CAP enhances chemotherapy response in BHH spheroids but impairs efficacy in MRH spheroids with high chemotherapy dosage

To determine the optimal CAP treatment time and GEM/PCX concentrations for a combination therapy, we investigated the effect of multiple monotherapy CAP treatment times, followed by a dual titration of both CAP treatment times and GEM/PCX concentrations in combination on cell viability (Figure 5.1). Mono-CAP treatment reduced cell viability in a time-dependent manner in both PDAC spheroid models, with 120 seconds inducing the strongest cytotoxicity (Figure 5.1b and c). When combined with a chemotherapy titration (T1–T7; see Table 5.2 above), differential responses were observed. At low GEM/PCX doses, BHH spheroids were more sensitive to the combination than MRH spheroids (Figure 5.1d and e). Conversely, at high GEM/PCX doses, MRH spheroids exhibited a stronger response than BHH (Figure 5.1d and e). Normalization to mono-CAP conditions (Figure 5.1e and f) revealed that in BHH spheroids, cytotoxicity was enhanced when combining CAP and GEM/PCX treatments across the dose range, especially at lower concentrations (Figure 5.1f). Interestingly, in MRH spheroids, CAP showed an increased efficacy at low doses but attenuated the response at higher doses, with a paradoxical increase in viability at the highest GEM/PCX concentrations with 120s of CAP treatment (Figure 5.1g). These results highlight the model-dependent and dose-dependent nature of CAP and chemotherapy interactions.

5.4.2 Monotherapies show differential selectivity across tumor models

Mono-CAP treatment and mono-chemotherapy both reduced PCC and PSC proportions in 3D PDAC spheroids but differed in their selectivity and tumor-type specificity (Figure 5.2a-d and Supplementary Figures S5.1-5.4). In MRH spheroids, CAP selectively reduced PCCs while largely sparing or even modestly preserving PSCs (Figures 5.2b and d, S5.2-5.4). In contrast, in BHH spheroids, CAP acted non-selectively, significantly reducing both PCC and PSC areas, suggesting a broader cytotoxic profile in this context (Figures 5.2a and c, S5.1, S5.3 and S5.4).

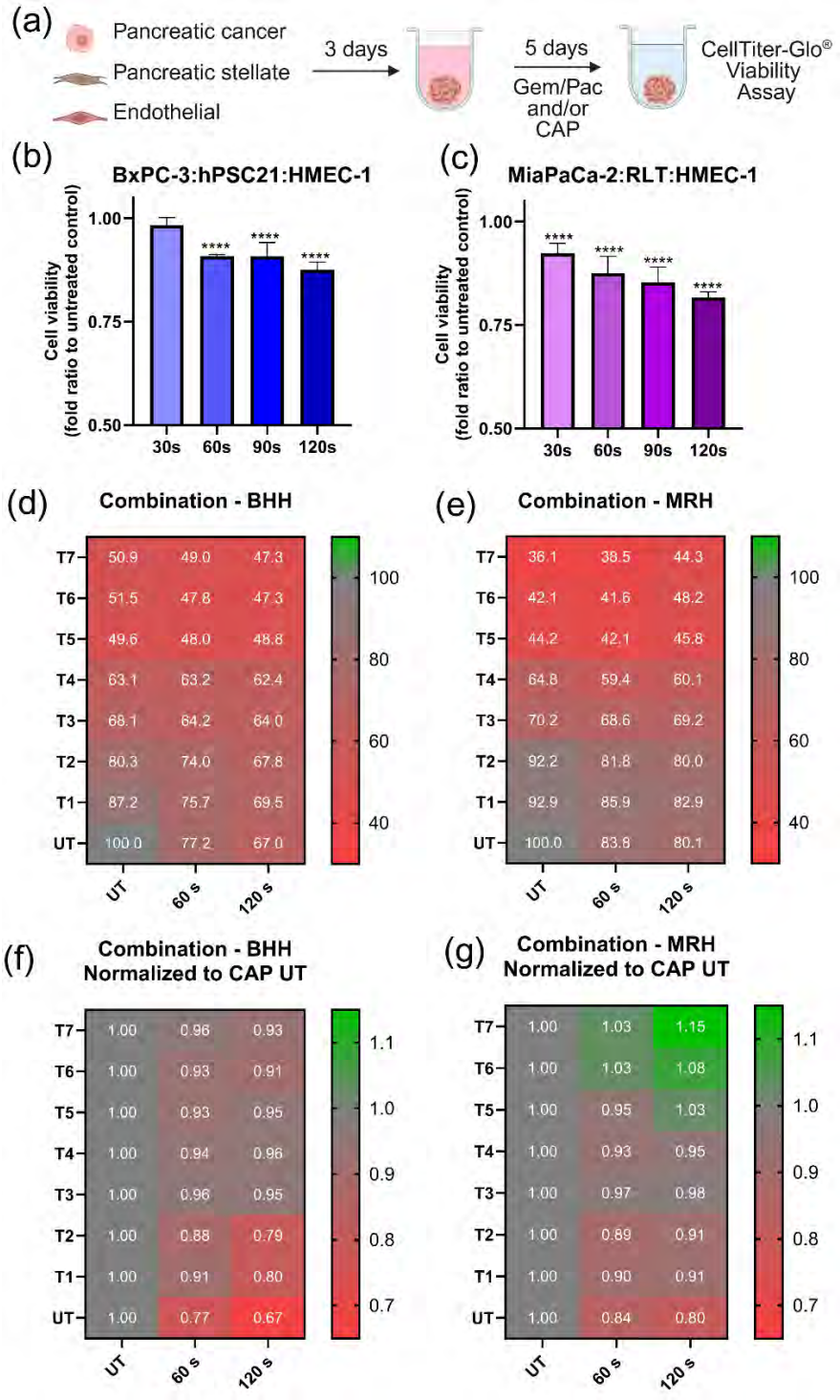

Figure 5.1. *CAP reduces viability and modulates chemotherapy response in PDAC spheroids. (a) Experimental setup showing TCC spheroid formation, CAP exposure (30-120s), chemotherapy treatment, and viability assay. (b-c) Normalized cell viability to untreated controls for CAP treated spheroids (30-120s) for BHH (b) and MRH (c) spheroids. (d–g) Viability heatmaps for BHH (b) and MRH (c) spheroids treated with GEM/PCX (T1–T7) and CAP (60s, 120s) and normalized to the CAP untreated for BHH (f) and MRH (g) spheroids. Data are represented as mean ± SEM are shown (n≥7 from 3 independent experiments). Statistical significance is compared to the untreated control (value = 1.00 due to normalization). ****p < 0.0001. UT = untreated.*

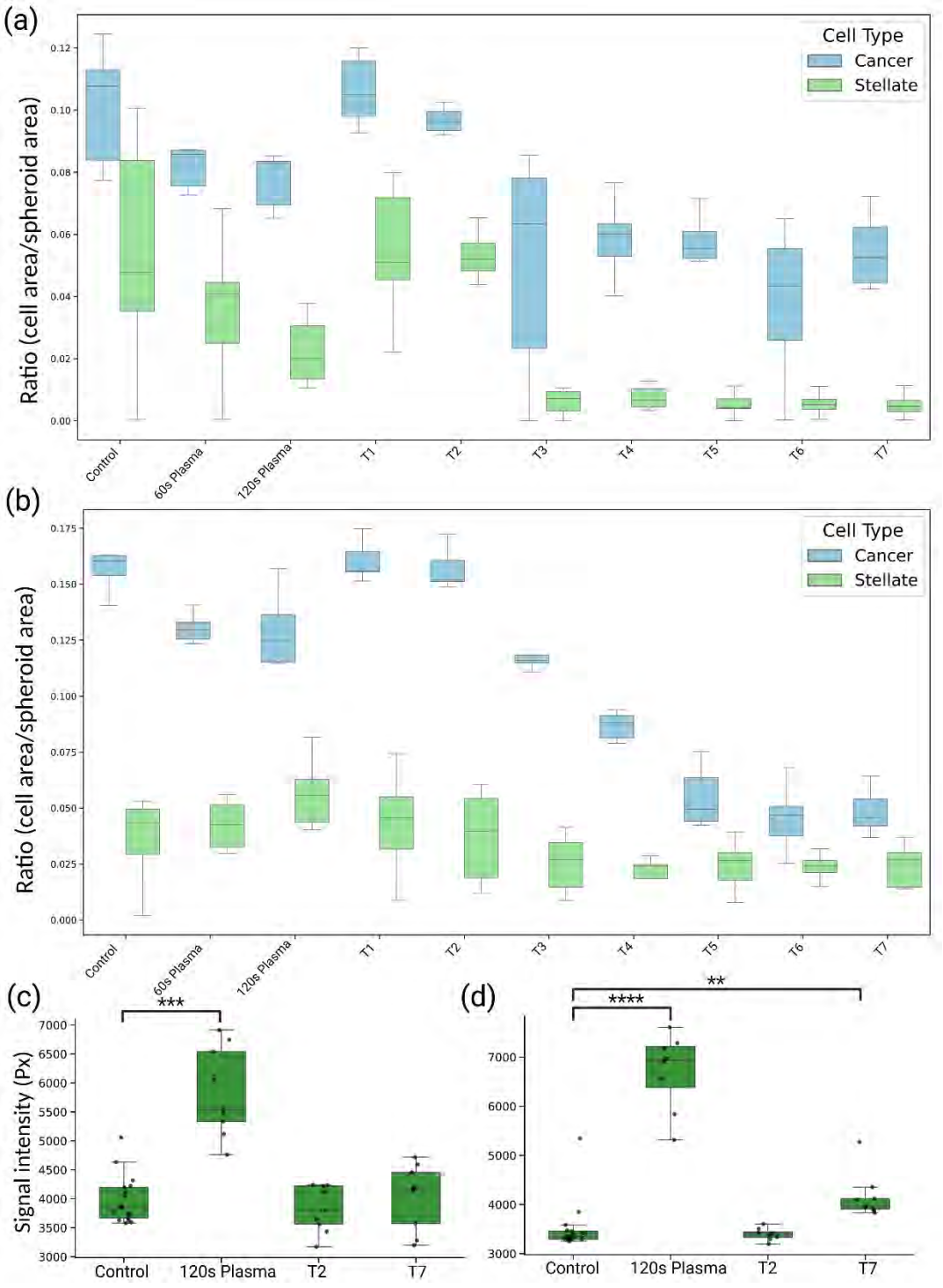

Figure 5.2. *Differential effects of CAP and chemotherapy on cell proportions and oxidative stress in BHH and MRH spheroids. (a, b) Box plots showing the effect of CAP (60s, 120s) and chemotherapy (T1–T7) on cancer (blue) and stellate (green) cell proportions in BHH (a) and MRH (b) spheroids. (c, d) Oxidative stress intensity measured after 72 hours in BHH (c) and MRH (d) spheroids following treatment with 120s CAP, T2, or T7 compared to untreated control. Data represent cell type proportions relative to total spheroid area (a-b) or oxidative intensity measured by CellRox™ Orange (c-d) with n≥7 from 3 independent experiments. *p < 0.05, **p < 0.01, ***p < 0.001, ****p < 0.0001.*

Mono-chemotherapy showed a strong dose-dependent reduction in PCC proportions across both models, with T5–T7 producing the most pronounced effects (Figure 5.2a and b). However, this effect came at the cost of PSC viability, especially in BHH spheroids where stellate damage occurred abruptly between T2 and T3 and plateaued thereafter (Figure 5.2a and b). Mono-CAP treatment clearly induced oxidative stress in both BHH and MRH spheroids 72 hours post-treatment, while mono-chemotherapy did not, highlighting the different mechanisms of action of CAP compared to GEM/PCX (Figure 5.2c and d), and thus, the rationale of the combination therapy.

5.4.3 Treatment-induced structural disruption reflects cytotoxic effects

Morphological features of spheroids further reflected the cytotoxic impact of treatments. Across both models, spheroid roundness consistently dropped post-treatment, indicating structural destabilization and loss of cell-cell cohesion at the edges of the spheroid (Figures 5.3 and S5.1-5.4). This effect intensified with higher chemotherapy doses and with the addition of CAP for nearly all conditions (Figures 5.3, S5.1-5.4). Spheroid area did not follow a consistent dose-response pattern. In some conditions, particularly those with extensive cell death (e.g., high-dose GEM/PCX conditions), area increased slightly over time (Figures 5.3 and S5.1-S5.4). This likely reflects loosening of spheroid structure rather than true growth, caused by cell loss in the spheroid core. Mono-CAP treatment (120s) in BHH spheroids showed such a pattern, with increased area accompanied by decreased cell content, consistent with a disintegration phenotype (Figures 5.3, S5.1, S5.3 and S5.4).

5.4.4 Combination therapy yields limited synergy and depends on tumor models

Combining chemotherapy with CAP yielded largely additive effects on cancer cell killing, with true Bliss synergy was detected only at lower chemotherapy doses (T1–T3) and predominantly in MRH spheroids (Figure S5.5). Higher-dose combinations generally showed neutral or antagonistic interactions, suggesting limited benefit of adding CAP at high cytotoxic loads (Figures 5.3, S5.4 and S5.5). Selectivity profiles further emphasized tumor-type specificity.

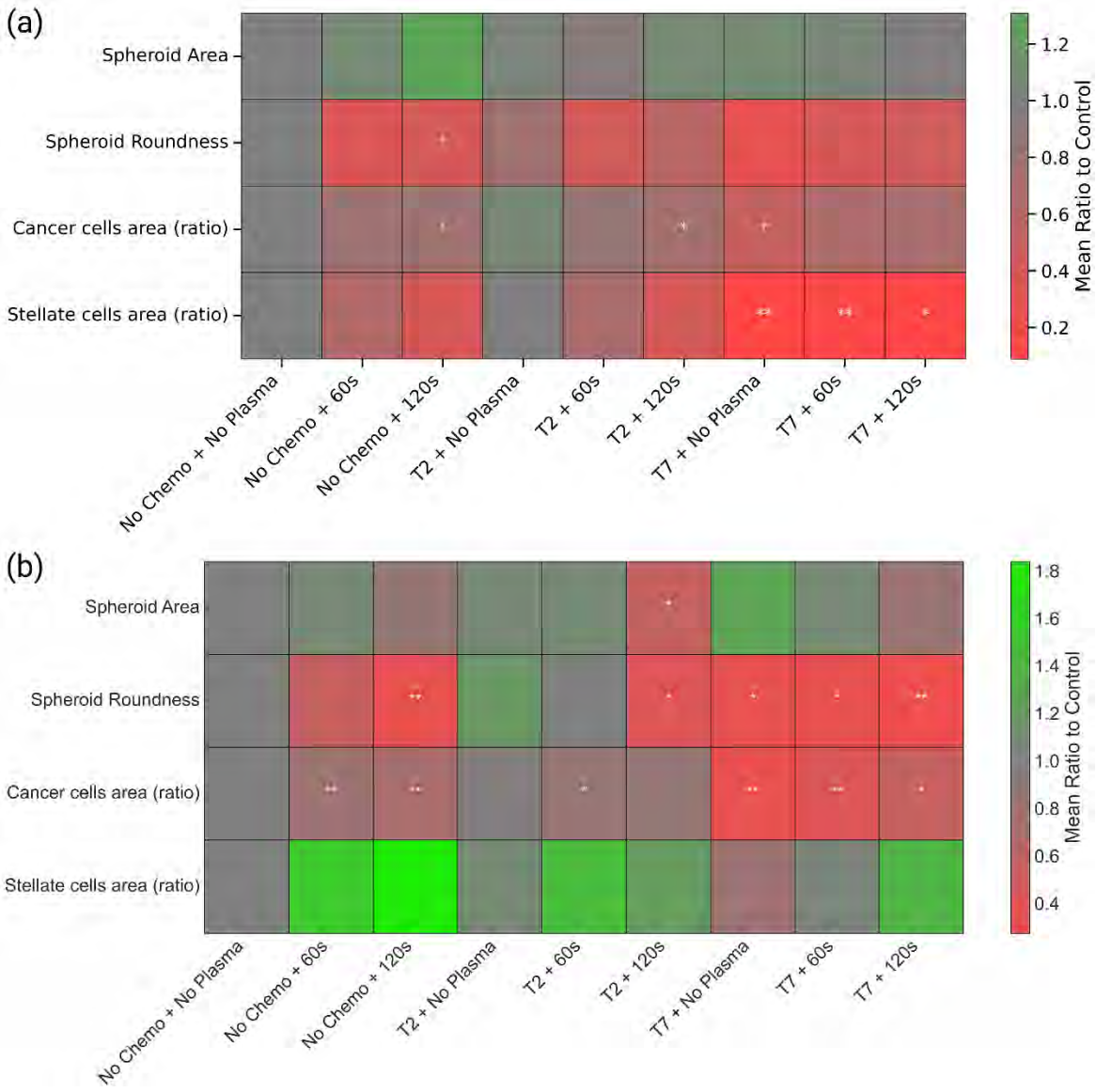

Figure 5.3. *CAP enhances treatment response in BHH spheroids at low chemotherapy dose and preserves stromal components in MRH spheroids. Heatmaps showing the mean effect of different treatments on image-based parameters relative to untreated controls in (a) BHH and (b) MRH TCC spheroids. Treatments include chemotherapy (No chemo, T2, T7) with or without CAP (No plasma, 60s, 120s). Measured parameters include PCC and PSC area (as a ratio to the total spheroid area), spheroid area, and roundness. Red indicates a reduction and green an increase relative to control. *p < 0.05, **p < 0.01.*

In MRH spheroids, CAP preserved PSCs when combined with chemotherapy, particularly at lower doses, indicating a protective interaction (Figures 5.3, S5.2 and S5.4). This effect was absent in BHH spheroids, where CAP enhanced stellate cell damage regardless of chemotherapy dose (Figures 5.3, S5.1 and S5.4).

The findings from the image analysis underscore the influence of tumor-type context in shaping responses to CAP and chemotherapy combinations. While MRH spheroids exhibited greater selectivity during mono-CAP treatment (reducing cancer cells while preserving PSCs), this benefit did not consistently translate to combination settings.

At higher chemotherapy doses, CAP treatment even appeared to attenuate efficacy in MRH spheroids. Conversely, in BHH spheroids, CAP enhanced the effect of chemotherapy across the full dose range, however with decreasing efficiency towards higher chemotherapy doses, but did so at the cost of selectivity, significantly reducing both cancer and stellate cell populations. These data emphasize the need for tumor-type-informed optimization of GEM/PCX-CAP strategies in PDAC, balancing efficacy with preservation of stromal components. These differences between MRH and BHH spheroids demonstrate that the responses to CAP–chemotherapy combinations vary substantially between tumor types, reflecting the heterogeneity observed in PDAC.

5.4.5 CAP does not improve chemotherapy-induced tumor suppression in the CAM model

Using the CAM model, we wanted to further evaluate the efficacy of GEM/PCX and CAP treatment on tumor growth for both tumor models (Figure 5.4). A clear dose-dependent decrease in tumor weight was observed for both tumor models upon chemotherapy titration, with the highest GEM/PCX concentrations (432/86.4 GEM/PCX µg/kg) significantly reducing tumor weight in BH tumors (Figure 5.4b and c). This dose was selected for a further combination study.

Combination treatment with CAP and high-dose GEM/PCX was subsequently tested across three independent repeated experiments (Figures 5.4d-e and S5.6). Results show that chemotherapy consistently reduced tumor weight in repeats 1 and 3 for both BH and MR

models, as it did in the chemotherapy titration experiments (Figures S5.6 and 5.4). In contrast, mono-CAP treatment had no significant effect, and combination treatment did not outperform mono-chemotherapy (Figures 5.4d-e and S5.6). Repeat 2 showed aberrant results for both tumor models, with unexpectedly small untreated tumors and increased tumor weight in the combination group, suggesting possible experimental variation in the turkey CAM model or cell culture, or unnoticed technical issues (Figure S5.6). Overall, these findings confirm the efficacy of high-dose GEM/PCX in reducing tumor burden, while CAP does not consistently enhance therapeutic outcome in the used turkey in ovo CAM model.

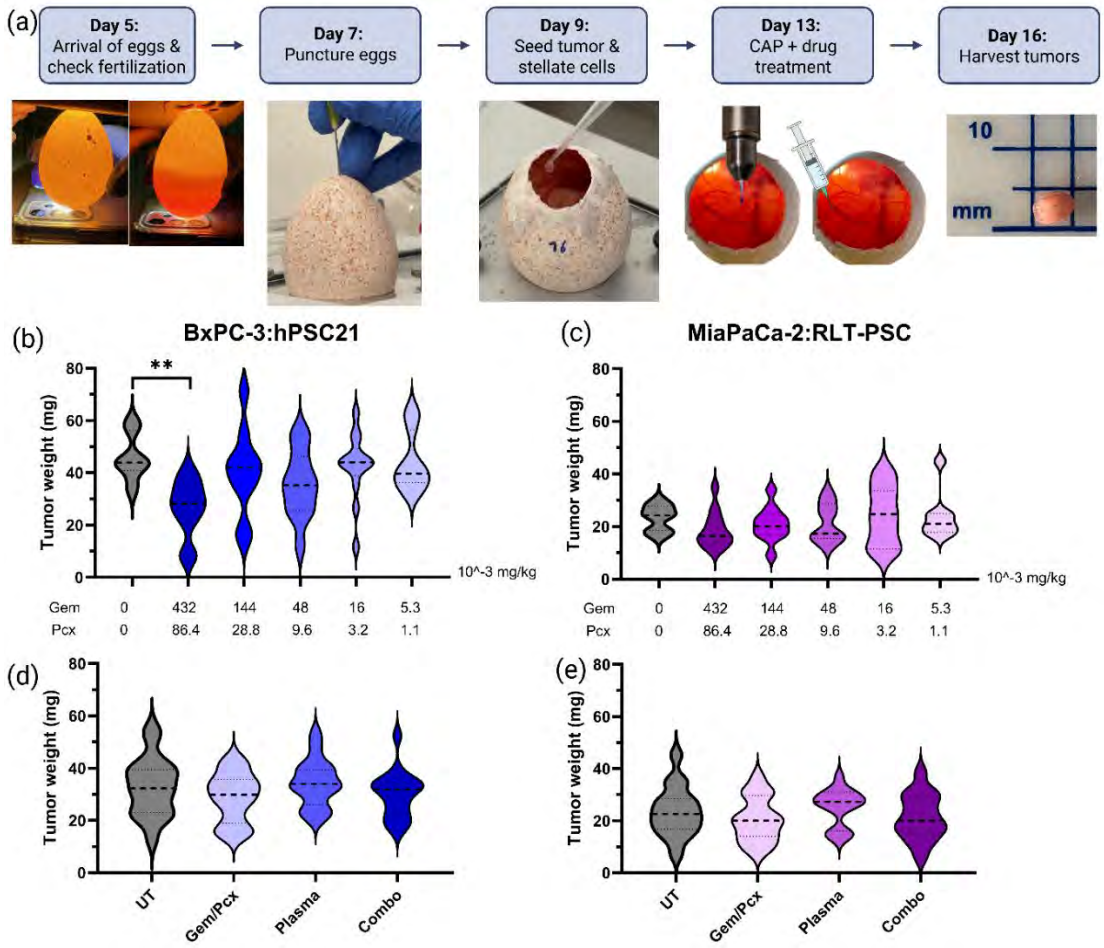

Figure 5.4. *In ovo CAM model workflow and treatment effects on tumor growth. (a) Schematic of the experimental timeline showing fertilized egg preparation, PCC and PSC seeding, CAP and GEM/PCX treatment and tumor harvesting. (b-e) plots showing tumor weight measurements in a chemotherapy titration (GEM/PCX) for BH (b) and MR (c), and following treatment with mono-chemotherapy (0.432 mg/kg GEM and 0.0864 mg/kg PCX, mono-CAP (120 s), or their combination for BH (d) and MR (e). GEM/PCX doses (mg/kg) are indicated below each group. Combination treatment includes CAP exposure followed by GEM/PCX injection. Data are represented as mean ± SD (n ≥ 8 of three independent experiments). Horizontal dashed lines indicate group medians. **p < 0.01.*

5.5 Discussion

Our findings provide valuable insights into the complex interplay between CAP and chemotherapy, highlighting both the promise and limitations of this combination therapy in PDAC. Interestingly, CAP demonstrated differential responses dependent on chemotherapy dosage and tumor model, emphasizing the importance of carefully considering tumor heterogeneity and treatment dosages.

Mono-CAP treatment at shorter durations (60s) demonstrated clear cytotoxic effects, particularly in MRH spheroids. This aligns with earlier studies showing that intermediate CAP treatment times can effectively induce cytotoxicity [24, 25]. However, our data indicated that combining CAP with chemotherapy yielded limited synergy and is only evident at lower chemotherapy doses. This aligns with the idea to lower chemotherapy dosages, when combined with sensitizing modalities such as CAP, to mitigate systemic toxicity and economic costs associated with high-dose chemotherapy regimens. The potential advantages of lower chemotherapeutic dosages on a longer treatment schedule as anti-angiogenic therapy have indeed been argued [26], which could enhance quality of life for patients while maintaining therapeutic efficacy in a combination strategy. However, at higher chemotherapy dosages, particularly in MRH spheroids, CAP exposure unexpectedly attenuated treatment efficacy, paradoxically increasing cell viability. This phenomenon could be attributed to the induction of cellular stress responses and antioxidant mechanisms at excessively high stress levels, however this should be investigated. Previous research indicates that heightened oxidative stress can trigger adaptive cellular survival pathways, including upregulation of antioxidants like glutathione and enzymes such as catalase and superoxide dismutase, thereby reducing therapeutic effectiveness [27]. Our observations strongly suggest that a balance must be maintained, where CAP exposure intensity and chemotherapy dosage is sufficient to induce cytotoxic stress. In addition, research has shown that the combination of CAP and GEM on in vitro mono-culture MiaPaCa-2 cells did not outperform mono-CAP treatment but did significantly outperform both monotherapies in an orthotopic in vivo PDAC model [28]. Although a different CAP device and monocultures were used, the in vitro findings are

consistent with our observations at high chemotherapy doses combined with CAP. The divergence across models likely reflects differences in organismal context, microenvironment, and how compounds (GEM/PCX drugs and CAP-derived RONS) are delivered to the tumor. In vitro, GEM/PCX remain in the culture medium for several days, so high-dose regimens can saturate cytotoxicity, leaving little room for CAP to add an increased effect. In vivo, by contrast, drug exposure is transient because of distribution, metabolism, and clearance, which can unmask combination effects. In the turkey CAM in ovo model, chemotherapy produced a measurable effect, but CAP efficacy might have been limited by incomplete surface exposure: tumors often grow inward beneath the CAM, reducing access and hindering uniform CAP exposure.

Interestingly, our study observed notable differences between the tumor models in response to mono-CAP treatment and its combination with chemotherapy. In MRH spheroids, CAP demonstrated selective cytotoxicity, targeting cancer cells preferentially and preserving PSCs. Conversely, BHH spheroids showed non-selective cytotoxicity, impacting both cancer and stromal cells equally. These findings are consistent with previous reports suggesting tumor-type-specific sensitivities to treatment in general, possibly due to variations in the TME, cellular composition, known as intra- and intertumoral heterogeneity, highlighting the importance of including this heterogeneity in 3D tumor models [29-31]. We demonstrated that our TCC model can capture these effects, pointing towards its clinical relevance.

Our in ovo CAM model results further supported the limited clinical potential of combining high-dose chemotherapy with CAP. Surprisingly, mono-CAP treatment was insufficient to significantly impact tumor growth, and combined treatment did not enhance chemotherapy-induced tumor suppression. Our previous work using the CAM model in chicken eggs showed that 60s of CAP treatment on MR tumors was sufficient to induce significant cytotoxicity [25]. This, however, was achieved with an older, and different version of the kINPen®, specifically made for lab-purposes (kINPen®IND). In addition, the chicken and turkey CAM model might not be fully comparable, as the turkey embryo

growth is slower (29 days of embryonic development until hatching) compared to the chicken embryo (21 days of embryonic development until hatching).

Given these outcomes, exploring lower CAP and chemotherapy doses in combination using this model could be beneficial to avoid triggering pro-survival mechanisms associated with high cellular stress, potentially improving therapeutic efficacy, while reducing side effects, cytotoxicity and cost for patients. Furthermore, future research can also explore alternative combinations, such as CAP paired with immunotherapy, which might exploit the immunomodulatory effects of CAP-generated RONS to potentially enhance anti-tumor immunity [12, 13, 32-34].

Overall, our data show that responses to CAP-chemotherapy combinations in PDAC are strongly context dependent. CAP combined with low-dose GEM/PCX enhanced antitumor activity and suggested a route to GEM/PCX dose reduction, whereas its added benefit diminished at higher chemotherapy doses. Divergent responses of MRH and BHH spheroids caution against generalizing from a single model and point to including tumor heterogeneity and optimization of CAP parameters and drug dosing, with other potential exploration of combinations such as immunotherapy.

5.6 Conclusion

In conclusion, our findings emphasize the complex interactions between CAP and chemotherapy in PDAC, highlighting tumor heterogeneity and therapeutic dosages as crucial factors influencing outcomes. Combining CAP with lower chemotherapy doses showed potential by enhancing efficacy, which could be beneficial for PDAC patients due to a reduced systemic toxicity and economic costs. However, higher doses of chemotherapy in combination to CAP attenuated this enhanced cytotoxic effect. The observed tumor-specific responses suggest the importance of tailoring treatment strategies accordingly. The limited impact observed in our CAM model supports that the combination of high CAP and chemotherapy doses does not provide a better treatment outcome, and alternative approaches, like CAP combined with the low-dose chemotherapy or with immunotherapy,

should be explored. Future research should aim to refine these combinations to maximize therapeutic efficacy and improve clinical outcomes in PDAC.

5.7 Supplementary material

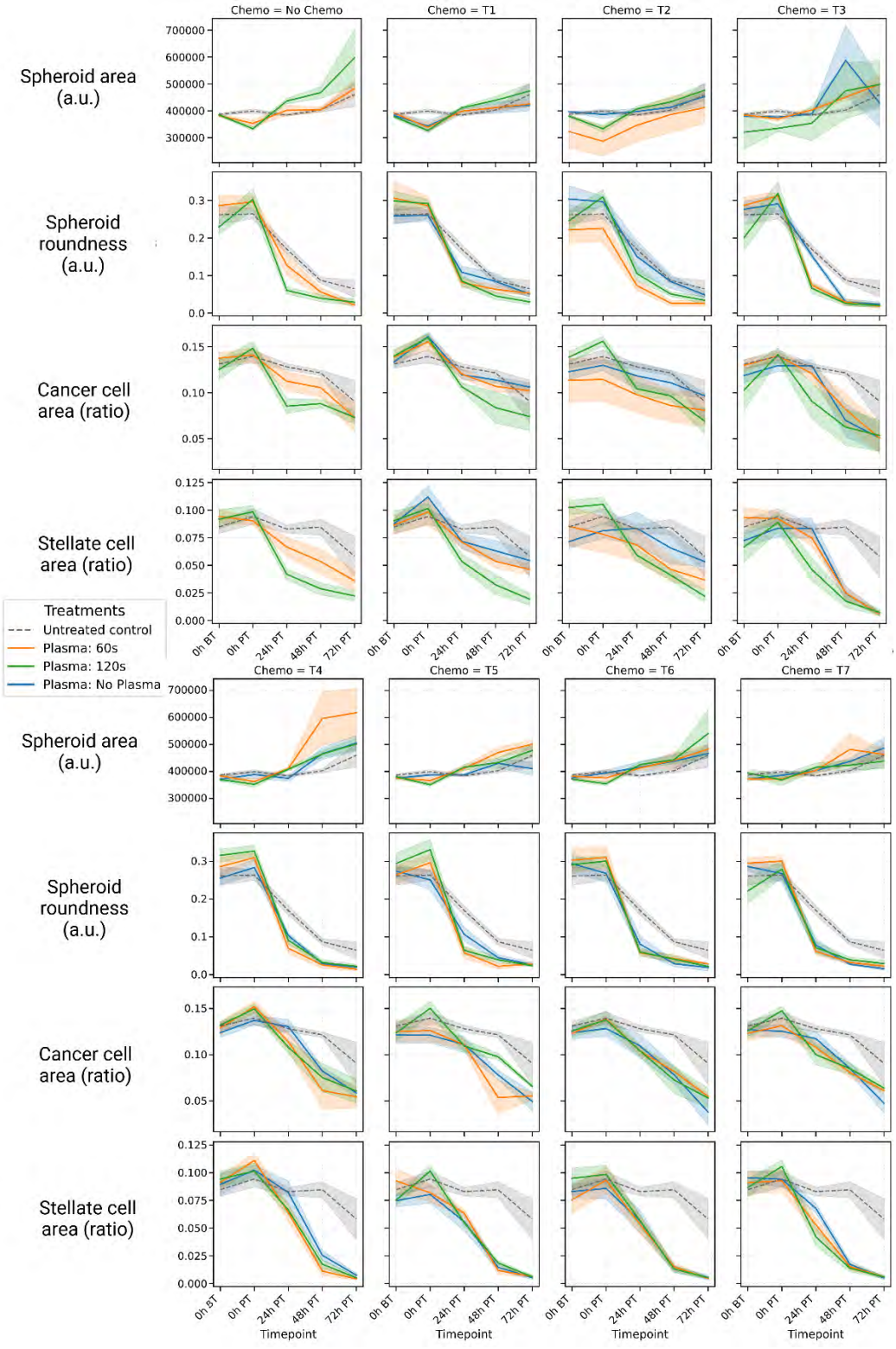

Supplementary Figure 5.1. *Time-course plots showing spheroid area, spheroid roundness, PCC area, and PSC area in BHH spheroids treated with different chemotherapy conditions (No Chemo, T1–T7) in combination with CAP exposure (No Plasma, Plasma 60s, Plasma 120s). Each plot represents the mean ± SD of quantified image-based parameters across three independent repeated experiments with each three technical replicates.*

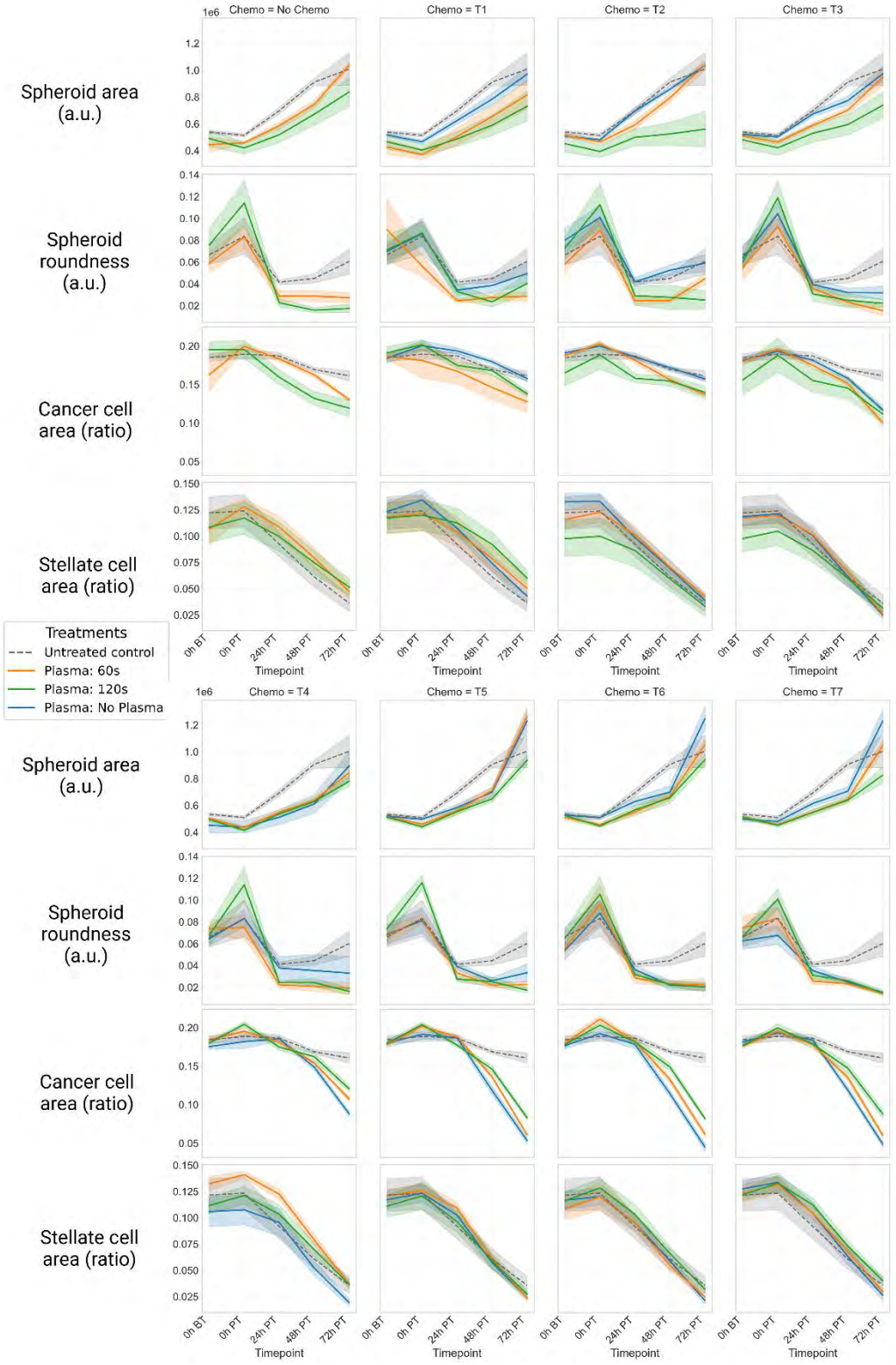

Supplementary Figure 5.2. *Time-course plots showing spheroid area, spheroid roundness, PCC area, and PSC area in MRH spheroids treated with different chemotherapy conditions (No Chemo, T1–T7) in combination with CAP exposure (No Plasma, Plasma 60s, Plasma 120s). Each plot represents the mean ± SD of quantified image-based parameters across three independent repeated experiments with each three technical replicates.*

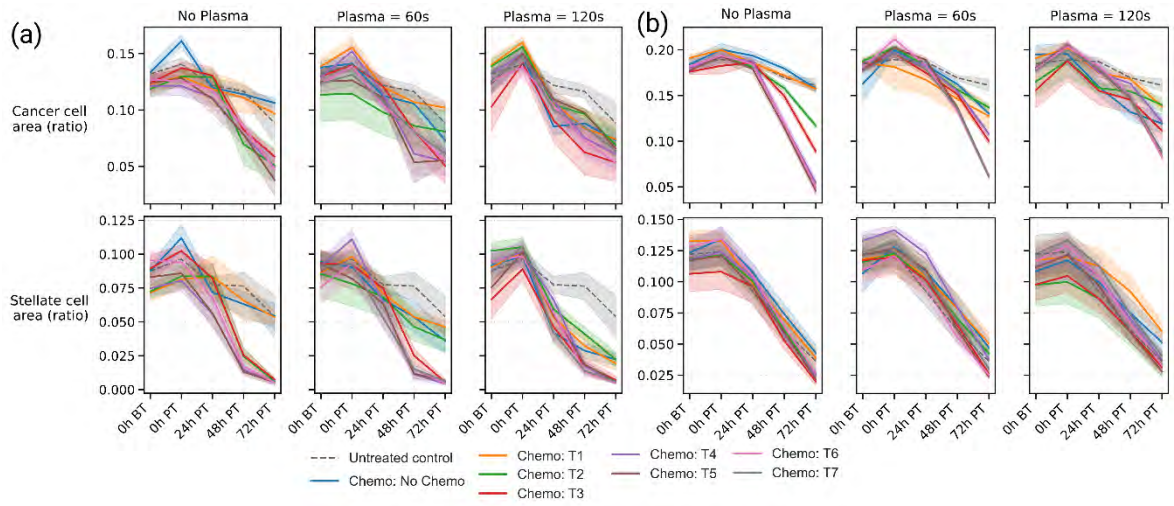

Supplementary Figure 5.3. *Time-course plots showing PCC area and PSC area in BHH and MRH spheroids treated with different chemotherapy conditions (No Chemo, T1–T7) in combination with CAP exposure (No Plasma, Plasma 60s, Plasma 120s). Each plot represents the mean ± SD of quantified image-based parameters across three independent repeated experiments with each three technical replicates.*

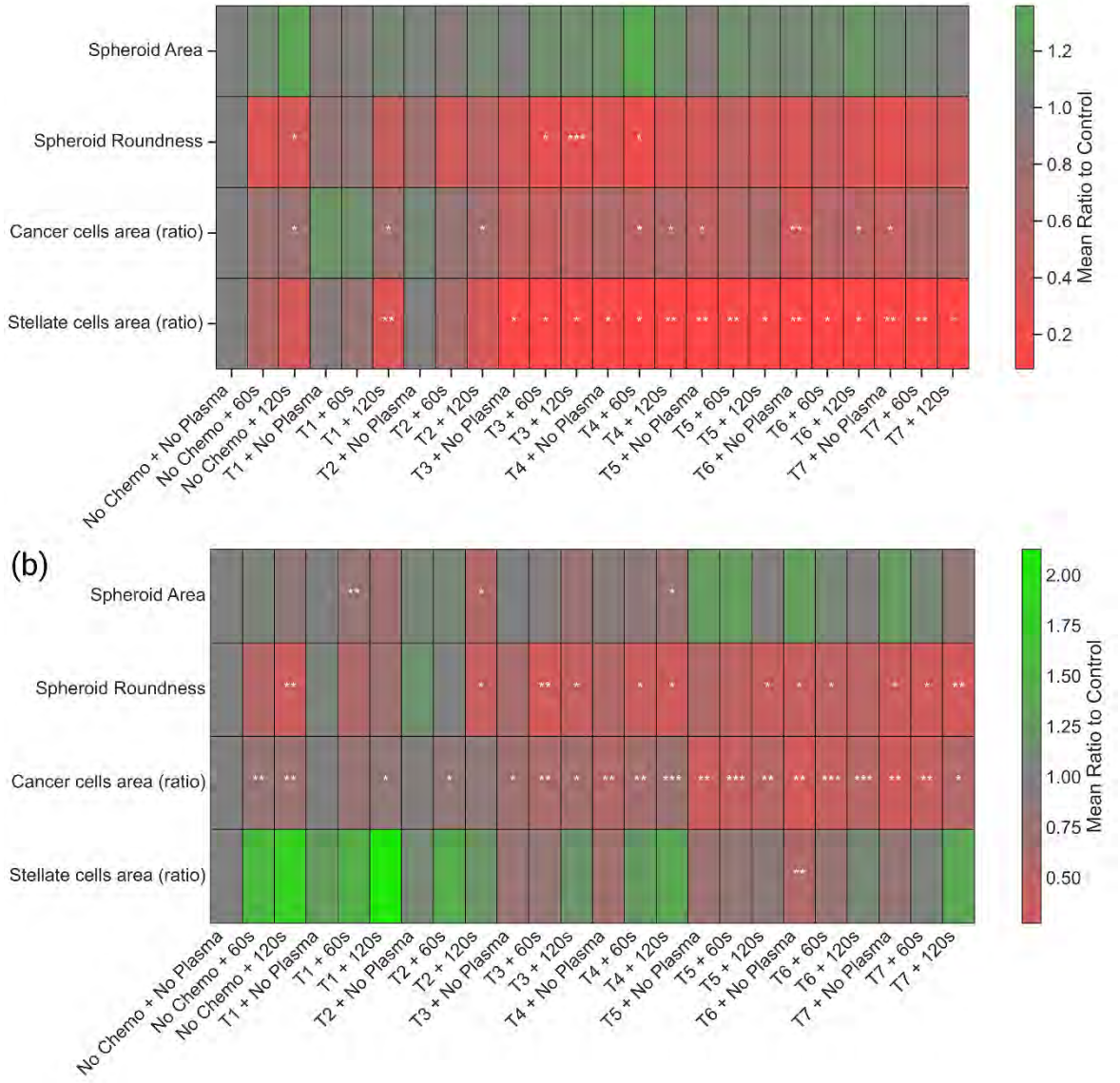

Supplementary Figure 5.4. *CAP enhances treatment response in BHH spheroids at low chemotherapy dose and preserves stromal components in MRH spheroids. Heatmaps showing the mean effect of different treatments on image-based parameters relative to untreated controls in (a) BHH and (b) MRH spheroids. Treatments include chemotherapy (T1–T7) with or without CAP (60s, 120s). Measured parameters include PCC and PSC area (as a ratio to the total spheroid area), spheroid area, and roundness. Blue indicates a reduction and red an increase relative to control. *p < 0.05, **p < 0.01, ***p < 0.001.*

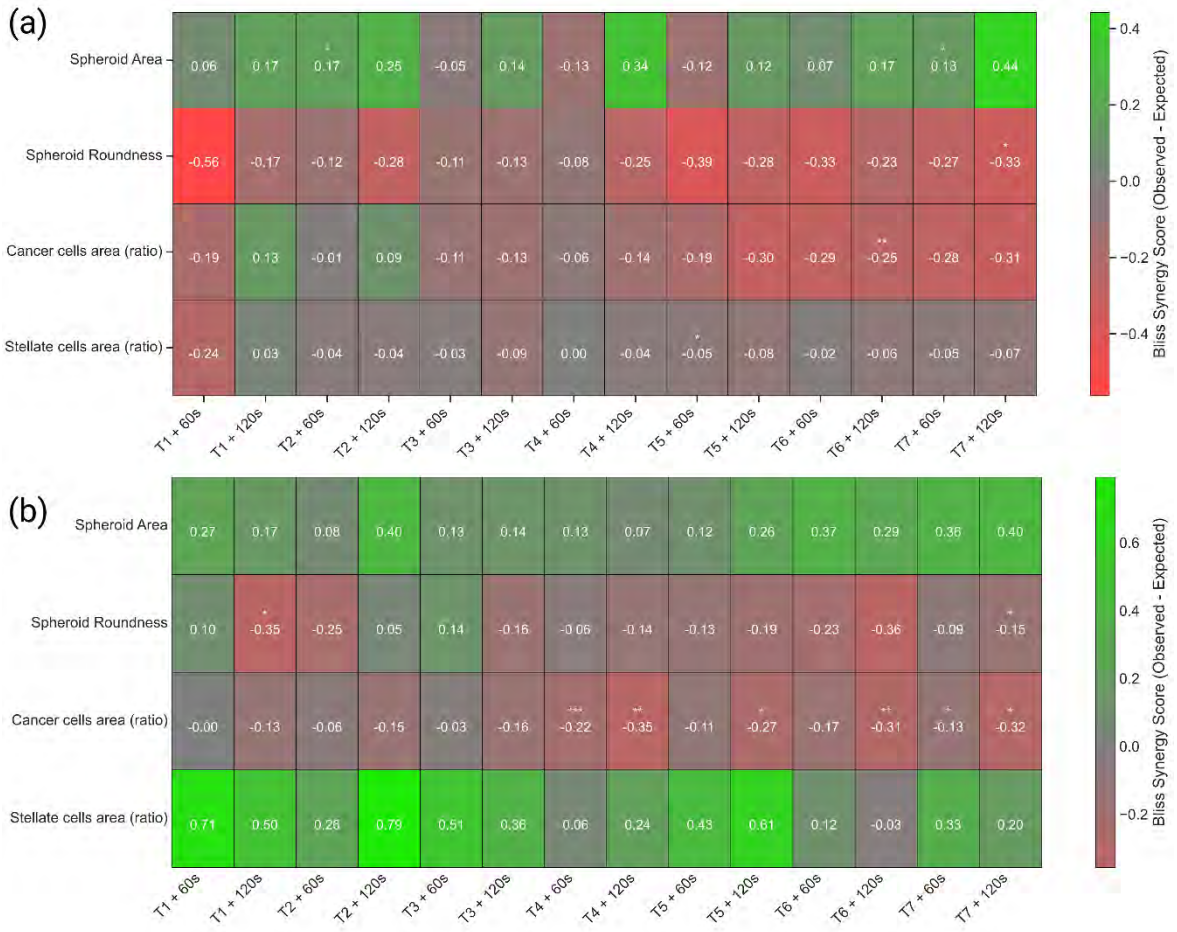

Supplementary Figure 5.5 *CAP-chemotherapy synergy differs by tumor type, with MRH spheroids showing stromal-selective synergy. Bliss synergy heatmaps for combinations of chemotherapy (T1–T7) and CAP (60s or 120s) in (a) BHH and (b) MRH spheroids. Positive scores (green) indicate synergistic effects, while negative scores (red) indicate antagonism. In BHH spheroids, synergy is observed mainly in cancer cell reduction, while in MRH spheroids, strong synergy is seen in PSC preservation. Asterisks indicate statistical significance of the observed vs. expected effects (*p < 0.05, **p < 0.01, ***p < 0.001).*

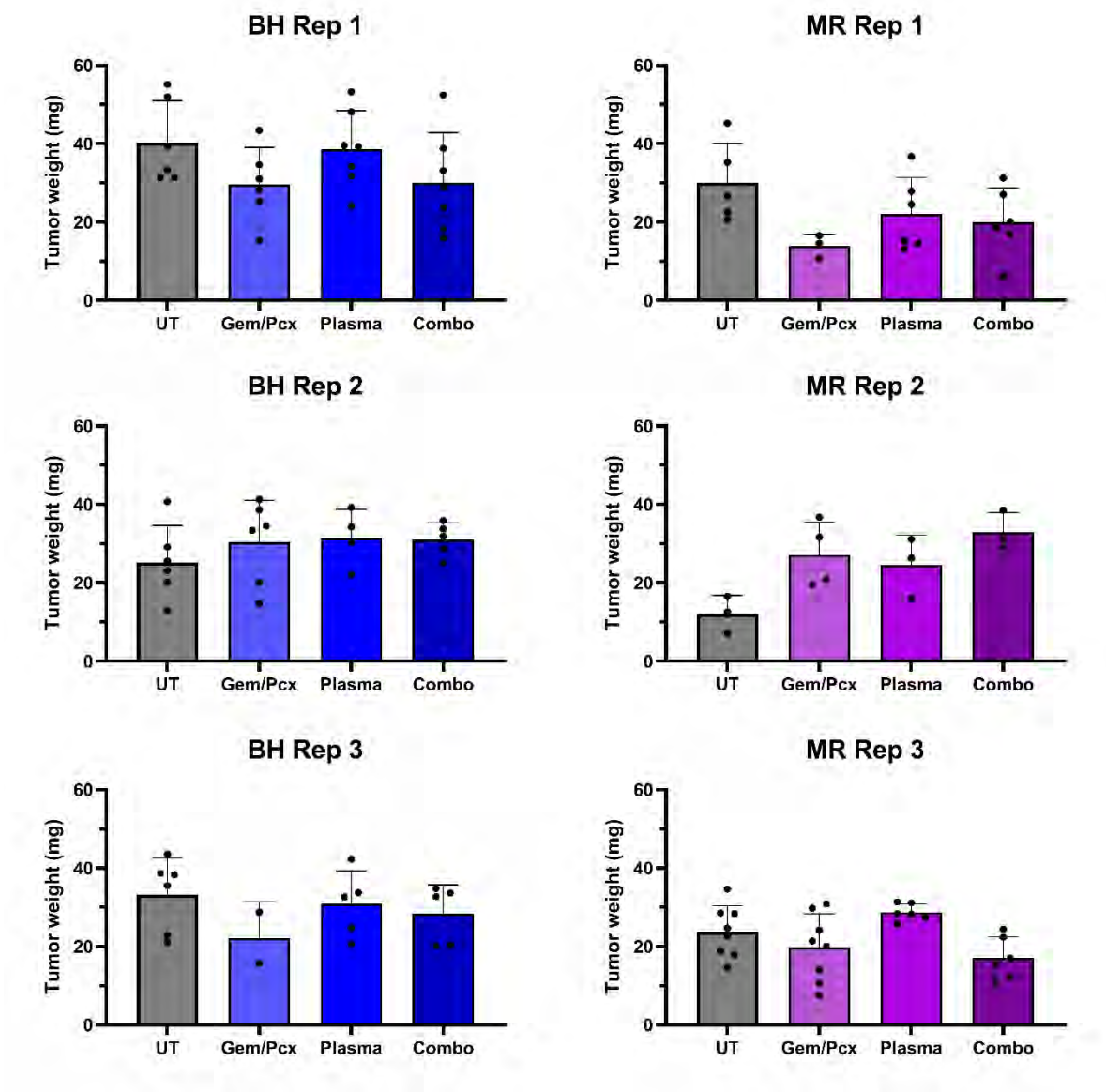

Supplementary Figure 5.6. *Combination treatment effects on tumor weight in BHH and MRH models per replicate. Bar graphs showing tumor weight measurements across three independent experimental replicates (Rep 1–3) for BHH (left) and MRH (right) tumors treated with GEM/PCX), CAP, or their combination (Combo). Data are represented as mean ± SD (n ≥ 2). UT = Untreated.*

5.8 References

1. Siegel, R.L., A.N. Giaquinto, and A. Jemal, *Cancer statistics, 2024.* CA Cancer J Clin, 2024. **74**(1): p. 12-49.
2. Sung, H., J. Ferlay, R.L. Siegel, M. Laversanne, I. Soerjomataram, A. Jemal, et al., *Global Cancer Statistics 2020: GLOBOCAN Estimates of Incidence and Mortality Worldwide for 36 Cancers in 185 Countries.* CA Cancer J Clin, 2021. **71**(3): p. 209-249.
3. Jiang, B., L. Zhou, J. Lu, Y. Wang, C. Liu, L. You, et al., *Stroma-Targeting Therapy in Pancreatic Cancer: One Coin With Two Sides?* Front Oncol, 2020. **10**: p. 576399.
4. Smith, C., W. Zheng, J. Dong, Y. Wang, J. Lai, X. Liu, et al., *Tumor microenvironment in pancreatic ductal adenocarcinoma: Implications in immunotherapy.* World J Gastroenterol, 2022. **28**(27): p. 3297-3313.
5. Orlandi, E., C. Citterio, E. Anselmi, L. Cavanna, and S. Vecchia, *FOLFIRINOX or Gemcitabine Plus Nab-paclitaxel as First Line Treatment in Pancreatic Cancer: A Real-World Comparison.* Cancer Diagn Progn, 2024. **4**(2): p. 165-171.
6. Dominguez, A.A., M.T. Perz, Y. Xu, L.G. Cedillo, O.D. Huang, C.A. McIntyre, et al., *Unveiling the Promise: Navigating Clinical Trials 1978-2024 for PDAC.* Cancers (Basel), 2024. **16**(21).
7. Verloy, R., A. Privat-Maldonado, E. Smits, and A. Bogaerts, *Cold Atmospheric Plasma Treatment for Pancreatic Cancer-The Importance of Pancreatic Stellate Cells.* Cancers (Basel), 2020. **12**(10): p. 2782.
8. Orth, M., P. Metzger, S. Gerum, J. Mayerle, G. Schneider, C. Belka, et al., *Pancreatic ductal adenocarcinoma: biological hallmarks, current status, and future perspectives of combined modality treatment approaches.* Radiat Oncol, 2019. **14**(1): p. 141.
9. Wu, Y., C. Zhang, K. Jiang, J. Werner, A.V. Bazhin, and J.G. D'Haese, *The Role of Stellate Cells in Pancreatic Ductal Adenocarcinoma: Targeting Perspectives.* Front Oncol, 2020. **10**: p. 621937.
10. Privat-Maldonado, A., A. Schmidt, A. Lin, K.D. Weltmann, K. Wende, A. Bogaerts, et al., *ROS from Physical Plasmas: Redox Chemistry for Biomedical Therapy.* Oxid Med Cell Longev, 2019. **2019**: p. 29.
11. Van Loenhout, J., T. Flieswasser, L. Freire Boullosa, J. De Waele, J. Van Audenaerde, E. Marcq, et al., *Cold Atmospheric Plasma-Treated PBS Eliminates Immunosuppressive Pancreatic Stellate Cells and Induces Immunogenic Cell Death of Pancreatic Cancer Cells.* Cancers (Basel), 2019. **11**(10).
12. Lin, A., J. De Backer, D. Quatannens, B. Cuypers, H. Verswyvel, E.C. De La Hoz, et al., *The effect of local non-thermal plasma therapy on the cancer-immunity cycle in a melanoma mouse model.* Bioeng Transl Med, 2022. **7**(3): p. e10314.
13. Zivanic, M., A. Espona-Noguera, A. Lin, and C. Canal, *Current State of Cold Atmospheric Plasma and Cancer-Immunity Cycle: Therapeutic Relevance and Overcoming Clinical Limitations Using Hydrogels.* Adv Sci (Weinh), 2023. **10**(8): p. e2205803.

14. Dai, X., K. Bazaka, E.W. Thompson, and K.K. Ostrikov, *Cold Atmospheric Plasma: A Promising Controller of Cancer Cell States.* Cancers (Basel), 2020. **12**(11).
15. Hadefi, A., M. Leprovots, M. Thulliez, O. Bastin, A. Lefort, F. Libert, et al., *Cold atmospheric plasma differentially affects cell renewal and differentiation of stem cells and APC-deficient-derived tumor cells in intestinal organoids.* Cell Death Discov, 2022. **8**(1): p. 66.
16. Aggelopoulos, C.A., A.M. Christodoulou, M. Tachliabouri, S. Meropoulis, M.E. Christopoulou, T.T. Karalis, et al., *Cold Atmospheric Plasma Attenuates Breast Cancer Cell Growth Through Regulation of Cell Microenvironment Effectors.* Front Oncol, 2021. **11**: p. 826865.
17. Verloy, R., A. Privat-Maldonado, J. Van Audenaerde, S. Rovers, H. Zaryouh, J. De Waele, et al., *Capturing the Heterogeneity of the PDAC Tumor Microenvironment: Novel Triple Co-Culture Spheroids for Drug Screening and Angiogenic Evaluation.* Cells, 2025. **14**(6).
18. Chen, L., S. Wang, Y. Feng, J. Zhang, Y. Du, J. Zhang, et al., *Utilisation of Chick Embryo Chorioallantoic Membrane as a Model Platform for Imaging-Navigated Biomedical Research.* Cells, 2021. **10**(2).
19. Miebach, L., J. Berner, and S. Bekeschus, *In ovo model in cancer research and tumor immunology.* Front Immunol, 2022. **13**: p. 1006064.
20. Kundekova, B., M. Macajova, M. Meta, I. Cavarga, and B. Bilcik, *Chorioallantoic Membrane Models of Various Avian Species: Differences and Applications.* Biology (Basel), 2021. **10**(4).
21. Nowak-Sliwinska, P., T. Segura, and M.L. Iruela-Arispe, *The chicken chorioallantoic membrane model in biology, medicine and bioengineering.* Angiogenesis, 2014. **17**(4): p. 779-804.
22. Jesnowski, R., D. Furst, J. Ringel, Y. Chen, A. Schrodel, J. Kleeff, et al., *Immortalization of pancreatic stellate cells as an in vitro model of pancreatic fibrosis: deactivation is induced by matrigel and N-acetylcysteine.* Lab Invest, 2005. **85**(10): p. 1276-91.
23. Hamada, S., A. Masamune, T. Takikawa, N. Suzuki, K. Kikuta, M. Hirota, et al., *Pancreatic stellate cells enhance stem cell-like phenotypes in pancreatic cancer cells.* Biochemical and Biophysical Research Communications, 2012. **421**(2): p. 349-354.
24. Bekeschus, S., E. Freund, C. Spadola, A. Privat-Maldonado, C. Hackbarth, A. Bogaerts, et al., *Risk Assessment of kINPen Plasma Treatment of Four Human Pancreatic Cancer Cell Lines with Respect to Metastasis.* Cancers (Basel), 2019. **11**(9).
25. Privat-Maldonado, A., R. Verloy, E. Cardenas Delahoz, A. Lin, S. Vanlanduit, E. Smits, et al., *Cold Atmospheric Plasma Does Not Affect Stellate Cells Phenotype in Pancreatic Cancer Tissue in Ovo.* Int J Mol Sci, 2022. **23**(4).
26. Jan, N., S. Sofi, H. Qayoom, A. Shabir, B.U. Haq, M.A. Macha, et al., *Metronomic chemotherapy and drug repurposing: A paradigm shift in oncology.* Heliyon, 2024. **10**(3): p. e24670.
27. Trachootham, D., J. Alexandre, and P. Huang, *Targeting cancer cells by ROS-mediated mechanisms: a radical therapeutic approach?* Nat Rev Drug Discov, 2009. **8**(7): p. 579-91.

28. Brulle, L., M. Vandamme, D. Ries, E. Martel, E. Robert, S. Lerondel, et al., *Effects of a non thermal plasma treatment alone or in combination with gemcitabine in a MIA PaCa2-luc orthotopic pancreatic carcinoma model.* PLoS One, 2012. **7**(12): p. e52653.
29. Le Compte, M., E.C. De La Hoz, S. Peeters, F.R. Fortes, C. Hermans, A. Domen, et al., *Single-organoid analysis reveals clinically relevant treatment-resistant and invasive subclones in pancreatic cancer.* NPJ Precis Oncol, 2023. **7**(1): p. 128.
30. Le Compte, M., N. Komen, I. Joye, M. Peeters, H. Prenen, E. Smits, et al., *Patient-derived organoids as individual patient models for chemoradiation response prediction in gastrointestinal malignancies.* Crit Rev Oncol Hematol, 2021. **157**: p. 103190.
31. Li, X., H.E. Francies, M. Secrier, J. Perner, A. Miremadi, N. Galeano-Dalmau, et al., *Organoid cultures recapitulate esophageal adenocarcinoma heterogeneity providing a model for clonality studies and precision therapeutics.* Nat Commun, 2018. **9**(1): p. 2983.
32. Lin, A., Y. Gorbanev, J. De Backer, J. Van Loenhout, W. Van Boxem, F. Lemiere, et al., *Non-Thermal Plasma as a Unique Delivery System of Short-Lived Reactive Oxygen and Nitrogen Species for Immunogenic Cell Death in Melanoma Cells.* Adv Sci (Weinh), 2019. **6**(6): p. 1802062.
33. Verswyvel, H., *Boosting cancer immunotherapy : the immunogenic and therapeutic potential of non-thermal plasma in head and neck cancer*. 2025, University of Antwerp: UAntwerp Repository. p. 253.
34. Yan, D., J.H. Sherman, and M. Keidar, *Cold atmospheric plasma, a novel promising anti-cancer treatment modality.* Oncotarget; Vol 8, No 9, 2016.

CHAPTER 06

DISCUSSION AND FUTURE PERSPECTIVES

6.1 General discussion

This PhD thesis aimed to explore a novel combination strategy for PDAC, one of the most lethal and treatment-resistant cancer types. Previous CAP research on PDAC that included PSCs are limited and have mostly investigated cell death, ICD, ECM remodeling, EMT and metastasis [1-4]. Additionally, CAP research on angiogenesis has shown that the stimulation of endothelial cell proliferation, migration, tube formation and angiogenesis is possible, however, this has not been investigated on a tumor model [5-7]. Given the prominent role of the TME in limiting vascular perfusion and drug delivery, especially due to the desmoplastic stroma orchestrated by the PSCs, this research was developed around evaluating CAP in combination with chemotherapy in advanced 3D co-culture models. The PhD thesis was driven by two central hypotheses: (i) that low-dose CAP treatment could stimulate angiogenesis in PDAC models and thereby improve chemotherapy delivery and efficacy; and (ii), that high-dose CAP could contribute additional cytotoxic effects alongside chemotherapy via a different mechanism of action than GEM/PCX.

Chapter 3 focused on the critical need to replicate the heterogeneity and complexity of the PDAC TME for effective drug screening and angiogenic evaluations. To this end, we developed a panel of novel TCC spheroid models composed of PCCs, PSCs, and ECs. These spheroids reflected inter- and intratumoral heterogeneity observed in patient tumors and allowed for the investigation of structural organization, drug penetration, and endothelial behavior. Drug screening experiments revealed differential chemotherapy responses across spheroid models, influenced by cellular composition and architecture, while angiogenesis assays indicated distinct levels of endothelial stimulation dependent on the spheroid makeup. These findings emphasized the limitations of traditional 2D and monoculture models and underscored the relevance of TCC spheroids as an in vitro platform that better mimics the PDAC TME [8-10]. Importantly, the study showed that interactions between cancer cells and stromal components significantly affect drug resistance and angiogenic signaling. As such, these models offer a robust and flexible system to study personalized therapeutic responses and could be expanded to include

immune cells or patient-derived organoids for even greater translational potential [11]. This work demonstrates that replicating tumor heterogeneity is essential for acquiring translational insights and refining drug screening strategies in PDAC. This was confirmed in Chapter 5, in which two different tumor types were evaluated upon CAP treatment and chemotherapy and showed a differential tumor-type-specific response.

The first hypothesis of this PhD thesis was investigated in **Chapter 4** and addressed the therapeutic potential of CAP as an angiogenic modulator using the optimized TCC spheroids and an in ovo turkey CAM model. The goal was to explore whether CAP could enhance vascularization in PDAC, thereby improving drug delivery in this poorly perfused tumor type. However, both in vitro and in ovo experiments revealed that low-dose CAP treatment preserved vascular quiescence. Endothelial tube formation was inhibited in a dose-dependent manner, and VEGF-A secretion from spheroids declined with longer exposure. In the in ovo model, no significant changes in vessel density were observed, although a slight increase in tumor weight was noted at very short treatment durations. While other studies have reported pro-angiogenic effects under different conditions [5-7, 12-15], our findings suggest that low-dose CAP delivered by the kINPen MED using argon gas is not suitable to stimulate angiogenesis in PDAC. Instead, it appears to maintain the suppressed vascular phenotype of this tumor type. These results highlight the highly context-dependent effects of CAP, in which treatment modality, dose, device, and gas composition all influence the amount and type of produced RONS and therefore the biological response [16]. In addition, RONS such as H_2O_2, nitric oxide NO·, and hydroxyl radicals ·OH are potent regulators of angiogenesis, but their effects are strongly concentration- and context-dependent. Low levels of H_2O_2 stimulate endothelial proliferation, migration, and tube formation by upregulating VEGF [17-20], whereas high concentrations cause cytotoxicity [17, 18, 21]. This hormetic response is also known to be cell line dependent [22]. Mechanistically, H_2O_2 promotes angiogenesis through iNOS and ets-1 induction [20], while NO· contributes via vasodilation and VEGF-mediated chemotaxis of endothelial cells [23-26], though inhibitory effects have also been reported [27]. In line with this, DBD plasma induced angiogenesis via FGF-2 release, with H_2O_2 and ·OH as key mediators [6, 13, 15],

and kINPen treatment promoted angiogenesis in vivo in a murine wound model [28]. Together, these findings underscore that plasma-induced angiogenesis arises from a delicate balance of RONS whose effects can shift between pro-angiogenic and cytotoxic depending on dose and context. Thus, although CAP remains promising for selective cytotoxicity, its use as a pro-angiogenic agent requires significant parameter optimization. The key conclusion is that the angiogenic potential of CAP is not universal and it must be critically evaluated within relevant disease models and CAP parameters such as treatment time, dose, device, gas composition, distance to the target, etc.

In exploring the interplay between CAP treatment and chemotherapy, **Chapter 5** revealed a dose-dependent and tumor-type-specific response in advanced PDAC models. Using both TCC spheroids and the in ovo turkey CAM model, we tested various combinations of CAP and chemotherapy (GEM/PCX) across different treatment conditions. The results showed that combining CAP with low-dose chemotherapy led to limited but measurable additive effects, supporting the concept of using CAP as a sensitizing strategy to lower the required chemotherapy dose. This approach could reduce side effects and treatment costs while preserving therapeutic efficacy [29]. However, at higher chemotherapy doses, CAP unexpectedly diminished treatment efficacy in certain tumor models, possibly due to the induction of antioxidant defense mechanisms that counteract oxidative stress [30]. In particular, MRH spheroids exhibited a paradoxical increase in cell viability after CAP exposure in combination with high-dose chemotherapy. We also found that the cytotoxic effects of CAP varied between tumor models, with some showing selective targeting of cancer cells and others showing non-selective cell death, which clearly highlights the influence of TME heterogeneity on treatment response, similar to patient heterogeneity. These results emphasize the importance of understanding the tumor-specific microenvironment when designing CAP-based (and other) therapies.

This PhD thesis underscores that CAP is a highly complex treatment modality, with outcomes depending critically on treatment time, tumor type and model, gas composition, and the used device, as highlighted by our comparisons to literature in each chapter. This can cause cross-study variability and complicates cross-study interpretation and

emphasizes the need for either device-specific applications following sufficient validation or deeper mechanistic investigations into the role of distinct reactive species and their generation for commonly used devices in standardized conditions. Nevertheless, this complexity also represents a strength of CAP, as it opens the possibility to fine-tune CAP parameters toward specific biological outcomes. Importantly, the field is moving increasingly toward combination therapies, particularly with chemotherapy and immunotherapy, where CAP has already demonstrated promising potential [31-34]. However, most of these studies again employ different plasma sources, limiting reproducibility and comparability. Moreover, this PhD thesis highlights the critical importance of dose optimization in combined strategies for our conditions: while low-dose CAP with chemotherapy may yield additive or even synergistic effects offering the possibility to lower chemotherapy doses for patients, excessive dosing can attenuate cytotoxicity, as observed in one of our tumor models. Thus, careful consideration of both the CAP device and treatment parameters considering the study hypothesis is essential for translating CAP from experimental promise to clinically robust applications. In addition, this differential response in our tumor models signifies the importance of using multiple cell lines, preferably as co-cultures, to both include heterogeneity and the TME.

6.2 Future perspectives

The findings of this PhD thesis underscore the potential of CAP as an innovative addition in the treatment of PDAC. However, several critical directions remain to be explored to fully harness and translate CAP's therapeutic potential.

One promising avenue is the use of low-dose CAP as a pro-angiogenic strategy to improve chemotherapeutic drug delivery. Although the current work using the kINPen®MED did not show clear angiogenic stimulation, the choice of device and CAP parameters may play a decisive role. Devices like the SteriPlas® or purpose-built plasma sources engineered to enhance production of specific RONS, such as, NO·, ·OH, and H_2O_2, may be more effective in promoting angiogenesis [6, 13, 15, 17-20, 23-26]. Future research should focus on

selecting or customizing CAP sources based on their RONS output and aligning these with specific therapeutic goals, such as vascular remodeling in hypoperfused tumors like PDAC.

Furthermore, the combination of CAP with chemotherapy remains a complex but promising area of research. This PhD thesis revealed that CAP-chemotherapy synergy is highly dose- and context-dependent. Thus, fine-tuned optimization of treatment regimens, particularly regarding CAP dosimetry and chemotherapy scheduling, is essential. The concept of using CAP as an adjunct to low-dose chemotherapy is especially appealing, as it could reduce systemic toxicity, lower treatment costs, and improve quality of life for patients. To this end, more studies are needed to systematically map the dose-response interactions between CAP and cytotoxic agents across different tumor types and microenvironments.

Beyond chemotherapy, combining CAP with immunotherapy represents a high-impact frontier. CAP has been shown to induce immunogenic cell death and modulate immune responses through oxidative stress signaling, including PDAC [1, 34-38]. Integrating CAP with immune checkpoint inhibitors or other immune-targeting agents could potentiate anti-tumor immunity, especially in PDAC, which is traditionally immunologically cold [39]. Future work should therefore investigate the immunomodulatory effects of CAP in 3D co-culture and in vivo models that include immune cell populations.

Despite the growing preclinical evidence, several translational barriers remain. CAP's limited depth of penetration, typically only a few hundred micrometers, presents a challenge for treating deep-seated tumors. Furthermore, CAP is inherently a local therapy and is currently not able to treat all tumor types as broadly or systemically as conventional drugs. Therefore, selecting appropriate cancer types and clinical contexts for CAP research is crucial (e.g. head and neck cancer or melanoma). Tumors located near accessible surfaces or those that can be reached through minimally invasive methods may be more amenable to CAP-based therapies. Additionally, reactive species generated by CAP may be neutralized by biological fluids such as blood, further limiting their bioavailability and therapeutic efficacy [40]. Addressing these challenges will require innovative delivery

strategies for hard-to-reach tumors, such as endoscopic CAP administration (e.g. colon cancer), localized hydrogels, or nanoparticle-assisted CAP systems.

Finally, clinical adoption of CAP as a cancer therapy will require significant standardization efforts. The variability in CAP sources, treatment conditions, and biological models has made cross-study comparisons difficult. International collaborations are increasingly working toward establishing consensus protocols and regulatory pathways. These should include guidelines for CAP dosimetry, treatment reproducibility, and long-term safety. Addressing these regulatory and ethical considerations will be critical for enabling clinical trials and ensuring the safe and effective translation of CAP technology into routine oncology practice.

In summary, while CAP is not yet a clinical reality in PDAC treatment, its multimodal potential, ranging from cytotoxicity to immune activation, warrants continued investigation. Refinement of CAP delivery, dosimetry, and combination strategies, alongside regulatory standardization, will be key to unlocking its full clinical utility.

6.3 References

1. Van Loenhout, J., T. Flieswasser, L. Freire Boullosa, J. De Waele, J. Van Audenaerde, E. Marcq, et al., *Cold Atmospheric Plasma-Treated PBS Eliminates Immunosuppressive Pancreatic Stellate Cells and Induces Immunogenic Cell Death of Pancreatic Cancer Cells.* Cancers (Basel), 2019. **11**(10).
2. Kumar, N., P. Attri, S. Dewilde, and A. Bogaerts, *Inactivation of human pancreatic ductal adenocarcinoma with atmospheric plasma treated media and water: a comparative study.* Journal of Physics D: Applied Physics, 2018. **51**(25): p. 255401.
3. Freund, E., C. Spadola, A. Schmidt, A. Privat-Maldonado, A. Bogaerts, T. von Woedtke, et al., *Risk Evaluation of EMT and Inflammation in Metastatic Pancreatic Cancer Cells Following Plasma Treatment.* Frontiers in Physics, 2020. **Volume 8 - 2020**.
4. Privat-Maldonado, A., R. Verloy, E. Cardenas Delahoz, A. Lin, S. Vanlanduit, E. Smits, et al., *Cold Atmospheric Plasma Does Not Affect Stellate Cells Phenotype in Pancreatic Cancer Tissue in Ovo.* Int J Mol Sci, 2022. **23**(4).
5. Arndt, S., P. Unger, M. Berneburg, A.K. Bosserhoff, and S. Karrer, *Cold atmospheric plasma (CAP) activates angiogenesis-related molecules in skin keratinocytes, fibroblasts and endothelial cells and improves wound angiogenesis in an autocrine and paracrine mode.* J Dermatol Sci, 2018. **89**(2): p. 181-190.

6. Arjunan, K.P., G. Friedman, A. Fridman, and A.M. Clyne, *Non-thermal dielectric barrier discharge plasma induces angiogenesis through reactive oxygen species.* J R Soc Interface, 2012. **9**(66): p. 147-57.
7. Duchesne, C., S. Banzet, J.J. Lataillade, A. Rousseau, and N. Frescaline, *Cold atmospheric plasma modulates endothelial nitric oxide synthase signalling and enhances burn wound neovascularisation.* J Pathol, 2019. **249**(3): p. 368-380.
8. Brüningk, S.C., I. Rivens, C. Box, U. Oelfke, and G. ter Haar, *3D tumour spheroids for the prediction of the effects of radiation and hyperthermia treatments.* Scientific Reports, 2020. **10**(1): p. 1653.
9. Pape, J., M. Emberton, and U. Cheema, *3D Cancer Models: The Need for a Complex Stroma, Compartmentalization and Stiffness.* Front Bioeng Biotechnol, 2021. **9**: p. 660502.
10. Tomas-Bort, E., M. Kieler, S. Sharma, J.B. Candido, and D. Loessner, *3D approaches to model the tumor microenvironment of pancreatic cancer.* Theranostics, 2020. **10**(11): p. 5074-5089.
11. Zhu, Y., E. Kang, M. Wilson, T. Basso, E. Chen, Y. Yu, et al. *3D Tumor Spheroid and Organoid to Model Tumor Microenvironment for Cancer Immunotherapy*. Organoids, 2022. **1**, 149-167 DOI: 10.3390/organoids1020012.
12. Haertel, B., K. Eiden, A. Deuter, K. Wende, T.v. Woedtke, and U. Lindequist. *Differential effect of non-thermal atmospheric-pressure plasma on angiogenesis*. 2014. Letters in Applied NanoBioScience.
13. Priya Arjunan, K. and A. Morss Clyne, *Hydroxyl Radical and Hydrogen Peroxide are Primarily Responsible for Dielectric Barrier Discharge Plasma-Induced Angiogenesis.* Plasma Processes and Polymers, 2011. **8**(12): p. 1154-1164.
14. Kang, S.U., H.J. Kim, S. Ma, D.Y. Oh, J.Y. Jang, C. Seo, et al., *Liquid plasma promotes angiogenesis through upregulation of endothelial nitric oxide synthase-induced extracellular matrix metabolism: potential applications of liquid plasma for vascular injuries.* Cell Commun Signal, 2024. **22**(1): p. 138.
15. Kalghatgi, S., G. Friedman, A. Fridman, and A.M. Clyne, *Endothelial cell proliferation is enhanced by low dose non-thermal plasma through fibroblast growth factor-2 release.* Ann Biomed Eng, 2010. **38**(3): p. 748-57.
16. Privat-Maldonado, A., A. Schmidt, A. Lin, K.D. Weltmann, K. Wende, A. Bogaerts, et al., *ROS from Physical Plasmas: Redox Chemistry for Biomedical Therapy.* Oxid Med Cell Longev, 2019. **2019**: p. 29.
17. Huang, S.S. and R.L. Zheng, *Biphasic regulation of angiogenesis by reactive oxygen species.* Pharmazie, 2006. **61**: p. 223-229.
18. Anasooya Shaji, C., B.D. Robinson, A. Yeager, M.R. Beeram, M.L. Davis, C.L. Isbell, et al., *The Tri-phasic Role of Hydrogen Peroxide in Blood-Brain Barrier Endothelial cells.* Sci Rep, 2019. **9**(1): p. 133.
19. Chua, C.C., R.C. Hamdy, and B.H. Chua, *Upregulation of vascular endothelial growth factor by H2O2 in rat heart endothelial cells.* Free Radic Biol Med, 1998. **25**(8): p. 891-7.

20. Yasuda, M., Y. Ohzeki, S. Shimizu, S. Naito, A. Ohtsuru, T. Yamamoto, et al., *Stimulation of in vitro angiogenesis by hydrogen peroxide and the relation with ETS-1 in endothelial cells.* Life Sci, 1999. **64**(4): p. 249-58.
21. Whang, W.K., H.S. Park, I. Ham, M. Oh, H. Namkoong, H.K. Kim, et al., *Natural compounds,fraxin and chemicals structurally related to fraxin protect cells from oxidative stress.* Exp Mol Med, 2005. **37**(5): p. 436-46.
22. Park, W.H., *The effects of exogenous H2O2 on cell death, reactive oxygen species and glutathione levels in calf pulmonary artery and human umbilical vein endothelial cells.* Int J Mol Med, 2013. **31**(2): p. 471-476.
23. Noiri, E., E. Lee, J. Testa, J. Quigley, D. Colflesh, C.R. Keese, et al., *Podokinesis in endothelial cell migration: role of nitric oxide.* Am J Physiol, 1998. **274**(1): p. C236-44.
24. Pipili-Synetos, E., S. Kritikou, E. Papadimitriou, A. Athanassiadou, C. Flordellis, and M.E. Maragoudakis, *Nitric oxide synthase expression, enzyme activity and NO production during angiogenesis in the chick chorioallantoic membrane.* Br J Pharmacol, 2000. **129**(1): p. 207-13.
25. Shimizu, S., M. Kageyama, M. Yasuda, D. Sasaki, S. Naito, T. Yamamoto, et al., *Stimulation of in vitro angiogenesis by nitric oxide through the induction of transcription factor ETS-1.* The International Journal of Biochemistry & Cell Biology, 2004. **36**(1): p. 114-122.
26. Murohara, T. and T. Asahara, *Nitric oxide and angiogenesis in cardiovascular disease.* Antioxid Redox Signal, 2002. **4**(5): p. 825-31.
27. Isenberg, J.S., *Nitric oxide modulation of early angiogenesis.* Microsurgery, 2004. **24**(5): p. 385-91.
28. Arndt, S., A. Schmidt, S. Karrer, and T. von Woedtke, *Comparing two different plasma devices kINPen and Adtec SteriPlas regarding their molecular and cellular effects on wound healing.* Clinical Plasma Medicine, 2018. **9**: p. 24-33.
29. Jan, N., S. Sofi, H. Qayoom, A. Shabir, B.U. Haq, M.A. Macha, et al., *Metronomic chemotherapy and drug repurposing: A paradigm shift in oncology.* Heliyon, 2024. **10**(3): p. e24670.
30. Trachootham, D., J. Alexandre, and P. Huang, *Targeting cancer cells by ROS-mediated mechanisms: a radical therapeutic approach?* Nat Rev Drug Discov, 2009. **8**(7): p. 579-91.
31. Gjika, E., S. Pal-Ghosh, M.E. Kirschner, L. Lin, J.H. Sherman, M.A. Stepp, et al., *Combination therapy of cold atmospheric plasma (CAP) with temozolomide in the treatment of U87MG glioblastoma cells.* Sci Rep, 2020. **10**(1): p. 16495.
32. Brunner, T.F., F.A. Probst, M. Troeltzsch, S. Schwenk-Zieger, J.L. Zimmermann, G. Morfill, et al., *Primary cold atmospheric plasma combined with low dose cisplatin as a possible adjuvant combination therapy for HNSCC cells-an in-vitro study.* Head Face Med, 2022. **18**(1): p. 21.
33. Chen, G., Z. Chen, D. Wen, Z. Wang, H. Li, Y. Zeng, et al., *Transdermal cold atmospheric plasma-mediated immune checkpoint blockade therapy.* Proceedings of the National Academy of Sciences, 2020. **117**(7): p. 3687-3692.

34. Verswyvel, H., *Boosting cancer immunotherapy : the immunogenic and therapeutic potential of non-thermal plasma in head and neck cancer*. 2025, University of Antwerp: UAntwerp Repository. p. 253.
35. Azzariti, A., R.M. Iacobazzi, R. Di Fonte, L. Porcelli, R. Gristina, P. Favia, et al., *Plasma-activated medium triggers cell death and the presentation of immune activating danger signals in melanoma and pancreatic cancer cells.* Sci Rep, 2019. **9**(1): p. 4099.
36. Lin, A., Y. Gorbanev, J. De Backer, J. Van Loenhout, W. Van Boxem, F. Lemiere, et al., *Non-Thermal Plasma as a Unique Delivery System of Short-Lived Reactive Oxygen and Nitrogen Species for Immunogenic Cell Death in Melanoma Cells.* Adv Sci (Weinh), 2019. **6**(6): p. 1802062.
37. Zivanic, M., A. Espona-Noguera, A. Lin, and C. Canal, *Current State of Cold Atmospheric Plasma and Cancer-Immunity Cycle: Therapeutic Relevance and Overcoming Clinical Limitations Using Hydrogels.* Adv Sci (Weinh), 2023. **10**(8): p. e2205803.
38. Min, T., X. Xie, K. Ren, T. Sun, H. Wang, C. Dang, et al., *Therapeutic Effects of Cold Atmospheric Plasma on Solid Tumor.* Front Med (Lausanne), 2022. **9**: p. 884887.
39. Maru, S.Y. and E.M. Jaffee, *Pancreatic cancer is feeling the heat.* J Immunother Cancer, 2024. **12**(10).
40. Lin, A., E. Biscop, C. Breen, S.J. Butler, E. Smits, and A. Bogaerts, *Critical Evaluation of the Interaction of Reactive Oxygen and Nitrogen Species with Blood to Inform the Clinical Translation of Nonthermal Plasma Therapy.* Oxid Med Cell Longev, 2020. **2020**: p. 9750206.

CHAPTER 07

SUMMARY

7.1 Summary

Pancreatic ductal adenocarcinoma (PDAC) is one of the most aggressive malignancies, with a five-year survival rate below 10%. This poor prognosis is largely due to its late diagnosis, rapid metastatic spread, and resistance to conventional therapies. One of the main drivers of this resistance is the unique tumor microenvironment (TME), which is dominated by a dense fibrotic stroma. A key component of this stroma are the pancreatic stellate cells (PSCs), which contribute to therapy resistance by remodeling the extracellular matrix, suppressing immune responses, and creating a hypoxic, nutrient-poor, hypovascular and drug-impermeable environment. These challenges have prompted the search for novel treatment approaches that can overcome the barriers imposed by the TME.

Cold atmospheric plasma (CAP), a non-thermal partially ionized gas rich in reactive oxygen and nitrogen species, has emerged as a promising anti-cancer modality. CAP exerts oxidative stress on cells, leading to apoptosis and immune activation. While CAP has shown strong cytotoxic potential in various cancers, its behavior in complex tumor models like PDAC remains poorly understood, especially in the context of a complex TME. This PhD thesis aimed to investigate the dose-dependent effects of CAP in 3D PDAC models and assess its interaction with angiogenesis and chemotherapy, with the goal of defining its therapeutic value in the treatment of pancreatic cancer.

To this end, advanced 3D co-culture spheroid models were developed that include PDAC cells, PSCs, and endothelial cells. These models reflect the heterogeneity and complexity of the PDAC TME more accurately than conventional 2D monocultures. Using these models, I first investigated whether CAP could modulate the vasculature, potentially promoting angiogenesis in the hypovascular setting of PDAC. The data showed that low-dose CAP did not induce angiogenesis. Instead, it preserved vascular quiescence, reduced VEGF-A secretion, while other growth factors remained unchanged, and slightly diminished endothelial tube formation in vitro. Further validation in the turkey in ovo chorioallantoic membrane (CAM) model showed that vascularization within and around the tumor remained largely unchanged upon low-dose CAP treatment. These findings challenge the

assumption that CAP's oxidative stress could reprogram the vasculature in PDAC and suggest that its effects are highly context-dependent regarding the used CAP device, gas composition, distance to the target, tumor model, cancer type, among others.

Next, the therapeutic potential of combining CAP with the standard chemotherapeutics gemcitabine and paclitaxel was explored. Across spheroids derived from two distinct tumor types, MiaPaCa-2:RLT-PSC:HMEC-1 (MRH) and BxPC-3:hPSC21:HMEC-1 (BHH) (cancer:stellate:endothelial cells), CAP monotherapy reduced cancer cell viability, with varying selectivity depending on the tumor model. In MRH spheroids, CAP preserved stellate cell integrity and enhanced the cytotoxicity of low-dose chemotherapy, suggesting a possible dose-sparing strategy. In BHH spheroids, however, CAP exerted broader cytotoxic effects, damaging both cancer and stellate cells, and failed to synergize effectively with high-dose chemotherapy. Notably, in some conditions, the combination of high-dose chemotherapy and CAP resulted in reduced efficacy compared to chemotherapy alone, potentially due to the activation of cellular stress responses that promote survival under extreme oxidative pressure. These findings were further validated in the CAM model, which confirmed the cytotoxic effects of intravenous administration of chemotherapy. The combination of direct CAP treatment with chemotherapy did not significantly outperform monotherapies, again emphasizing the complexity of the interactions between treatment components and tumor context. These results highlight that CAP's therapeutic potential lies not in uniform application but in carefully tuned regimens adapted to tumor- and application-specific characteristics.

Taken together, this work demonstrates that CAP is a potent yet complex therapeutic tool whose effects depend strongly on treatment dose, tumor type, and the surrounding microenvironment. While CAP alone or in combination with chemotherapy can induce strong cytotoxic responses, its effects on stromal and vascular components must be considered to avoid unintended consequences, such as major stromal damage, loss of selectivity or promotion of cancer cells. The co-culture models developed in this thesis represent valuable platforms for preclinical evaluation of anti-cancer strategies, and are

therefore not limited to CAP treatment, underscoring the importance of mimicking tumor complexity when testing new therapies.

In conclusion, this thesis provides novel insights into the role of CAP in the treatment of PDAC. It shows that CAP does not promote angiogenesis in the PDAC setting, at least not for the studied conditions, and that its combination with chemotherapy must be carefully optimized to avoid counterproductive effects. Future research should focus on further finetuning optimization parameters, such as, CAP device, gas composition, distance of the device nozzle to the sample depending on the used tumor model and proposed research hypothesis. Another promising future perspective is combining CAP with immunotherapy and integrating immune components into 3D models to assess the full potential of CAP in overcoming the immunosuppressive PDAC microenvironment. By tailoring CAP application to tumor-specific vulnerabilities, it may become a valuable addition to multimodal PDAC treatment strategies.

7.2 Samenvatting

Pancreasductaal adenocarcinoom (PDAC) is een van de meest agressieve vormen van kanker, met een vijfjaarsoverleving van minder dan 10%. Deze slechte prognose is grotendeels te wijten aan de late diagnose, snelle metastasering en resistentie tegen conventionele therapieën. Een belangrijke oorzaak van deze resistentie is de unieke tumormicro-omgeving (TMO), die wordt gedomineerd door een vast fibrotisch stroma. Een essentieel onderdeel van dit stroma zijn de pancreas stellaatcellen (PSCs), die bijdragen aan therapieresistentie door de extracellulaire matrix te hermodelleren, immuunreacties te onderdrukken en een hypoxische, nutriëntarme, hypovasculaire en slecht doordringbare omgeving te creëren. Deze uitdagingen hebben geleid tot de zoektocht naar nieuwe behandelingsstrategieën die de barrières opgelegd door de TMO kunnen doorbreken.

Koud atmosferisch plasma (Eng: cold atmospheric plasmas; CAP), een niet-thermisch en gedeeltelijk geïoniseerd gas dat rijk is aan reactieve zuurstof- en stikstofdeeltjes, is een veelbelovende antikankerbehandeling. CAP veroorzaakt oxidatieve stress in cellen, wat leidt tot apoptose en immuunactivatie. Hoewel CAP een sterk cytotoxisch potentieel heeft aangetoond in verschillende kankertypes, is het gedrag in complexe tumormodellen, zoals PDAC nog onvoldoende begrepen, vooral binnen de context van een complexe TMO. Dit doctoraatsonderzoek had als doel de dosisafhankelijke effecten van CAP in 3D PDAC-modellen te onderzoeken en de interactie ervan met angiogenese en chemotherapie te evalueren, met als uiteindelijk doel de therapeutische waarde ervan in de behandeling van pancreaskanker te definiëren.

Hiervoor werden geavanceerde 3D co-cultuur sferoïdemodellen ontwikkeld die PDAC-cellen, PSCs en endotheelcellen omvatten. Deze modellen weerspiegelen de heterogeniteit en complexiteit van de PDAC-TMO nauwkeuriger dan conventionele monoculturen. Aan de hand van deze modellen werd eerst onderzocht of CAP de vasculatuur kon moduleren, met als doel angiogenese te bevorderen in de hypovasculaire omgeving van PDAC. De resultaten toonden echter aan dat lage doses CAP geen angiogenese induceerden. Integendeel, CAP behield vasculaire rust, verlaagde de VEGF-A-secretie, terwijl andere

groeifactoren onveranderd bleven, en verminderde lichtjes de tubulaire vorming van endotheelcellen in vitro. De vascularisatie binnen en rond de tumor in het in ovo chorioallantois membraan (CAM) model van de kalkoen bleef grotendeels onveranderd na behandeling met lage dosis CAP. Deze bevindingen ondermijnen de hypothese dat oxidatieve stress van CAP de vasculatuur in PDAC zou kunnen herprogrammeren, en suggereren dat de effecten sterk contextafhankelijk zijn, onder andere in functie van het gebruikte CAP-apparaat, gascompositie, afstand tot het doelweefsel, tumormodel en kankertype.

Vervolgens werd het therapeutisch potentieel onderzocht van CAP in combinatie met de standaardchemotherapieën gemcitabine en paclitaxel. In sferoïden afgeleid van twee verschillende tumortypes, MiaPaCa-2:RLT-PSC:HMEC-1 (MRH) en BxPC-3:hPSC21:HMEC-1 (BHH) (kanker-:stellaat-:endotheelcellen), verminderde CAP-monotherapie de overleving van kankercellen, met wisselende selectiviteit afhankelijk van het tumormodel. In MRH-sferoïden bleef de integriteit van stellaatcellen behouden en werd de cytotoxiciteit van lage dosis chemotherapie versterkt, wat wijst op een mogelijke dosisbesparende strategie. In BHH-sferoïden daarentegen oefende CAP bredere cytotoxische effecten uit, met schade aan zowel kankercellen als stellaatcellen, en werd geen effectieve synergie met hoge dosis chemotherapie waargenomen. Opmerkelijk is dat in bepaalde omstandigheden de combinatie van hoge dosis chemotherapie met CAP resulteerde in een verminderde effectiviteit ten opzichte van chemotherapie alleen, mogelijk door de activatie van cellulaire stressreacties die overleving bevorderen bij extreme oxidatieve stress. Deze bevindingen werden verder gevalideerd in het CAM-model, dat de afzonderlijke cytotoxische effecten van chemotherapie bevestigde. De combinatiebehandeling van CAP en chemotherapy presteerde niet beter dan de monotherapieën, wat opnieuw de complexiteit van de interacties tussen behandelingscomponenten en tumorkenmerken benadrukt. Deze resultaten tonen aan dat het therapeutisch potentieel van CAP niet ligt in een uniforme toepassing, maar in zorgvuldig afgestemde regimes die aangepast zijn aan tumor- en toepassingsspecifieke kenmerken.

Gezamenlijk toont dit werk aan dat CAP een krachtig maar complex therapeutisch instrument is, waarvan de effecten sterk afhankelijk zijn van de dosis, het tumortype en de omliggende micro-omgeving. Hoewel CAP, alleen of in combinatie met chemotherapie, sterke cytotoxische reacties kan opwekken, moeten de effecten op stromale en vasculaire componenten worden overwogen om ongewenste gevolgen, zoals ernstige stromale schade, verlies van selectiviteit of de bevordering van kankercellen te vermijden. De co-cultuurmodellen die in dit proefschrift zijn ontwikkeld, vormen waardevolle platformen voor preklinische evaluatie van anti-kanker strategieën (en dus niet gelimiteerd zijn tot CAP behandeling) en onderstrepen het belang van het nabootsen van tumorcomplexiteit bij het testen van nieuwe therapieën.

Tot slot biedt dit proefschrift nieuwe inzichten in de rol van CAP bij de behandeling van PDAC. Het toont aan dat CAP geen angiogenese bevordert in de context van PDAC, tenminste met de gebruikte condities in dit proefschrift, en dat combinaties met chemotherapie zorgvuldig geoptimaliseerd moeten worden om contraproductieve effecten te vermijden. Toekomstig onderzoek zou zich moeten richten op het verder verfijnen van optimalisatieparameters, zoals het type CAP-apparaat, de gascompositie, de afstand van de uitlaat van het apparaat tot het monster afhankelijk van het tumormodel en de onderzoekshypothese. Een andere veelbelovende toekomstige richting is de combinatie van CAP met immunotherapie en het integreren van immuuncomponenten in 3D-modellen om het volledige potentieel van CAP te beoordelen bij het doorbreken van de immuunsuppressieve micro-omgeving van PDAC. Door CAP-toepassing af te stemmen op tumorspecifieke kwetsbaarheden, kan het een waardevolle aanvulling worden op multimodale behandelingsstrategieën voor PDAC.

CHAPTER 08

CURRICULUM VITAE

Personalia

Name	Ruben Verloy
Date of birth	04/12/1996
Place of birth	Edegem, Belgium
Nationality	Belgian
Current affiliation	Plasma Lab for Applications in Sustainability and Medicine – ANTwerp (PLASMANT) Center for Oncological Research (CORE) University of Antwerp Campus Drie Eiken Universiteitsplein 1, 2610 Wilrijk, Belgium
Email	ruben.verloy@uantwerpen.be

Education and scientific career

2020 - Present **PhD Researcher**

"Cold atmospheric plasma's dose-dependent effect in 3D pancreatic Cancer Models: From Vascular Quiescence to Cytotoxic Combination Strategy"

Promotors: Prof. dr. Annemie Bogaerts, Prof. dr. Evelien Smits, and Dr. Angela Privat Maldonado

Plasma Lab for Applications in Sustainability and Medicine - ANTwerp (PLASMANT)

Center for Oncological Research (CORE)

University of Antwerp

2018 – 2020 **Master of Chemistry, University of Antwerp, BE** – *Great Distinction*

"The effect of cold atmospheric plasma treatment on the activation of pancreatic stellate cells"

Supervisors: Prof. dr. Annemie Bogaerts, Prof. dr. Evelien Smits, and Dr. Angela Privat Maldonado

Plasma Lab for Applications in Sustainability and Medicine - ANTwerp (PLASMANT)

Center for Oncological Research (CORE)

University of Antwerp

2015 – 2018 **Bachelor of Chemistry** – *Honours Student*

"Ruthenium-catalyzed reductive arylation of N-(pyridin-2-yl)amides and recycling of the directing group"

Supervisors: Prof. Dr. Bert Maes and Evelien Renders

Organic Synthesis (ORSY)

University of Antwerp

2017 – 2018 **Internship**

Supervisor: Griet Stoffels

Quality Control

Johnson & Johnson Geel

Scientific output

Articles

2025 **Verloy, R.,** Privat-Maldonado, A., Van Audenaerde, J., Rovers, S., Zaryouh, H., De Waele, J., Quatannens, D., Peeters, D., Roeyen, G., Deben, C., Smits, E. and Bogaerts, A. (2025). Capturing the Heterogeneity of the PDAC Tumor Microenvironment: Novel Triple Co-Culture Spheroids for Drug Screening and Angiogenic Evaluation. *Cells*, 14(6):450. doi:10.3390/cells14060450.

Rovers, S., Van Audenaerde, J., **Verloy, R.,** De Waele, J., Brants, L., Hermans, C., Lau, H.W., Merlin, C., Moller Ribas, M., Ponsaerts, P., Van Laere, S., Lardon, F., Wouters, A., Fisher, S.A., Van Meerbeeck, J., Marcq, E. and Smits, E. (2025). Co-targeting of VEGFR2 and PD-L1 promotes survival and vasculature normalization in pleural mesothelioma. *Oncoimmunology, 14*(1), 2512104. doi:10.1080/2162402X.2025.2512104.

Verloy, R., Peeters, E., Privat-Maldonado, A., Rovers, S., Lau; H.W., Brants, L., De Waele, J., Deben, C., Smits, E. and Bogaerts, A. Low-dose cold atmospheric plasma treatment

preserves vascular quiescence in 3D tumor-stroma-endothelial models of pancreatic cancer in vitro and in ovo. ***Manuscript submitted to NPJ Precision Oncology***.

Verloy, R., Privat-Maldonado, A., Palmiotto, G., Rovers, S., Peeters, E., Brants, L., Lau, H.W., De Waele, J., Deben, C., Smits, E. and Bogaerts, A. Balancing cytotoxicity and resistance: dose-dependent and tumor-type specific response to cold atmospheric plasma-chemotherapy combinations in advanced 3D PDAC models. ***Manuscript in preparation for submission.***

Oliveira, MC, Privat-Maldonado A, Heirman P, **Verloy R**, Smits E and Bogaerts A. Effect of cold atmospheric plasma on cancer cell communication via gap junctions: an in silico and experimental approach. ***Manuscript in preparation for submission***.

2023 Heirman, P., **Verloy, R.,** Baroen, J., Privat-Maldonado, A., Smits, E. and Bogaerts, A. (2024). Liquid treatment with a plasma jet surrounded by a gas shield: effect of the treated substrate and gas shield geometry on the plasma effluent conditions. *Journal of Physics D: Applied Physics,* 57(11), 115204. doi:10.1088/1361-6463/ad146b.

2022 Privat-Maldonado, A., **Verloy, R.,** Cardenas Delahoz, E., Lin, A., Vanlanduit, S., Smits, E., and Bogaerts, A. (2022). Cold Atmospheric Plasma Does Not Affect Stellate Cells Phenotype in Pancreatic Cancer Tissue in Ovo. *International Journal of Molecular Sciences,* 23(4). doi:10.3390/ijms23041954.

2020 **Verloy, R.,** Privat-Maldonado, A., Smits, E., & Bogaerts, A. (2020). Cold Atmospheric Plasma Treatment for Pancreatic Cancer-The Importance of Pancreatic Stellate Cells. *Cancers (Basel),* 12(10), 2782. doi:10.3390/cancers12102782.

Oral presentations

2024 **10th International Conference on Plasma Medicine and 9th International Workshop on Plasma for Cancer Treatment |** Portorose, Slovenia

Revolutionizing pancreatic cancer therapy with the combination of chemotherapy and cold atmospheric plasma using the turkey in ovo model

2023 **2nd Annual Meeting of COST Action PlasTHER |** Bologna, Italy

Eliminating the effects of ambient conditions during a plasma jet treatment of a liquid sample with a gas shield

2022 **9th International Conference on Plasma Medicine |** Utrecht, Netherlands

Triple co-culture spheroid model of pancreatic cancer for anti-cancer & angiogenic plasma research

Poster presentations

2025 **Final Annual Meeting of COST Action PlasTHER |** Barcelona, Spain

Cold atmospheric plasma combined with chemotherapy in innovative 3D pancreatic cancer models

2023 **8th International Workshop on Plasma for Cancer Treatment |** North Carolina, USA

Heterogeneous triple co-culture spheroid model of pancreatic cancer to improve plasma research

EACR Goodbye Flat Biology | Berlin, Germany

Development of a heterogeneous triple co-culture 3D spheroid model of pancreatic cancer for anti-cancer and angiogenic studies

UAntwerp Cancer Research Day | Antwerp, Belgium

Development of a heterogeneous triple co-culture 3D spheroid model of pancreatic cancer for anti-cancer and angiogenic studies

2022 **UAntwerp Cancer Research Day |** Antwerp, Belgium

Triple co-culture spheroid model of pancreatic cancer for plasma research

1st Training School of COST Action PlasTHER

Triple co-culture spheroid model of pancreatic cancer for plasma research

2021 **7th International Workshop on Plasma for Cancer Therapy |** Online

Triple co-culture spheroid model of pancreatic cancer for plasma research - **Bob Barker Award for Best Poster Presentation**

Other scientific achievements

Science communication

2025 **Bob Barker Award for Best Poster Presentation at the 7th International Workshop on Plasma for Cancer Therapy**
"Triple co-culture spheroid model of pancreatic cancer for plasma research"

Project management

2024 **Student supervision**
I guided Emma Peeters, a Master's student from the University of Antwerp, throughout her research project entitled "*The investigation of the proangiogenic cold atmospheric plasma treatment for pancreatic cancer in the turkey in ovo CAM model*" from January to June 2024.

2021 **FWO Strategic Basic Research PhD Fellowship Grant**
I was awarded with an FWO Strategic Basic Research PhD Fellowship Grant from the Research Foundation Flanders (FWO), supporting innovative doctoral research. This competitive funding enabled the full-time pursuit of my PhD on cold atmospheric plasma treatment against pancreatic cancer.

2020-2025
Student supervision
Each semester during my PhD, I supervised chemistry practical sessions for first-year bachelor students. This included guiding them through experimental procedures, ensuring lab safety, and supporting their understanding of fundamental chemical concepts.

CHAPTER 09

ACKNOWLEDGEMENTS

Acknowledgements – Dankwoord

Vijf jaar geleden begon ik aan een avontuur waarvan ik toen nog niet wist hoe uitdagend, leerrijk en verrijkend het zou worden. Het behalen van dit doctoraat was niet mogelijk geweest zonder de hulp, steun en inspiratie van de mensen rondom mij, waarvoor ik mijn oprechte dank wil uitspreken.

Angela, oof, where do I start?! It's been over 5 years now since I've joined you doing egg experiments before I even started my master's thesis to see whether I would be interested in the plasma-medicine research, and I sure was! Covid wasn't easy on all of us, but we made it work with you doing more experiments and I doing more analysis of results. Quickly after that I became your first PhD student so it was an exciting start for both of us! Over the years I was able to learn so much from you. All the tips and tricks you've gathered over the years were all coming my way and I tried to absorb as much as possible, not always successfully at first, but hey I kept trying! :) Obviously, I am very grateful for all of that because I was able to grow so much from these things, and I believe that's great supervision/leadership to motivate and allow people to grow. This also caused a flip side on me though, and in a moment of lacking sufficient resilience, it got too much for me. You've not only been there at my highs cheering me on (because you really did!), but also had to pick me up from the ground and get me going again. As you talked and walked me through this somewhat harder period, I could see how you genuinely care for your PhD students and how much it means to you that we're not only learning and growing, but that we're also proud of ourselves in what we achieve. So thank you for ALL of that and for being there in the difficult times as well! :) Now onto some fun things: I still remember how we went for a beer in Lisbon and you felt so sorry for dragging us to a "terrible" bar, but honestly it was a very fun night! It was also nice to form a sports group with you, Maxime and Fanny and how we went for a quick training outside and just suffered together! I will remember you as a very caring and punctual person and as I'm learning spanish with duolingo I'll end with some spanish: estoy muy feliz con mi graduacíon y me siento emocionado para mi futura gracias por todo lo aprendido! I wish you all the best!

Annemie, jou wil ik vooral heel erg bedanken voor de kans die je mij gaf! Ik weet nog goed wanneer ik op zoek was naar de juiste plek voor mijn master thesis en PhD dat ik hier heel goed over wilde nadenken. En ondanks ik altijd dacht dat ik in organische chemie ging verder gaan, voelde het heel goed en vertrouwd bij jou en bij het plasma-medicine onderzoek, en om toch iets medischer te gaan dan puur chemie. Vijf jaar later heb ik hier absoluut geen spijt van! Dus bedankt dat je toen in mij geloofde :) Ik denk niet dat ik ooit al iemand heb ontmoet die altijd zo vriendelijk is, met een lach op het gezicht en dat siert je echt enorm! Ik denk ook dat er niemand bestaat die fijner is om mee te communiceren via e-mail dan jij! Je antwoordt altijd zeer snel op e-mails, zelfs wanneer je out-of-office of op vakantie bent! En soms vraag ik me echt af of je geen dubbelganger hebt zodat je dit allemaal kan blijven volhouden. Nee, het bewijst vooral hoe je jouw onderzoeksgroep met hart en ziel hebt opgebouwd en nog steeds leidt. De smileys mag ik natuurlijk niet vergeten, want die maken de e-mails toch altijd luchtig en fijn om te lezen :) Nog veel succes met de verdere groei van PLASMANT, ik ben benieuwd waar je de groep nog naartoe zult brengen!

Evelien, vandaag wil ik graag voor de laatste keer een kaartje nemen, en dat is een fluogroen want het is toch een bijzondere dag waarop ik wellicht een beetje nerveus ben maar vooral gelukkig en trots ben dat ik mijn PhD op een goede manier heb kunnen afronden. Toen ik aan mijn PhD startte kende ik jou nog niet van eerder les te hebben gehad van jou, en je kwam mij als een zeer professionele en serieuze persoon over. En dat is zeker waar op de werkvloer, maar daarnaast heb ik me enorm geamuseerd met jou en hard gelachen om allerlei anekdotes en verhalen. Een grappig verhaal vertellen uit je verleden breekte telkens weer het ijs en zorgde voor de inzet van een leuke avond bv. op conferenties in Utrecht, Slovenië en Barcelona. Of het nu op een terrasje was in Utrecht, in een jacuzzi in Slovenië of in een roos restaurant in Barcelona, je greep telkens je kans om ons buiten het werk ook beter te leren kennen en dat was enorm fijn! Ook op het werk stond je deur en inbox open om tips of feedback te geven en vond je het mentaal welzijn van je PhD studenten niet onbelangrijk, waarvoor dank! Ik denk dat we je ook wel mogen kronen als de queen of teambuildings want je zit vaak in het winnende team! De laatste keer mocht ik hier deel van uitmaken dus een betere afsluiter kon ik me niet bedenken.

Zeker de editie waarbij je mij ondersteunde om over het touw te springen en ik je daardoor bijna op de grond duwde zal ik niet snel vergeten (nogmaals sorry daarvoor)! Bedankt voor de geweldige begeleiding, leuke momenten en veel succes met de toekomst van STIG & CORE.

I would also like to thank my jury, **Prof. Dr. An Wouters, Dr. Abraham Lin, Prof. Dr. Cristina Canal and Dr. Augusto Stancampiano** for reading and evaluating my PhD thesis. I have enjoyed our fruitful discussions where I was able to express my view on the field of plasma-oncology and its exciting future. Additionally, thank you for the interesting times and discussions on conferences throughout these years.

An, bedankt voor de tijd die we samen bij CORE hebben gedeeld en voor je bemoedigende en ondersteunende woorden. We hebben samen één keer de jaarlijkse teambuilding mogen organiseren en toen besloten we naar de zoo te gaan. Dat is voor mij één van de mooiere herinneringen aan CORE: samen alle ideeën bedenken, foto's maken die de anderen moesten nabootsen en natuurlijk het organiseren van de teambuilding zelf! Dankjewel daarvoor en veel succes met je TACTT groep.

Filip, jij bent zeker en vast één van de meest inspirerende mensen die ik ken! De manier waarop jij streeft naar een betere (en gezondere) toekomst voor iedereen is bewonderenswaardig en bewijst dat jouw plek als diensthoofd van CORE, vicerector van de UA en decaan van de faculteit geneeskunde en gezondheidswetenschappen meer dan correct is. Ik weet nog dat je moest bellen met journalisten om iets op te nemen voor het nieuws (als ik het mij goed herinner). Je kwam hiervoor naar het MacLab, want ze hadden graag een labo achtergrond, maar ik was daar net een experiment aan het uitvoeren. Je verontschuldigde je meerdere keren voor het storen, maar het enigste dat ik erover dacht is hoe geweldig het was om jouw inspirirende woorden live te horen! Bedankt voor alles!

Sophie, mijn office buddy, maar dat is niet het enige dat we al die jaren deelden! Van vastberadenheid om alle Harry Potter poppetjes te verzamelen tot een gave om in een slappe lach te belanden door een opluchtende en synchrone zucht. In jou heb ik echt een vriendin voor het leven gevonden en ik hoop je niet te verliezen door de afstand. Maar no

worries, ik blijf je wel gewoon spammen met Instagram reels of random What's App berichtjes zodat je me niet vergeet, hihi! Wanneer ik echt een dieptepunt bereikte en ik even mezelf verloor had je dit al snel afgelezen aan mijn gezicht en houding. Bedankt om altijd te willen luisteren en me er door te krijgen. Zonder jou naast mij had het nooit hetzelfde geweest! Nou, daar zit ik dan met traantjes in m'n ogen terwijl ik dit schrijf. Wat was het fijn om de legendarische Anita (die mij ondertussen beter kent dan mezelf denk ik haha), AJ, Stewie en Teddy te leren kennen in Frankrijk. Ook zij steelden een plekje in mijn hart! We werden er beste vrienden met de lemur aapjes, al bleef ik toch eerst liever op afstand staan bij Laura! Ook leerde ik een andere kant van jou kennen wanneer je achter het stuur kroop haha! Je bracht me in de wereld van bookbinding, en al vond ik het de eerste keren wel lang duren en moest je me nauwkeurig begeleiden of m'n boeken waren crooked, tegen het einde vond ik het toch jammer dat we er klaar mee waren! M'n Bridgerton en HP boeken zullen me altijd blijven herinneren aan die leuke momenten, waar "twellef" echt z'n eigen leventje is gaan leiden! Samen naar pretparken gaan deden we als de besten, waar we onze gekke kantjes helemaal konden loslaten. Ook al heb ik je misschien gehoorschade bezorgt, plezier was gegarandeerd! Mij beïnvloeden en verslaafd maken aan iets kon je als de beste, al was dit meestal niet je bedoeling denk ik, maar het bewijst wel hoe goed je mij kent en hoe goed je wist wat ik leuk zou vinden! Drag Race is nog een andere gemeenschappelijke interesse van ons, dus trokken we naar Gent voor Bianca del Rio, waar we echte ghostbusters werden en het kind in ons loslieten! Wie had gedacht dat dat laatste uurtje vrije tijd zo leuk ging worden! "I want one if you want one" werd ons motto en al snel hadden we souvenirs voor Ole en Luc, een lekkere wafel op, en koekjes gekocht voor thuis. Kalkoentjes weggooien (sorry kalkoentjes) verliep niet altijd vlot bij mij, maar gelukkig was jij er om mij te supporteren (lees "mij uit te lachen"). Bedankt om hier vandaag fysiek aanwezig te zijn vanuit Noorwegen en mijn office buddy, assistent vandaag, bookbinding teacher, en mede-obsessieve collector te zijn geweest al die jaren. Jij hebt werkelijk een gouden hart en ik ben zo dankbaar dat ik mocht ondervinden hoe je dit deelt met je vrienden! Bedankt voor alles en ik kan niet wachten om te zien waar het leven jou nog brengt, want je talenten blijven maar opduiken. Als je ooit met één van je

creatieve passies zou verder gaan, sta ik op de eerste rij om je aan te moedigen zoals jij bij mij deed met Rubelle Scents!

Maxim, de chaotische mastermind! Dat jij je eigen manier van aanpak en organisatie hebt, of het gebrek eraan ;), was duidelijk, maar het sierde je wel! Je wist toch perfect waar je mee bezig was en waar je naartoe wilde. Ook het vergaren van nieuwe literatuur en kennis doe je met twee vingers in de neus (ik kon in elk geval niet volgen!). Niet alleen in PDAC en 3D modellen waren we beiden geïnteresseerd, maar ook in "de cryptos"! Maandagochtenden waren standaard "en Ruben wat denkte van de cryptos? Ziet het er goed uit?" en de week kon weer beginnen! Bier drinken is iets waar we dan weer helemaal niet gelijkaardig in zijn, ik lust het totaal niet, jij drinkt het per halve liters ;) Merci voor de leuke jaren waarin we met Sophie (en anderen voor korte en lange periodes) onze leuke bureau hebben mogen delen. Veel succes met Sightera!

Sofie, Soffeeeee, wat was het fijn om met jou de bureau te delen! Één van onze highlights was toch wel samen een appartement delen in Berlijn tijdens de conferentie! Gezellig samen nog een theetje drinken, wat babbelen en elkaar beter leren kennen. Maar ook in de bureau was het altijd een goede sfeer met jou erbij. Wanneer ik weer nood had aan een neusspray, of glas in m'n oog had was je telkens weer m'n redder in nood ;) Het dokter zijn zit echt in jouw genen met je zorgende karakter en intelligentie, en een harder werker ben je sowieso! Dat had ik al door vanaf week 1 waarin je een review artikel schreef! Keep up the hard work, veel success met het afronden van je thesis!

Gijs, de nieuwste aanwinst van het TUSC-team! Je kwam het NL team versterken op CORE en we zaten al vrij direct vast doordat jij bepaalde belgische woorden niet kenden en andersom ik jouw NL accent niet altijd kon verstaan. Maar hey, met wat extra uitleg zijn we er telkens wel uitgeraakt! Toen ik op weekend ging iets "dieper" in Nederland was het op maandagochtend heel grappig om te ontdekken dat ik blijkbaar in jouw hometown ben geweest, hoe toevallig was dat! Bedankt voor de leuke momenten in onze bureau en je geïnteresseerde vragen over hoe het gaat met bepaalde experimenten of thesis schrijven. Veel succes nog met jouw PhD!

Odeta, jou wil ik vooral bedanken voor je openheid! Aan oppervlakkige small-talk doe jij niet mee, het was fijn om échte gesprekken te voeren. Ook ging je telkens goedlachs van start met de teambuildings en was je vastberaden om de opdrachten met succes te beëindigen. Nu jouw PhD er ook zo goed als op zit, is het tijd dat je jezelf op de eerste plaats zet! Veel succes hierbij.

Mauranne, my little sis! Het werkleven zal nooit meer hetzelfde zijn zonder jou! :(Ik ga jou echt héél hard missen (zoals jij het altijd zegt haha)! Wij waren echt twee handen op één buik en begrepen elkaar meteen, zelfs telepathisch! Tijdens je master thesis merkten we snel dat het een gouden match was, en ik voelde me vereerd dat je naast je begeleiders ook bij mij kwam vragen naar mijn mening of advies over kleine dingen. Wanneer we het moeilijk hadden met FWO, slechte resultaten of we gewoon even overprikkeld waren konden we altijd bij elkaar terecht voor een luisterend oor en om even opgepept te worden om er terug in te vliegen. We hebben ook zoveel onvergetelijke momenten! :) Zoals even gek dansen op roxy dekker in onze hotelkamer op conferentie! Of hoe we 15 min moesten wandelen naar de spa om dan in onze badjas op straat te belanden en we niet meer bijkwamen van het lachen, hahaha! Daarna hebben we ook weer de avond van ons leven gehad op een hilarisch dansfeestje met al de plasma medicine mensen, en grepen we nipt naast die “early carreer award” en “lifetime achievement award” haha! Onze telepathie was altijd on point, zelfs in die zenuwslopende momenten! Samen hotdogs verkopen voor het goede doel (ons kankeronderzoek) en skydiven kunnen we ondertussen ook als de beste! Maar af en toe hebben we onze “me-time” nodig en zakken we af naar de McDo voor een paar chicken nuggets. Hmmm! Voor mij blijf je altijd dé vinted-queen die enkele euros (of zelfs lucht) omtovert in botjes of een handtas, die haar ikea mand op de brommer naar huis brengt of gewoon uit het niets roept tijdens mijn uitleg “shhhh ik moet niezen” en dan in de zon kijkt maar het toch wééral mislukt! Onze portie luchthaven miserie hebben we wel gehad voor de komende 10 jaar, maar wat ik er wel uit geleerd heb is om niet meer met de trein te gaan naar een luchthaven, en om niet mee op te gaan in jouw emoties want dan wordt het alleen maar erger! Wanneer de muziek aanging of de stempelkaart vol was wist ik hoe laat het was; wat hebben we toch hard gelachen en oooh wat ga ik al die

verhalen en momenten missen! Ik woon misschien nu in het verre Arendonk, maar altijd welkom om met de trein tot Turnhout te komen waar ik je oppik voor een gezellige avond! Dit is geen goodbye maar wel tot snel! Love you!

Jöran, (in mijn hoofd nog steeds Jöranosaurus, sorry), mijn mede gas bottle buddy (al hebben jullie me niet veel nodig gehad haha). Ik heb jouw werkethiek en attitude altijd beaamd: consistent vroeg op de bureau en gedisciplineerd en hard aan het werk. Daarbovenop ben je altijd positief en enthousiast, wat het enorm aangenaam maakte om met jou een gesprekje in het lab te voeren of naar Walibi te trekken. Jij die in de botten door het slijk gaat om een gas bottle te vervangen ga ik niet snel vergeten haha! Samen kregen we het hele team over dat touw tijdens de teambuilding, en wat was ik blij dat jij geen lab rat was, want alleen had dat niet gelukt! Ik wens jou en Marine het beste toe en hoop dat jullie een leuk plekje vinden om samen te wonen :) WALIBI

Adrien, my fellow rage gamer. Too bad we didn't get to play a lot of games together (probably because we would have ragequitted after a minute, haha just kidding). But I did enjoy when you got me addicted to Palworld! Be sure to let me know if you find anything else, you know my gaming taste by now anyway! I don't think I'll ever meet someone so outspoken and strongly opinionated as you, but I do know that underneath that tough armor there's a very caring person. Good luck with finishing your own thesis and whatever comes after!

Jasper, de lego, marvel, F1 en sporty guy! Wat ik aan jou heel fijn vond was dat onze "hey" kon uitdraaien op een hele deepdive over Marvel films of toekomstplannen en het gesprek niet oppervlakkig bleef maar dat je oprecht geïnteresseerd bent om een leuk gesprek te voeren, dat is misschien de diep-kempische klik haha! Alvast bedankt daarvoor. Ik wist dat je sportief was, maar toen ik die foto zag binnenkomen van 5km aan 3:59/km dacht ik, wow, wat doe ik hier eigenlijk in de running club?! Niet normaal! Competitiviteit zit zeker in jouw genen, dus jij wint met lopen, maar, we all know I would've beaten you with karting if I was there ;) Ik zie je nog wel eens in Mol of Arendonk of via Hanne, maar alvast veel succes met de laatste fase van je PhD!

Emma, mijn eerste student & superbrain (want ja, voor mij blijf je toch altijd een beetje mijn student ;)). Wat ben ik trots dat jij mijn master student was! Je begon eraan in een moeilijke periode met je knie, en het was ongelooflijk om te zien hoeveel veerkracht en doorzettingsvermogen jij hebt! Ik heb je nog vaak gevraagd of je nog last hebt, en ik hoop dat het antwoord hierop ooit een dikke NEE is! Jouw ability om alles te onthouden is echt niet normaal, ik voelde me telkens dom dat ik weer een belangrijk detail vergeten was, maar goed dat ik jou had in die momenten! Ik hoop ook dat je ooit terug eieren kan eten zonder dat de geur je doet denken aan het MacLab en dat je ooit terug een ei kan openen zonder het gevoel te hebben dat je het in een medium fles moet weggooien omdat het niet bevrucht is of de CAM niet gedropt is haha! Je bent een echte Formule 1 fan en door jou ben ik mij er nu ook in aan het verdiepen! Jammer dat ik er bij het karten niet bij was om in je slipstream te hangen en dan voorbij te vliegen ;) Bedankt voor alle samenwerking en hulp, en veel succes met je PhD.

Julie, chapeau hoe jij je studies combineert met een PhD! Ik heb jouw oprechte interesse om even te vragen hoe het gaat met experimenten of paper/thesis schrijven erg geappreciëerd! En wie had gedacht dat die lieve, onschuldige Julie zo'n professionele pokerface had zeg?! We zaten er helemaal naast als het ging over jouw leugens & waarheden haha! Succes met het behalen van je PhD en het afronden van je studie :)

Laura, but when did I ever call you that right, LG? You were my lab buddy since the start and we self-claimed Flow 3 as ours, it became our *Wonderland* at T4! We would both be early in the lab, join each other, and get our lab frustrations out. Another trashbin we had to get rid of, or empty drawers in the morning we had to refill. But also talking about other stuff that distracted us until one of us made a mistake, a very *All Too Well* moment, oops! We both did not have the best of luck when it came to getting positive outcomes, but we learned to *Shake it off* and get going again. I'm really going to miss my lab buddy! We've had so many lunches where you joined Sophie and I in our office where we could stop behaving nicely and just be our crazy selves, *the squad goals* were real. We even went on a holiday to France together to meet Sophie's parents and went on a walk with the horsies, which was fun but also a real adventure for both of us, we were totally *Fearless*. At first we

were a bit hesitant about Teddy too, but we got to appreciate his way of saying "*You Belong With Me* human" as a good thing after all. When Sophie and I went to interact with the monkeys, you preferred a safe distance, but at least we had the perfect photographer then, it was a real *Picture to Burn*, just kidding, it was great ;) I admire your sportyness and it was super cool going bouldering with you, seeing you thrive in your personal habitat, and you were doing it in so much *Style*. Learning it from you was a blast! We also learned bookbinding from our teachers and at first we were like *two kids in a cardigan* not knowing what we were doing, but at the end you were faster than the speed of light! And there are so many more good memories: BBQ at my place (*the Last Great American Dynasty* party vibe), going to the Christmas market (*'tis the damn season*), your housewarming (your *Begin Again* with Pedro). But honestly, I truly hope this is not the *End Game* of our story <3

Lisa, m'n rollercoaster co-screaming buddy! Onze tijd gaat al lang terug, tot in de 1e Bachelor! Toen vond ik jou al een super positief ingesteld en enthousiaste persoon, en dat is nog niets veranderd! Het was heel fijn om terug re-united te worden op CORE om dat verder te zetten, and we sure did haha! In Slovenïe op conferentie hebben we ons echt mega goed geamuseerd, bv. op de dance party, én maar strijk gaan van het lachen! Maar ook tijdens de rollercoasters kwamen we ook niet meer bij van het lachen, en stikten we zelfs soms tussen het om de beurte lachen en schreeuwen door haha! In Walibi hebben we hun echt laten zien hoe wij aan attracties doen, en we hebben dat verder gezet in de Efteling, good vibes only, Eftelabubuuuuuu, ik wou dat ik even terug naar dat weekend kon ;) Maar ook werden we bookbinding buddies en ik weet dat jij altijd even hard uitkeek naar de pizzzzaaaa als mij haha! Wicked zal ik voor altijd aan jou associëren en als ik ooit iemand nodig heb voor een "stop de band" ronde tijdens een quiz dan bel ik jou! "You're all I can think of, every drop I drink up, <nu jij>" :) Als laatste, laat ik jou al mijn pizzastukken na die nog op op mijn shellef staan in de ijskast omdat ik die vergeten was zellef mee naar huis te nemen, maar je zal wel snel moeten zijn want om klokslag twellef uur komt de wolef alles opeten! Blijf die bubbely zellef dat je bent en we zien elkaar sowieso nog terug!

Jana, jouw luisterende oor en begripvolle gesprekken zal ik missen. Verder valt niet te ontkennen hoe enorm behulpzaam jij bent. Jij stond werkelijk altijd klaar om te helpen waar je kon, bedankt om bv. mijn platen eens te scannen met de spark. Je steun tijdens de opstart van Rubelle heb ik ook enorm gewaardeerd. Daarnaast hebben we ook leuke tijden gehad op conferenties zoals in Slovenië & Bologna! Veel succes nog met je uitdagende PhD maar je bent een harde werker dus ik heb er alle vertrouwen in! :)

Tias, m'n teambuilding buddy! Enkel jaren geleden begonnen we samen aan ons PhD, we zaten echter in andere bureaus en hebben niet gigantisch veel contact gehad eigenlijk, en eerlijk gezegd vind ik dat wel jammer want de momenten die wel wel samen spendeerde bv. op teambuildings waren top! Op de teambuilding van Who's The Lab Rat bv. hebben we het toch super leuk gehad samen :) Ik zeg niet dat we de beste speurders waren haha maar we gingen er wel helemaal voor! De laatste teambuilding bewezen we wel dat we goede speurders zijn! En weeral heb ik me toen hard geamuseerd met jou. En het winnen ervan aan het einde van ons PhD was toch wel de kers op de taart :) Verder vond ik je als collega ook heel behulpzaam! Ik had nooit het gevoel dat er een vraag te veel was dus bedankt voor die leuke collegiale houding :) En succes met je nieuwe avontuur na dit PhD.

Aminur, my Bollywood friend! I still haven't watched one of those Bollywood movies you sent me, apologies! But now I should have some more time on my hands to finally do that! :) You started your PhD with me as your lab mentor, so I had some extra opportunities to get to know you! You came across as a shy person in the beginning, but once you warmed up, I got to experience your sense of humor and once we got started it was amazing haha! Also had a good time with you on the Barcelona conference, especially in the pink restaurant! Good luck with everything!

Yannick, wat ik bij jou enorm appreciëerde was je vriendelijkheid en behulpzaamheid. Tijdens een STIG meeting bv. ben jij veruit één van de meest geïnteresseerde mensen in de ruimte die opbouwende feedback geeft. Dat viel me niet enkel op bij mijn eigen presentaties, maar ook bij anderen, bedankt om op die manier aan iedereen zijn onderzoek bij te dragen! Verder zaten we twee keer in hetzelfde teambuilding team waarin ik mij

super hard geamuseerd heb dus bedankt voor die leuke momenten en om de winst binnen te slepen met je geweldige verhaal! Succes met je uitdagende vervolg als klinisch bioloog.

Chloé, Brian, Liesbeth, Pieterjan, Daniel, Charlotte, Pierre, Karin, we've not had many opportunities to get to know each other that much because you've only recently joined or our paths crossed very little in- & outside of the lab, but I want to wish you the best and good luck with finish your own PhD's (for those that still have to)!

Jorrit, the superman of the lab, niet normaal wat jij combineert in je werk & leven, zonder verlies van kwaliteit, ik kijk daar echt naar op! Je stond altijd klaar om te helpen of feedback te geven, ookal moest je dit om 1u 's nachts doen op een slaap te kort. Het was heel fijn dat we samen een teambuilding samen mochten organiseren, waar ik je tegelijkertijd beter heb leren kennen als persoon in plaats van post-doc, hiervoor gingen we bv. samen naar de zoo met Ho Wa en je gezin om alles verder te bedenken van vragen en opdrachten, wat een leuke dag! Gesprekken even een vage wending geven kan je als de beste, maar wat kristalhelder is, is je voorkeur voor rijpe bananen, ooh wee dacht ik als ik een banaan met groene plekjes mee had genomen! Tijdens de teambuilding van Who's The Lab Rat hebben we zeker ons steentje bijgedragen om mensen over het touw te krijgen, dat was te zien aan onze schouders! Bedankt ook om me tijdelijk te adopteren als PhD Student tijdens Angela haar maternity leave. Ik probeerde niet veel tijd van je weg te nemen, omdat je al zoveel te doen had, maar het was heel fijn dat ik op iemand kon rekenen voor een brainstorm of wat feedback wanneer nodig. Toen ik me had buitengesloten op het labo was ik zo blij dat jij thuis was zodat ik even je badge kon lenen, anders had ik toch wel even een probleem! Je talent om de meest toepassellijke memes/GIFs te vinden tijdens een What's App gesprek ga ik zeker missen! Bedankt voor een leuke tijd en succes met je welverdiende carrière (waar die ook naartoe mag gaan).

Jonas, toen ik jou leerde kennen zat je nog in Australïe en hebben we een online meeting gehad over mijn PhD project. Ik vond dat toen wel spannend want ik vond dat super indrukwekkend dat jij daar zat voor je onderzoek! Bedankt om mee te willen brainstormen over mijn PhD project toen ik voor FWO aan het schrijven was, maar ook voor daarna nog met je flow cytometry hulp en om mij hier in te begeleiden! Het was ook enorm fijn om

uitgenodigd te zijn op jullie trouwfeest, dat was een fantastische avond vond ik, om met heel de groep samen te zijn en vooral om jullie te vieren. Bedankt voor die hulp, input, feedback en leuke tijd!

Debbie, m'n yoga buddy! Hoe grappig en toevallig was dat om plots in dezelfde yoga les te zitten samen! Ik vond dat alvast wel fijn :) Jouw goedlachsheid en enthousiasme was elke keer weer besmettelijk, maar daardoor heb je mij ook wel goed kunnen misleiden als Lab Rat, dus well done! Bedankt voor een fijne tijd samen op CORE (en tijdens de yoga les).

Hanne, mijn mede entrepeneur haha! Gust en fluffy friends en Rubelle Scents take over the world :)! Onze tijd gaat al lang terug want jij was al voor mij in CORE en ik keek toen op naar jou en Eline als meer ervaring Plasma-onco PhD studenten :) Maar niet enkel de plasma-onco groep hadden we gelijk maar ook onze miserie met nek- of schouderproblemen :(Onze sessies aan kiné en warmtekussens hebben we wel gehad daarmee! Nu wonen we ook allebei in het verre Mol & Arendonk dus begrijpen we elkaars struggles met de lange afstand als geen anderen! Maar het voordeel is wel dat we nu samen kunnen gaan tennissen met Mich en Luc :) In Slovenië hebben we ons rot geamuseerd op de beach dance party, ik weet echt niet of ik ooit al zohard gelachen heb als toen, dat was echt een legendarische avond! Heel recent ben ik dan mee in Ferem Lokaal gestapt met Rubelle Scents en ik zou echt in geen andere concept store willen staan want nu betekent het dat we nog langer kunnen samenwerken! Ik kijk al uit naar de dagen dat we hopelijk eens kunnen samen staan in de winkel! Misschien kan je zelfs Patsy die we samen in Utrecht kochten als inspiratie gebruiken voor een fluffy friend van te maken! Dit is zeker geen afscheid dus tot de volgende tennismatch of shopday :)!

Hannah, mijn quadruple L buddy en zo veel meer! Van samen Lab experimenten uitvoeren tot Lab cleans doen, samen Lunchen, maar ook altijd Lachen, gieren en brullen met elkaar. Jij was één van de weinigen waarmee ik echt een next-level gesprek mee kon voeren waarin er geluisterd werd naar elkaar, tranen werden weggeveegd of zelfs luidkeels gelachen werd. In ieder geval, de support was er altijd in twee richtingen. Voor mij ben je toch wel de karaoke queen en hoop ik dat we dit nog eens opnieuw kunnen doen :) Ook super leuk dat je helemaal afrees naar het verre Arendonk om samen in de Vapiano te gaan eten in

Eindhoven omdat je dit nog niet kende, en daarna in de jacuzzi te springen. Altijd welkom voor meer van die avondjes :) We vonden elkaar ook telkens om samen naar Walibi te gaan, balletjes in de Ikea of lekkere pasta in Bavet te gaan eten. Ik ben ook nog steeds zooooo dankbaar dat ik via jou (en Laura) naar Taylor Swift kon gaan! Oh my god dat was iets dat ik niet zag aankomen, maar wel hard op hoopte, en was echt een super leuke avond! Hannah, een lab clean of karaoke avond zal nooit meer hetzelfde zijn zonder jou dus daarom heb ik een afscheidscadeau voor jou (ookal is dit geen echt afscheid hoop ik). En dat is dat ik nog een laatste keer de liquid nitrogen man zal nadoen met extra overtuiging, speciaal voor jou! Dan kan je nog eens goed lachen haha. Tot binnekort! :)

Delphine, de motiverende & organisatorische kracht binnen CORE! Van leuke initiatieven zoals de runners club voor de halve marathon opstarten tot mee de organisatie op je nemen van het winterconcert of BE-PRECISE, Delphine zegt daar geen nee tegen, sterk! Daarnaast vond ik het fijn dat je eens kwam checken hoe het bv. ging met het submitten van m'n paper en vond ik het zot dat je RuPaul's Drag Race kende, dat hoor ik niet vaak :) Veel succes met je volgende stappen!

Sanne, mijn FELASA buddy en de vrouw van de grappige geluidjes ;) Toen ik jou de eerste keer zag waren we op een teambuilding en je leek mij al meteen een super vlotte en enthousiaste persoon. Daarna hebben we samen ons FELASA diploma gehaald en wat was dat voor een geweldige periode! Samen met Birgit hebben we gelachen dat het niet meer normaal was! Maar ook wel hard gestudeerd en soms kleine stressjes gehad; belachelijk maar toch waren we zenuwachtig om onze "handen te wassen" dus hebben we dat op CORE nog eerst extra geoefend. Muizen restrainen was écht niet ons ding en we stonden daar met knikkende knieën af te zien. Chapeau hoe jij hebt door gebeten en uiteindelijk een muizen expert bent geworden! Daarna zijn we elks wat ons eigen pad ingegaan, maar je zorgde ervoor om toch nu en dan eens in het labo te verschijnen (wat je zat vooral bij de muizen) met je gekke geluidjes zoals *bop bop bop*, wat altijd voor een lach op mijn gezicht zorgde! Bedankt voor de leuke momenten en veel succes nog met je PhD af te ronden!

Christophe D, ik vind het heel straf hoe jij TUSC en je robotics screening platform hebt opgebouwd en zo hebt bijgedragen om het niveau van CORE toch naar een hoger niveau te tillen. Zonder de Spark en drug printer alleen al was mijn PhD een pak lastiger geweest! Toen ik de robot heb laten crashen met een plaat die ik er was vergeten uit te halen dacht ik even dat je me ging lynchen, wat was ik blij dat het zonder schade kon opgelost worden! Ik heb het nog geprobeerd om met cupcakes goed te maken, ah nee sorry dat waren mijn kalkoeneieren ;) Veel succes met je ambitieuze toekomst!

Ho Wa, I mean Howhaaaaaaat?! Of zeg ik beter Howasabi, Howarm, Howasmachien, Howafel, Howater, Howazig, Howalvis, Howaakhond van CORE, I mean you know I could keep going if you want, right haha? Wat ga ik jou missen! Jij bent echt veel te goed voor deze wereld, soms moet je eens leren “nee” te zeggen ;) Maar ik was toch blij dat je ja zei op mijn onbevruchte kalkoeneieren zodat ik ze niet moest weggooien. Dus het was wel handig om te weten bij wie ik moest zijn als de meerderheid me zou afwijzen ;) “Stay” van Justin Bieber zal altijd ons lijflied blijven en telkens dat ik het hoor sta ik weer in die karaokezaal met jou haha! Samen die teambuilding voorbereiden was ook echt top! Dagje in de zoo rondlopen en onze gedachten loslaten om de gekste vragen te verzinnen :) Bedankt voor die leuke tijd en om alle labfrustraties te delen.

Louize, de superhulp! Jij stond echt altijd klaar om te helpen waar nodig, wat een zaligheid! We hebben samen wel wat kalkoeneieren doorstaan en naaldjes optrekken heb je nu wel genoeg gedaan voor een tijdje haha, sorry daarvoor! Ik bewonder echt je positieve en enthousiaste ingesteldheid, dat maakte het altijd leuk om samen te werken. Je leert ook heel graag bij en vond het daarom ook leuk om mee te werken aan de eierenexperimenten omdat je hier weer iets uit kon leren! Zaterdagochtenden zijn vanaf nu voor vtm go tijdens het ontbijt als ik het niet vergeet of niets anders gepland heb haha!

Christophe H, mijn crypto buddy! Tegen een babbeltje hier en daar zeg je geen nee tegen, en onze gesprekken gingen vaak over crypto, maar het was fijn om iemand, buiten mijn vader, te hebben om hier helemaal in op te gaan! Ik ben er zeker van dat we nog contact zullen houden om verdere strategieën te bespreken, dus die crypto meetings moeten we dan nog eens organiseren. Bedankt ook om altijd te willen helpen wanneer ik iets nog niet

goed kende in verband met stainen, cryosections maken en andere dingen! Tot op de volgende meeting ;)

Hilde, bedankt voor jouw hulp met allerlei stainings! Het einde van Gotcha met jou en Astrid was héél spannend, bedankt voor deze zenuwslopende strijd! :)

Céline, je bent overlaatst verhuisd naar de verre kempen bij mij en de Verswyvels, welcome to the team! Jammer dat ik je geen kalkoen kon bezorgen, dat had toch wel grappig geweest om een labkalkoen te hebben :) Wie weet zien we elkaar nog eens in oud-turnhout of omstreken!

Inge, je bent nog maar pas bij CORE, en toch heb ik het gevoel dat we al een leuke band hebben opgebouwd. Je bent altijd geïnteresseerd om te vragen hoe het gaat en je luistert écht. Veel succes nog met jullie huis in de ardennen verder te bouwen en vanaf nu weet ik dat je mij niet het zwijgen wilt opleggen maar dat je hard aan het nadenken bent ;)

Felicia, guuuuurl, ik ga onze kiki momentjes echt missen! Me wie moet ik nu twerken in het labo op het gepiep signaal? Wie komt mij nu redden als ik in de kelder vast zit? Het was goed om te weten that somebody was having my back! Ga ook wel echt jouw haar missen haha! You know I love it, hoe jij altijd leuke kapsels hebt! Had nooit gedacht dat jij into Anime zou zijn, maar wat ben ik blij dat je mij hebt beïnvloed into Anime hahaha, maar ben wel nog steeds teleurgesteld dat je Nocturne nog niet hebt gezien! Hoe lang moet ik nog wachten?! Merci voor al die leuke en grappige labmomentjes!

Andreia, you are the sweetest! Loved going to the pizza hut with you when you only started in the lab recently. It was nice to get to know you better right away. We've had our discussion on belgian supermarkets, you know, and I think we can conclude that you should stop going to the colruyt! I hope you agree with me and that you can find your love for belgian supermarkets soon once you've tried different ones ;) Thanks for the short, but fun times together!

Dana, merci voor alle leuke labmomentjes! Maar ook voor daarbuiten, we gingen samen klimmen met Ho Wa en Laura, en al waren we niet zo goed als hun (uiteraard), we deden wel ons best! Daarna gingen we nog gezellig samen eten in de Lunch Garden. Ik dacht ook

dat ik een goede duolingo buddy had gevonden voor samen een quest mee te spelen, maar wanneer ik dit startte bleek jij al gestopt te zijn met DuoLingo... Daar ging m'n quest haha! Hopelijk zie ik je toch nog terug verschijnen en kunnen we eens battlen in een league ;)

Astrid, jij bent gewoon zo schattig (sorry) :D ! Altijd zo lief en nederig (tenzij wanneer er eten gedeeld moet worden of de vraag nog maar gesteld wordt), dat is echt jouw superkracht! Ik vond het heel tof om jou als collega te hebben, ook al miste wel elkaar soms in het labo (ik vroeg, jij laat). De Gotcha finale tussen ons was enorm zenuwslopend en bedankt om er een waardige strijd van te maken! Samen naar het Taylor Swift: The Eras Tour concert gaan was echt zaaaaalig! Heb mij toen echt zo hard geamuseerd met samen te staan zingen en dansen, en je weet als mensen jou lastig vallen, ik ben daar om ze op hun plaats te zetten hé ;) Ik ben benieuwd naar jouw volgende avontuur als onderzoeker want je bent er echt voor in de wieg gelegd, succes!

Eline, mijn mede chemie Plasmateer! Wat jammer dat we niet meer tijd samen hebben kunnen spenderen op PLASMANT/CORE want dat was toch wel een leuke tijd en het voelt ook al zo lang geleden ondertussen! Samen op conferentie gaan in Utrecht was echt gezellig en ik zal nooit één van de hilarischte momenten ooit vergeten dat je instinctief een stap opzij deed alsof je nog kon weglopen en verstoppen om niet betrapt te worden maar ook instant besefte dat dat te laat was haha! Als we even een snackje nodig hadden dan moesten we ook maar even de consequenties dragen zeker (al waren die er eigenlijk niet). Het in ovo experiment heb ik wel wat van jou geleerd en ik weet nog goed dat ik je vroeg "hoeveel eieren heb je ooit al laten vallen per ongeluk", en je zei "geen enkel", en nog geen 2 minuten later liet je een ei vallen haha oeps, I jinxed it, sorry! Ik heb het uiteindelijk ook voor gehad dus je bent niet de enige ;) Pengu of Patsy of Perry (want ik weet eigenlijk niet meer dewelke van mij was oeps) staat nog steeds op mijn kast dus The Three Plasmateers blijven zo toch nog verder bestaan! Bedankt om hier aanwezig te zijn en voor de leuke tijd samen!

Abraham, the karaoke legend and globe trotter of CORE! You've already left CORE for quite some time, but I still remember the good old days! We did not only go for karaoke in Antwerp, but also on conference in Utrecht! I loved how you gave it your ALL like it was a

sing-off competition haha! You also took us for a Skydiving session, which I think was just for fun but it turned out to be a great teambuilding activity for the plasma-onco team! You were always in for some fun or a party, and you're such an enthusiastic person which I loved. Everyone turns happy when you're around, it's just infectious! Thanks as well for being a jury for my PhD thesis and for a fruitful discussion. Who knows maybe I'll bump into you somewhere around the world ;)

Gabriele, thank you for your insanely hard work on the Arivis data and for being so swift about the analysis when a change was needed! Your eagerness and ability to learn are impressive and I think you have great future ahead! Thanks for everything!

Rani, Pepjin, jullie ken ik natuurlijk al langer dan enkel tijdens mijn PhD :) Jullie waren al een grote steun en toeverlaten tijdens de Bachelor en Master opleiding en wat jullie beiden siert is jullie enorm groot hart voor jullie vrienden (en uiteraard ook je eigen families). Van klasweekends tot karting, bowling, uitgaan, attractieparken, practicamomentjes, … we hebben echt al zoveel leuke dingen samen meegemaakt! Ik ben heel blij dat we deze trend hebben kunnen verderzetten tijdens ons PhD, en in het buitenland omdat we samen naar CERN of op conferentie konden gaan, wie kan dat zeggen over zijn vrienden? Wij! :) Ook jullie aanmoediging bij alle spannend momenten zoals examens, presentaties, verdedigingen, etc. zijn mij niet voorbij gegaan en waren voor mij heel waardevol! Bedankt voor deze tijd en tot snel!

I would also like to thank some other PLASMANT people in specific: **Cecilia, Sarah, Mac, Lisa, Priyanka, Karen and Karel.** Thank you for the great times at conferences, in the lab and for discussions during our meetings. As well as your help in placing orders (sorry for being so "urgent" that often!).

Luc, mijn allerliefst hubbyke, jij bent werkelijk te goed voor deze wereld en soms vraag ik me af hoe ik het geflikt heb om jou aan de haak te slagen 6 jaar geleden. Slechts enkele maanden later begon ik aan mijn master thesis in PLASMANT & CORE. Dat wil zeggen dat jij mij al bijna 6 jaar weet praten over sferoïds, kalkoeneieren en plasma, en vandaag eindelijk kan zien wat ik exact bedoelde daarmee en hoe ik de cellen "bliksemde" (zoals jij

het uitlegt aan anderen). Ik heb dit traject niet alleen afgelegd want jij was er voor elke stap die ik maakte, zowel voorwaarts, als achterwaarts. Je was trots op mij bij het behalen van de prijs voor de beste poster presentatie en mijn FWO beurs. Je stond klaar om mij te knuffelen wanneer ik terug kwam van een conferentie omdat we elkaar toch telkens miste. Je maakte me weer vrolijk wanneer ik teleurgesteld was met onverwachte resultaten of een mislukt experiment en moedigde me weer aan met “nog ff volhouden manneke” wanneer het allemaal wat te veel werd. Duizend maal bedankt en ik hou heel veel van jou!

Mama, Papa, Ellen, bedankt om altijd mijn veilige thuishaven te zijn geweest, mij te accepteren en graag te zijn om wie ik ben en mij te laten geloven dat ik alles aankan! Jullie hebben uiteraard een grote rol gespeeld in waar ik tot nu toe sta in het leven en dat ik dit PhD heb kunnen afronden. Jullie gaven mij de kansen, steun en liefde die nodig waren om dit te bereiken en ik ben ontzettend dankbaar voor dit alles en de band die we met elkaar hebben. Ik zie jullie graag!

Aan heel mijn **familie** (het zijn te veel namen om op te noemen), jullie zijn stuk voor stuk schatten van mensen die ik hier vandaag heel graag bij had en die mij als sinds klein Rubentje steunen en enkel het beste met me voor hebben, bedankt voor alle mooie momenten en steun!

Jessica, Sofie, mijn allerliefste best friends! Bedankt voor jaren plezier, avondjes uit, weekendjes weg, ontelbare loopjes, luisterende oren, en duizend keer meer! Bij jullie kan ik 150% mezelf zijn en al mijn vreugde, en soms ook miserie kwijt. Bedankt om naar mijn gezaag te luisteren over mislukkende experimenten maar ook om mij aan te moedigen bij succesvolle mijlpalen zoals vandaag! Onze tijd is zeker nog niet voorbij, alhoewel, Jessica jij het ons wel moeilijk maakt hoor ;) Maar ik weet dat onze vriendschap internationaal reikt en dat we elkaar sowieso nog terug zien in België of het buitenland <3